2013

The Design of Novel Nano-Sized Polyanion-Polycation Complexes for Oral Protein Delivery

This thesis is submitted to the University of Hertfordshire in partial fulfilment of the requirements of the degree of Doctor of Philosophy

Ambreen Ayaz Khan

School of Pharmacy
University of Hertfordshire
Hatfield
Hertfordshire
AL10 9AB
United Kingdom

DECLARATION

I declare that:

(i) This thesis is based on the author's original work.

(ii) All the prose herein has been written by the author, except where acknowledgement has been given to the others.

(iii) All the results and figures in this thesis have been devised and produced by the author, except where acknowledged.

Signed *Ambreen Ayaz* **Date:** October 2013

Name: Ambreen Ayaz Khan

Programme title: Research PhD/MPhil/MA/MSc by Research Schedule A

ACKNOWLEDGEMENT

I take this opportunity to express my sincere thanks to all those who supported me in this project. I express my gratitude to Dr. Woei Ping Cheng for her continuous support and advice throughout the project. She encouraged me to learn an entirely new field and broadened my academic interests. I am truly grateful to Dr. Matt Traynor for his sincere guidance and useful suggestions. I am also thankful to him for the moral support and good advice that sparked my interest and determination. There is no doubt if I say that I have been mentored by the leading experts and best advisors on the subject. I extend my thanks to all the technical staff. In particular, I express my deepest appreciation to, James Stanley, Virendra Shah, Di Francis and Lee Rixon for their enormous help which allowed me to get things working on time. I gratefully acknowledge the grant from the University of Hertfordshire that made this research possible. I thank all my friends for the support that they have given to me in my life outside work. I am deeply indebted to my husband for his endurance and love; for helping me out in difficult times and for doing all that I could not do. Special thanks to my parents and parents-in-law for their continuous prayers and their so much belief in me which renewed my strength and confidence every day and kept me going.

LIST OF TABLES

Chapter 1

Chapter 2

Chapter 3

Chapter 4

Chapter 5

LIST OF FIGURES

Chapter 1

Chapter 2

Chapter 3

Chapter 4

Chapter 5

LIST OF ABBREVIATIONS

Alg-CS	Alginate-chitosan
APECs	Polycation-polyanion-protein polyelectrolyte complexes (ternary complexes)
ATP	Adenosine triphosphate
CLDN4	Claudin 4
CM-H_2DCFDA	Carboxy methyl- di-fluoro di-hydro fluorescein di-acetate
CPPs	Cell-penetrating peptides
CS-PLGA	Chitosan -modified poly(lactic)-co-glycolic acid
Da10	(dimethylamino) naphthalene-1-sulfonyl chloride
DADMAC	Diallyl-dimethyl-ammonium chloride
DAPI	Diamino-2-phenylindole
DLS	Dynamic Light Scattering
DMEC	Dimethylethyl chitosan
DMSO	Dimethyl sulfoxide
DS	Dextran sulfate
DTPA	Diethylene triamine penta-acetic acid
ELISA	Enzyme linked immunosorbent assays
EMEM	Eagles minimal essential medium
FAE	Follicle associated epithelium
FBS	Foetal bovine serum
GALT	Gut-associated lymphoid tissue
GC	Glycol chitosan
GIT	Gastrointestinal tract
GLA	Gluteraldehyde
GPC	Gel Permeation Chromatography
GSH	Glutathione
HBSS	Hank's balanced salt solution
HCG	Glycol chitosan -5β- cholanic acid conjugate nanoparticles
HGC	Hydrophobically modified glycol chitosan
HPLC	High performance liquid chromatography
HTCC	N-(2-hydroxyl) propyl-3-trimethyl ammonium chitosan chloride
IL	Insulin loaded
IL-6	Interleukin-6
LA	Linoleic acid
LMWH	Low molecular weight heparin
LPS	Lipopolysacchride
M-cells	Microfold cells
MPS	Mononuclear phagocyte system
MTT	3-4,5 dimethyl thialzol2,5 diphenyl tetrazolium bromide
MW	Molecular weight
NAcHis-GC	N-acetyl histidine-conjugated glycol chitosan
NEAA	Non- essential amino acids
NIL	Non-insulin loaded
NLC	Nanostructured lipid carriers
Pa2.5	Palmitoyl grafted Polyallylamine
Pa2.5R	Rhodamine labelled Palmitoyl grafted Polyallylamine

PAA	Polyacrylic acid
PAEMA	Poly[N-(2-aminoethyl)methacrylamide trifluoro acetate
PAH	Polyallylamine
PAMAM	Poly amidoamine
PBS	Phosphate buffer tablets
PBS	Phosphate buffered saline
PCL-g-PDMAEMA	Polycaprolactone-graft-poly(N,N-dimethylaminoethyl methacrylate)
PDI	Polydispersity index
PECs	Amphiphilic polyelectrolyte complexes (Binary complexes)
PEG	Polyethylene glycol
PEI	Polyethylenimine
P-gp	P- glycoprotein
PLGA	Poly(lactic-co-glycolic acid
PLL	Poly(L-lysine)
PMAP	Poly(methylaminophosphazene) hydrochloride
PMLA	Poly (β-malic) acid
PCL-g-PDMAEMA /DNA/PGA-g-PEG	Poly(e-caprolactone)-graft-poly(N, N dimethylaminoethyl methacrylate-DNA- polyglutamic acid-graft-polyethylene glycol
PPS	Propanesulfonate
PVA	Poly(vinyl alcohol)
QPa2.5	Quaternized polyallylamine
QPa2.5R	Rhodamine labelled Quaternized polyallylamine
RBITC	Rhodamine B isothiocyanate
RCEC	Rabbit conjunctival epithelial cells
RhB	Rhodamine B
RhB-CHNP	Rhodamine B (RhB) labeled chitosan hydrochloride grafted nanoparticles
RhB-CMCNP	Rhodamine B (RhB) labeled carboxymethyl chitosan grafted nanoparticles
ROS	Reactive oxygen specie
RP-HPLC	Reverse phase high performance liquid chromatography
RPM	Revolutions per minute
sCT	Salmon calcitonin
SNOCC	N-sulfonato-N,O-carboxymethylchitosan
sPECs	Standard polyelectrolyte complexes (Binary complexes),
SPHC	Superporous hydrogel composite
SQV	Saquinavir
TEC	Triethyl chitosan
TEER	Transepithelial electrical resistance
TEM	Transmission Electron Microscopy
TJs	Tight junctions
TMB	3, 3´-5, 5´-tetramethylbenzidine
TMC	Trimethyl chitosan
TNFα	Tumor necrotic factor alpha
TPP	Tripolyphosphate
$ZnSO_4$	Zinc sulfate
ZO-1	Zonula occludens
ZP	Zeta potential

ABSTRACT

Introduction

Oral delivery of proteins faces numerous challenges due to their enzymatic susceptibility and instability in the gastrointestinal tract. In recent years, the polyelectrolyte complexes have been explored for their ability to complex protein and protect them against chemical and enzymatic degradation. However, most of the conventional binary polyelectrolyte complexes (PECs) are formed by polycations which are associated with toxicity and non-specific bio-interactions. The aim of this thesis was to prepare a series of ternary polyelectrolyte complexes (APECs) by introduction of a polyanion in the binary complexes to alleviate the aforementioned limitations.

Method

Eight non-insulin loaded ternary complexes (NIL APECs) were spontaneously formed upon mixing a polycation [polyallylamine (PAH), palmitoyl grafted-PAH (Pa2.5), dimethylamino-1-naphthalenesulfonyl grafted-PAH (Da10) or quaternised palmitoyl-PAH (QPa2.5)] with a polyanion [dextran sulphate (DS) or polyacrylic acid (PAA)] at 2:1 ratio, in the presence of $ZnSO_4$ (4µM). A model protein i.e., insulin was added to a polycation, prior to addition of a polyanion and $ZnSO_4$ to form eight insulin loaded (IL) APECs. PECs were used as a control to compare APECs. The complexes were characterised by dynamic light scattering (DLS) and transmission electron microscope (TEM). *In vitro* stability of the complexes was investigated at pH (1.2-7.4), temperature (25˚C, 37˚C and 45˚C) and ionic strength (NaCl-68mM, 103mM and 145mM). Insulin complexation efficiency was assessed by using bovine insulin ELISA assay kit. The *in vitro* cytotoxicity was investigated on CaCo2 and J774 cells by MTT (3-4,5 dimethyl thialzol2,5 diphenyl tetrazolium bromide) assay. All complexes were evaluated for their haemocompatibility by using haemolysis assay, oxidative stress by reactive oxygen species (ROS) assay and immunotoxicity by *in vitro* and *in vivo* cytokine generation assay. The potential of the uptake of complexes across CaCo2 cells was determined by flow cytometry and fluorescent microscopy. The underlying mechanism of transport of complexes was determined by TEER measurement, assessment of FITC-Dextran and insulin transport across CaCo2 cells.

Results

NIL QPa2.5 APECs (except IL QPa2.5-DS) exhibited larger hydrodynamic sizes (228-468nm) than all other APECs, due to the presence of bulky quaternary ammonium moieties. QPa2.5 APECs exhibited lower insulin association efficiency (≤40%) than other APECs (≥55%) due to a competition between the polyanion and insulin for QPa2.5 leading to reduced association of insulin in the complexes. DS based APECs generally offered higher insulin association efficiency (≥75%) than PAA based APECs (≤55%) due to higher molecular weight (6-10kDa) of DS. In comparison to other complexes, Pa2.5 PECs and APECs were more stable at varying temperature, ionic strength and pH due to the presence of long palmitoyl alkyl chain (C_{16}) which reduced the chain flexibility and provided stronger hydrophobic association. The cytotoxicity of polycations on CaCo2 and J774 cells is rated as PAH>Da10=Pa2.5>QPa2.5. The introduction of PAA in Pa2.5 and Da10 brought most significant improvement in IC_{50} i.e., 14 fold and 16 fold respectively on CaCo2 cells; 9.3 fold and 3.73 fold respectively on J774 cells. In comparison to other complexes, Da10 (8mgml^{-1}) induced higher haemolytic activity (~37%) due to a higher hydrophobic load of 10 percent mole grafting of dansyl pendants. The entire range of APECs displayed ≤12% ROS generation by the CaCo2 cells. The degree of *in vitro* TNFα production (QPa2.5≥Da10≥Pa2.5=PAH) and *in vitro* IL-6 generation (QPa2.5≥Pa2.5=PAH≥Da10) by J774 cells established an inverse relationship of cytotoxicity with the cytokine generation. Similar to MTT data, the introduction of PAA in APECs brought more significant reduction in *in vitro* cytokine secretion than DS based APECs. Pa2.5-PAA brought the most significant reduction in both *in vitro* and *in vivo* cytokine generation. All the formulations were able to significantly reduce original TEER, however did not demonstrate appreciable paracellular permeation of a hydrophilic macromolecular tracer of paracellular transport i.e., FITC Dextran. The uptake study revealed internalisation of APECs predominantly by a transcellular route. Transcellular uptake of IL QPa2.5 (≤73%), IL QPa2.5-DS (67%) was higher than their NIL counterparts, whereas the uptake of NIL Pa2.5 (≤89%), NIL Pa2.5-PAA (42%) was higher than their IL counterparts.

Conclusion

In essence, amphiphilic APECs have shown polyanion dependent ability to reduce polycation associated toxicity and they are able to facilitate transcellular uptake of insulin across CaCo2 cells.

Chapter 1

INTRODUCTION

1 INTRODUCTION

Oral delivery of proteins has been attempted for many years to offer a convenient and non-invasive route, however, several challenges still remain before successful oral delivery of proteins can be achieved [1, 2]. Figure 1.1 displays a schematic diagram of the barriers to the absorption of proteins in the gastrointestinal tract (GIT). The oral delivery of proteins is strictly limited due to their chemical and physical instability in the GIT [3, 4]. The proteins require a minimum degree of lipophilicity to partition into the cell membrane [5] but the hydrophilic nature, high molecular weight and tertiary conformation of proteins prevent their passive diffusion across the lipophilic cell membrane [6-8]. On the other hand, the cell-cell tight junctions (TJs) limit their paracellular absorption as only molecules smaller than 200 Da can permeate across the paracellular junctions [5].

The whole length of the small intestine comprises of the dense and well-organized microvilli at the apical surfaces of the enterocytes [7]. The surface of epithelial cells is covered by a thin layer of mucus, made of glycocalyx and glycoproteins, produced by the goblet cells [9]. It acts as a diffusional barrier for large macromolecules and selectively allows the permeation of biomolecules like nutrients, water and small molecules [10]. Electrostatic repulsion between protein drugs and the mucus layer (negatively charged) has been found to prevent the contact of protein drug and the absorptive epithelial cells [7]. Thus, an orally administered protein drug must be able to infiltrate through the mucus layer before reaching the surface of intestinal epithelium. The mucus layer also serves as an enzymatic barrier [9, 11]. The pre-systemic degradation of protein by proteolytic enzymes in the GIT lead to a low bioavailability [12-14]. Therefore, if proteins are to be successfully delivered by the oral route, they must be able to resist chemical and enzymatic degradation in the GIT, and traverse the intestinal epithelium without undergoing extensive metabolism [15].

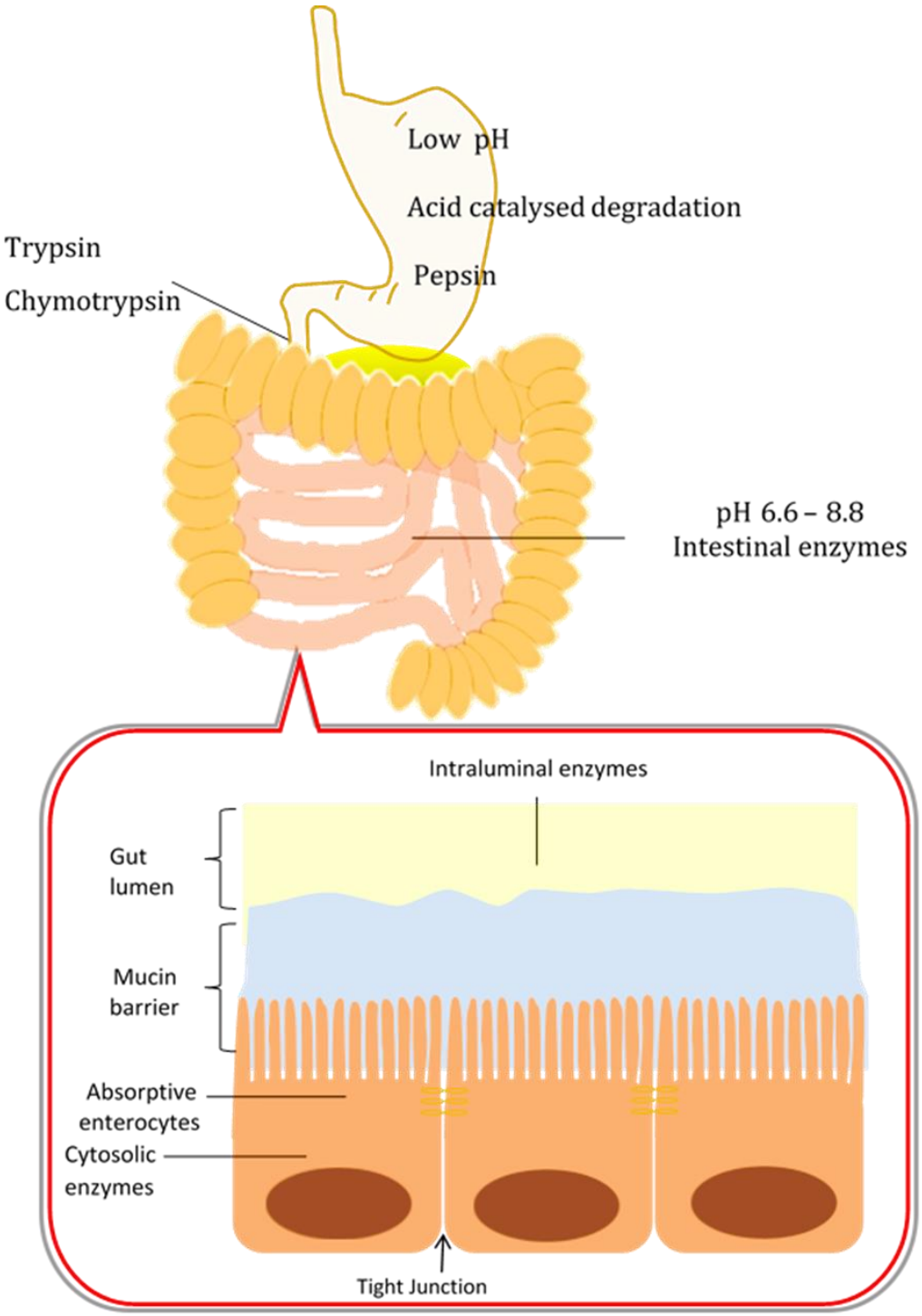

Figure 1.1 Barriers to oral protein delivery

An important obstacle to the absorption of proteins is the extreme pH range in the GIT which can denature the proteins and render them biologically inactive [1]. The gut luminal pH varies from highly acidic in the stomach (pH 1.2-3.0) to weakly acidic to basic in the intestine (small intestine pH 6.5- large intestine 8.0) [8]. The acidic environment in the stomach causes acid catalysed degradation of proteins [4, 16, 17]. Under the influence of pH and the enzymes, the proteins are broken down into their constituent amino acids which do not have actual biological activity like the original proteins [18, 19].

Pepsin is the primary proteolytic enzyme produced in the stomach and has been found to be responsible for approximately 10% to 20% of total protein degradation [20, 21]. Proteolytic enzymes such as proteases and peptidases also play an important role in denaturing the proteins [4, 16, 17]. The intestinal proteases are located in three major sites defined as intraluminal, membrane bound or cytosolic proteases [7, 20]. The membrane-bound and cytosolic proteases are particularly active against di- and tri-peptides and form an important barrier to the absorption of biologically active peptides across the intestinal mucosa [7, 20].

Despite all these challenges to oral protein delivery, a large number of proteins are under clinical investigation and over 30 proteins have been approved by the FDA [19]. Polypeptide drugs such as desmopressin, cyclosporin A [22] Gefitinib [23] Imatinib [24] have all been developed as oral dosage forms. Further efforts are still being made to progress orally administered proteins. A number of different approaches are being used to avoid the barriers to oral protein delivery but each approach has its own advantages and limitations.

1.1 APPROACHES USED TO ENHANCE ORAL PROTEIN DELIVERY

Much attention has been paid to overcome the barriers to oral protein delivery and to maintain the biological activity of proteins in the body [25]. A large number of approaches have been used to promote oral protein delivery, such as the use of enzyme inhibitors, penetration enhancers, mucoadhesive polymers and polymeric nano-drug delivery systems [2, 8]. Despite a great deal of progress being made today, oral protein delivery still presents a significant challenge.

1.1.1 Enzyme inhibitors

Enzyme inhibitors inhibit the proteolytic activity of protein digesting enzymes such as trypsin and chymotrypsin. The co-administration of enzyme inhibitors (protease inhibitors) and protein formulations has been shown to prevent or delay the rate of degradation of protein and thus increase the rate of protein absorption [26]. Proteolytic enzymes require divalent cations such as Ca^{2+} or Zn^{2+} within their active site (as a cofactor) for their functional enzymatic activity [27]. The chelation of these cations by using polyanionic enzyme inhibitors, e.g., carbomers and poly(acrylates) have been shown to circumvent the enzymatic barrier [28, 29]. Carbomers have been shown to facilitate the paracellular transport of the proteins by chelating ions; this has however been shown to cause irreversible damage to the GIT epithelium [28].

Yomamoto *et al.* studied the effect of a number of enzyme inhibitors on protein absorption and found that sodium glycocholate, camostat mesilate, and bacitracin were efficient excipients in reducing insulin degradation in the large intestine, but, not in the small intestine [30]. This was because a considerably higher concentration of enzyme inhibitors was required to maintain their effectiveness in the enzyme rich small intestine which could possibly lead to disturbed digestion of nutritive proteins [14, 31]. It was later found that the co-administration of enzyme inhibitors and mucoadhesives tend to improve the absorption of drugs without requiring high concentrations of enzyme inhibitors [31]. Recently, Su *et al.* used diethylene triamine penta-acetic acid (DTPA), as a protease inhibitor and conjugated it with a mucoadhesive drug-delivery system to form DTPA- poly(γ-glutamic acid)-chitosan nanoparticles. The idea was to concentrate the enzyme inhibitory activity within a localised zone of the intestinal mucosa by using the mucoadhesive properties of chitosan. This system demonstrated a substantial protective effect against the intestinal proteases resulting in enhanced insulin absorption and significant reduction in the blood glucose levels [31]. A similar approach was used

to prepare polymer–inhibitor conjugates carboxymethylcellulose-bowmann-birk and carboxymethylcellulose- ellastinal inhibitor which although demonstrated strong enzyme inhibiting activity towards chymotrypsin and carboxypeptidases, presented systemic intoxications, disturbed digestion of nutritive proteins and hypertrophy as well as hyperplasia of the pancreas [1, 26, 27]. Due to the toxicological concerns associated with enzyme inhibitors, efforts are being directed to improve the absorption of protein drugs by using a number of other different approaches.

1.1.2 Penetration enhancers

Penetration enhancers (PEs) are known to promote the intestinal absorption of poorly permeable therapeutic proteins either by permeabilizing the mucus layer, enhancing transport across the epithelial cell membrane or by opening the TJs [2, 32]. A variety of PEs have been used to enhance the macromolecular permeability across the intestinal epithelium including surfactants, bile salts and fatty acids, chelating agents, salicylates and phosphonate derivatives [2, 33, 34]. However, most of these compounds, if not all, have failed due to the inherent toxicities related to their mechanisms of action. Fatty acids, monoglycerides, bile salt and surfactants have all been shown to increase the permeability of epithelial cells by the partial solubilisation of cell membrane [2, 35]. In this way, they damage the cell membranes leading to local inflammation or may even increase the non-specific absorption of luminal contents and pathogens by solubilising the phospholipids and membrane proteins [35, 36]. These effects have been a major setback in the progress of PE's. However, recently, Chun *et al.* have shown that the addition of bile salts to pravastatin sodium could enhance drug absorption by mechanism other than solubilising behaviour, i.e., through the paracellular route and P-glycoprotein (P-gp) inhibition [34]. Likewise, Gupta and co-workers reported dimethyl palmitoyl ammonio propanesulfonate to be a non-toxic penetration enhancer and a potent alternative for providing enhanced oral uptake of peptides [2]. Such reports suggest that the attempts to enhance oral protein delivery using permeation enhancers are back in favour. In fact, sodium caprate (C10), a potent PE, has reached the clinical trial (phase II) [37, 38]. It was considered to exert its enhancing effect mainly via the paracellular route and by inhibiting the P-gp efflux pumps [39]. Its surfactant-like properties at high doses (100mM) have been shown to increase the bioavailability of associated protein drugs [38, 39]. However, histological examination revealed that the increase in permeability was related in part to superficial epithelial damage [38]. These

findings once again increase the demand for safer alternatives of PE such as cell-penetrating peptides (CPPs).

Over the last few decades, CPPs have become an important class of permeation enhancers because of their remarkable ability to traverse the cell's plasma membrane in a non-toxic and highly efficient manner [40]. The first CPP was discovered while investigating the ability of the human immunodeficiency virus (HIV) transactivation protein (TAT) to penetrate the cells and so named as HIV type 1 (Tat) [41]. Later on a range of different CPPs were discovered such as penetratin transcription factor derived from Antennapedia (pAntp) [42], transportan [43] and polyarginine [44]. A preliminary *in vivo* study using Tat revealed that Beta-galactosidase, a macromolecule, which was previously considered impermeable to cells, was taken up by cells in a cell-type independent manner, when covalently cross-linked to Tat [45]. Soon after this study, it was recognised that CPP have the potential to act as a carrier to achieve successful intracellular delivery of poorly permeable therapeutic macromolecules. It was found that a small amino acid sequence of CPP, approximately 10–30 residues long, mostly positively charged, cargo the peptide and proteins inside the cell. It is now known that Tat are taken up by the cells via an endocytotic pathway by interaction between the positively charged arginine of CPP and the negatively charged proteoglycan on the cell membrane surface [40]. They have also been reported to be internalised by lipid raft-dependent endocytosis involving either macropinocytosis [46], caveolae dependent endocytosis [47] or clathrin dependent endocytosis [48]. They can translocate through the membranes of numerous cells because of their low cell specificity and deliver their cargo into the cytoplasm by directly perturbing the lipid bilayer structure of the cell membrane or by endocytosis [40]. The cytotoxicity analysis demonstrated that antennapedia, TAT, transportan and polyarginine display no significant toxicity even at 100 mM concentrations [40]. However, further efforts are required in this field to explore their potential for clinical use.

1.1.3 Mucoadhesive polymers

Mucoadhesive polymers have evolved as a promising alternative for improving the transport of peptides and proteins. They function by adhering to the mucosal wall by non-specific electrostatic interactions and transiently enhance the mucosal permeability by opening TJs or by permeabilising the mucus lining [49]. The prolonged contact of the delivery system with the mucosa facilitates their transport across the mucous layer

[49, 50]. The mucoadhesive polymers like chitosan, alginate, polyacrylate and cyclodextrins are thought to reach the epithelial cell surface by interpenetrating the mucous layer followed by association with the negatively charged units on the cell membrane via electrostatic interaction.

Colloidal carriers made of chitosan have been widely investigated as carriers for protein delivery [13, 49]. They have favourable biological properties such as biocompatibility and biodegradability [51-53]. Chitosan based systems have demonstrated the facilitation of paracellular transport of large hydrophilic macromolecules by opening the TJs of mucosal membranes [4, 54-56]. This behaviour of chitosan has been attributed to its bio-adhesive property. The positively charged amino groups of chitosan interact with the negatively charged sites on the cell surfaces, thereby transiently open the TJs to facilitate paracellular transport [49].

Recently, Tahtat *et al.* found that association of chitosan with alginate increased the adherence percentage of alginate/chitosan beads to the mucosal surface of the rat intestine to 90%, compared to 35% for pure alginate beads [50]. This behaviour was associated with the interaction of the d-glucosamine residue of chitosan with the sialic acid residues of mucin by electrostatic interaction; thus facilitating more efficient absorption [50].

Despite several advantages, chitosan presents problems such as limited aqueous solubility [57]. A number of chitosan derivatives have been synthesised to improve its properties including trimethylchitosan chloride (TMC) [4, 58], N-(2-hydroxyl) propyl-3-trimethyl ammonium chitosan chloride (HTCC) [51, 59] and thiolated chitosans [60, 61]. TMC has demonstrated higher aqueous solubility than chitosan and carries a permanent positive charge regardless of the pH [57, 58]. Both TMC and HTCC allow mucoadhesion and penetration enhancement across intestinal epithelium [58, 59]. A number of different thiolated polymers (thiomers) such as thiolated chitosan and polyacrylates, have also been used as mucoadhesive polymers for enhancing oral delivery of hydrophilic macromolecular drugs because of their ability to form covalent bonds with the cysteine-rich subdomains of mucus glycoproteins via thiol/disulfide exchange reactions [60, 62, 63]. They act as enzyme inhibitors, permeation enhancers and efflux pump inhibitors as well as being capable of protecting the incorporated peptide and protein drugs against enzymatic degradation in the intestine [64, 65].

However, their stability in solutions is a major concern which may reduce their efficacy [61, 62]. In addition, the drawback associated in using non-specific mucoadhesive systems (first generation) is that adhesion may occur at sites other than those intended. Therefore, current efforts focus on designing specific and targeted mucoadhesion systems within the GIT as well as other polymer based systems which can provide a site specific platform for oral delivery of proteins.

1.1.4 Polymeric nano-drug delivery systems

In recent years, incorporation of proteins into polymeric nano-drug delivery systems has proved to be a very promising approach for their oral delivery [66-68]. Polymeric nanocarriers are submicron-sized (10-1000 nm in diameter) colloidal particles [69, 70]. They are of particular interest, because of their ability to deliver the challenging therapeutic agents, such as proteins [69, 71, 72] and DNA [73, 74]. The most widely used and FDA approved polymers include poly(lactic acid) (PLA), poly(glycolic acid) (PGA) and poly(lactide-co-glycolide) (PLGA) and their co-polymers because of their biocompatibility [69].

A variety of polymeric nano-sized drug carrier systems have been developed e.g., nanospheres [75], nanocapsules [76, 77], polymeric micelles [78] and polymeric polyelectrolyte complexes [54, 79]. The choice of a suitable polymeric system is crucial and it depends on the properties of the polymers such as polymer architecture, surface charge, protein association efficiency and uptake profile [69, 80].

Different types of nanostructures can be obtained from similar polymers, depending on the method of preparation [81]. Chitosan, and its derivatives and polyethylene glycol (PEG) have also been used to fabricate various forms of nanostructures [49, 55, 79, 82]. Some of the commonly used polymeric nano-sized systems are described below.

1.1.4.1 Polymeric nanospheres and nanocapsules

The term nanoparticle collectively refers to the nanospheres and nanocapsules (Figure 1.2) [20]. Nanocapsules are vesicular systems in which the solubilized or solid drug is confined to an aqueous or oily core surrounded by a unique polymer membrane [81, 83, 84]. The oily core allows entrapment of a lipid-soluble drug, whereas, an aqueous core enables encapsulation of water-soluble drugs [85-87]. Nanospheres are solid matrix type structures in which the drug is homogeneously dispersed in the bulk

matrix or confined to the particle surface [20, 81, 87-89]. In general, nanocapsules are spherical in shape but nanospheres may have other shapes [85].

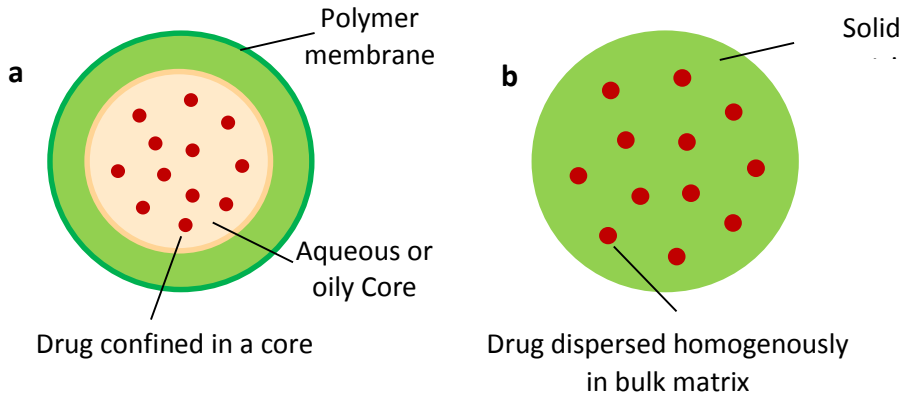

Figure 1.2 Schematic representation of (a) Nanocapsule (b) Nanosphere

Nanoparticles have been prepared by a number of different techniques, predominantly via emulsion based techniques such as emulsion solvent evaporation, and emulsion solvent diffusion techniques [69]. These techniques commonly involve the use of organic solvents, toxic chlorinated compounds, heat and vigorous agitation that may potentially be harmful to the associated proteins and peptides [53, 69]. Many of these methods can easily disrupt the delicate protein structure rendering the protein inactive. In addition, many of the nanoparticle preparation methods require a surfactant to stabilize the dispersed phase in an emulsion based technique. Some of the nanoparticles have shown limitations in terms of their biodegradability, toxicity and biocompatibility. In addition, the majority of nanoparticles have experienced rapid clearance from the systemic circulation, and have ended up almost exclusively in the mononuclear phagocyte system (MPS). In order to avoid these problems, techniques have been designed to manipulate the surface of nanoparticles to achieve the desired properties [90, 91]. PEG is a hydrophilic flexible, non-ionic and biodegradable polymer [59]. Surface modification of polymers with PEG allow an increase in the circulation time and also provides thermodynamic stability to the particles [92]. It also tends to avoid or reduce the interactions of nanoparticles with the blood proteins [93]. These properties have been utilised by several researchers. Zhu and colleagues prepared PEG grafted chitosan-N-trimethylaminoethylmethacrylate chloride (CS-TM–PEG) copolymers not only to improve the solubility of chitosan in a physiological environment but also to enhance biocompatibility and reduce their interaction with blood cells and proteins [92] PEGylated nanosystems have also demonstrated the

ability to adhere to the mucosa. Recently, PEG modified starch acetate nanoparticles were prepared by Minimol *et al.* for controlled delivery of insulin. These nanoparticles were non-cytotoxic and demonstrated greater bioadhesiveness than chitosan [90].

Nanoparticles have demonstrated high protein loading efficiency, protection of protein degradation in GIT and ability to facilitate protein uptake [94]. Pan *et al.* prepared insulin-loaded chitosan nanoparticles which demonstrated high protein loading and biocompatibility [49]. Recently, Shu *et al*. prepared glutathion responsive polyelectrolyte nanocapsules composed of cysteamine conjugated chitosan (CS-SH) and dextran sulfate (DS), which protected protein drugs from destruction by gastric acid and allowed release of the protein inside the cells [95]. The drug was released intracellularly under the effect of intracellular glutathion secretion [95]. Polymeric nanoparticles, e.g. amine-modified graft polyesters, chitosan nanoparticles [96] or thiolated trimethylchitosan nanoparticles [97] have all been shown to increase the bioavailability of insulin. All these reports indicate the potential of nanoparticles to achieve oral protein delivery, however, the methods of fabrication of nanoparticles are very complex and use expensive reagent [20]. This is the reason that suitable large-scale production is essentially restricted [98]. This leads to the consideration of designing polymeric systems with simple techniques which do not require toxic chemicals, heat or vigorous agitation.

1.1.4.2 Polymeric micelles

Polymeric micelles gained a lot of interest in recent years due to their simple and versatile fabrication process. They are formed spontaneously by the self-assembly of amphiphiles in an aqueous medium, generally as a result of hydrophobic or ion pair interactions between polymer segments [99]. The hydrophobic groups on the polymeric chains are directed towards the internal zone of the particle while the hydrophilic groups such as poly(ethylene glycol) and poly(ethylene oxide) are directed towards the solvent (Figure 1.3) [100, 101]. This behaviour reduces the contact of the hydrocarbon chain with water and acts as a driving force for micelle formation (or micellization) [100, 102]. The hydrophobic inner core is capable of protecting the drug from the aqueous environment and against premature enzymatic degradation, whereas the hydrophilic portion provides stability by forming a tight shell around the micellar core by forming hydrogen bonds with the surroundings water molecules [103-105].

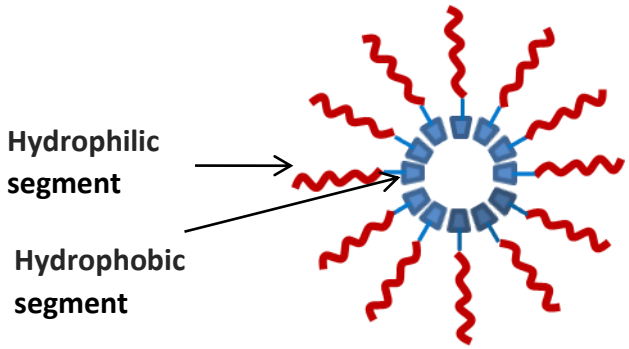

Figure 1.3 Schematic representation of a micelle

In comparison to nanoparticles which display a static and stable structure, polymeric micelles form dynamic structures which are formed by diverse molecular architecture such as block copolymer and graft copolymer [15]. Aliabadi and coworkers prepared methoxy poly(ethylene oxide)-b-poly(ε-caprolactone) (PEO-b-PCL) micelles as alternative vehicles for the solubilization and delivery of CsA [106]. Although, these micelles demonstrated higher CsA to vehicle loading, and superior controlled drug delivery properties, they required organic solvents, low temperatures and sophisticated methods for their fabrication.

The advanced drug delivery approaches allow spontaneous self-assembly of micelles and simple fabrication process which are viewed as major advantages compared to solid nanoparticle [15]. Other key advantages of polymeric micelles is their thermodynamic stability in physiological solution, low cytotoxicity and high entrapment efficiency [98, 107]. However, this makes them more suitable for intravenous administration and is the reason why most micelle based formulations are administered intravenously [98, 107]. Nevertheless, numerous research groups have now focused on oral administration of micelles [107, 108]. In this context, Li and coworkers fabricated polyanionic copolymer mPEG grafted-alginic acid (mPEG-g-AA)-based polyion complex (PIC) micelles which demonstrated enhanced oral absorption of salmon calcitonin (sCT) [107]. These micelles were found to be internalised by Caco-2 cells predominantly via endocytosis [107].

The hydrophobic character of the core of a micelle enables efficient entrapment of hydrophobic drugs, however, it is difficult to entrap hydrophilic drugs such as protein [81], and thus the use of polymeric micelles for protein delivery has been limited [15,

109]. However, Lee *et al.* recently successfully developed protein loaded polyionic complex (PIC) micelles which contained a block copolymer with poly(ethylene glycol) (PEG) as a neutral block and a poly(amino acid) as an ionic block. These micellar systems demonstrated high stability, reduced immune response, and prolonged circulation time [108]. More recently, glucose-responsive complex micelles i.e., phenylboronic acid-contained block copolymer PEG-b-P(AA-co-APBA) and a glycopolymer P(AA-co-AGA) [110] and monomethoxy poly(ethylene glycol)-b-poly(L-glutamic acid-co-N-3-L-glutamylamidophenylboronic acid) [111] have been prepared for protein delivery and have demonstrated higher glucose-responsiveness and glucose triggered insulin release. The self-assembling character of amphiphiles have also been utilised for the fabrication of polyelectrolyte complexes by ion pair interactions. It is considered that this system will associate with a protein drug to form complexes for oral delivery.

1.1.4.3 Polyelectrolyte complexes

Polyelectrolyte complexes are an important class of nanocarriers which have shown tremendous potential for protein delivery in the past few decades [68, 112]. Polyelectrolytes are polymers containing ionisable groups [113]. In a suitable polar solvent (generally water), the ionisable groups acquire charge by releasing low molecular weight ionic moieties called counter-ions [79, 114]. The charged polymeric chains tend to remain expanded in the solution due to electrostatic repulsion between the like charges on the polymeric chains. This effect prevents the polymeric chains from coming closer and forming agglomerates [115, 116]. However, any condition causing neutralisation of the surface charges (e.g., salt) leads to coiling of the polymer chains around itself leading to aggregation [117]. Many important biological macromolecules are polyelectrolyte in nature e.g., DNA and RNA. A large number of naturally occurring and synthetic polyelectrolytes have been used in biopharmaceutics for drug and protein delivery purposes. Some of the commonly used polyelectrolytes include chitosan, polyacrylates, poly (lactide-co-glycolide) (PLGA), polyethylenimine (PEI), poly (L-lysine) (PLL), chondroitin sulfate and alginate.

The ability of polyelectrolytes to form complexes with oppositely charged polymers or protein provides prospects for the oral delivery of protein. The charged polymeric chains interact with the oppositely charged polymers or proteins to form polymer-

polymer, polymer-protein and polymer-protein-polymer complexes, predominantly via electrostatic interactions. The polyelectrolyte complexes formed between amphiphilic polymers and proteins may provide an additional contribution of hydrophobic association resulting in higher stability and protein association efficiency.

1.1.4.3.1 Types of polyelectrolyte complexes

There are three main types polyelectrolyte complexes employed in the protein delivery systems, namely the standard polyelectrolyte complexes (sPECs - binary complexes), amphiphilic polyelectrolyte complexes (PECs - binary complexes), and polycation-polyanion-protein polyelectrolyte complexes (ternary complexes) which can be formed in the absence (aPECs) or presence (APECs) of a cross-linker (Figure 1.4). sPECs are formed by the association of oppositely charged polymer and protein whereas, PECs are formed by the association of an amphiphilic polymer and a protein. A number PECs have been developed for the oral protein delivery [118, 119]. Recently, Thompson *et al*. demonstrated the potential of using novel comb shaped PECs for the oral delivery of protein [120]. These PECs demonstrated the ability to prevent enzymatic degradation, exhibited paracellular absorption, and high complexation efficiency. The amphiphilic quaternary ammonium palmitoyl polyallylamine (QPa) demonstrated the ability to produce nanocomplexes with cationic peptides (i.e., sCT) [118], as well as anionic peptides (i.e., insulin) [121], due to contribution of both electrostatic and hydrophobic associations in their formation. This shows the ability of PECs to deliver both the cationic and anionic proteins using this system [118, 121].

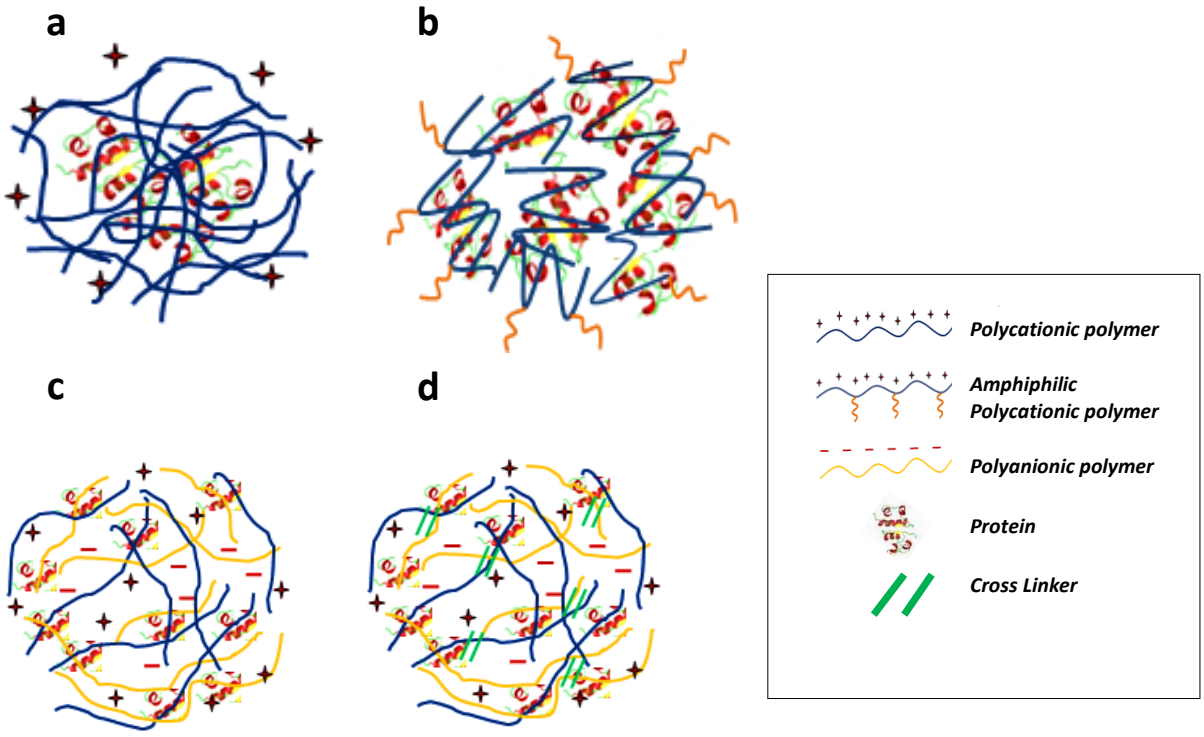

Figure 1.4 Types of polyelectrolyte complexes (a) Standard complexes – sPECs (b) Amphiphilic complexes - PECs (c) Polycationic-Polyanionic protein complexes - aPECs (d) Polycationic-polyanionic protein complexes stabilised by cross-linker - APECs

APECs are formed by the complexation of a polycation with a polyanion and a protein. They can be formed in the presence or absence of cross-linkers such as zinc sulphate ($ZnSO_4$) [122], tripolyphosphate (TPP) [123, 124] which facilitate their formation. The cross-linkers are low molecular weight ions which are considered to bridge the polymeric chains [125]. Divalent and multivalent ions reinforce the polymeric chains and thus induce the formation of ionically cross-linked systems [125]. They can facilitate the formation of stable and homogenous colloidal dispersions. Previously, Jintapattanakit *et al.* demonstrated the use of TPP counter ion to cross link trimethyl chitosan (TMC) as a carrier for insulin [4]. This system produced stable, uniform and nanosized trimethyl chitosan (TMC) and polyethylene glycol graft-TMC copolymer complexes. They demonstrated that increasing cross-linker concentration resulted in increased particle sizes, association efficiency, process yield and decreased zeta potential (ZP) and polydispersity index (PDI) of PECs [124]. These complexes prevented insulin degradation at 50˚C and displayed an inhibitory effect towards trypsin [4].

APECs allow formation of fine-tuned complexes whereby desirable size and charge can be obtained by changing the ratio of polycation: polyanion: cross-linker. Recently, Zheng and colleagues prepared chitosan-polyaspartic acid PECs of efficient drug delivery properties by using gluteraldehyde (GLA) as a cross linker. Their study showed that the mean size of PECs could be adjusted by changing GLA concentration [113].

APECs have been shown to significantly lower the toxicity associated with polycations in the binary systems. Tiyaboonchai and colleagues prepared polyethylenimine-dextran sulphate- DNA PECs, stabilised by $ZnSO_4$ through ionic interaction. Interestingly, these PECs possessed efficient transfection efficiency of DNA and a 10 fold reduction in toxicity in the presence of dextran sulphate (DS) [73].

Moreover, polyelectrolyte complexes have demonstrated significant absorption across *in vitro* and *in vivo* models and increased bioavailability of proteins. Sarmento and colleagues prepared alginate-chitosan (Alg-CS) by using calcium chloride as a cross-linker. An *in vivo* study in streptozotocin induced diabetic rats showed that oral application of these Alg-CS insulin PECs was able to reduce basal serum glucose level up to 40% for over 18h [126]. All these findings show that polyelectrolyte complexes, as a nano-drug carrier system, hold tremendous promise for the oral delivery of the therapeutic proteins. However, there are numerous factors which influence the stability of these colloidal systems, therefore, it is very important to understand the underpinning concepts of the formation and stability of PECs to produce stable colloidal dispersions.

1.1.4.3.2 Factors influencing the stability of colloidal dispersions

There are a variety of factors which govern the formation and stability of PECs [4, 79]. The charge density of the complexes has been identified as one major factor which accounts for the stability of the complexes [79]. The magnitude of the charge density of the polymers determines the degree of electrostatic interaction between the oppositely charged polymers and proteins which in turn is responsible for maintaining the complex stability [115]. The high positive charge allows the attachment of complexes to the anionic cell membrane and increases the residence time in the GIT and subsequently enhances the bioavailability. However, the excess cationic charge has been shown to cause high toxicity and *in vivo* instability, due to non-specific interactions and protein adsorption [127, 128]. Efforts have been made to reduce the

cytotoxicity and improve the stability of the delivery system either by surface modification of the polymer with safer hydrophobic moieties such as palmitoyl graft [129], hydrophilic moieties such as PEG and quaternary ammonium moieties [129, 130] or by introduction of a polyanion [131] in the complex to reduce the charge density. It has been found that attaching a hydrophilic non-ionic block or side chain e.g., poly(ethylene oxide) (PEO) to the polyelectrolyte can improve stability of the system [132]. Wang *et al.* reported that the hydrophobic (linoleic acid-LA) and hydrophilic (poly (β-malic) acid-PMLA) modification of chitosan contributed to suppress non-specific adsorption. In addition, hydrophobic LA grafting also promoted resistance against enzymatic degradation and cellular uptake through the clathrin-mediated pathway while hydrophilic PMLA substitution inhibited these effects [130].

The ratio of polymer and protein and the nature of the ionic group have a significant impact on both the degree of interaction and the physical properties of polyelectrolyte complexes [71, 79]. The non-stoichiometric ratios of polymers form soluble complexes [133-135], whereas, polymers with 1:1 stoichiometry form insoluble and electroneutral complexes which tend to destabilize and flocculate [134]. The insoluble stoichiometric PECs are ideal materials for several large-scale industrial applications e.g. as membrane materials, coatings, binders, and flocculants, but, remain poorly investigated for drug delivery applications due to their electro-neutral behaviour [135]. Recently, ternary insoluble stoichiometric interpolyelectrolyte complexes of insulin with biodegradable synthetic polymers, poly(methylaminophosphazene) hydrochloride (PMAP) and dextran sulfate (DS) (Insulin-PMAP-DS) were prepared by Burova and co-workers under conditions imitating the human gastric environment (pH 2, 0.15 M NaCl). The findings showed complete immobilization of insulin in the complexes. These ternary complexes dissolved and dissociated under conditions imitating the human intestinal environment (pH 8.3, 0.15 M NaCl) liberating free insulin and soluble binary Insulin-PMAP complexes. The results showed an almost 100% protection of insulin against proteolytic degradation [136]. These findings establish the potential of ternary insoluble stoichiometric complexes in oral protein delivery.

Nonstoichiometric complexes are ideal for pharmaceutical applications. They have been prepared by numerous groups including chitosan-dextran sulfate CS-DS complexes [137], PEG graft trimethyl chitosan copolymer- insulin complexes [67], CS-DS-amphotericin B complexes [55], PEI-DS-insulin [122], polysodium styrenesulfonate - nonionic poly(ethylene oxide) ether methacrylate complexes [135].

Several research groups have demonstrated that the mixing order and mixing ratio also play an important role in the formation and stability of polyelectrolyte complexes [138]. Muller *et al.* prepared polyelectrolyte complexes between poly(ethyleneimine) (PEI) and poly(acrylic acid) (PAA) and showed that the size and internal structure of PEI/PAA particles could be regulated by parameters such as mixing order and mixing ratio [139]. All these properties reflect the numerous advantages of polyelectrolyte complexes as a protein delivery.

1.1.4.3.3 Advantages of polyelectrolyte complexes

Polyelectrolyte complexes are of particular interest due to their attractive advantages and numerous applications in the biomedical field. They are an inexpensive, biocompatible and versatile substitute to the current polymeric delivery strategies [115]. Firstly, the process of fabrication of polyelectrolyte complexes is very simple and mild [79]. Moreover, polyelectrolyte complexes are formed spontaneously in solvents such as water and do not require high heat, toxic chlorinated compounds or organic solvents for their preparation, thereby reducing the possible toxicity and other undesirable effects of the reagents [115, 140]. Polyelectrolyte complexes are formed via electrostatic interactions which not only allow easy complexation but also avoid the use of chemical modification of the polymer and protein by covalent interactions [140]. Some of the polyelectrolyte complexes, if not all, act to protect proteins from proteolysis in the GIT, resulting in a prolonged retention of the protein activity [72, 84, 141, 142]. The novel comb-shaped amphiphilic polyelectrolytes (QPa) prepared for the oral delivery of insulin [121, 129] and sCT [118] have been reported for their ability to protect insulin and sCT from the *in vitro* gastrointestinal enzymatic degradation by pepsin, trypsin, elastase, or chymotrypsin. Despite the many advantages of polyelectrolyte complexes, their interaction with cells such as nanotoxicity and mechanism of uptake has not been widely explored.

1.2 NANOTOXICOLOGY AND *IN VITRO* TESTING

Nanotoxicology is a modern branch of toxicology which has revolutionised the evaluation of nanocarrier toxicity in the recent years [143]. It essentially identifies the adverse nano-bio interactions. It provides better understanding on, how different nanomaterial properties affect their biological response. Nanostructures may be efficient as drug delivery systems; however, there is an increasing concern about their potential toxicity which may arise following their *in vivo* administration. So far, most of the nanotoxicological studies have been conducted on inorganic nanoparticle such as iron oxide, ZnO, CuO, MgO and TiO_2 [144, 145] and carbon nanostructures [146-148]. However, currently, there has been limited research done on the evaluation of nanotoxicity of polymeric nanostructures which may delay their progress to clinics (Duncan & Gaspar, 2011). This knowledge is crucial to understand the biocompatibility of polymeric nanostructures and their interaction with the cells. Therefore, a comprehensive nanotoxicological characterisation of nanocarriers is required for every study [15].

1.2.1 Challenges to the polymer based nano-structures

Generally, the success of polymeric nano-structures strongly relates to their pharmacological and toxicological properties [149]. However, the properties which favour drug delivery may result in undesirable toxic effects. The cationic charge of the polycationic systems is one good example of a property which although favours drug delivery, is associated with toxicity. The positive charge on the nanocarriers has been found to be essential for their initial contact with the negatively charged cell membrane and consequently for the cellular uptake [150]. A large number of polycationic polymers such as PEI, PLL and polyallylamine (PAH) have been implicated in the charge dependent toxicity [143, 151, 152]. These polycations possess primary amino groups on their backbone which have been found to be the primary origin of their toxicity [153]. However, it has been shown that modification of primary amines by groups such as PEG or imidazoyl grafting is able to decrease the charge density on the polymer backbone and hence decreases the toxicity associated with the polycation [152]. Similarly, glycolation of PAH [154] and PEI [155] have been shown to decrease the positive charge and hence the polycation associated cytotoxicity.

High molecular weight polymers have been implicated in inducing a greater degree of toxicity than low molecular weight polymers [156]. Fischer and co-worker have

shown that low molecular weight PEI displays significantly less cytotoxicity than high molecular weight counterparts [156, 157]. Mao *et al.* has also shown that the cytotoxicity of TMC increased with the increasing MW such that 5kDa TMC chitosan was completely non-toxic compared to 400kDa which exhibited an IC_{50} of 15µgmL^{-1} [67].

Polymer based nano-structures are formed from a diverse polymer architecture, for example amphiphilic polymers form polymeric micelles while dendrimers are globular three dimensional structures. Therefore, the adverse effects of nanostructures may arise from a combination of factors such as nano-structure chemistry, size, shape and electromagnetic properties [158]. The high surface area to volume ratio of nanostructures can lead to increased chemical reactivity and biological activity [150]. The increased chemical reactivity results in production of reactive oxygen species (ROS), including free radicals which is one of the primary mechanisms of nano-carrier toxicity and the cause of most of the pro-inflammatory effects. *In vitro* and *in vivo* studies using nanostructures of different composition and particle sizes have shown cell and tissue damage due to ROS production as a major contributory factor in the inflammation and toxicity. ROS production has been found in a diverse range of nanostructures including carbon fullerenes, carbon nanotubes and nanoparticle metal oxides [159]. However, this behaviour is not well explored for polymeric nanostructures.

The intrinsic surface properties of nano-structures e.g., hydrophobicity and hydrophilicity also play an important role in causing toxicity. The exposure of nanocarriers to the blood may cause them to be adsorbed onto the surface of erythrocytes which may lead to the failure of cellular regulatory mechanisms or even haemolysis of cells. On the other hand, nanocarriers can also activate inflammatory and immunological responses and may affect both local and distant tissues and organ function.

As a result of polymer heterogeneity, nanostructures might interact with the cells in a large number of ways. In order to advance the polymer based nanostructures to clinical use, it is important to select a range of appropriate *in vitro* tests to understand the molecular events leading to toxic events.

1.2.2 Challenges to *in vitro* toxicity testing for polymer based nanostructures

Cell based *in vitro* models can play an important role in analysing the toxic effects of nanomedicines. The challenges to the *in vitro* toxicity testing of polymer based nano-structures extend from selecting appropriate cell lines to using more relevant, robust and validated *in vitro* methodologies which cover aspects such as route of administration, time and dose related toxicities. The literature is rich with an impressive array of *in vitro* assays (Table 1.1). The most commonly used assays include cell viability assays, particularly 3-4,5 dimethyl thialzol2,5 diphenyl tetrazolium bromide (MTT), 3-(4,5-dimethylthiazol-2-yl)-5-(3-carboxymethoxyphenyl)-2-(4-sulfophenyl)-2H-tetrazolium) (MTS), (2,3-bis(2-methoxy-4-nitro-5-sulfophenyl)-5-[(phenylamino)carbonyl]-2H-tetrazolium hydroxide) (XTT) [160, 161], lactate dehydrogenase assay (LDH), adenosine triphosphate (ATP), trypan blue [144, 160] and neutral red uptake assay (Hillegass et al., 2010). Other less commonly employed assays include haemocompatibility, immunogenicity and cellular uptake studies (Table 1.1 and 1.2) [162]. There are techniques to measure other endpoints such as inflammatory potential, genotoxicity and carcinogenicity but these are least employed because of their complexity and difficulty in interpretation [162]. These and several other techniques are in general consideration by the regulatory authorities and may add to the mechanistic understanding of the underlying toxicity of nano-structures [51].

Before performing *in vitro* testing, a number of questions should be considered, for example, 1) do the polymeric nanostructures alter cellular metabolism and specialized cell functions?; 2) how are they taken up by the cells and do they reside in the cells?; 3) do they mediate effects like inflammation, immunostimulation and immunosuppression? [163]; 4) do they have tendency to damage DNA and other cellular organelles? ; 5) How are they metabolised and eliminated from the body?; 6) how sensitive and specific are the toxicological data? [164, 165]. Due to the biological complexity, toxicity may be generated as a result of a number of mechanisms. Therefore, there is a need to employ a range of different *in vitro* tests to cover all related endpoints. It is essential to prioritise and standardise *in vitro* testing depending on which endpoint correlates well with the route of administration and physical and chemical properties of the formulation. The notion is to achieve a standard battery of assays to evaluate the safety of polymeric nanostructures for a better clinical correlation.

Table 1.1 Summary of *In Vitro* assay systems used in the assessment of nanotoxicity

		Assay	Principle	Detection	Detection Method
Basal Toxicity	**Cell Viability Assays**	Tetrazolium based assay MTT, XTT, WST-1	Metabolic activity	Formazan product	Spectrophotometry
		LDH	Membrane integrity	LDH release	Spectrophotometry
		Trypan Blue	Membrane integrity	Uptake of dye by dead cells	Counting of unstained viable cells
		Propidium Iodide	Membrane integrity	Stain the nucleus of dead cells	Fluorometry
		Annexin-V	Translocation of Phosphatidyleserine to outer surface of cell	Apoptosis	Fluorometry
		ATP	ATP generation by live cells	ATP content	Luminometry
Specialized Toxicity	**Oxidative Stress**	ROS assay	Measurement of ROS	ROS	Fluorometry / luminometry
		Lipid Peroxidation	Oxidative degradation of membrane lipids	Cell membrane damage	Fluorometry
	Immuno-toxicity	Cytokine Production	ELISA	Cytokines protein content	Spectrophotometry
	Genotoxicity	Micronucleus assays	Cellular imaging	Chromosomal and genomic mutation	Fluorometry
		Alkaline comet Assay	Single cell gel electrophoresis	Chromosomal and DNA damage	Fluorometry

1.2.2.1 Types of in vitro toxicity testing

1.2.2.1.1 Basal cytotoxicity

Basal cytotoxicity assays are usually performed as initial assessments to determine general toxicity (Table 1.1) [160, 166]. The end point employed is usually IC_{50} (inhibitory concentration 50%), i.e., the concentration required to kill 50% of the cell population [167]. Once the IC_{50} or no observable effect level (NOEL) and sub lethal concentrations have been established, more relevant mechanistic endpoints can be determined by specialised toxicity assays (Table 1.1). However, this should proceed only if suitable *in vitro* results are achieved. In order to validate the findings, experiments should be performed on more than one cell line and at several different time points [160].

1.2.2.1.2 Specialised toxicity

The specialised toxicity assays determine cell-selective mechanistic toxicity capacity and specialized end-points like alteration in cellular metabolism, specific cellular functions and signalling pathways (Table 1.1) [160, 166]. The polymeric nanostructures can elicit an immune response which triggers the release of various cytokines or chemokines and may initiate a cascade of biochemical reactions. They may induce oxidative potential by the release of ROS which can further lead to altered metabolic and regulatory processes of cells, DNA damage, altered signalling pathway or gene expression [168]. Therefore, specialised *in vitro* assays can add to the understanding of the underpinning mechanism at the molecular and cellular level. They can expand our understanding related to the safety, biological activity and interaction of polymeric nanostructures in the body. The type of assay and endpoint to be employed can be improvised depending on the route of administration, type of cell line and special cellular functions [160].

1.3 UPTAKE AND TRANSPORT

The elucidation of uptake and intracellular trafficking of the polymer based nano-structures is commonly performed to determine their efficacy as targeted delivery systems. However, the uptake and trafficking may cause nanocarrier-cell interaction which can potentially lead to unwanted effects. The concentration, size and surface charge of the polymer based nano-structures can affect cellular uptake as well as potentially lead to undesirable uptake [165]. Uptake studies are mainly conducted on

cell culture models such as CaCo2, MDCK, LLC-PK1, 2/4/A1, TC-7, HT-29, IEC-18 [169, 170]. Quantification and visualisation of nanostructures at a cellular and subcellular level enable the understanding of transport and localisation of nanocarriers within the cell and cellular organelles. A number of valuable tools are used to determine the mechanism and rate of uptake of nanostructures e.g. confocal laser scanning microscope and transmission electron microscope (TEM) (Table 1.2) [166, 171]. Particle quantification can also be carried out via fluorescently labelled nanostructures using a flow cytometry [141, 166].

Table 1.2 Summary of techniques used to assess the *in vitro* uptake and transport of formulations across cells

		Assay	Principle	Detection	Detection Method
Uptake & transport studies	**Transport Studies**	Cell based Transport Model	Apical – to – basal bidirectional transport	Permeability	Two – chamber system, TEER, Fluorometry
	Non invasive study	Confocal Microscopy	Visualisation	Detection and localisation	Microscopy, Fluorometry
		Transmission electron microscopy	Visualisation	Detection and localisation	Microscopy
		Fluorescence activated cell sorting	Flow cytometry	Uptake and quantification	Fluorometry

The transport of substances across the intestinal epithelia occurs via different routes namely paracellular, passive transcellular, carrier/receptor mediated transcytosis and via M cells in Payer's Patches, as briefly described below [96, 172, 173]. Figure 1.5 displays the various modes of uptake of biomolecules by the cells.

1.3.1 Paracellular Transport:

Paracellular transport is the passive movement of solute between the adjacent cells across the intestinal epithelial barrier. Intestinal epithelial cells lie very close to each other such that they form TJs between the cells [174]. The TJs are dynamic structures formed by a collection of macromolecular proteins confined to the apical region of epithelial cells termed as zonula occludens [175]. It has been found that the TJs are built from almost 40 different proteins, including claudin, occludin and zonula occludens-1 (ZO-1) [27, 174].

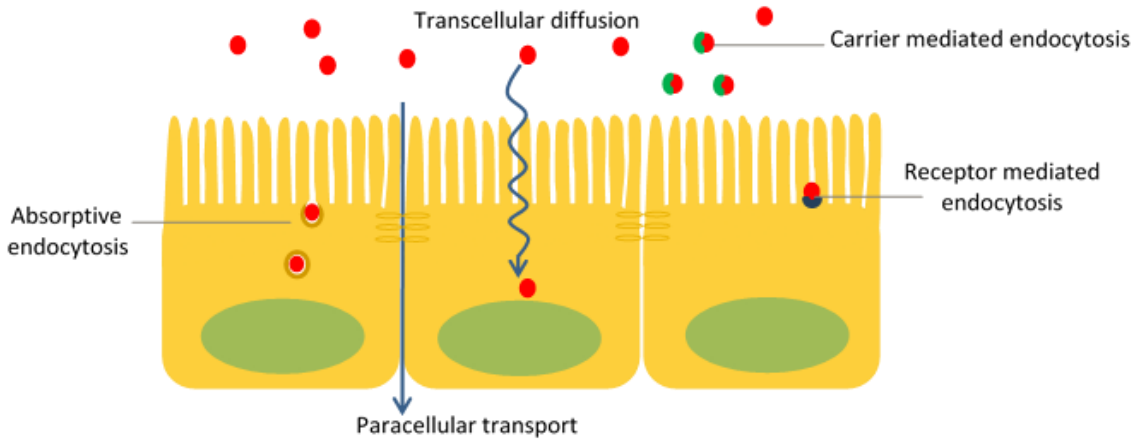

Figure 1.5 Mechanism of uptake of biomolecules by intestinal enterocytes

Claudins are considered as the primary tight junction-forming proteins which have pore-like properties [176]. They act as intercellular adhesion molecules and form a paracellular seal [174]. The claudin based pores of 4 Aº radius are most often quantified by transepithelial electrical resistance (TEER). The resistance varies along the scale from tight to leaky epithelia [174, 176]. Immunohistological studies confirm that claudins form a distinct intact ring/pore around the periphery of individual cells [177]. Studies have shown alteration in the staining pattern of the ring following incubation with various polycations. Martien and co-workers have shown reduction in claudin staining around the apical part of the cell following treatment with thiolated chitosan nanoparticle suspension for 4 h. The discontinuous staining in some areas along with the presence of intracellular staining implied disruption of cell–cell contacts and

removal of claudin into vesicles inside the cell [177]. However, after removal of the nanoparticle suspension, the intact staining around the cell periphery was observed again indicating re-establishment of the cell integrity [177]. Similar finding have been reported by Yeh *et al.* who reported the redistribution of the TJ protein claudin 4 (CLDN4). The normal continuous ring appearance of claudins between adjacent cells was disrupted and fluorescence signal of CLDN4 became weaker after treatment with chitosan [178].

ZO-1 are cytosolic proteins which interact with each other, and serve as a platform to link the TJs to the cytoskeleton. ZO-1 interacts with multiple other TJ regulatory proteins to organize them to control TJs function. It is thought to be a linkage molecule between occludins and actin cytoskeleton [179, 180]. It has been shown to control the paracellular permeability by connecting to the perijunctional actin and myosin [180]. The subcellular localisation of ZO-1 has been investigated by numerous research groups [181-185]. A number of researches have indicated the role of translocation of ZO-1 in altering the paracellular permeability. Smith *et al.* reported that chitosan mediates TJs disruption by translocation of TJ proteins from the membrane to the cytoskeleton [182]. They observed that chitosan causes a dose-dependent reduction in TEER of up to 83% of CaCo2 monolayers and a corresponding increase in horseradish peroxidase permeability across the monolayer which was found to be 18 times greater than the control. The ZO-1 protein appears as a continuous ring between the adjacent cells before incubation with nanocarriers [186]. Immunofluorescent localisation of ZO-1 elucidated the loss of membrane-associated ZO-1 from discrete areas. Analysis of cellular fractions showed a dose-dependent loss of ZO-1 and occludin from the cytosolic and membrane fractions into the cytoskeletal fraction [182].

A similar study done by Ranaldi *et al.* compared the effects of chitosan and other polycations (polyethylenimine, poly-L-lysines) on the TJ [183]. Their results showed that all polycations investigated were able to induce a reversible increase in the TJ permeability. This effect was associated with morphological changes in the F-actin cytoskeleton, and the localization of tight junctional proteins [183]. Vllasaliu and co-workers studied the effect of chitosan nanoparticles on the distribution of ZO-1. They found that the chitosan nanoparticles produce a sharp and reversible decrease in TEER and increased the permeability of two FITC-dextrans (FDs), FD4 (MW 4 kDa) and

FD10 (MW 10 kDa). In addition, chitosan nanoparticles produced changes in ZO-1 distribution indicating a TJs effect, however, no improvement in permeability of chitosan nanoparticles was observed [184]. Lin *et al.* reported similar findings according to which the incubation of cells with the CS-coated poly-γ -glutamic acid nanoparticles caused a discontinous staining pattern of ZO-1 proteins with a corresponding reduction in the TEER values indicating the opening of TJs [179].

There have been studies which have reported contradictory findings. One good example is of the study done by Rosenthal and co-worker which elucidated that chitosan affects both, the paracellular and the transcellular resistance. However, no effects on expression and subcellular distribution of TJ proteins or the actin cytoskeleton were observed. They indicated that the reversible absorption-enhancing chitosan effect is actually due to the changes in intracellular pH caused by the activation of a chloride-bicarbonate exchanger [181]. There have been reports which indicate the relation of other factors in the permeation enhancement properties of polymers. Li and co-workers related the permeation enhancement property of carbopol polymers to the chelation of extracellular or tight-junctional Ca^{2+} by charged polymer's carboxylate groups. Depletion of extracellular Ca^{2+} results in opening of epithelial TJs, thereby facilitating paracellular transport [187].

A plethora of reports on similar polymers state differences in their mechanism of uptake. These differences might mean that the uptake of these polymers is occurring by a combination of different pathways. It is also possible that these polymers were able to open the TJs with or without causing a substantial transport of nanocarriers. This means that even if polymers are able to open up the TJs, it is difficult to explain the paracellular uptake of particles >50 nm by a widening of the intercellular spaces. These effect have been reported by Ma and co-workers where the paracellular pathway was not adequately widened to allow the passage of a substantial amount of insulin molecules across the cell monolayer [188]. These findings have led researchers to consider the uptake of nanocarriers by a transcellular pathway. The transcellular pathway has been widely reported to transport macromolecules and particles across absorptive epithelial cells which is briefly described below.

1.3.2 Transcellular Transport

Transcellular transport refers to the transport of substance across the cell membrane. It occurs by energy in dependent or independent mechanisms such as receptor/ carrier mediated endocytosis or adsorptive endocytosis respectively (Figure 1.5) [172]. Adsorptive endocytosis involves internalisation of nanocarriers without requiring receptors or carriers for their uptake [22]. It is preceded by nonspecific interactions of a ligand with the cell membrane. As no ligand-specific receptors have been identified for most of the polycations, therefore, the polycations are considered to interact with the cell membranes by nonspecific electrostatic interactions. Chitosan has been shown to enter the cells by various endocytic processes, however, predominantly by adsorptive endocytosis [189]. N-acetyl histidine conjugated glycol chitosan has been shown to be internalised by adsorptive endocytosis [190]. These nanocarriers have been reported to localise in the endosomes and undergo time dependent exocytosis. Adsorptive endocytosis depends primarily on the size and surface properties of adsorbed material, therefore, offers potential for delivering the macromolecules and colloidal carriers into the cells [141]. Positively charged particles with a size ≤100nm are readily internalised via adsorptive endocytosis, however, particles 100-500nm have also been reported to be taken up by adsorptive endocytosis but with a lesser tendency [191].

The receptor and carrier mediated endocytosis are energy-dependent, saturable endocytic pathways initiated by ligand binding to specific cell membrane receptors or transporters at the apical cell membrane [141, 192]. The macromolecular proteins such as insulin are internalised by receptor mediated endocytosis [22]. However, since all nanocarriers do not have specific receptors for internalisation, research has been focused on incorporating specific ligands to the polycations to allow cell-specific uptake by receptor-mediated mechanisms [193]. The polycations have been linked with ligands, such as folate [194-196] transferrin [197, 198], galactose [199] and vitamin [200] for receptor specific recognition and effective endocytosis.

The two commonly investigated endocytic pathways include classical clathrin mediated endocytosis and caveolae-mediated endocytosis [201, 202]. These endocytic mechanisms are distinguished by the composition of their coat, size of the detached vesicles, and fate of the internalised material [201].

1.3.2.1 Clathrin mediated endocytosis:

Clathrin-dependent endocytosis is a well characterised receptor-mediated endocytosis (Figure 1.6) [203, 204]. It occurs at clathrin coated sites which contain receptors specific to the ligands to be internalised [204]. Clathrin are cytosolic proteins associated with the formation of endocytic vesicles [203]. The plasma membrane comprises of specific domains called clathrin-coated pits [203]. These coated pits are able to concentrate large extracellular molecules that are internalised by receptor-mediated endocytosis, e.g., folate, vitamins, transferrin, galactose and antibodies.

Once the ligand is bound to the membrane receptors, a signal is sent to generate membrane coating at the receptor sites. This is followed by the invagination of plasma membrane to capture the receptor-ligand complex. Later on, the invagination buds and pinches off from the plasma membrane and gives rise to clathrin-coated vesicles. Once internalised the vesicles loose the clathrin coats, which is a prerequisite for mediation of their fusion with the early endosomes [203]. The endosomes fuse with the acidic lysosomes which result in sequestration followed by degradation of the cargo therapeutics by lysosomal enzymes [201]. The system is saturable because the ligand is internalized with the receptor, however the uptake returns to normal when the receptors recycle to the surface.

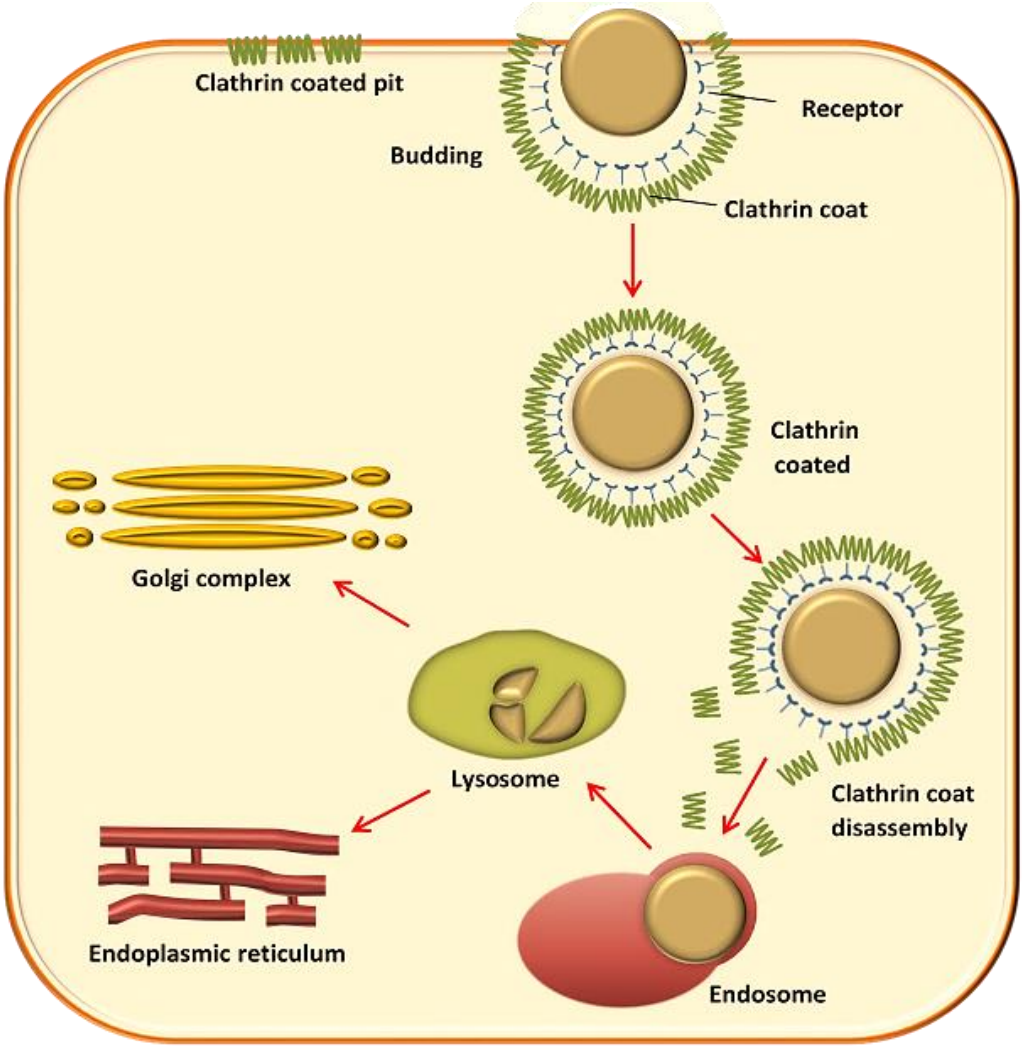

Figure 1.6 Schematic diagram of clathrin mediated endocytosis

Clathrin inhibitors such as chlorpromazine inhibit the receptor recycling by disrupting the assembly-disassembly of clathrin and hence are used to elucidate the clathrin-mediated endocytosis [188, 205]. A plethora of nanocarriers systems have been shown to be internalised by clathrin-mediated endocytic process. Tahara and co-workers reported that chitosan (CS)-modified PLGA nano-structures (CS-PLGA) are preferentially taken up by human lung adenocarcinoma cells (A549 cells) by an energy dependent mechanism [206]. The uptake of particles was reduced at lower temperatures and in hypertonic growth medium confirming uptake by a clathrin-mediated endocytic process [206]. Another similar study reported the cellular uptake of chitosan nanoparticles as a saturable process which was found to be concentration and temperature dependent [188]. The uptake was unaffected by co-administered filipin (inhibitor of caveolae pathway and clathrin-independent endocytic pathway). However,

chlorpromazine reduced the number of coated pit-associated receptors at the cell surface indicating the internalisation via clathrin-mediated endocytosis [188]. Huang and colleagues also used chitosan nanoparticles but showed a contradictory result where uptake was neither inhibited by chlorpromazine nor filipin [207]. However, since the cellular uptake of chitosan nanoparticles was temperature dependent, these findings led them to conclude internalisation of chitosan nanoparticles predominantly mediated by the adsorptive endocytosis initiated by nonspecific interactions between nanoparticles and cell membranes and in part by the clathrin-mediated process.

It is important to note here that nanocarriers with similar composition have been shown to exhibit different mechanisms of endocytosis [190]. The variation in the uptake mechanism can be explained by the differences in their physicochemical properties. Harush-Frenkel reported that positively charged nanoparticles internalised rapidly via the clathrin-mediated pathway whereas negatively charged nanoparticles showed reduced rate of endocytosis and did not utilize clathrin-mediated endocytosis pathway [208]. Particle size also determines the route of uptake and the mode of endocytosis. It has been reported that clarthrin-mediated endocytosis allows endocytosis of particles ≤ 100nm in diameter [191]. However, this size limit does not agree well with the sizes of the drug delivery nano-structures which are commonly larger in size than 100 nm.

1.3.2.2 Caveolae mediated endocytosis:

Caveolae mediated endocytosis is a form of non-classical endocytic pathways which is based on the balance between caveolin-1 and the raft lipids (Figure 1.7). Caveolins are integral membrane proteins of 21kDa, which are responsible for formation of flask-shaped plasma membrane invaginations, 60–80 nm in diameter called caveolae [203, 204, 209]. Caveolae are formed by the assembly of highly hydrophobic membrane domains called lipid raft domains [202, 210]. They have a unique morphology mainly composed of cholesterol and sphingolipids [202].

The formation of caveolae is dependent on the expression of caveolin-1 in non-muscle cells and caveolin-3 in muscle cells [210]. Cells that do not express caveolins have no caveolae [209]. Once caveolae are internalised they form caveolar vesicles. Researches have shown multicaveolar assemblies of caveolae which appear as bunches

of grapes [204]. The caveolar structures and vesicles travel to the intracellular distribution centres called caveosome [203]. The caveosomes are distinct from endosomes in terms of content and pH [202]. The internalized ligands or membrane constituents reside in caveosomes, and are sorted either to the Golgi complex, or to the endoplasmic reticulum [211].

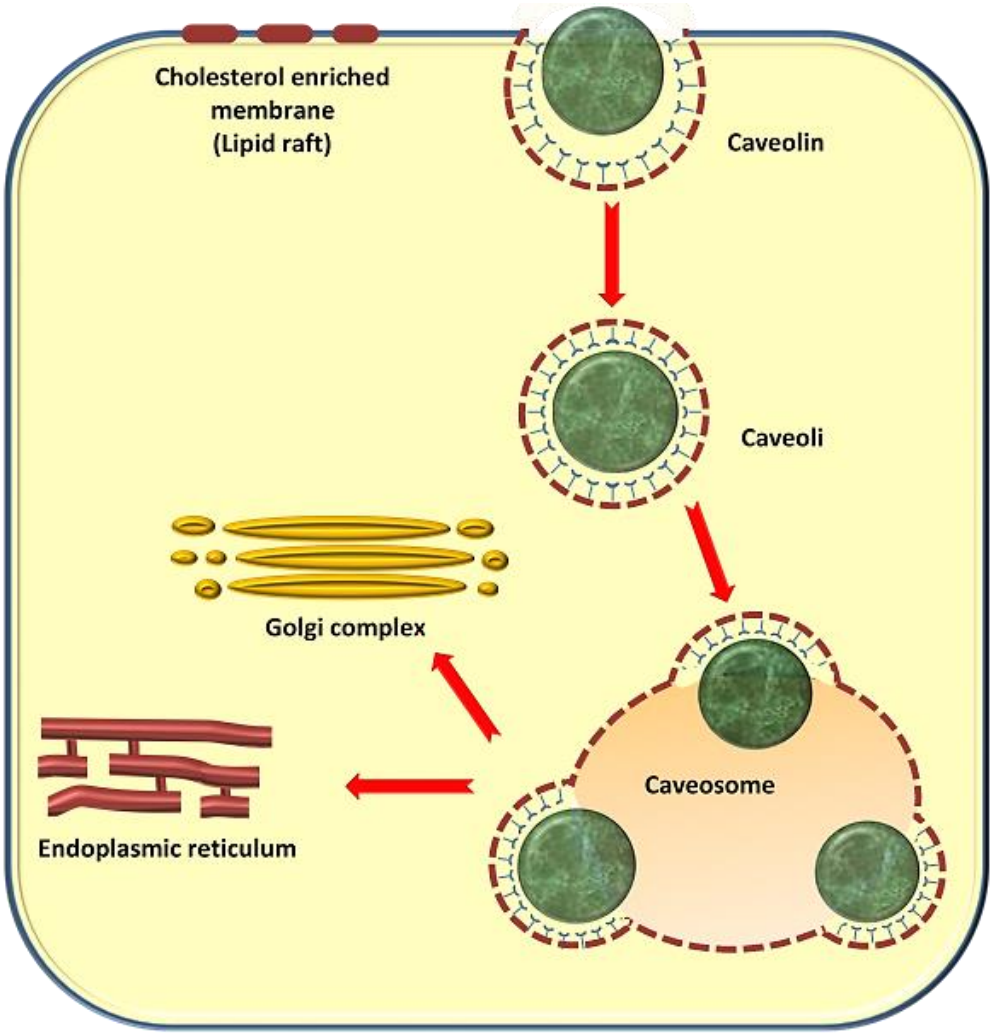

Figure 1.7 Schematic diagram of caveolae mediated endocytosis

A number of nanocarriers have been reported to be taken up by caveolae mediated endocytosis. Chung and co-worker reported that oligonucleotide-coated histidine-conjugated polyallylamine complexes (PAA-HIS/DNA) could specifically recognize adenosine receptors on the cell surface and were taken up by adenosine receptor mediated process. Uptake experiments with various endocytic inhibitors indicated that,

after receptor/ligand binding, oligonucleotide-coated PAA-HIS/DNA/complexes were mainly internalized via caveolae-mediated pathway [212]. Similar results have been shown by Van der Aa and colleagues. They showed that poly(2-(dimethylamino)ethyl methacrylate (pDMAEMA) and polyethylenimine (PEI) complexed DNA co-localise with fluorescently-labelled transferrin and cholera toxin after internalisation by COS-7 cells, which indicates uptake via the clathrin and caveolae-dependent pathways [213]. Blocking the uptake with route specific inhibitors only resulted in a marginal decrease in polyplex uptake indicating that the uptake routes of polyplexes are interchangeable. However, despite a minor effect of inhibitors on polyplex internalisation, blocking the caveolae-mediated uptake route resulted in an almost complete loss of polyplex-mediated gene expression. On the other hand, gene expression was not negatively affected by blocking the clathrin-dependent route of uptake indicating more important role of caveolae mediated uptake in polyplex uptake [213]. These findings indicate that uptake of particles may occur by one or more than one pathway, however, it may vary with the particle properties and type of cell. Although, the data on the uptake of nanocarriers by caveolae-mediated endocytosis proposes a size limit of 50-80nm diameter, however there are contradictory reports [191]. Rejman *et al.* has shown internalisation of nanoparticles having a diameter below 200 nm by clathrin-mediated endocytosis [214]. However, it was shown that as the size of the particles increased up to 500 nm, caveolae mediated internalisation pathway became the predominant pathway for the uptake of particles [214].

1.3.2.3 Gut-associated lymphoid tissue (GALT) system:

GALT is not only an essential component of immune system in the digestive tract but is also associated with the process of particle uptake via oral route [215] (Figure 1.8). GALT comprises of well-organized lymphoid tissues, such as mesenteric lymph nodes and Peyer's Patches and diffusely scattered lymphocytes in the intestinal lamina propria [216]. Peyer's Patches are macroscopic aggregates of lymphoid nodules, few centimetres in length present exclusively in the lowest portion of the small intestine, the ileum [217]. The Peyer's Patches play an important part in the immune surveillance system (antigen sampling) of luminal contents and directly stimulate immune response within the mucosa [217].

The lymphoid tissues of the digestive system are lined by specialized layer of intestinal enterocytes known as follicle associated epithelium (FAE) [217]. The FAE lining forms a dome shaped region over the follicle which serve as depot for the immune cells, such as T and B lymphocytes and dendritic cells [218]. It is distinguished from the intestinal epithelium covering the villi by low digestive enzymes levels, less pronounced brush border, infiltration of immune cells such as B cells, T cells, macrophages and dendritic cells and most importantly specialized epithelial cells called microfold cells (M-cells) [217, 219]. The notable feature of M cells which make them different from other epithelial cells are absence of surface microvilli and the normal thick mucus layer [219]. M cells have been shown to transport antigens from the lumen to the sub-epithelial dome [219].

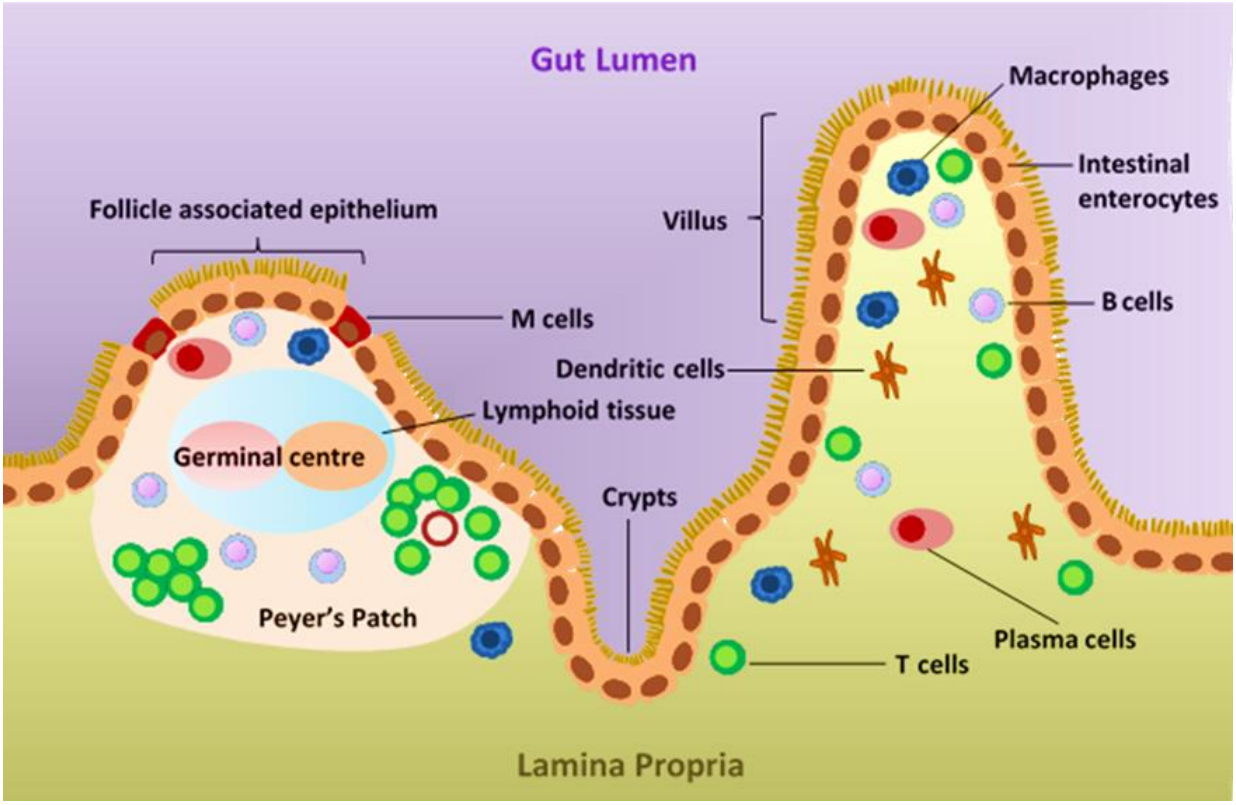

Figure 1.8 Schematic diagram of gut associated lymphoid tissue

The uptake of polymeric nanocarriers from M cells allows a direct way into the lymphatic system. Their high transcytotic activity makes them an interesting choice for drug delivery. This route favourably avoids first pass metabolism. Since M-cells do not express P-glycoprotein efflux pumps, therefore, decrease the likelihood of cellular efflux of nanocarriers [217]. In addition, uptake via M cells prevents the need to

traverse the thick glycocalyx coating present on the epithelial cells [217, 220]. Additionally, since M-cells are known to have a limited number of lysosomes [220], the intracellular degradation of nanocarriers can be prevented. All these favourable findings have led researchers to consider uptake of nanocarriers via M cells.

Researchers have used M cell specific ligands at the nanoparticle surface to target M cells. Garinot and co-workers prepared antigen-loaded PEGylated Poly(ε-caprolactoneco-ethylene glycol -based nanoparticles (PCL–PEG), which were grafted with M cell specific ligand i.e., RGD peptide. Formulation was targeted to β1 integrins expressed at the apical surface of M cells. The RGD ligand at the surface of the nanoparticles increased the transport of the nanoparticles across the M cell in *in vitro* co-cultures [221]. In a similar study, integrin targeting was studied by investigating the transport of arginine-glycine-aspartate (RGD)-coated nanoparticles across the ileal specimens. Integrin targeting with RGD has been shown to dramatically improve the nanoparticle transport across the FAE [222]. However, it is being considered that, since the number of M-cells in FAE is very low, the potential of uptake of nanocarriers by M cells may be limited [220]. Secondly, the nanocarriers encounter large quantities of local macrophages upon translocation via M cells which may phagocytise the particle. However, whether the particle will be taken up or not or will be phagocytised essentially depends on the particle properties such as size, charge and M cell specific ligands on the surface of particles.

1.4 CONCLUSION

Polyelectrolyte complexes offer the prospect and promise for the oral delivery of proteins. However, conventional carrier systems such as binary polyelectrolyte complexes are associated with toxicity related issues which severely limit their clinical use. The fabrications of systems which are able to alleviate the toxicity of the conventional systems are in high demand to fulfil the promise of oral delivery of protein. The APECs are fabricated in this project to circumvent the limitations of previously formed binary polyelectrolyte carrier systems. The analysis of basic toxicity as well as specialised toxicity of carrier systems is essential to determine the magnitude and mechanism of toxicity. This will help to establish the effect of polymer based nanocarriers on the cellular functions as well as regulatory and metabolic processes. It is equally important to determine the cellular uptake and trafficking of polymeric nanostructures in biological systems to understand and predict their fate *in vivo*. Employing a number of assays in different cell lines will contribute towards a better correlation between *in vitro* and *in vivo* studies.

1.5 AIM

The aim of this study was to fabricate non-insulin loaded (NIL) and insulin loaded (IL) ternary polyelectrolyte complexes (APECs) between (i) amphiphilic PAH with different hydrophobic groups i.e., 5-(Dimethylamino) naphthalene-1-sulfonyl chloride (Da10) and palmitoyl moiety (Pa2.5); and quaternised Pa2.5 and (ii) polyanions (PAA & DS), and compare their physicochemical properties, stability, biocompatibility, uptake and transport with binary complexes (PECs).

1.5.1 Objectives

- Synthesis of modified polyallylamine by grafting hydrophobic (Pa2.5 & Da10) and hydrophilic (QPa2.5) pendant groups on PAH backbone
- Fabrication of NIL and IL PECs and APECs
- Determination of insulin association efficiency of PECs and APECs
- Determination of stability of IL PECs and APECs at various ionic strengths (68mM, 102mM, and 145mM of NaCl), temperature (37˚C & 45˚C) and pH (1.2 and 6.6)

- Determination of cytotoxicity of PECs and APECs on CaCo2 cells assessed using the MTT assay
- Determination of haemocompatibility of PECs and APECs assessed using the haemolysis assay
- Determination of effect of PECs and APECs in inducing oxidative stress assessed by the reactive oxygen specie (ROS) generation assay
- Determination of the effect of PECs and APECs in *in vitro* and *in vivo* immunotoxicity by investigation of cytokine (IL-2, IL-6 and TNFα) generation
- Determination of the drop in the percentage TEER on exposure to free insulin, PECs and APECs.
- Determination of the paracellular flux of FITC-Dextran across CaCo2 cell monolayers.
- Quantitative analysis of the permeation of insulin across CaCo2 cell monolayer.
- Evaluation of the uptake of various PECs and APECs by CaCo2 cells using flow cytometry and fluorescent microscopy.

Chapter 2

POLYMER SYNTHESIS AND CHARACTERISATION

2 POLYMER SYNTHESIS AND CHARACTERISATION

2.1 AMPHIPHILIC POLYMER

Amphiphilic polymers have demonstrated significant potential in protein delivery [118]. They consist of hydrophobic and hydrophilic segments which can self-organise in aqueous media to form well defined nano-structures like micelles and vesicles [223, 224]. A hydrophobic segment forms the inner core and contributes to hydrophobic interactions while a hydrophilic segment maintains the polymer solubility and stability in aqueous environment by forming hydrogen bonds with the surrounding water molecules [119, 225]. Amphiphilic polymers commonly exist as block copolymers, which are fabricated via copolymerisation of hydrophilic and hydrophobic monomers (Figure 2.1) [119, 224]. However, nowadays comb shaped amphiphilic polymers are gaining a lot of interest.

Comb shaped polymers are formed by grafting hydrophobic and/or hydrophilic pendant groups on a homopolymer or copolymer backbone which gives rise to a comb-like architecture (Figure 2.1) [224, 226]. The hydrophilic pendant groups such as poly (ethylene glycol) (PEG) [227] or quaternary ammonium moieties are added to improve water solubility of the polymer [226]. These comb-shaped amphiphilic polymers have proven very versatile due to their ability to form different supra-molecular structures in the aqueous environment such as solid nanoparticles, polymeric micelles, vesicles and polyelectrolytes [119, 228]. Recently, Thompson *et al.* demonstrated the potential of using novel comb shaped polymers to form polyelectrolyte complexes for oral protein delivery [119].

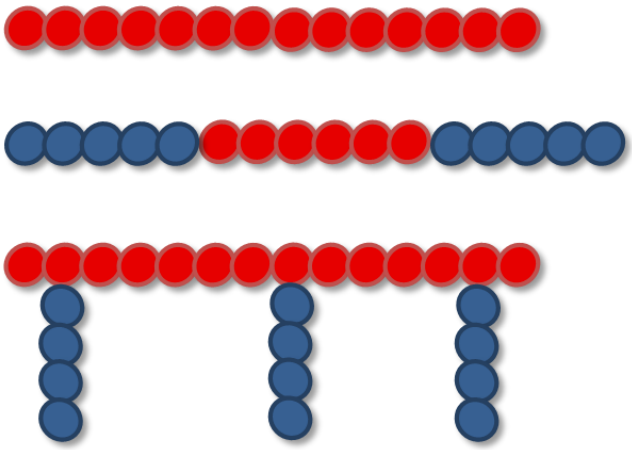

Figure 2.1 Schematic diagram of (a) homopolymer (b) block copolymer (C) comb shaped polymer

In this study, comb shaped amphiphilic polymers were synthesised by grafting hydrophobic or hydrophilic groups onto a water-soluble homopolymer polyallylamine backbone (PAH). PAH is a synthetic cationic polymer prepared by polymerization of allylamine. It has a long alkyl chain with a high density of primary amino groups (-NH_2^+) (Figure 2.5). PAH was selected because of the ease of performing modification at the primary amine site which allows grafting of hydrophilic and hydrophobic moieties by simple nucleophilic substitution and addition reactions [229]. Its cationic nature enables this polymer to interact electrostatically with negatively charged proteins and polymers [152]. The positive charge also allows interaction with negatively charged proteoglycans of the cell membrane, leading to enhanced uptake [154]. The cross-linked PAH is currently used clinically as an oral phosphate binder [230]. Unlike other polycationic polymers (e.g., polyethylenimine, poly-l-lysine), PAH is less toxic, a property which makes it suitable for pharmaceutical applications [120]. However, the presence of primary amines in PAH still confers some degree of cytotoxicity [152, 231].

It has been shown that the modification of primary amines on PAH can lead to a reduction of cytotoxicity [120, 152, 154]. Boussif *et al.* has shown that the glycolation of PAH with hydrophilic methyl glycolate is able to reduce the cytotoxicity of unmodified PAH. Similarly, Pathak *et al.* demonstrated that PAH modified with imidazolyl is less toxic than unmodified PAH. All these reports showed that PAH has a lower cytotoxicity index in its modified form, due to a reduction of primary amines on the polymer backbone [152]. Therefore, in this study, PAH was grafted with the

hydrophobic pendant group (5-(Dimethylamino) naphthalene-1-sulfonyl chloride - dansyl) and palmitoyl moiety - Pa2.5); and a hydrophilic moiety (quaternary ammonium moiety - QPa2.5).

Thompson and colleagues studied the effect of the degree and type of hydrophobic and hydrophilic substitution on the properties modified PAH based nanocomplexes [119]. They reported that the hydrophilic and hydrophobic modifications of PAH lead to substantial differences in the physicochemical properties of the complexes. The substitution of primary amines on the PAH lead to a significant reduction in the positive charge density. They also reported that the hydrophobic grafting reduces the flexibility of the PAH backbone. Alternatively, the hydrophilic polymers tend to increase the inter chain repulsion due to a permanent positive charge on its surface [120]. In this project, the degree of substitution was devised in a manner to retain sufficient number of primary amino groups on the PAH backbone, to complex with oppositely charged polymer and protein for subsequent studies.

To confirm the success of modification on the polymer, a number of techniques are needed to characterise the polymers. Elemental analysis, nuclear magnetic resonance spectroscopy (NMR) and gel permeation chromatography (GPC) are very useful and commonly used techniques applied for the analysis of polymer properties, like elemental composition [232, 233].

2.2 CHARACTERISATION OF POLYMERS

2.2.1 Elemental Analysis

Elemental analysis is performed to characterize the organic compound for its elemental composition [233]. It can identify the elements in an organic compound by qualitative (type of elements present) or quantitative analysis (relative number of atoms) [234, 235].

The most common type of elemental analysis is carbon, hydrogen and nitrogen known as CHN analysis [236]. In addition, analysis for atoms such as halogens i.e., sulphur, chlorine, and fluorine can also be performed. CHN analysis is performed by a CHN elemental analyser by combustion analysis. A schematic representation of an elemental analyser is shown in Figure 2.2.

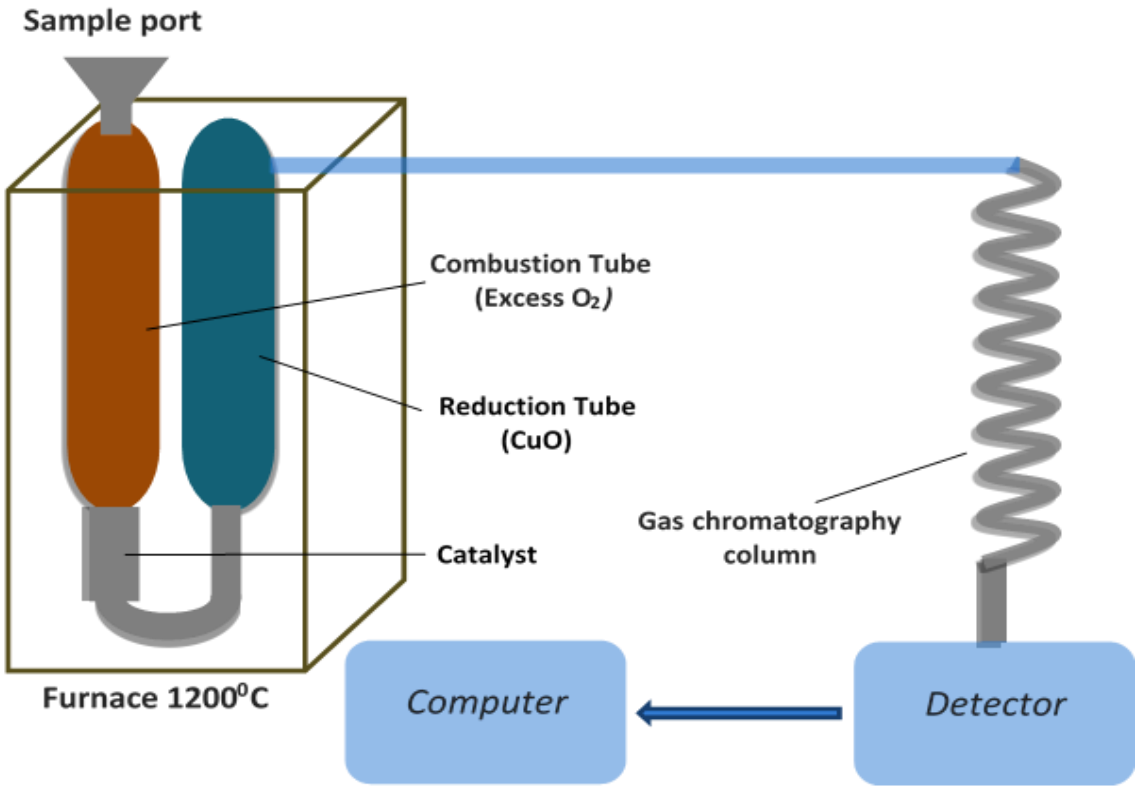

Figure 2.2 Schematic diagram of an elemental analyser

A small amount of unknown sample is burnt in the presence of oxygen at high temperature (>1000°C) [233, 235]. The combustion mixture passes over a layer of catalyst (e.g., chromium trioxide and tungsten trioxide) which enables the complete combustion of the sample. As a result, all of the carbon in the compound is converted to carbon dioxide and all of the hydrogen in the compound is converted to water vapours [235]. The resulting gas mixture (CO_2, H_2O, nitrogen oxides and remaining oxygen) then flows through a silica tube packed with copper granules called copper turnings, which form a reduction column (500 °C) [237]. In this column, the gases such as nitric/nitrous oxides are reduced to unreactive elemental nitrogen (N_2) [235, 237, 238]. The leaving gas stream (CO_2, H_2O and N_2) is swept by the high purity helium, used as the carrier gas into the detector for quantitative analysis [238, 239].

The micro-analytical detection system allows quantitative analysis of the final product. The most commonly used analysis for determination of gas content is gas chromatography, a method that can separate each gas. In most of the instruments, the separated gases are carried to a thermal conductivity detector which detects the

elements and determines their relative amounts [235]. The thermal conductivity detector generates an electrical output signal proportional to the concentrations of each of the individual elements [240]. The percentage of each element can be calculated from the integrated weight values [237].

2.2.2 Nuclear magnetic resonance spectroscopy (NMR)

Nuclear magnetic resonance spectroscopy is a well-established technique, commonly referred as NMR [241]. It is a versatile analytical technique that utilizes the magnetic properties of atomic nuclei for compositional and structural characterisation of molecules [242-244]. It is extensively used for the determination of structure of polymers. [244]. Figure 2.3 displays a schematic illustration of NMR spectroscopy.

As virtually all organic molecules carry protons, therefore, the Proton Nuclear Magnetic Resonance (^{1}H NMR) provides information about the hydrogen present in a mole. The nuclei of atoms generally have a defined characteristic spin [244]. The spinning protons generate a magnetic field around themselves, which allow them to move in a random fashion called a magnetic moment (μ) [242]. However, when the protons (^{1}H) are placed in an external magnetic field, they absorb electromagnetic radiation at a specific frequency and resonate [245]. The frequency of resonance of a proton is called its chemical shift [246]. In an NMR spectrum, the x- axis expresses the chemical shift (in ppm) against the intensity of absorption on y-axis [245].

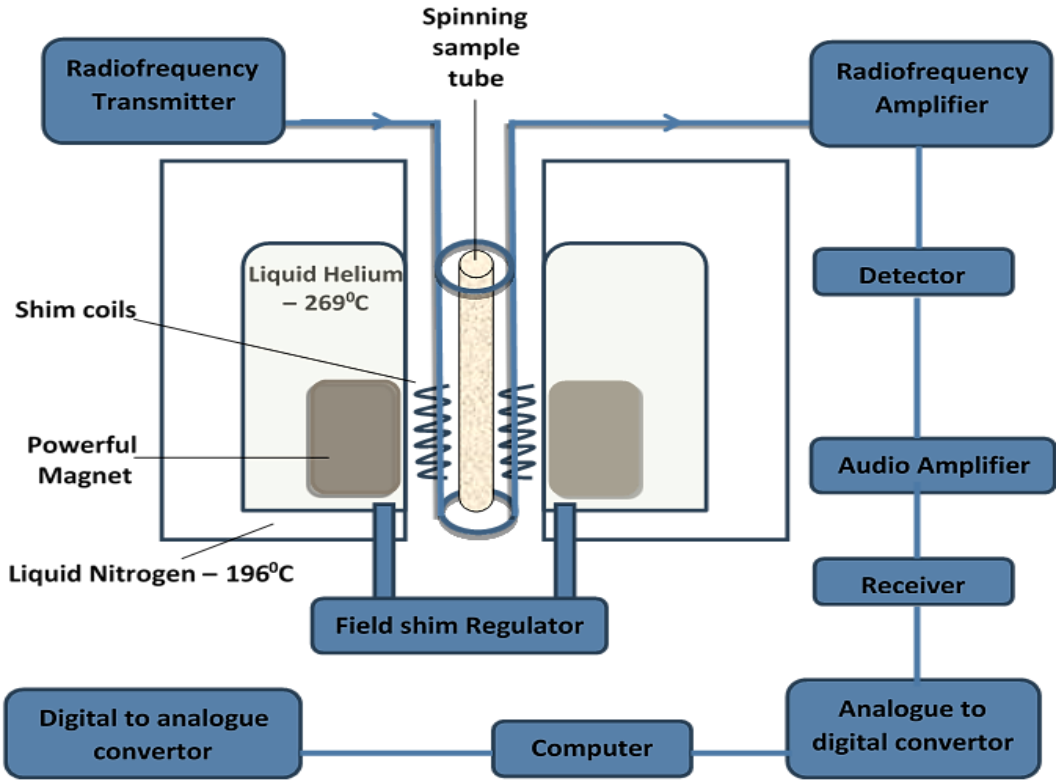

Figure 2.3 Schematic illustration of NMR spectroscopy

The difference in the absorption of the electromagnetic radiation by different protons is due to the distinct electron densities and dissimilar chemical environments around them [244]. Therefore, each chemically discrete proton or group of protons generate a distinct resonance in the NMR spectra. The area measured under the NMR resonance represents the relative number (not the absolute number) of the chemically distinct protons in that chemical shift. The electrons around the proton act as a barrier and shield the proton from the applied magnetic field, and so prevent them from generating a high chemical shift. This phenomenon is termed the nuclear shielding [242]. The shielded proton, therefore, present only a small chemical shift [244]. Conversely, the removal of electrons by the electron withdrawing groups reduces the electron density around the proton and de-shields the protons. This effect allows the protons to generate a higher chemical shift [242].

Different functional groups have different characteristic chemical shifts. Figure 2.4 displays a schematic diagram of some typical chemical shift in ^{1}H NMR spectra. The shielded protons undergo lower chemical shifts and appear on the right hand side of the axis, which is called the up field. On the other hand, the de-shielded protons undergo

higher chemical shifts and appear on the left hand side called the down field side (increase in ppm). Trends in the proton NMR chemical shift are influenced by factors such as distance from the unsaturated groups (e.g., aromatic). The unsaturated groups are de-shielded and hence appear towards the down field side (left; increase in ppm) [247]. More precisely, a large chemical shift in a ^{1}H-NMR spectrum corresponds to a proton that either has relatively little electron density around it, or is lying adjacent to the electron withdrawing groups. Similarly, a small chemical shift represents a proton that has greater electron density around it, indicating no adjacent electron withdrawing groups [248].

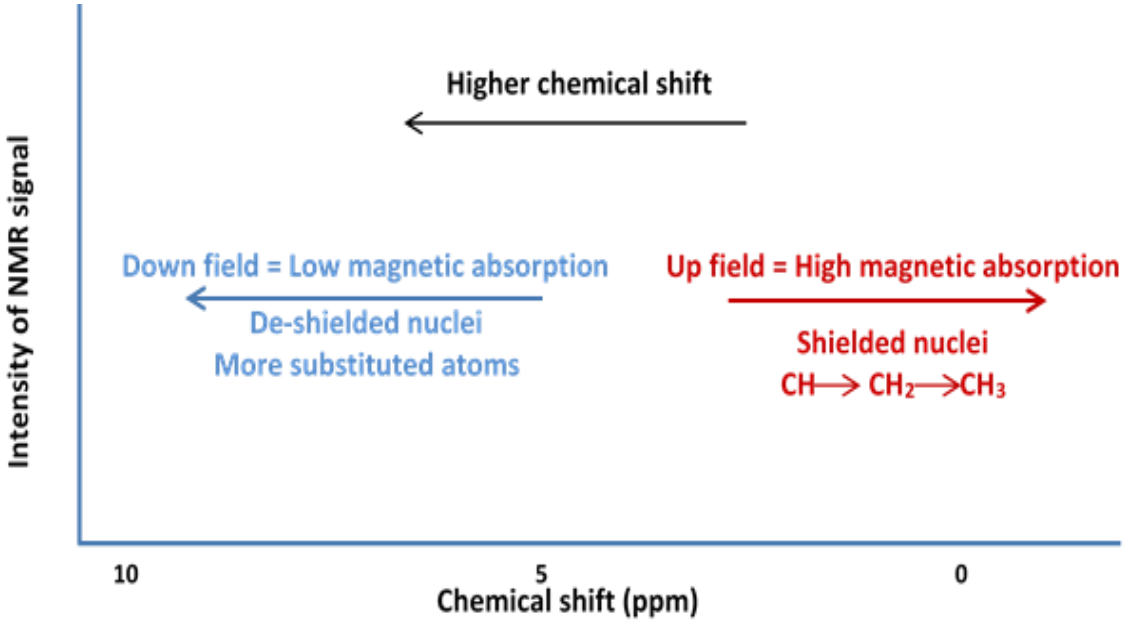

Figure 2.4 Schematic representation of some typical chemical shifts in ^{1}H NMR

2.2.3 GPC

GPC, also known as Size Exclusion Chromatography is a rapid and reliable technique for polymer characterisation [233]. It is a chromatographic technique that separates molecules on the basis of the molecular size. The analytes are pumped through the specialized columns containing a microporous packing material. The smaller analytes penetrate the pores more easily, therefore, are retained for longer time in these pores [241]. Alternatively, the larger analytes are retained for a less time in the pores and are eluted quickly. In this way, a range of molecular weights can be separated and

determined [241]. The comb shaped polymers can further be characterised by GPC to determine their molecular weight and size [233, 249].

2.3 AIM

The hydrophobic and hydrophilic modification of PAH backbone.

2.3.1 Objectives:

- Substitution of hydrophobic (palmitoyl (Pa2.5) and dansyl (Da10)) and hydrophilic (QPa2.5) moieties on PAH backbone.
- Characterisation of polymers by elemental analysis and ^{1}H NMR spectroscopy to confirm grafting of hydrophobic and hydrophilic moieties on to the PAH backbone.

2.4 MATERIALS AND METHODS

2.4.1 Materials

Materials	Supplier
Amberlite 96 resin	Fluka, UK
Dansyl chloride	Sigma Aldrich, UK
Deionised water milliq apparatus	Millipore, UK
Deuterated Water	Sigma Aldrich, UK
Dialysing membrane (7 and 12-14kDa cut-off limit)	Medicell international Ltd, UK
Diethyl ether	Fisher Scientific, UK
Dioxane	Fisher Scientific, UK
Ethanol	Fisher Scientific, UK
HCl	Sigma Aldrich, UK
Methanol	Fisher Scientific, UK
Methyl Iodide	Sigma Aldrich, UK
PAH-HCl	Sigma Aldrich, UK
Palmitic acid N hydroxy succinimide ester	Sigma Aldrich, UK
Polyallyllamine hydrochloride (MW= 15KDa)	Sigma Aldrich, UK
Sodium Carbonate	Sigma Aldrich, UK
Sodium Hydrogen Carbonate	Sigma Aldrich, UK
Sodium hydroxide	Fisher Scientific, UK
Sodium Iodide	Sigma Aldrich, UK

2.4.2 Method

2.4.2.1 Conversion of polyallylamine hydrochloride (PAH-HCl) to PAH free base

PAH-HCl (10g) was dissolved in 100mL of deionised water. 1M NaOH was added into the PAH-HCl solution under gentle magnetic stirring, until pH 13 was achieved. The resulting solution was stirred for one hour. The solution was then dialysed with a visking tube of Mw cut-off = 7 kDa, against 5L of water with at least 12 water changes in 24 h [120]. The dialysate was freeze dried for 48h using inoLab WTW series pH 720 Mechatech System Freeze Drier. PAH was recovered as a white rubbery solid. Figure 2.5 represents the chemical structure of PAH.

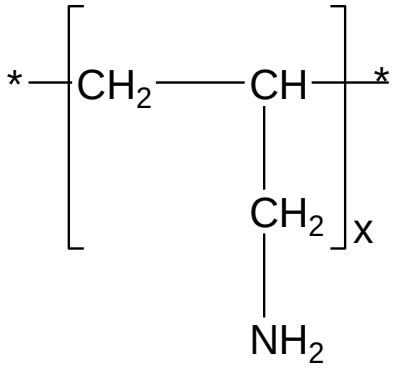

Figure 2.5 Chemical Structure of PAH

2.4.2.2 Synthesis of modified polymers

The synthesis of all polymers was performed using the method reported by Thompson *et al.* and briefly described as below [120].

2.4.2.2.1 Synthesis of palmitoyl 2.5-polyallylamine (Pa2.5)

Briefly, a solution of palmitic acid-N-hydroxysuccinimide ester (0.304 g in 100mL ethanol) was added drop-wise to the PAH solution (PAH free base 2 g in 100mL deionised water). Sodium hydrogen carbonate (2.35 g) was gradually added to the solution over 1 h. The reaction was stirred for 72 h at 500 rpm. The solvent was then evaporated in the rotary evaporator and the residue was dissolved in 50mL of deionised water. The solution was subsequently dialysed against 5L of water with 12 water changes (molecular weight cut-off=12-14 kDa). The dialysate was then freeze dried and collected as a white cotton-like solid [120]. Figure 2.6 presents the chemical reaction of synthesis of Pa2.5.

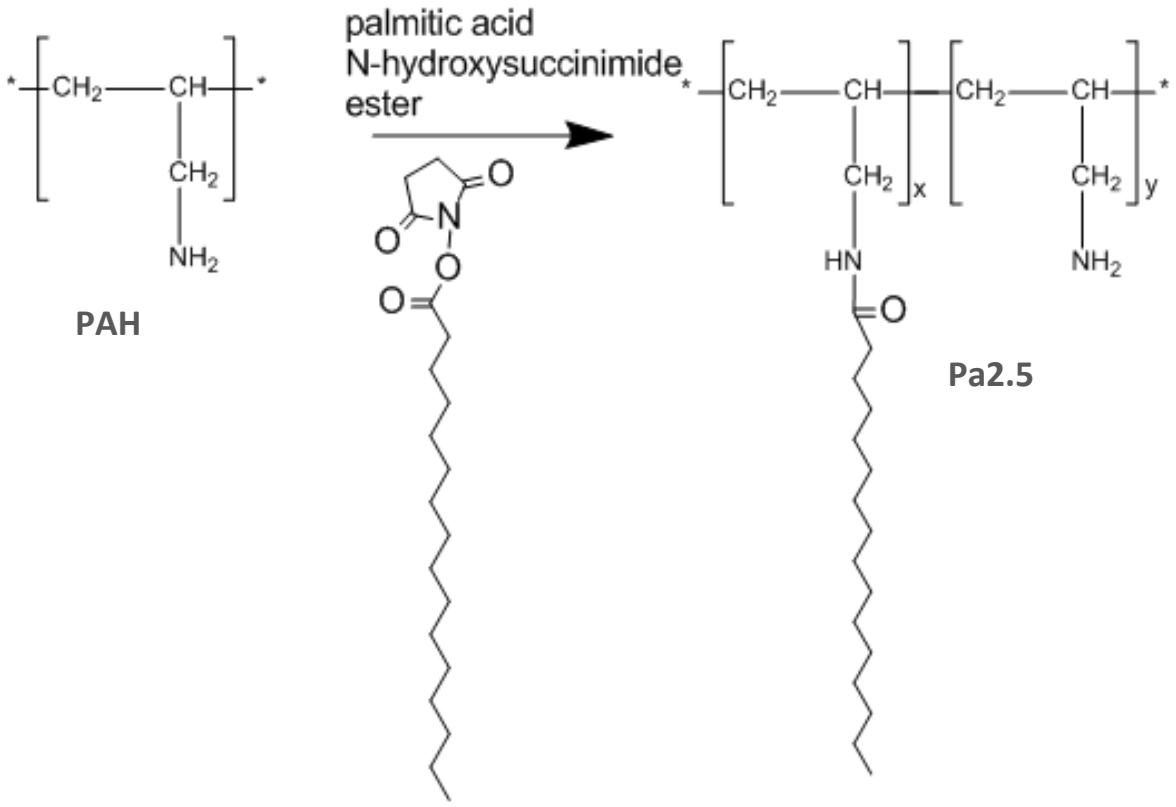

Figure 2.6 Chemical reaction of the synthesis of Pa2.5

2.4.2.2.2 Synthesis of Quaternary ammonium amphiphilic polymer (QPa2.5)

Pa2.5 (0.6 g) was dissolved in 100mL of methanol. Sodium hydroxide (0.557 g) and sodium iodide (0.25 g) were added into the Pa2.5 solution and stirred until completely dissolved. Methyl iodide (3.5 mL) was added into the mixture and the reaction was carried out at 36°C, over 3 h under nitrogen atmosphere. The supernatant was poured off and diethyl ether (400mL) was added to the white precipitate. The solution was then left to settle overnight at 25°C. The diethyl ether was then decanted and the precipitate was dried overnight. The dried precipitate was dissolved in 100mL of 1:1 (v/v) mixture of ethanol and distilled water and dialysed as described above section 2.4.2.2.1. The dialysate was then passed through an amberlite 93 exchange resin column (30mL), which had been previously washed with HCL (2 M, 100mL) and titrated to neutral pH with distilled water. The resulting clear elute was then freeze dried as above and collected as a white cotton-like solid [120]. Figure 2.7 presents the chemical reaction of quaternisation of Pa2.5 to QPa2.5.

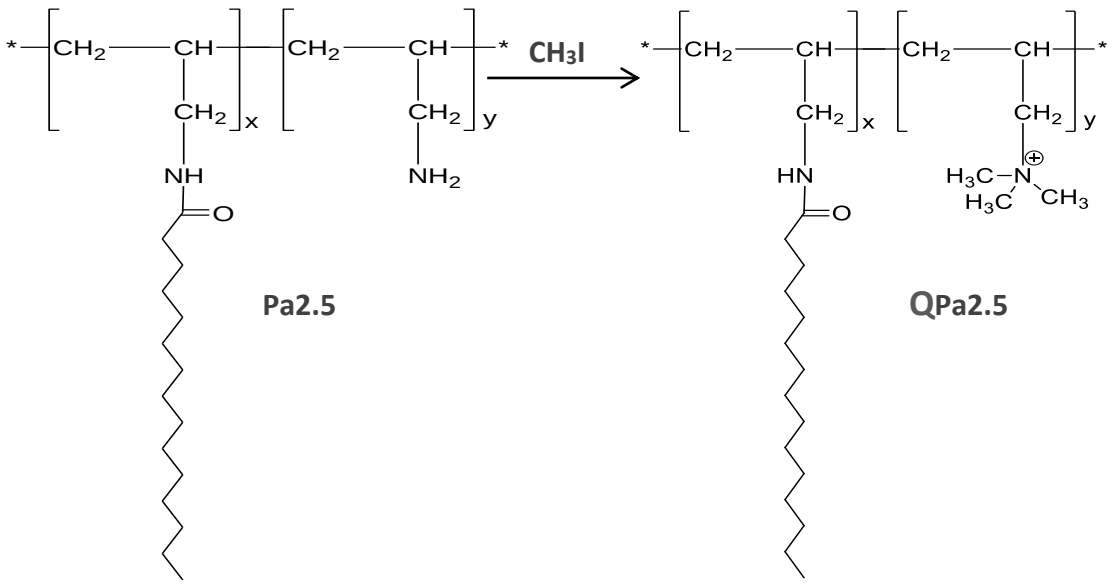

Figure 2.7 Chemical reaction of synthesis of QPa2.5

2.4.2.2.3 Synthesis of Dansyl 10-polyallylamine (Da10)

The PAH free base was dissolved in 150mL dioxane: water (1:1v/v). Sodium carbonate (0.185g) was added and the solution was stirred until it was completely dissolved. Dansyl chloride (0.472g) was dissolved in dioxane (20mL), and was added drop wise to the polymer solution over 2h at 0˚C. The reaction was stirred for 4h at 0˚C, followed by 8 h stirring at room temperature. The solvent was evaporated and the residue washed 3 times with diethyl ether. The precipitate was then dissolved in doubly distilled water and dialyzed as mentioned above in section 2.4.2.2.1 and freeze dried for 48h [120]. The Da10 was recovered as a yellow fluffy solid. Figure 2.8 presents the synthesis of Da10.

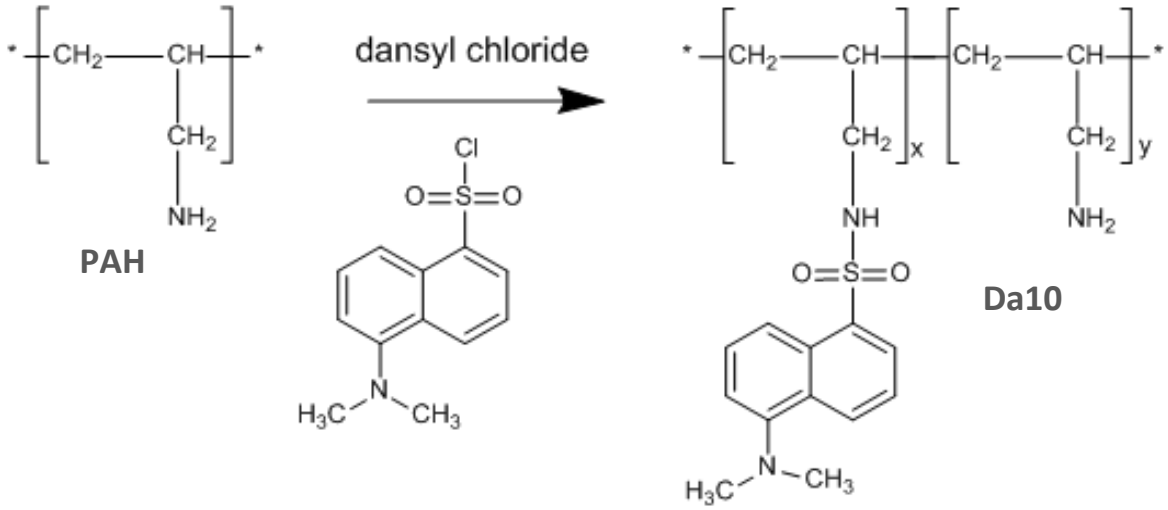

Figure 2.8 Chemical reaction of synthesis of Da10

2.4.2.3 Characterisation of polymers

2.4.2.3.1 Elemental analysis

Synthesised and unmodified polymers were characterized for their carbon, hydrogen and nitrogen contents by elemental analysis. 4 mg samples were analysed using a Flash EA® 1112 Elemental Analyser. The determination of percentage by weight of C, H and N was based on the quantitative "dynamic flash combustion" method as provided by Medac Ltd. The analysis was performed by combusting the sample at 1000˚C in oxygen in the presence of a catalyst under controlled conditions. The gases (CO_2, H_2O and N_2) were separated by gas chromatography.

2.4.2.3.2 Nuclear magnetic resonance spectroscopy (^{1}H NMR)

The polymers were characterized by ^{1}H-NMR. A total of 3-5mgmL^{-1} of the polymer was dissolved in deuterated water (D_2O), sonicated for 5min at maximum amplitude and allowed to cool down. The samples were filtered through cotton and loaded into the NMR tube (0.8 mL). The spectrums were obtained using JEOL 600 MHz Ultrashield spectrometer. Each spectrum is an average of 64 scans acquired at room temperature.

2.5 RESULTS

2.5.1 Polymer Yield

Table 2.1 demonstrates the initial molar feeds and percentage yield of the various polymers.

Polymer yield was calculated by the following formula:

$$\% \text{ Yield} = \frac{\text{Weight of product}}{\text{Weight of reactants}} \text{ X } 100$$

The polymer percentage yield of hydrophobically modified polymers was found to be >80%. Unlike hydrophobically modified polymers, the quaternised polymer demonstrated a lower yield of <66%.

Table 2.1 Properties of polymers (mean±SE)

Polymer	***Type of grafting***	***Initial molar feed ratio***	***% Yield(mean±SE) (n=≥3)***	***Physical appearance***
PAH	-	-	*95%*	*Transparent sticky rubber like*
Pa2.5	*Palmitoyl*	*1:0.025*	*86%*	*White cotton like*
Q Pa2.5	*Quaternised palmitoyl*	*1:0.025*	*65%*	*White cotton like*
Da10	*Dansyl*	*1:0.10*	*82%*	*Yellow cotton like*

2.5.2 Elemental analysis

2.5.2.1 PAH

Table 2.2 presents the findings from the elemental analysis of PAH. Using equation 1, the molar ratios were calculated from the percentage weight obtained from the elemental analysis. Subsequently, the molar ratio relative to nitrogen was calculated by using equation 2.

$$Element's\ molar\ ratio\ (x) = \frac{Element's\ weight\ \%\ obtained\ from\ elemntal\ analysis}{Elemental\ molecular\ weight}$$

Equation 1

$$Element's\ molar\ ratio\ relative\ to\ N\ (x') = \frac{Element's\ molar\ ratio\ (x)}{Element's\ molar\ ratio\ of\ N}$$

Equation 2

For PAH, the element molar ratio relative to nitrogen was found to be 3.05:7.87:1 (Table 2.2), which is in good agreement with 3 C's, 7 H's and 1 N theoretical atoms ratio of the empirical formula of the PAH monomer (Figure 2.5).

Table 2.2 Calculation of the empirical formula of PAH

	Elements		
	C	H	N
Element weight % obtained from elemental analysis	57.07	12.27	21.77
Element molar ratio (x)	4.76	12.27	1.56
Element molar ratio relative to N (x′)	3.05	7.87	1.0

2.5.2.2 Modified polymers

Table 2.3 demonstrates the elemental analysis results of the modified polymers. The molar ratio and molar ratio relative to nitrogen were calculated from the aforementioned equations 1 & 2 and subsequent calculations were performed by using the following equations 3 and 4.

$$Moles\ of\ element\ in\ the\ grafted\ group\ of\ modified\ PAH = Element's\ molar\ ratio\ relative\ to\ N\ of\ the\ modified\ polymer - Element's\ molar\ ratio\ relative\ to\ N\ of\ the\ PAH\ (x')$$

Equation 3

$$Percentage\ mole\ modification = \frac{Moles\ of\ carbon\ in\ the\ grafted\ group\ present\ in\ the\ modified\ PAH}{Number\ of\ carbon\ atoms\ present\ in\ the\ grafted\ moiety}\ x\ 100\%$$

Equation 4

Mole modification of the Pa2.5 and Da10 groups on the modified polymers was determined relative to PAH. The number of extra moles in modified polymers were determined by calculating the difference in the moles of PAH (3.05 moles) from Pa2.5 and Da10 given as (3.75-3.05 = 0.70 extra moles of carbon) and (4.06 - 3.05 = 1.01 extra moles of carbons) respectively (refer to Table 2.3). These results demonstrate that, for every 1 mole of nitrogen in Pa2.5, there were 3.75 moles of carbon and 12.34 moles of hydrogen. For each mole of nitrogen in QPa2.5, there were 6.54 moles of carbon and 17.64 moles of hydrogen. In addition, for every 1 mole of nitrogen in Da10 there were 4.06 moles of carbon and 9.18 moles of hydrogen.

On the other hand, the extra moles of carbon atom from quaternary amine moieties was determined relative to Pa2.5 i.e., 6.54- 3.75= 2.79 extra moles of carbon. The mole modification of various polymers was calculated from equation 4, as 4.3%, 46.6% and 8.4% for Pa2.5, QPa2.5 and Da10 respectively.

Table 2.3 Calculation of the % mole modification and empirical formula of modified PAH i.e., Pa2.5, QPa2.5 and Da10

Polymers	**Pa2.5**			**QPa2.5**			**Da10**		
Elements	**C**	**H**	**N**	**C**	**H**	**N**	**C**	**H**	**N**
Element weight % obtained from elemental analysis	52.2	10.80	16.26	26	7.41	5.99	47.51	8.91	13.6
Element molar ratio (x) (Equation 1)	4.35	10.80	1.16	2.16	7.47	0.42	3.95	8.91	0.97
Element molar ratio relative to N (x') (Equation 2)	3.75	12.34	1.0	5.15	17.64	1.0	4.06	9.18	1.0
Moles of the respective element in the grafted moiety (Equation 3)	0.70	4.47	0	1.40	5.3	0	1.01	1.31	0
% modification (Equation 4)		4.3%			46%			8.4%	

2.5.3 Nuclear Magnetic Resonance

Each peak in the spectrum was identified and assigned a value based on the number of protons resonating at that chemical shift (δ). Peak areas were acquired by the integration of the ^{1}H NMR spectra of protons. The mole modification of the polymers was calculated from the ^{1}H NMR spectra by using the equation 5. A summary of the corresponding chemical shifts for each attached hydrophobic/hydrophilic group and percentage mole modification is tabulated in Table 2.4.

$$\text{Percentage mole modification} = \frac{\text{Integration value of the peak i / number of protons i}}{\text{Integration value of } CH_2 \text{ PAH peak at } \delta_{2.5}) \text{ / number of protons of } CH_2 \text{ PAH}} \times 100$$

Equation 5

2.5.3.1 ^{1}H NMR spectra of PAH

The proton chemical shifts of ^{1}H NMR spectra of PAH in D_2O were achieved as CH_2 (A) = $\delta_{1.05,\ 1.1 \text{ and } 1.2}$, CH (B) = $\delta_{1.43}$, = CH_2 (C) = $\delta_{2.5,\ 2.8}$ (Figure 2.9). The integration ratio of these peaks was found to be 97:52:100, respectively. This ratio correlates well with the theoretical 2:1:2 proton ratios in the PAH structure (Figure 2.5).

$$CH_2 : CH : CH_2$$

$$\frac{100}{52.2} : \frac{52.2}{52.2} : \frac{97.15}{52.2}$$

$$1.91 : 1 : 1.86$$

The two protons connected to the nitrogen atom are indiscernible in the NMR spectra, due to the fast exchange with deuterated solvent.

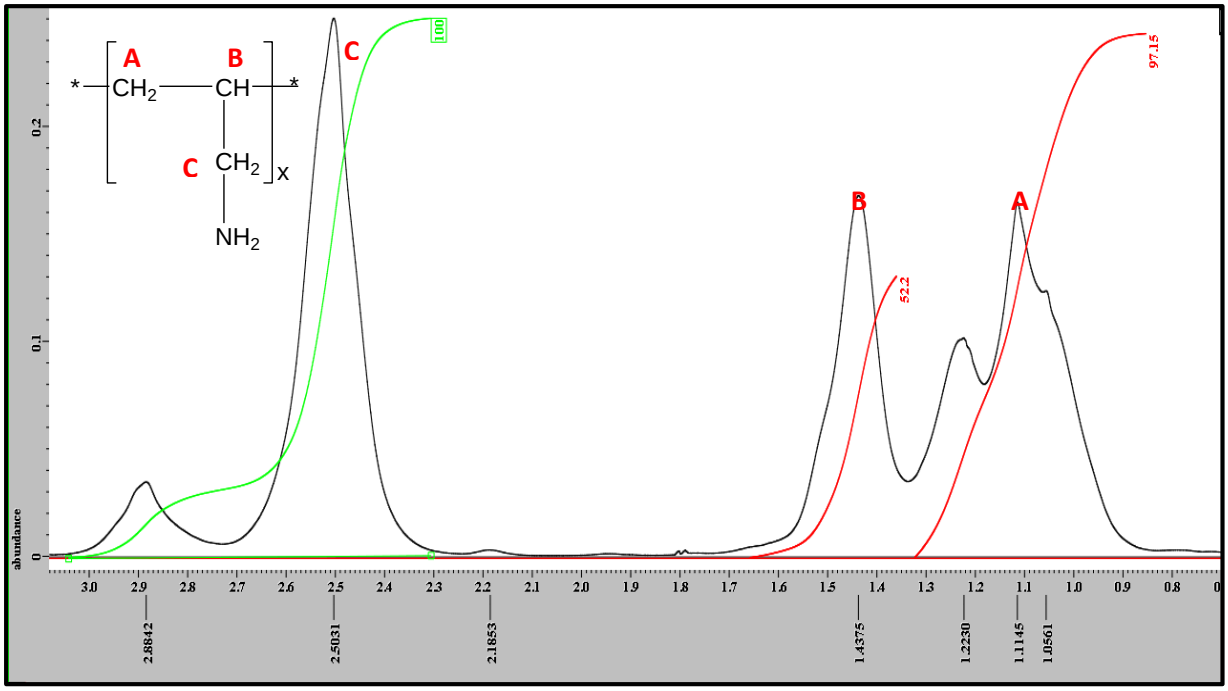

Figure 2.9 ^{1}H NMR spectra of PAH in D_2O conducted by 600 MHz spectrometer at 25 °C.

2.5.3.2 ^{1}H NMR spectra of Pa2.5

The ^{1}H NMR spectra of Pa2.5 in D_2O provides information regarding the palmitoylation of PAH on the primary amines. The proton chemical shifts of ^{1}H NMR spectra of Pa2.5 in D_2O were achieved as CH_3 (A) = $\delta_{0.73,}$ CH_2 (B) = $\delta_{1.05, 1.12, 1.14, 1.16}$, CH (C) = $\delta_{1.5}$ and CH_2 (D) = $\delta_{2.6, 2.7}$ of PAH (Figure 2.10; Table 2.4). In comparison to the PAH spectra, an additional small peak appeared much up field at $\delta_{0.73}$, just before the CH_2 proton peak of PAH (Figure 2.10, A). This peak corresponds to the terminal CH_3 and CH_2 proton in the palmitoyl pendant group. The $\delta_{0.73}$ appears poorly resolved due to the overlapping between the peaks i.e., CH_3 peaks from Pa2.5 and the CH_2 peak from PAH. The grafting percentage was therefore calculated by comparing the CH_3 peaks from Pa2.5 with the CH_2 peak from PAH at $\delta_{2.5}$, as the signal appeared clear with no overlapping between the peaks in this region. The grafting percentage of Pa2.5 at peak at $\delta_{0.73}$ in the ^{1}H NMR spectra was calculated as follows:

$$\textit{Grafting percentage} = \frac{\textit{Integration value of the } \delta_{0.73} \textit{ / number of protons in palmitic } CH_3 \textit{ peak}}{\textit{Integration value of } \delta_{2.5} \textit{ / number of protons in PAH } CH_2} \times 100$$

$$\frac{(8.57 / 3)}{(100 / 2)} \times 100 = 5.7\ \%$$

The percentage grafting of Pa2.5 was found to be 5.7%, which is close to the initial molar feed ratio.

Table 2.4 Summary of the chemical shifts, number of protons attached to hydrophobic/ hydrophilic group generating resonance and the percentage mole modification

Polymer	Peak (δ)	No of protons	% Mole modification
Pa2.5	0.73	3	5.7%
QPa2.5	3.19-3.2	9	40.6%
Da10	7.5- 8.28	6	7.7%

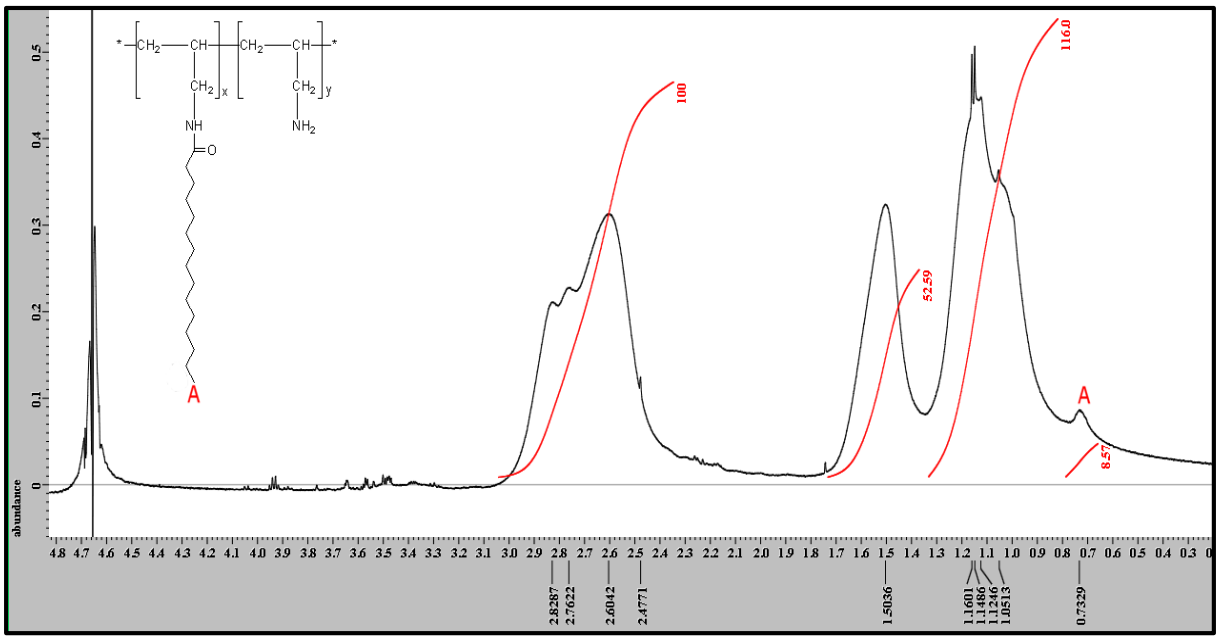

Figure 2.10 ^{1}H NMR spectra of Pa2.5 in D_2O conducted by 600 MHz spectrometer at 25 °C.

2.5.3.3 ^{1}H NMR spectra of Da10

The ^{1}H NMR spectra of Da10 in D_2O showed an expanded spectrum consisting of multiple peaks from 7.5- 8.28 ppm (Figure 2.11; Table 2.4). In relation to PAH, two additional peaks i.e., at $\delta_{3.4\text{-}3.5}$ and at $\delta_{6.9\text{-}8.5}$ were obtained. These peaks correspond to the CH_3 proton groups linked to the nitrogen atom of the dansyl moiety (peak A in Figure 2.11) and protons of the naphthalene ring (peaks B-F in Figure 2.11) respectively. The grafting percentage from peaks (B-F in Figure 2.11) at $\delta_{7.5\text{-}8.3}$ was calculated as given below.

Grafting percentage

$$= \frac{\textit{Integration value of the } \delta_{8.3} \textit{ / 6 protons from } CH_3 \textit{ group attached to N of dansyl moiety}}{\textit{Integration value of } \delta_{2.5} \textit{ / number of protons in PAH } CH_2} \times 100$$

$$= \frac{(23.27 \,/\, 6)}{(100/\,2)} \times 100 = 7.7\%$$

The results indicate that 7.7% of the dansyl moiety was grafted on the PAH backbone, which appears to be in good agreement with the 8.4% obtained from the elemental analysis.

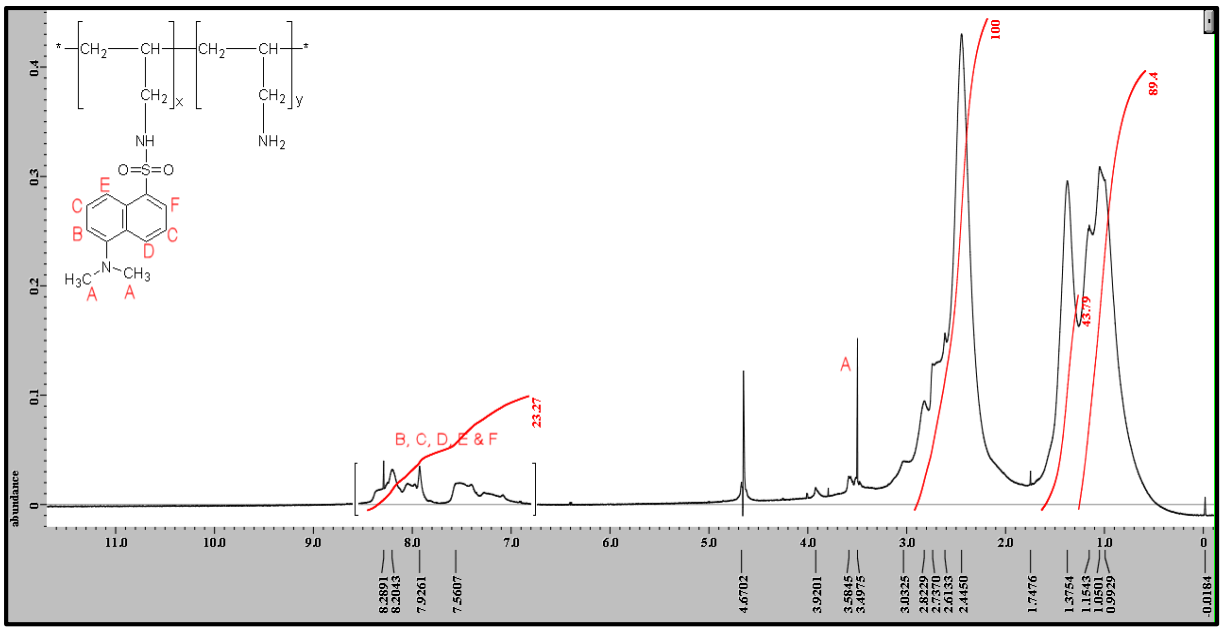

Figure 2.11 ^{1}H NMR spectra of Da10 in D_2O conducted by 600 MHz spectrometer at 25 °C.

2.5.3.4 ^{1}H NMR spectra of QPa2.5

Figure 2.12 shows the ^{1}H NMR spectra of QPa2.5 in D_2O. The ^{1}H NMR spectra of QPa2.5 showed additional peaks in comparison to the PAH spectra. The additional peak was found at $\delta_{3.19\text{-}3.2}$ in the ^{1}H NMR spectra after quaternisation of Pa2.5 (Figure 2.12, A). This peak corresponds to the quaternary ammonium moiety. This confirms the presence of quaternary ammonium moieties in the polymers. The grafting percentage from peaks $\delta_{3.19\text{-}3.2}$ in the ^{1}H NMR spectra after quaternisation of Pa2.5 was calculated as given below

Grafting percentage

$$= \frac{\text{Integration value of the } \delta_{3.2} \text{ / 9 protons in } CH_3 \text{ attached to quaternary ammonium moiety}}{\text{Integration value of } \delta_{2.5} \text{/ number of protons in PAH } CH_2} \times 100$$

$$\frac{(182\ /\ 9)}{(100/2)} \times 100 = 40.6\%$$

The grafting percentage (40.6%) calculated from peaks at $\delta_{3.19\text{-}3.2}$ corresponds well with the level of quaternisation obtained from the elemental analysis (46.6%).

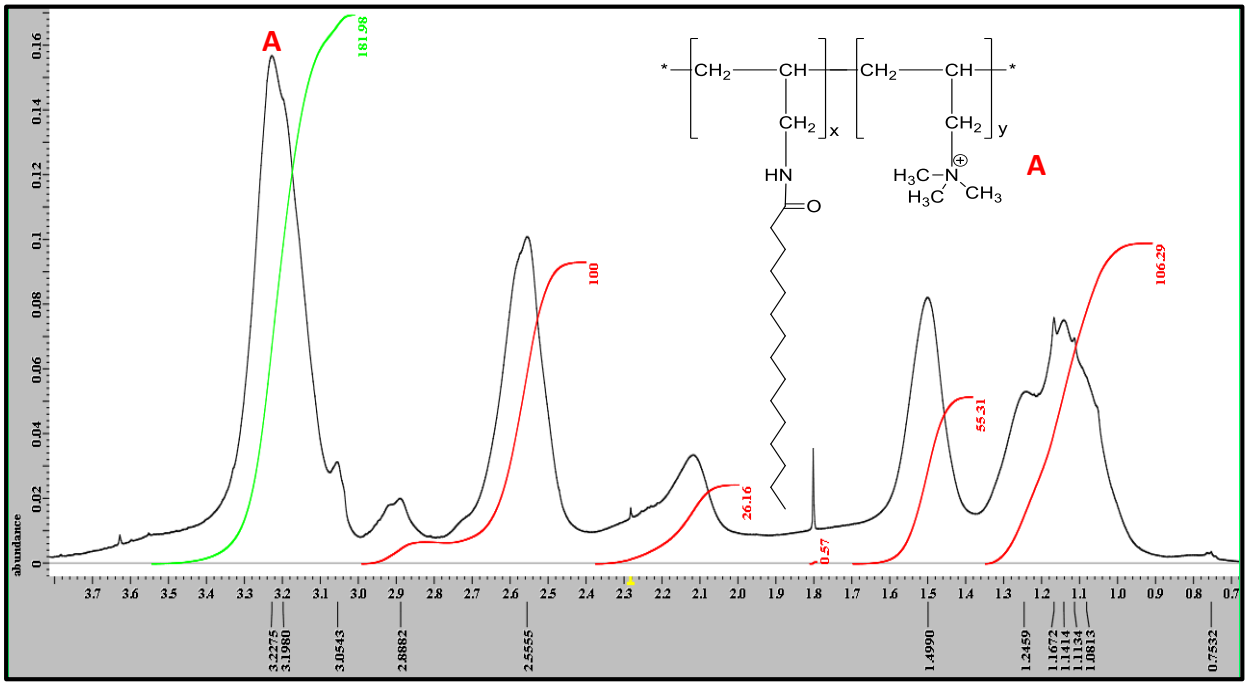

Figure 2.12 ^{1}H NMR spectra of QPa2.5 in D_2O conducted by 600 MHz spectrometer at 25°C.

2.6 DISCUSSION

PAH has previously been used in the gene-delivery systems due to the presence of primary amine functional groups, which allowed it's complexation with the negatively charged DNA [153]. The primary amine functional groups are also suitable sites for chemical modifications. Numerous reports have shown the ability of the modified PAH, like imidazolyl modified PAH [152], polyethylene glycol grafted PAH [250] and glycolated PAH [154] to reduce the cytotoxicity index compared to the unmodified PAH.

In this project, a hydrophilic (QPa2.5) and two hydrophobic combed-shaped amphiphilic polymers (Pa2.5 and Da10) were synthesised successfully by grafting hydrophilic and hydrophobic grafts on to the PAH backbone. All the modified polymers displayed good percentage yield; Pa2.5= 86%**,** QPa2.5= 65% and Da10= 82%. Presence of hydrophilic and hydrophobic grafting on the PAH backbone was confirmed and quantified by using elemental analysis and NMR spectroscopy. Elemental analysis data determined the elemental composition whereas the corresponding ^{1}H NMR spectra allowed determination of the approximate number of protons per structural unit.

The element molar ratios of the PAH obtained from the elemental analysis (3.05:7.87:1) corresponded well with the theoretical atoms ratio of the PAH monomer (3 C's, 7 H's and 1 N). The percentage grafting of the Da10 (8.4%) and Pa2.5 (4.3%) obtained from the elemental analysis were close to the initial molar feeds. The degree of quaternisation of Pa2.5 was found to be 46.6%. Thus the findings from the elemental analysis confirmed that hydrophobic (Pa2.5 and Da10) and hydrophilic (QPa2.5) moieties were successfully grafted on to the PAH backbone.

The proton assignments for the PAH on the ^{1}H NMR spectra were found to be, $\delta_{1.01,\ 1.1\ and\ 1.2}$ indicating CH_2 protons (A), $\delta_{1.35}$ - CH protons (B) and $\delta_{2.4}$ indicating CH_2 protons adjacent to NH_2 group (C). The chemical shift of proton in ($-NH_2$) is dependent upon the temperature, solvent, concentration and the neighbouring group. The signals from the proton attached to NH_2 group appeared obscured which may be ascribed to the fast exchange with deuterium. The integration ratio 1.91:1:1.86 of peaks of the PAH monomer determined from ^{1}H NMR relates well to the theoretical monomer structure of PAH (CH_2: CH: CH_2), i.e., 2 protons: 1 proton: 2 protons

The ^{1}H NMR spectrum of the hydrophobically substituted PAH i.e., Pa2.5 resonated a small singlet peak at $\delta_{0.73}$ for protons from the terminal CH_3 proton and CH_2 protons of palmitoyl pendant group. The percentage modification was found to be 5.7% from the ^{1}H NMR and 4.3% from the elemental analysis.

Aromatic protons are absorbed in a region between 6-8.5 ppm. Multiplet peaks were recognized in the absorption region from 7.5 to 8.2 ppm due to overlapping between protons of different carbons in the naphthalene rings, which were assigned to the protons of the dansyl group. This higher chemical shift ($\delta_{7.5\text{-}8.2}$) towards the downfield upon dansylation confirms the presence of aromatic signal from the naphthalene ring of the dansyl moiety. Due to the multiple peaks splitting, it was difficult to differentiate between peaks of various equivalent protons. However, the presence of these peaks indicate the grafting of dansyl moiety on to the PAH backbone. The percentage grafting of Da10 calculated from NMR (7.7%) was found to be in close agreement with the initial molar feed as well as the results achieved from elemental analysis (8.4%).

Signals of the methyl groups from the quaternary ammonium group appeared in the lower field i.e., 3.5ppm. The percentage modification achieved from the elemental analysis was 46.6% while 40.4% from ^{1}H NMR, which are again consistent with each

other. The small variation between findings achieved from elemental analysis and ^{1}H NMR results may be attributed to the integration boundaries setting. The data from ^{1}H NMR studies together with elemental analysis confirms the grafting of the hydrophobic and hydrophilic moieties on to the PAH backbone.

2.7 CONCLUSION

Hydrophobic and hydrophilic moieties were successfully grafted on to the PAH backbone. The degree of substitution was confirmed by elemental analysis and nuclear magnetic resonance and was found to be in agreement with each other.

Chapter 3

FABRICATION OF TERNARY POLYELECTROLYTE COMPLEXES

3 INTRODUCTION

3.1 POLYELECTROLYTE COMPLEXES

Polyelectrolyte complexes have emerged as a very useful means for the delivery of protein drugs. They are formed spontaneously by a simple process which is devoid of potentially harmful organic solvents and heat [251-253].

As mentioned in chapter one, the conventional binary polyelectrolyte complexes are generally fabricated by using positively charged polymers which are known to be associated with non-specific binding with other negatively charged entities in the body, such as serum proteins [3, 97]. These polycation based systems also associated with a higher toxicity index [157]. Shielding the positive charge on particles reduces the non-specific binding, whereby the polymer is not recognized as a foreign entity in the body and consequently is not opsonised [254]. In addition, shielding of the charge has also been shown to reduce the toxicity associated with the binary systems [153].

A number of strategies have been employed by researchers to reduce the positive surface charge and hence the likelihood of non-specific interactions and charge associated toxicity. These strategies involve the modification of surface either with moieties which can effectively shield the surface charge such as PEGylation with poly (ethylene glycol) [254] or layer by layer technique where alternating layers of polycation and polyanion are tailored to achieve the desired morphology, surface charge and surface composition [255]. Boussif *et al.* has shown that modification of PAH with hydrophilic methyl glycolates not only enhanced its ability to mediate gene transfer into cells but also decreased charge associated cytotoxicity [154].

Ternary polyelectrolyte complexes have shown to reduce the positive surface charge and hence the associated toxicity and non-specific interactions with the biocomponents [127, 131, 256]. Nimesh *et al.* has shown that polyallylamine-dextran sulphate-DNA (PAH-DS-DNA) nanoplexes considerably reduced the cytotoxicity associated with positive charge of polyallylamine [153]. A number of ternary polyelectrolyte systems such as poly(e-caprolactone)-graft-poly(N, N-dimethylaminoethyl methacrylate-DNA-polyglutamic acid-graft-polyethylene glycol complexes [127], polycaprolactone-graft-poly(N,N-dimethylaminoethyl methacrylate) [256] and polyanion/pDNA/PEI complexes [131] have been prepared recently to reduce the positive surface charge and

hence toxicity associated with the corresponding binary complexes. Peng *et al.* showed that adding different anions and controlling their concentrations reduced the nonspecific interactions and hence the toxicity of chitosan nanoparticles to the cell membranes [257]. Poly(acrylic acid) (PAA) and dextran sulphate (DS) are two commonly used polyanions which have been used to form ternary complexes by a number of research group [258-260].

3.1.1 Polyanions

3.1.1.1 Poly (acrylic acid) (PAA)

Poly (acrylic acid) (PAA) is a weak polyacid with high density of carboxylic acid units on its surface which are deprotonated to yield negatively charged moieties (COO^-) (Figure 3.1). The COO^- units are known to interact with the amines (NH_3^+) of proteins to form polyelectrolyte complexes [261].

PAA was chosen for the study because of its *in vivo* and *in vitro* biocompatibility [262]. Wang *et al.* coated CeO_2 nanoparticles with dextran or PAA due to their enhanced biocompatibility properties, low toxicity, and reduced clearance by the immune system [260]. Zhang *et al.* has shown the ability of PAA to crosslink with PAH and improve the stability of complexes via interaction between carboxyl of PAA and amine groups of PAH [263].

The carboxyl groups on surface of PAA form mucoadhesive bonds with the mucosal surface [264]. This allows it to adhere to the gastrointestinal mucosal lining and improve the complex uptake by intestinal enterocytes [265]. This property permits the PAA based delivery system to increase the bioavailability of associated drug.

PAA has been used as a scaffold for immobilization of biologically active molecules e.g., molecules containing amine groups such as proteins [266]. It has also been used to stabilize magnetic nanoparticles by providing electrostatic and steric repulsion against particle aggregation [261].

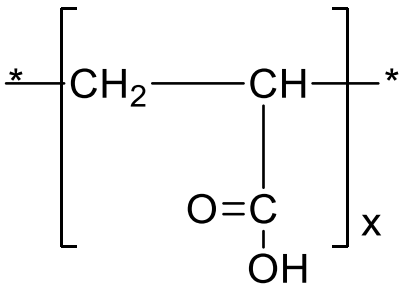

Figure 3.1 Chemical Structure of Poly(acrylic) acid

3.1.1.2 Dextran Sulphate (DS)

The polyanion dextran sulphate (DS) is a member of the family of glycosaminoglycan. It is a hydrophilic polysaccharides synthesized from the fermentation of sucrose by the enzymes, bacteria (*Leuconostoc mesenteroides*) or yeast [73]. It comprises of a branched chain of anhydroglucose units which contain approximately 2–3 sulphate groups per glucosyl unit (Figure 3.2) [267]. The presence of the sulphate groups (SO_4^{-2}) ensures strong electrostatic interactions with the amino groups of proteins and polycations [96, 137].

DS is used in this study because of its biodegradability and biocompatibility [96, 153]. It has widely been used as blood plasma substitute and as a delivery vehicle of drugs due to its good biocompatibility and aqueous solubility [268]. It is characterized by its high molecular weight (3000- > 1 000 000 Da) and low toxicity [260]. Its hydrophilic nature allows it to complex with the water soluble proteins [96]. DS benefits from its low pKa which permits a charged state over a broad pH range. DS has also been shown to act as a colloidal protectant via steric hindrance.

DS has been found capable of reducing the cationic charge of PEI nanoparticles [55]. Studies have shown that PEI and DS self-assemble at room temperature to complex amphotericin B [252], insulin [122] and DNA [269]. It has also been reported that DNA and insulin structures are protected when DS is used in the formulation of PEI-DS nanoparticles [55, 122].

DS has been used to prepare chitosan-DS by a number of research groups [55, 258, 270-272]. It has been used to complex anti-angiogenic hexapeptide (ARH peptide) [270], bovine serum albumin (BSA) [258], curcumin [271] and insulin [72]. The advantages of CS-DS nanoparticles [258, 270] are enhanced stability and increased mechanical strength over binary systems and CS-TPP microparticles [72]. The lower

stability and mechanical strength of binary systems and CS-TPP microparticles limit their usage as drug delivery systems. Pan *et al.* reported that chitosan-tripolyphosphate (CS-TPP) nanoparticles dissolved and dissociated at low pH in several minutes [49] whereas chitosan-DS complexes were stable in low pH [270]. Recently DS has also been used to complex modified chitosan such as glycol-chitosan (GCS) [273] and N-(2-hydroxyl) propyl-3-trimethyl ammonium chitosan chloride (HTCC) (Shu, Zhang, Wu, Wang, & Li, 2011) to spontaneously form methotrexate-loaded glycol-chitosan-DS (GCS–DS) and HTCC-DS respectively upon mixing DS aqueous solution (0.1% w/v) under magnetic stirring.

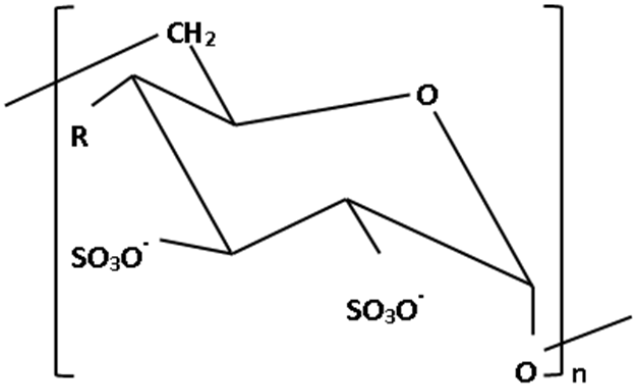

Figure 3.2 Chemical Structure of Dextran Sulphate

The present study aimed to incorporate a polyanion (PAA or DS) into the binary complexes (PECs, between polycation and protein) to form ternary complexes (APECs between a polycation, polyanion, protein) to alleviate the problems of toxicity and non-specific interactions associated with the binary complexes. Each polyanion (DS, 6-10KDa and PAA, 1.8KDa) was complexed with a polycation (PAH, palmitoyl grafted PAH (Pa2.5), dansyl grafted PAH (Da10) or quaternised palmitoyl PAH (QPa2.5) to form eight NIL ternary polyelectrolyte complexes (APECs). Insulin was used as a model protein to form eight IL ternary APECs. The PECs were used as a control. The effect of different hydrophobic groups (Pa2.5 and Da10) and quaternisation on the formation and stability of the APECs was established. The influence of polyanion on the physico-chemical properties, stability and insulin association efficiency of APECs was also investigated. The changes in formulation pH, temperature and ionic strength have significant effect on the stability of complexes [125]. Therefore, the stability of PECs and APECs was assessed and compared at varying pH (7.4, 6.6 and 1.2), ionic strength (NaCl 68mM, 102mM, and 145mM) and temperature (25^{o}C, 37^{o}C, 45^{o}C).

3.2 POLYELECTROLYTE INTERACTION AND COLLOIDAL STABILITY

The ability of a colloidal dispersion to resist aggregation is defined as colloidal stability [274]. The stability of the colloidal systems is well- explained by Derjiaguin, Landau, Verwey and Overbeek (DLVO) theory (Figure 3.3) [275]. This theory provides a concept for assessing the balance between repulsive and attractive interactions between two particles in a dispersion which serves for their stability [276]. It is based on the principle that the forces between two particles are determined by the sum of two forces i.e., van der Waals attractive forces and electrical double layer repulsive forces [277]. As the particles in a solution approach each other due to Brownian motion, an energy barrier resulting from the electrical repulsive forces prevent the particles from diffusing close to each other [278]. However, in case the repulsive forces are weak or if the particles collide with sufficient energy to overcome the energy barrier, the short-range Van der Waals attractive forces may pull the particles closer leading to aggregation or flocculation [278]. Therefore, a balance of the repulsive and attractive forces is required to maintain the stability of the particles which is essentially dependent on the magnitude of the surface charge.

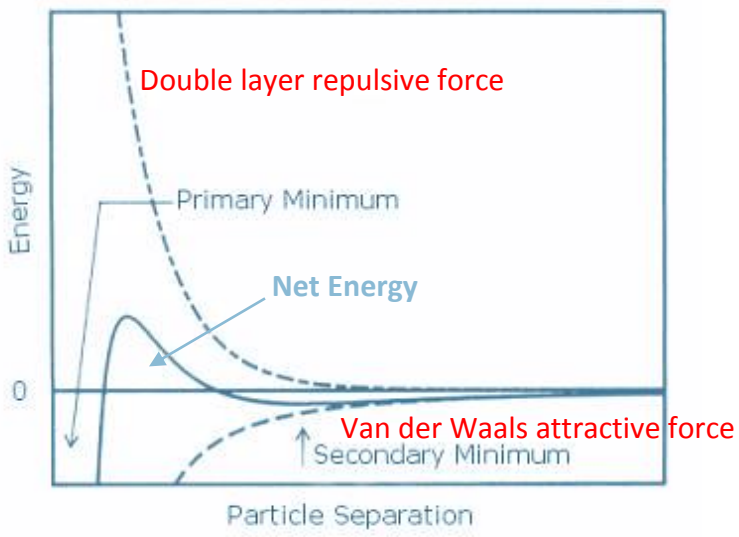

Figure 3.3 The interaction forces involved in a colloidal particulate system as stated by DLVO theory. The net energy is given by the sum of both attractive and repulsive forces when particles approach each other (Adapted from Malvern instrument ltd., 2004).

3.2.1 Factors influencing the formation and stability of polyelectrolyte complexes

3.2.1.1 Effect of pH on stability of ternary complexes

The formation of polyelectrolyte complexes requires the polymers/protein to be in an ionised state and bear opposite charges to mediate electrostatic interaction [79]. However, the degree of ionisation of charged groups of colloidal dispersions is affected by small changes in pH which subsequently affect the charge density of the polyelectrolyte solution [279, 280]. This is the reason that the formation of polyelectrolyte complexes occurs in a limited pH range, i.e., at pH values in the vicinity of pKa of the polymers/protein [125]. The acidic and basic groups of polymers exist in a protonated form at acidic pH and deprotonated form at alkaline pH. Therefore, the amino groups from the polyelectrolytes are ionised at an acidic pH (i.e., pH below their pKa) when they exist in their protonated form (NH_3^+) while remain deprotonated and hence unionised at pH above their pKa. On the other hand, the acidic groups such as carboxylic acid and sulfonyl groups are completely deprotonated/ionized (COO^-) at basic pH (i.e., pH above their pKa) and are protonated (COOH) at a pH below their pKa. Consequently, basic groups are ionised at acidic pH while acidic groups are ionised at alkaline pH [281]. This shows that the stability of the complexes depends upon the pH of the medium. It is essential that the polyelectrolyte complexes are stable at physiological pH of the stomach (pH 1.2−2.5) as well as the intestine (pH 6.6) to cargo the protein drug safely across the cellular barrier in the intestine. However, it is difficult to achieve a system which is stable at both stomach and intestinal conditions as both the cationic and anionic polyelectrolytes are required to be in their highly charged state to achieve optimum complexation and stability at aforementioned pH.

There have been investigations on the influence of formulation pH on the stability of polyelectrolyte complexes. Reschel *et al.* has shown that the stability of complexes formed by polycations depend on their basicity i.e., number of primary amine groups and their degree of dissociation. It was shown that the coagulation of poly[N-(2-aminoethyl)methacrylamide trifluoro acetate (PAEMA) complexes started at lower pH values than for poly(L-lysine) (PLL), which was assigned to its higher basicity [282]. By contrast, the lower basicity of PLL led to a higher degree of dissociation of amino groups of PLL compared to those of PAEMA. Burnova *et al.* investigated the effect of pH on ternary interpolyelectrolyte complexes of insulin-

poly(methylaminophosphazene) hydrochloride-dextran sulphate complexes (PMAP-DS). It was shown that under conditions imitating the human gastric environment (pH 2, 0.15 M NaCl), insulin-PMAP-DS complexes showed a complete immobilisation of insulin in the complexes. However, under conditions imitating the human intestinal environment (pH 8.3, 0.15 M NaCl), the ternary complexes were shown to dissolve and dissociate leading to free insulin and soluble binary insulin-PMAP complexes [136].

Investigations have been done to increase the stability and prevent the dissociation of complexes at a broader pH range. Quaternised groups have been introduced in polycations such as chitosan [259] and polyallylamine [120] to increase their stability at a wider pH range. It is thought that quaternisation can prevent the loss of protein drugs in the gastric cavity by generating electrostatic interaction at a wide pH range due to a permanently charged state [259]. At pH 6.0, TMC a quaternised derivative of chitosan and γ-PGA are ionised and therefore form spherical shaped polyelectrolyte complexes. γ-PGA has a pKa of 2.6 and therefore, at pH 1.2-2.0, most carboxylic groups on γ-PGA remain unionised. Hence, there was little electrostatic interaction between TMC25 and γ-PGA, leading to disintegration of the complexes. At pH values above 6.6, the free amino groups on TMC25 are deprotonated, thus again leading to the disintegration of nanoparticles [186]. These findings show that type of polyanion plays an important role in the stability of complexes.

DS has a much lower pKa (1.2) which ensures a charged state at highly acidic pH resulting in greater stability. This effect has been demonstrated by Shu and group who prepared polyelectrolyte complexes via electrostatic interaction between HTCC and DS and investigated their stability at various pH. Since there were more $N^{+}(CH_3)_3$ groups in HTCC and more ionised SO_4^{-2} groups in DS, at pH 1-2 (simulating the pH in stomach after meal), pH 2.5-3.7 (simulating the pH in the fasting stomach) and pH 6.0-6.6 (simulating the pH in the duodenum) [186], therefore strong electrostatic interactions resulted and so the complexes remained intact over a broader pH range [259].

3.2.1.2 Effect of ionic strength on stability of ternary complexes

Stability of colloidal dispersion may also be affected by increasing the ionic strength of the medium [113]. The addition of salt in the polyelectrolyte solution can screen the charge on the surface of particles leading either to reduction in the net charge or charge neutralisation [113]. Reduction in charge reduces the mutual electrostatic repulsion

between the particles and causes them to aggregate [279, 283]. Holappa *et al.* studied the effect of salt concentration (20 and 80mM NaCl solutions) on the complexes formed between a diblock copolymer (comprising of an anionic block and an electroneutral one, poly(ethylene oxide-block-sodium methacrylate), PEO block- PMANa) and a polycation, poly(methacryloyloxyethyl trimethylammonium chloride) [284]. It was shown that increasing the salt concentration increased the particle size which was attributed by authors to screening of the repulsive charges which resulted in the formation of bigger complexes [284]. However, numerous reports have indicated the role of salt in facilitation of complex formation [285]. Recently, Yousefpour and co-workers have shown a salt dependent interaction of doxorubicin-DS particles [285]. Besides, it has been shown by Sun *et al.* that the addition of NaCl up to 300mM did not bring any change in the size of complexes suggesting their stability in the salt conditions [54].

3.2.1.3 Effect of temperature on stability of ternary complexes

The temperature may or may not affect the polyelectrolyte complexes adversely. It may bring about a change in aqueous solubility of the polymers resulting in soluble, less soluble or insoluble systems [286]. It is thought that certain molecular interactions such as hydrogen bonding and hydrophobic effects are temperature dependent [287]. Therefore, an elevated temperature may favour/oppose polymer chain association leading to chain rearrangements which subsequently changes the particle conformation [288]. The hydrophilic segments of polymer chain may experience dehydration caused by the desolvation of water molecules upon increase in temperature. This may cause loss of interaction of polymer chain with water molecules leading to destabilisation of complexes [112]. Alternatively, the polymeric chains may acquire a more hydrophobic structure and hence stronger hydrophobic association leading to a shrinkage in size [288]. Kleinen *et al.* has shown that increase in temperature causes shrinkage in particle size which subsequently increases the colloidal stability [289]. Mao *et al.* also reported that elevated temperatures facilitated polyelectrolyte complex formation (Mao et al., 2001, 2005a).

3.2.1.4 Effect of formulation parameters on stability of ternary complexes

The formation and stability of polyelectrolyte complexes may be controlled by manipulating the formulation parameters. The mixing ratio of polycations and polyanions is a crucial parameter that controls the stability of complexes. Chen *et al.*

has shown that the particle size, surface charge and protein complexation efficiency are all dependent on the polycation: polyanion (Chitosan: DS) ratio [270]. Reduction in particle surface charge reduces the electrostatic interaction between polymeric chains resulting in change in particle sizes. The non-stoichiometric polycation/DNA complexes prepared with an excess of polycation have been shown to possess a positive surface charge [282]. However, the introduction of polyanion in binary complexes reduces the positive charge and hence the charge ratio. Chen *et al.* has shown that the charge of arginine-rich hexapeptide loaded nanoparticles changed from positive to negative on addition of the DS indicating that complexation has occurred [270].

Umerska *et al*. has shown that addition of hylauronic acid in chitosan at first either decreased the particle sizes slightly with decreasing hylauronic acid/chitosan ratio or did not change the size significantly [290]. However when the charge ratio reduced to an extent that polymers approached a charge equivalence point ($n-/n+ = 1$), the particle sizes rapidly increased and large aggregates were formed. This behaviour was attributed to a decrease in electrostatic repulsion between the particles as the net surface charge decreased [290]. Hu *et al.* has also shown that the ratio of chitosan to acrylic acid influenced the mean particle size [253]. The surfaces of chitosan–PAA nanoparticles was found to have positive charge of about 20–30mV at different ratio of chitosan to acrylic acid [253]. However, as the ratio of chitosan/acrylic acid increased, the ZP also increased and vice versa [253]. Tiyaboonchai and colleagues showed that as the charge ratio of PEI to DS increased from 0.5:1 to 3:1, the mean particle size decreased [122].

The polymer charge ratio has shown a considerable influence on the viscosity of colloidal dispersion [290]. When one of the polymers is used in excess, there are still molecules of that polymer which do not participate in the formation of complexes or which only weakly interact with the complexes, these polymer molecules are responsible for increasing the viscosity of the colloidal system [290].

Chen *et al*. has shown that the charge ratio of the two ionic polymers i.e., chitosan and DS affects the complexation efficiency of bovine serum albumin by altering the electrostatic binding with the protein [258]. The higher the charge ratio, the higher was the entrapment efficiency [258]. However, on the other hand, Peng *et al* has shown that adding different anions in chitosan and controlling their concentrations did not influence DNA encapsulation [257]. Saboktakin *et al.* investigated the effect of the

order of mixing of polymers and protein on the complexation efficiency of 5-aminosalicylic acid (5-ASA). They showed that the order of mixing had no effect on the complexation efficiency of 5-ASA as well as the size of 5-ASA-loaded chitosan-DS [291].

The polymer architecture has been found to have significant effect on the physicochemical properties of complexes [120]. Thompson *et al.* has shown that the level of grafting and type of hydrophobic pendant groups has an impact on the behaviour of the assemblies in water [120]. Increasing the hydrophobic load was shown to reduce the particle size. The authors attributed this effect to the ability of higher hydrophobic payload to shield the hydrophobic portions from water more effectively due to stronger hydrophobic interactions. On the other hand, their counterparts required more amphiphilic polymers to come together to achieve the same level of protection which resulted in an increase in hydrodynamic size of complexes with less hydrophobic payload [120].

The presence of hydrophobic moieties in copolymers also enhance the stability of complexes due to the added hydrophobic associations as compared to non-hydrophobic complexes. Filippov *et al.* has shown that the colloidal stability of polyplexes increases with increasing the hydrophobic cholesterol content in polycations [251]. The complexes prepared from polycations P17 with the lowest content of cholesterol showed the highest coagulation rate. The rate of coagulation was lower for the polyelectrolyte complexes prepared with polycations bearing higher amounts of cholesterol [251]. Reschel *et al.* has also shown a higher stability of (PAEMA)/DNA complexes, compared to PLL/DNA complexes which was attributed to a more hydrophobic nature of the polymer carbon chain [282].

The presence of bulky groups in the side chain of the polycation have been reported to have notable effects on the protein complexation efficiency and physicochemical properties of complexes [120, 292]. The permanent positive charge of bulky quaternised polymers have shown increased inter-chain repulsion and ability to counteract the hydrophobic interactions between grafts [120]. The bulky side chains on chitosan have shown significant steric hindrance effects that reduced the charge based interactions leading to low protein complexation efficiency [292].

A number of research groups have shown that the use of a cross-linker such as tripolyphosphate (TPP) or zinc sulfate ($ZnSO_4$) is essential for the formation and stability of the complexes [122, 293]. The cross-linker stabilises the particles through interactions with polymeric chains [73]. However, high concentration of TPP has been shown to be unfavourable, as it neutralised the positive charge of chitosan and led to aggregation of the complexes [294]. This is the reason that cross-linkers are used in a very low concentration to prevent aggregation of the polyelectrolyte complexes. Tiyaboonchai and colleagues studied the role of concentration of cross-linker ($ZnSO_4$) on the physicochemical properties of PEI-DS [122]. It was found that a concentration of 15–25μM $ZnSO_4$ was optimal in producing stable PEI: DS (1.5:1, pH 9 PEI solutions). It was also shown that as the amount of $ZnSO_4$ was increased, the particle size decreased [122]. Precipitation was observed at higher concentrations of $ZnSO_4$ (35μM). Formulations prepared without $ZnSO_4$ showed a mean particle size twice as large as before lyophilisation [122].

Umerska *et al.* prepared polyelectrolyte complexes composed of hyaluronic acid and chitosan which were found stable in the absence of cross-linker [290]. It was shown that chitosan (CL213 and G213) with a higher molecular weight produced larger and fast sedimenting chitosan-hyaluronic acid particles than the low MW chitosan. The authors attributed this effect to the presence of more amino groups on the long polymer chain of high MW polymer than low MW polymer which interacted with carboxyl groups of hyaluronic acid leading to large particles and aggregates [290].

A number of researches have shown the ability of polyelectrolyte complexes to protect protein conformation and activity from enzymatic degradation and at low pH [73, 122, 295]. PEG-graft-trimethyl chitosan-insulin nanocomplexes were shown to protect insulin from enzymatic degradation [295]. Similarly, PEI-DS have been reported to protect DNA [269] and insulin structures [122]. Tiyaboonchai and colleagues have shown that the structurally altered insulin, completely dissociates from PEI in higher (153mM NaCl) ionic strength medium and returns to a native-like conformation [122]. The insulin- poly(methylaminophosphazene-DS (Insulin-PMAP-DS) complexes have not only been shown to protect the insulin in the acidic conditions but also to preserve the insulin conformation [136]. Sarmento *et al.* reported that chitosan-DS complexes showed the preservation of immunogenic bioactivity of insulin [296]. This is the reason that all novel polyelectrolyte systems should be characterised

to determine their physicochemical properties such as particle size and surface charge to elucidate their formation and stability at various conditions.

3.3 CHARACTERISATION OF POLYELECTROLYTE COMPLEXES

The properties of polyelectrolyte complexes such as particle size, size distribution (PDI) and surface charge (ZP) have been identified as essential parameters for their characterisation [297, 298].

3.3.1 Particle size and size distribution

Particle size determination is the key step in the characterisation of polyelectrolyte complexes [297, 299]. It is a very useful indicator for determination of many properties of particulate materials. The colloidal particles have a size in the range between 1 to 1,000 nm which allows them to remain dispersed in the aqueous environment whereas larger particles >1 micron are susceptible to sedimentation [115, 300].

The colloidal dispersions rarely exist as monodisperse systems (one size) [301]. The more similar the size of particles in a particular system, the narrower is the size distribution [302]. On the other hand, a broad size distribution results from a wide range of particle sizes. A PDI closer to 0.1 on a scale from 0 to 1 is considered to have a homogenous particle population [302, 303]. A high PDI reflects a dispersion comprising of a number of different particle sizes. Each particle size may show different functionality such as uptake, biodistribution, immune generation and elimination (Table 3.1). The different particle sizes in a colloidal dispersion prevent the demarcation of size dependent functionality of particles. This makes the low PDI an essential requirement for a formulation [298].

Slight differences in particle size have significant implications on the cellular uptake, mechanisms of uptake process, biodistribution and bioavailability of the nanocarriers (Table 3.1) [297, 304]. The nanocarriers of size ≤200nm have shown efficient biodistribution and targeted delivery [302, 305, 306]. They have been shown to avoid uptake by reticuloendothelial system (RES) and mononuclear phagocytic system (MPS) and thus attain an extended circulation time as compared to the particles with larger diameter [305]. The smaller particles (20-30nm) undergo rapid renal excretion whereas large particles (>200nm) are phagocytized by the MPS of the lung, liver, spleen, and bone marrow [302, 305, 306]. Large particles (>200nm) have also been

reported to activate human complement system, and are rapidly cleared by Kupffer cells [305].

Numerous studies have reported that the uptake of particles increases with decreasing particle size [304, 305]. He *et al.* reported a size-dependent uptake of Rhodamine B labeled carboxylated chitosan grafted- bovine serum albumin nanoparticles where particle size ≤300 nm demonstrated higher uptake by gut enterocytes and M cells; and higher systemic biodistribution than the larger particle sizes (600 and 1000 nm) [304].

Table 3.1 A summary of the effects of nanocarriers' size on bio-functionality

Size of nanocarriers	Functionality
≤500nm	Endocytosis (Kulkarni et al.,2013)
≥200nm	Efficient phagocytosis [307] Activation of complement system (Paur et.al., 2011)
≤200nm	Efficient uptake (Hartig et al., 2007; Yin Win et al., 2005) Efficient bio-distribution (M. Gaumet et al., 2008; He et al., 2012) Avoid RES and MPS (X-M. Liu et al.,2004; Kulkarni & Feng, 2013) Extended circulation time (Kulkarni & Feng, 2013)
60-100nm	Receptor medicated uptake (Zhang et al., 2009)
<50nm	Paracellular transport (Kulkarni & Feng, 2013; Goldberg et al., 2003)
20-30nm	Rapid renal clearance (Kulkarni & Feng, 2013)

It has been reported by Kulkarni *et al.* that small sized polystyrene nanoparticles modified with the d-α-tocopheryl polyethylene glycol with a diameter of 100 nm demonstrated the highest uptake among range of particles tested [305]. These properties make the small particles 100-200 nm, more favourable delivery systems owing to their higher uptake and biodistribution [115, 308]. However, nanoparticles with large hydrodynamic sizes (600 and 1000 nm) have been shown to be phagocytized more efficiently by murine macrophages [304].

The size of particles also governs the route of particle uptake by the gut enterocytes such as paracellular passage (size < 50 nm) and endocytosis (size ≤500 nm) [305]. Zhang *et al.* has shown an upper limit of particle radii (60 nm) for receptor-mediated endocytosis [309]. All these investigations point towards the fundamental importance of measurement and control of the particle size of all delivery systems [88]. It is equally

important to determine the surface charge of particle which has been considered as the major factor in controlling the stability of the polyelectrolyte complexes.

3.3.2 Particle surface charge

ZP is an estimate of the surface charge of particles in colloidal dispersion [310]. The chemical groups on the surface of polyelectrolytes ionise in an aqueous solution to give a residual negative or positive charge on the particle surface, referred as the surface charge [310]**.** The oppositely charged ions form a counter-ion cloud around the ionised particles forming an electrical double layer (Figure 3.4) [311]. The net charge is thus derived not only from the surface charge but also from the surrounding counter-ions and reduced coions [280]. The inner region of the electrical double layer is known as the stern layer where the ions are strongly bound to the interfacial groups; whereas the outer region is called diffuse layer where the ions are less firmly associated [312]. There is an imaginary boundary in the diffuse layer called the hydrodynamic shear in which the ions and particles form a stable entity. The potential at this boundary is known as the zeta potential.

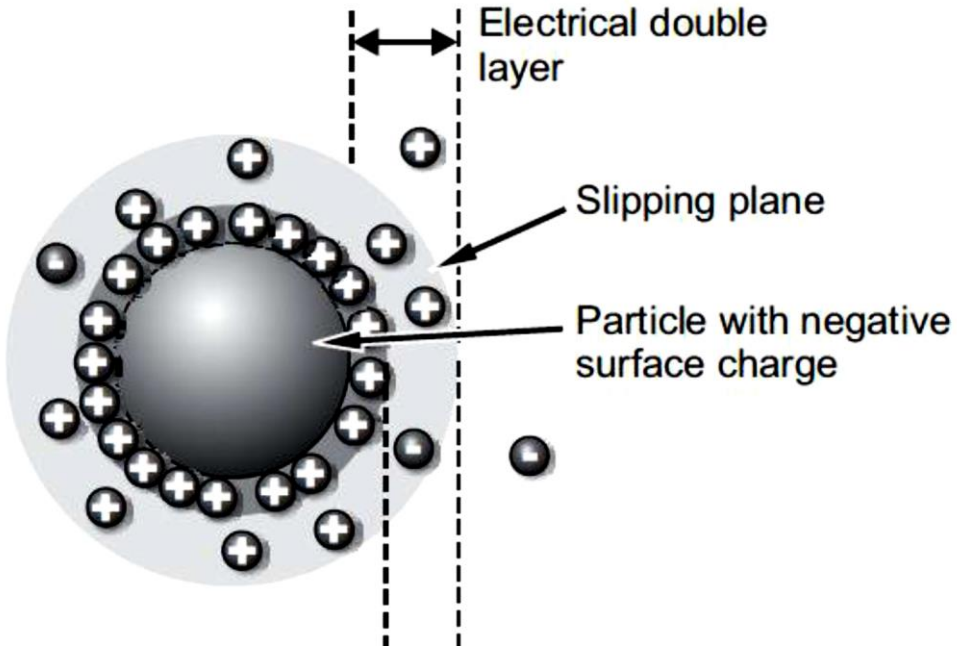

Figure 3.4 Schematic illustration of electrical double layer of a particle (Adapted from nanoComposix, 2012)

ZP is used to predict and control the colloidal stability [308, 313]. It is an indirect measure of the magnitude of the electrostatic repulsion between the particles [314]. ZP has an impact on a particle's tendency to associate with oppositely charged protein/polyelectrolyte [309]. A strong positive or negative charge is beneficial for electrostatic interactions with oppositely charged molecules, therefore large zeta potentials above (+/-) 30mV prevent aggregation and form an electrostatically stable dispersion [115, 315]. By contrast, the low ZP leads to a decrease in repulsive forces resulting in flocculation [314, 316].

ZP is often measured as a function of pH. A change in pH alters the degree of ionisation of polyelectrolytes and hence the ZP of particles. Dissociation of the acidic groups gives rise to a negatively charged particle surface whereas basic groups ionise to acquire a positively charged surface.

ZP also influences the uptake of particles by the cells and penetration of particles through the mucus layer of the GIT (de Campos, 2004). He *et al.* has shown that rhodamine B (RhB) labeled carboxymethyl chitosan grafted nanoparticles (RhB-CMCNP) and chitosan hydrochloride grafted nanoparticles (RhB-CHNP) bearing higher positive or negative surface charges are more attractive to macrophages than the nanoparticles with low surface charge [317]. The cellular uptake of positively charged RhB-CHNP-CPT increased with the increase in surface charge [317]. It was considered that nanoparticles with a higher positive charge exhibited a stronger affinity for the negatively charged cell membrane, accounting for its higher cellular uptake [317]. RhB-CMCNP of 150 nm in diameter displayed surface-charge-dependent cellular uptake, in the order -15 > -25 > -40 mV which was assumed to be due to the weakened electrostatic repulsion forces between the nanoparticles and the cell membranes.

Internalisation of NPs formed of cationic chitosan and its derivatives appeared to occur predominantly by adsorptive endocytosis [67, 205]. Harush-Frenkel and group has shown a low rate of endocytosis of the negatively charged (mPEG–PLA) nanoparticles which did not utilize clathrin-mediated endocytosis pathway [208]. On the other hand, positively charged (mPEG–PLA) NPs formed with cationic lipid stearylamine were internalized rapidly via the clathrin-mediated pathway [208].

3.3.3 Techniques for the physicochemical and morphological characterisation of PECs

Light scattering techniques are commonly used for the analysis of particle size and ZP [298]. In this study, dynamic light scattering (DLS) was employed to determine these physicochemical properties of the polyelectrolyte complexes. In addition, transmission electron microscopy (TEM) was used to characterize the morphological appearance of the polyelectrolyte carrier systems.

3.3.3.1 Dynamic Light Scattering

DLS, also called photon correlation spectroscopy or quasielastic light scattering is a valuable analytical technique for the analysis of submicron particulate systems (Figure 3.5) [299, 318]. It is used to determine the hydrodynamic size, PDI and ZP of particles. DLS determines these parameters by measuring the speed of motion of particles in a fluid medium referred to as "Brownian motion" (the erratic random movement of microscopic particles in a fluid, resulting from the continuous bombardment of the surrounding molecules).

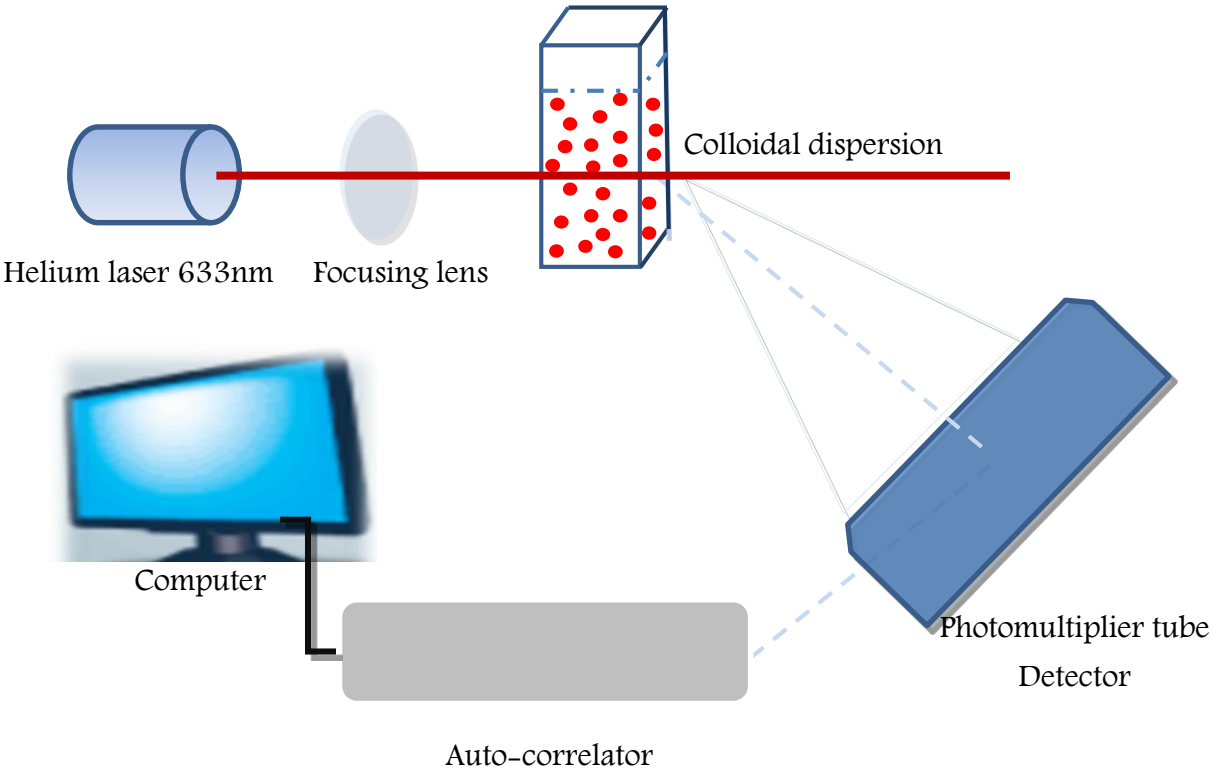

Figure 3.5 Schematic illustration of a Dynamic Light Scattering spectrophotometer

A DLS spectrophotometer is equipped with a 633nm helium-neon laser which is used as a standard light source. A monochromatic light from this laser passes through the nano-dispersed system and scatters in all directions upon interaction with the particles in the dispersion [319]. Since the particles undergo Brownian motion, significant intensity fluctuations are produced which are detected and analysed by an auto-correlation function which then yield the hydrodynamic radius of the particles [319]. These determinations are made on the basis of how fast the particles move within a system, due to the Brownian motion [299]. Generally, small particles move faster than larger particles at the same temperature.

ZP cannot be measured directly; however, it can be calculated from the electrophoretic mobility (the velocity of the particle in an electric field) of particles in a solution by DLS. When an electric field is applied, particles move towards the oppositely charged electrode [320]. As the amount of charge is proportional to the velocity of the particles, the ZP is estimated by measuring the velocity of the particles [314].

3.3.3.2 TEM

TEM is a very powerful tool used to study the morphological properties of nanoscale materials [321]. As the name indicates the principle of the technique is based on the transmission of a beam of electrons through the specimen via the condenser lens system to form an image [322]. The negatively charged electron beam passes through multiple electromagnetic lenses down the column and is focussed at a point. These focused electrons strike the specimen on the stage and bounce off, creating X-rays in the process which are converted into light signals [298]. These signals form an image which is focussed by the objective lens to a point and subsequently magnified by projector lenses onto an imaging device [322].

TEM produces high-resolution, two-dimensional, black and white images which allow direct visualisation of nano and microstructures [321]. It allows precise measurement of particle size and shape and can provide clear structural information. These properties make TEM a very reliable part for the characterisation of nanomaterials.

3.3.4 Quantification of protein complexation:

The protein association efficiency of the polyelectrolyte complexes is generally defined as the amount of protein bound to the polymer and is expressed as percentage association efficiency. Protein are complexed to the polyelectrolytes by electrostatic interaction. The amount of protein associated in polyelectrolyte complexes can be quantified by techniques such as high performance liquid chromatography (HPLC) [323] and enzyme linked immunosorbent assays (ELISA) [324].

3.3.4.1 High Performance Liquid Chromatography

HPLC is a chromatographic technique for quantitative and qualitative analysis of analytes in a sample. Among different types of chromatography, reverse phase high performance liquid chromatography (RP-HPLC) is commonly employed for identification and detection of peptide and proteins. It involves separation of molecules on the basis of their hydrophobicity [325].

RP-HPLC typically includes a sample injection device, high pressure pumps, column and a detector. The sampler takes the sample into the mobile phase stream which then transports it into the column. The pump provides the desired flow and composition of the mobile phase to the column [326]. The detector generates a signal which is proportional to the amount of sample coming out from the column, thus allows the quantitative analysis of the sample components. A digital microprocessor and user software provides the data analysis [326].

RP-HPLC is characterised for its excellent reproducibility and resolution. However, the main drawback is the irreversible denaturation of protein samples which reduces the biological activity of protein. For this reason the use of RT-HPLC for protein detection and quantification is discouraged and ELISA is preferred over it [327].

3.3.4.2 Enzyme Linked Immunosorbent Assay

ELISA is a commonly used biochemical technique for the detection of specific antigens in samples. It offers a simple and convenient method for the quantitative determination of proteins such as insulin in the samples [328]. The main advantage of ELISA is that it preferentially detects the active forms of protein and thus provides a good correlation to the bioactivity of protein [329].

A sandwich ELISA is a solid phase two-site enzyme immunoassay which is based on the direct sandwich technique [330]. The technique utilizes two antigen specific antibodies, i.e., a capture antibody bound to a solid phase and an enzyme linked detection antibody. The two monoclonal antibodies are directed against separate antigenic determinants on the protein molecule e.g., insulin [331]. The capture antibodies (peroxidase-conjugated anti-protein antibodies) first bind to the antigen (insulin) in the sample. Later on, anti-insulin antibodies are added which bind to antigen-antibodies conjugate. The bound conjugate is detected by reaction with a florescent marker such as 3, 3´-5, 5´-tetramethylbenzidine (TMB). The reaction is stopped by the addition of an acid, giving a colorimetric endpoint that is read spectrophotometrically.

3.4 AIM AND OBJECTIVES

3.4.1 Aim

Fabrication and characterisation of NIL and IL APECs for oral insulin delivery.

3.4.2 Objectives

- Preparation and characterisation of polycation solutions.
- Fabrication and characterisation of IL PECs.
- Fabrication and characterisation of NIL and IL APECs.
- Quantification of insulin in the PECs and APECs
- Determination of effect of pH (7.4, 6.6 and 1.2), temperature (25^{o}C, 37^{o}C and 45^{o}C), and ionic strength (68mM, 102mM, and 145mM of NaCl solution) on the stability of IL PECs and IL APECs.

3.5 MATERIALS AND METHODS

3.5.1 Materials

Materials	Supplier
0.8µM syringe filter (Millipore)	Fisher Scientific, UK
Amberlite 96 resin	Fluka, UK
Bovine insulin	Sigma Aldrich, UK
Bovine Insulin ELISA Kit	Meracodia, Sweden
Dansyl chloride	Sigma Aldrich, UK
Deionised water milliq apparatus	Millipore, UK
Dextran Sulfate (6-10KDa)	Sigma Aldrich, UK
Dialysing membrane (7 and 12-14kDa cut-off limit)	Medicell international Ltd, UK
Diethyl ether	Fisher Scientific, UK
Dioxane	Fisher Scientific, UK
Ethanol	Fisher Scientific, UK
Hydrochloric Acid	Fisher Scientific, UK
Methanol	Fisher Scientific, UK
Methyl Iodide	(Sigma Aldrich, UK
Palmitic acid N hydroxy succinimide ester	Sigma Aldrich, UK
Polyacrylic acid (1.8KDa)	Sigma Aldrich, UK
Polyallyllamine Hydrochloride (MW= 15KDa)	Sigma Aldrich, UK
Sodium Carbonate	Sigma Aldrich, UK
Sodium Hydrogen Carbonate	Sigma Aldrich, UK
Sodium hydroxide	Fisher Scientific, UK
Sodium Iodide	Sigma Aldrich, UK
Tris (hydroxymethyl) aminomethane	(Invitrogen) Fisher Scientific, UK

3.5.2 Method

3.5.2.1 Fabrication of PECs

3.5.2.1.1 Fabrication of polycation solutions (control)

Polycation solutions (8mgmL^{-1}) were prepared by dissolving 16mg of the polycation (PAH, Pa2.5, QPa2.5 or Da10) in 2mL of Tris buffer pH 7.4, under gentle magnetic stirring. The solutions were sonicated at maximum amplitude for 5min, using Soniprep 150 sonicator (MSE Ltd., UK) and were allowed to cool for 10min.

3.5.2.1.2 Fabrication of insulin loaded PECs (control)

The polycation solutions (4mgmL^{-1}) (PAH, Pa2.5, QPa2.5 or Da10) were prepared as described in section 3.5.2.1.1. Insulin stock solution (2mgmL^{-1}) was prepared by first dissolving the insulin powder in an acidic environment (150µL of 0.01 M HCl), followed by dilution with 0.1 M Tris buffer [332].

PECs were prepared by method reported by Thompson *et al.* [120]. Briefly, 2mL of 2mgmL^{-1} insulin solution in Tris buffer pH 7.4 was added drop wise into 2mL of 4mgmL^{-1} polycation solution under gentle magnetic stirring. The mixture was stirred at room temperature for 2h to form PECs. A final 2:1 polymer: insulin mass ratio was achieved. The following three PECs namely, IL Pa2.5, IL QPa2.5 and IL Da10 were produced spontaneously. Figure 3.6 depicts the schematic illustration of fabrication of PECs and APECs.

3.5.2.2 Fabrication of APECs

3.5.2.2.1 Fabrication of NIL APECs

Briefly, APECs were prepared in Tris buffer at pH 7.4 by adding 0.75mL of 8mgmL^{-1} of polyanion solution (DS or PAA) drop-wise into 1.5mL of 8mgmL^{-1} polycation solutions (PAH, Pa2.5, QPa2.5, and Da10) at a mass ratio 2:1 of Polycation:Polyanion. It was followed by addition of 250µL of 100µM $ZnSO_4$. The final volume was made up to 6mL with Tris buffer pH 7.4. APECs were spontaneously formed after stirring the solutions for 2h at room temperature. The following eight NIL APECs were produced namely, PAH–DS, PAH–PAA, Pa2.5–DS, Pa2.5-PAA, QPa2.5–DS, QPa2.5–PAA, Da10–DS and Da10–PAA.

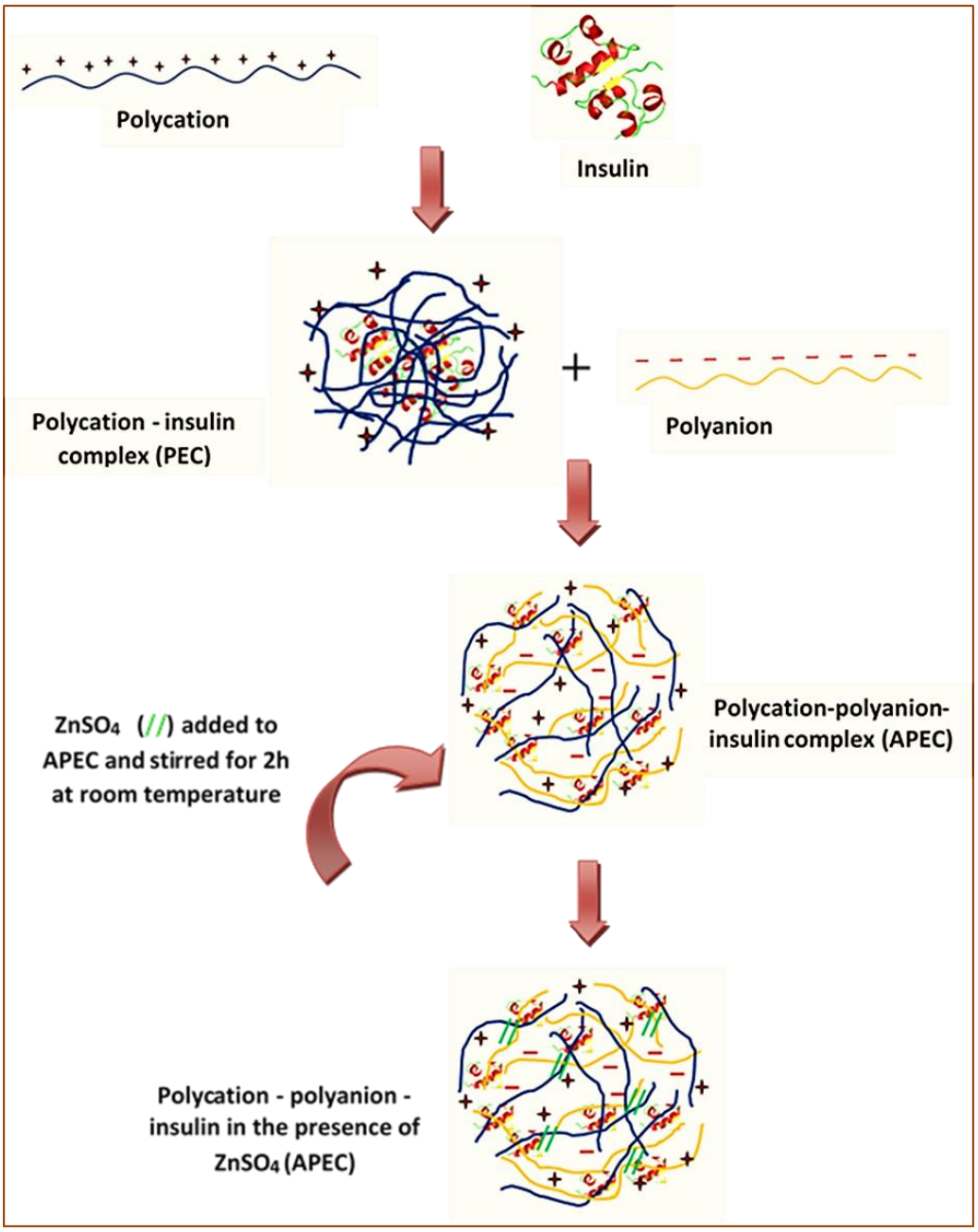

Figure 3.6 Schematic illustration of fabrication of PECs and APECs

3.5.2.2.2 Fabrication of IL APECs

1.25mL of insulin solution (2mgmL^{-1}) was added drop wise into 1.5mL of a polycation solution (8mgmL^{-1}) to achieve a polycation-insulin solution, which was stirred for 5 minutes under gentle magnetic stirring. 0.75mL of 8mgmL^{-1} of polyanion solution (DS and PAA) was added drop-wise into the polycation-insulin solution followed by addition of 250µL of 100µM $ZnSO_4$. The samples were stirred for 2h at

room temperature to allow formation of IL APECs. A final 2:1:0.42 of polycation: polyanion: insulin mass ratio was achieved. All solutions were filtered with a 0.8µM pore size filter. The following eight IL APECs were produced namely, IL PAH–DS, IL PAH–PAA, IL Pa2.5–DS, IL Pa2.5-PAA, IL QPa2.5–DS, IL QPa2.5–PAA, IL Da10–DS and IL Da10–PAA.

3.5.2.3 Characterisation of PECs and APECs

3.5.2.3.1 Measurement of particle size and zeta-potential

DLS measurements of the particle hydrodynamic size, ZP and PDI were performed at 25 ˚C on freshly prepared samples with a zetasizer 6.12 series (Malvern Instruments Limited, UK). Each measurement is representative of three distinct sets of data, given as mean± S.E (n=3).

3.5.2.3.2 Transmission electron microscopy analysis

A drop of PEC/APEC solution was mounted onto Formvar/carbon coated 200 mesh copper grid. It was dried down to a thin layer on a hydrophilic support film at room temperature. 1% aqueous methylamine vanadate (Nanovan; Nanoprobes, Stony Brook, NY, USA) stain was applied and the mixture air-dried. Specimens were zero-loss imaged with a LEO 912 energy filtering transmission electron microscope at 120 kV. Contrast optimised, zero-loss energy filtered digital images were recorded with a 14 bit /2K Proscan CCD camera [120].

3.5.2.3.3 Quantification of insulin association efficiency

The insulin was quantified by using bovine insulin ELISA immunoassay in accordance with the manufacturer's protocol as given below (Mercodia, Sweden).

i. Preparation of Enzyme Conjugate solution:

The required volume of enzyme conjugate solution 100µL/well was prepared by mixing enzyme conjugate in enzyme conjugate buffer (1:10). The solution was stirred gently to allow homogenous mixing.

ii. Preparation of Wash Buffer:

Wash buffer was prepared by diluting 40mL wash buffer in 800 mL distilled water.

iii. Preparation of Samples:

The IL PECs and APECs were prepared following the protocol stated previously (section 3.5.2.1.2 and 3.5.2.2.2). As the detection range of the ELISA test falls between 0.025-3μgL^{-1}, the samples were diluted serially to achieve a concentration of 1μgL^{-1} of insulin in samples.

iv. ELISA Plate Preparation:

Figure 3.7 displays the schematic illustration of the steps involved in the ELISA assay. 25μL of insulin calibrators and PEC/APEC samples were pipetted into appropriate wells of 96 well plate containing anti-insulin mouse monoclonal antibodies (mAB). 100μL of enzyme conjugate solution was added into each well. The plate was incubated on a plate shaker (Titramax, Heidolph, Germany) at 750 rpm for 2h at room temperature. The plate was washed 6 times with 700μL wash buffer per well to remove unbound insulin and enzyme conjugate solution. After the final wash, the plate was inverted and tapped against an absorbent paper. 200μL of substrate TMB was added into each well to act as a substrate for the enzyme conjugate solution. The plate was incubated for another 15 min at room temperature. Finally, 50μL of stop solution (sulphuric acid 0.5M, 50μL) was added to each well which changed the sample colour from blue to yellow. The plate was placed on the plate shaker for approximately 5 sec, to ensure appropriate mixing. The optical density was read at 450 nm, using a microplate reader (Synergy H4, Vermont, USA) and results were calculated as below.

v. Determination of association efficiency of the PECs and APECs:

The absorbance of the known insulin samples (1 mgmL^{-1} and 0.42mgmL^{-1}) which were diluted to achieve 1μgL^{-1} of insulin, were used as positive control (100%) and the absorbance of the sample containing no insulin was taken as a negative control. The value of the background absorbance of the negative control well was deducted from all the subsequent sample absorbance. The association efficiency was determined relative to the amount of insulin in the corresponding known insulin stock solution by the following equation:

$$\%\text{Association efficiency} = \frac{\text{Amount of insulin in unknown sample}}{\text{Amount of insulin in corresponding known sample}} \times 100$$

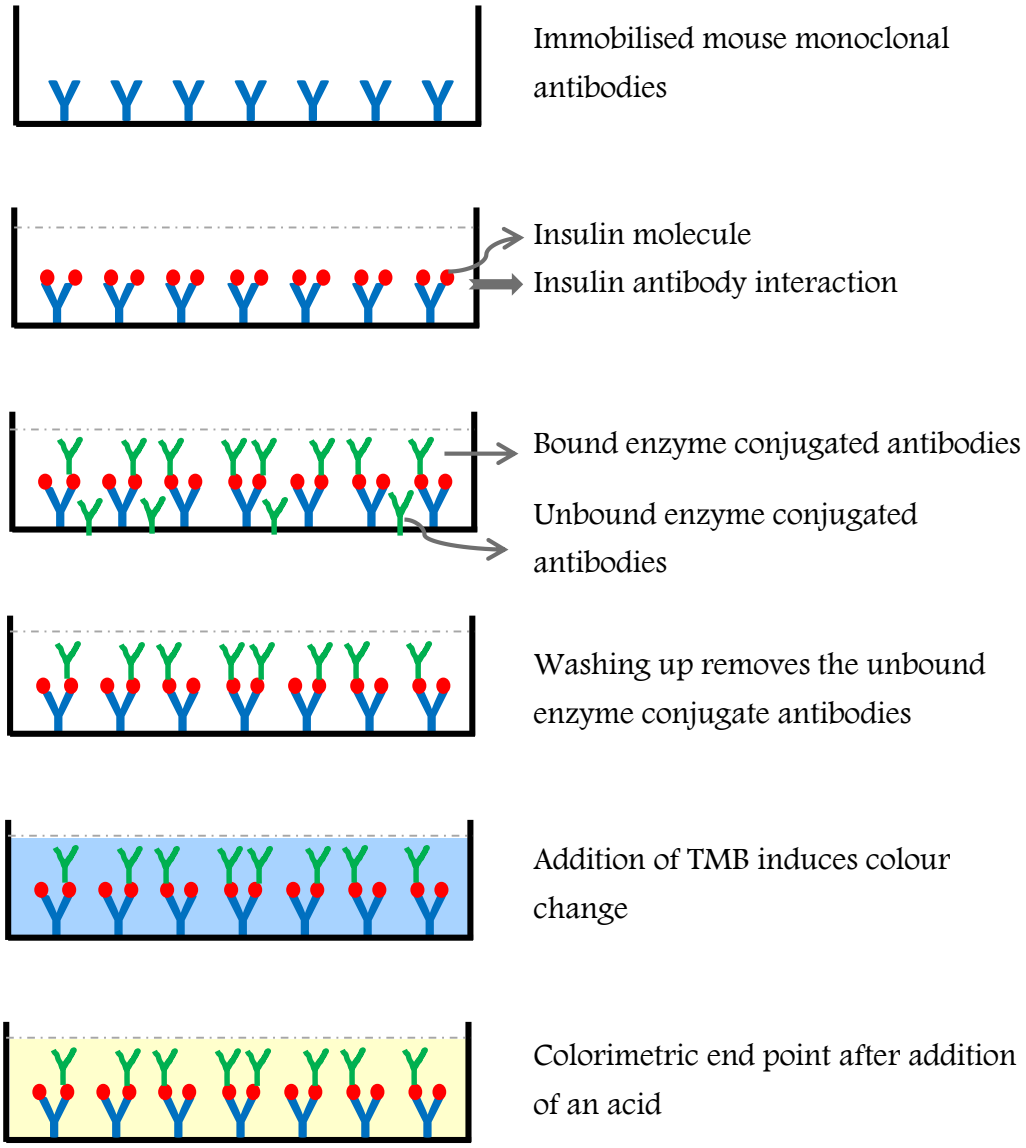

Figure 3.7 Schematic representation of quantification of insulin by Bovine Insulin ELISA

3.5.2.4 Stability studies

3.5.2.4.1 Effect of temperature

The IL PECs and APECs were prepared as described in section 3.5.2.1.2 and 3.5.2.2.2. They were incubated at 37˚C & 45˚C for 30mins and particle size, ZP and PDI were determined by DLS.

3.5.2.4.2 Effect of ionic strength

The influence of ionic strength on the stability of IL PECs and APECs was studied by incubating 6mL of the PECs/APECs solution with 338µL, 507µL and 721µL of 1.206M NaCl solution for 30min, to achieve final concentrations of 68mM, 102mM, and 145mM respectively. Particle size, ZP, and PDI were determined by DLS.

3.5.2.4.3 Effect of pH

The stability of IL PECs and APECs was investigated by incubating 2mL of sample at pH 1.2 and 6.6 for 4h and 6h respectively. The chosen pH reflects the pH in the stomach and small intestine respectively and the incubation time reflects the average residence time of a dosage form in these two regions. The samples were titrated to the respective pH by addition of required volume of 0.1M HCl (100-200µL/mL). The effect of pH on size and ZP was determined by DLS.

3.5.2.5 Statistical analysis

The samples were analysed for normal distribution. Statistical analysis was carried out using SPSS 20. One way analysis of variance (ANOVA) was performed using post hoc tukey's test. The values $p \leq 0.05$ were considered significant.

3.6 RESULTS

3.6.1 Characterisation of PECs and APECs

3.6.1.1 Dynamic light scattering

Table 3.2 represents the average size, ZP and PDI of polymer, PECs and APECs as determined by DLS. All formulations were obtained in a nanoscale range i.e., NIL polycation solutions (200-468nm), IL PECs (92-141nm), NIL APECs (78-435nm) and IL APECs (72-388nm). The introduction of polyanion (DS, PAA) in polycations (Pa2.5-200nm, Da10-208nm and QPa2.5-468nm) to form NIL APECs reduced the size of polycations. Polycations also demonstrated reduction in size upon complexation with insulin in PECs. However, the presence of insulin in APECs increased the size of APECs (except QPa2.5-DS and Pa2.5-PAA) compared to their NIL counterpart.

The general trend was a decrease in ZP of all PECs and APECs upon complexation with insulin. As expected, the introduction of polyanion was also able to reduce the ZP of all NIL and IL APECs. Among all APECs, the effect of reduction in ZP upon addition of polyanion was more pronounced in NIL QPa2.5 APECs (2.5 folds).

Table 3.2 Hydrodynamic size, ZP and PDI of NIL and IL PECs and APECs. The data represents the mean± SE of 3 experimental determinations.

	NIL polycation and APECS			***IL PECs and APECs***		
	Size(nm)	**ZP**	**PDI**	**Size(nm)**	**ZP**	**PDI**
PAH-DS	119±1	39±2	0.2±0.2	334±20	25±3	0.3±0.1
PAH-PAA	78±0.2	29±2	0.1± 0.0	94.2±0.4	0.06±3	0.1±0.0
Da10	208±0.2	32±3	0.1±0.0	92±1.2	26± 2	0.3±0.0
Da10-DS	91±3	23±2	0.1±0.08	96±1.2	22±3	0.2±0.2
Da10-PAA	101±2	29±4	0.1±0.02	106±0.8	25±4	0.2±0.0
Pa2.5	200±9	35±4	0.2±0.01	141±0.3	29±2	0.2±0.0
Pa2.5-DS	117±6	29±3	0.1±0.01	160±1.9	25±2	0.2±0.0
Pa2.5-PAA	122±15	29±2	0.1±0.02	101±2.7	25±2	0.2±0.0
QPa2.5	468±12	52±3	0.5±0.09	117±2.4	20±3	0.1±0.0
QPa2.5-DS	435±4	19±2	0.4±0.1	72±0.9	16±3	0.5± 0.0
QPa2.5-PAA	228±1	17±2.4	0.2±0.01	388± 29	7±2	0.5±0.0

3.6.1.2 Transmission electron microscopy analysis

Figure 3.8 displays the negatively stained TEM micrographs of various APECs. All APECs were found to be smooth and spherical structures. The sizes obtained were slightly smaller than the size achieved from DLS. Most of the APECs appeared as multicore structures (PAH-DS, Da10-PAA, Pa2.5-DS, Pa2.5-PAA and QPa2.5-PAA) surrounded by an outer layer.

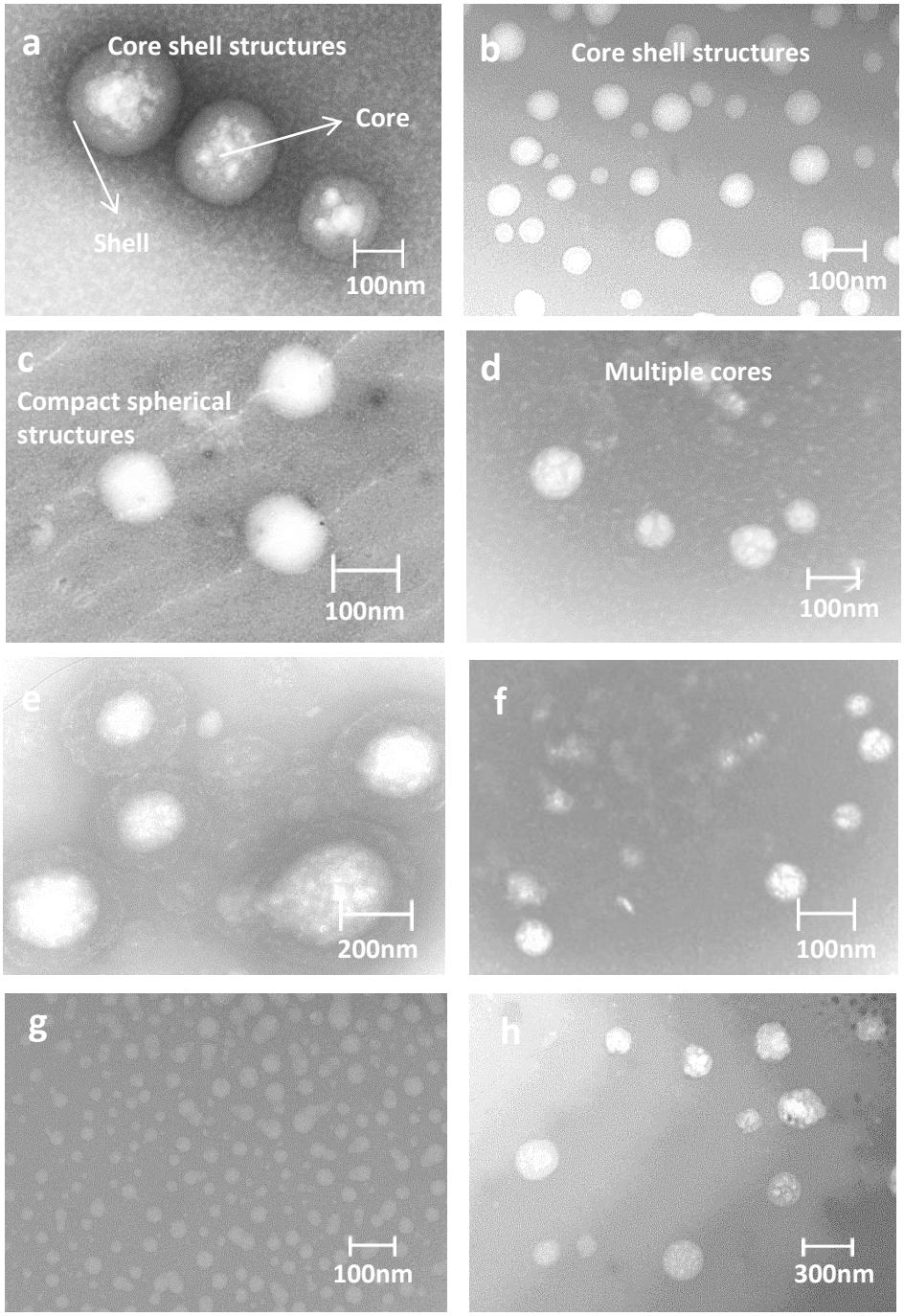

Figure 3.8 TEM micrographs of freshly prepared IL APECs insulin (a) PAH-DS (b) PAH-PAA (c) Da10-DS (d) Da10-PAA (e) Pa2.5-DS (f) Pa2.5-PAA (g) QPa2.5-DS (h) QPa2.5-PAA

3.6.1.3 Association Efficiency of PECs and APECs

Different PEC and APEC formulations exhibited different association efficiencies (Figure 3.9). There were no significant differences between association efficiencies of hydrophobically modified PECs (Pa2.5 and Da10) and their respective APECs (≥80%). However, introduction of polyanion in QPa2.5 significantly reduced the association efficiency of QPa2.5 PECs from ≥80% - ≤40%.

Among all APECs, the complexes formed by hydrophobically modified PAH i.e., Pa2.5 and Da10 displayed higher insulin complexation efficiency (>75%) than PAH-PAA and QPa2.5 based APECs (≤60% and ≤40%) respectively. These findings indicate that the type of polycation had an impact on the degree of insulin complexation. Pa2.5-DS, Da10-DS and PAH-DS demonstrated higher insulin association efficiency than their PAA based counterparts, substantiating the role of DS in mediating higher association efficiency.

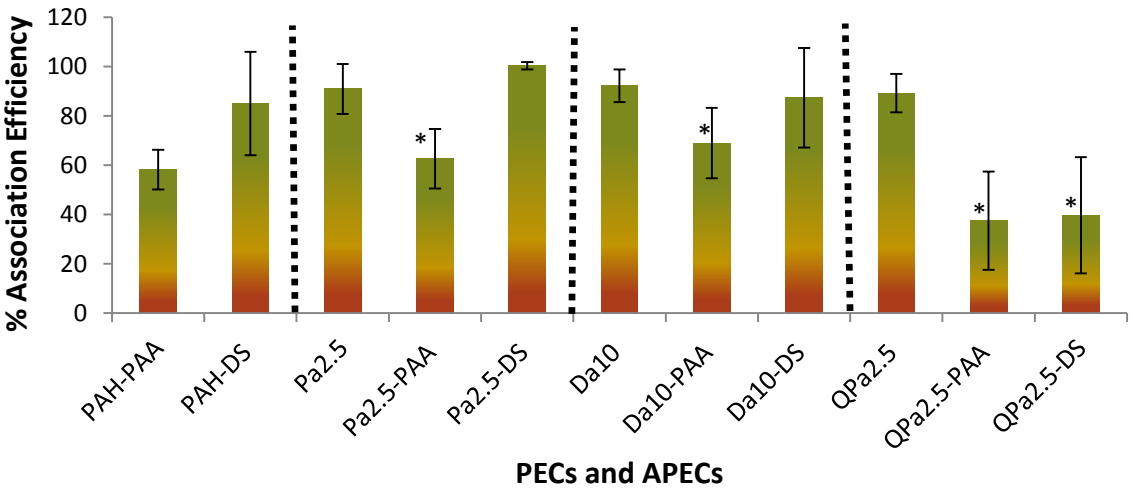

Figure 3.9 Percentage association efficiency of insulin in PECs and APECs. The data is expressed as mean± SE (n=3). Statistically significant differences ($p < 0.05$) APECs with PECs are indicated by asterisks.

3.6.1.4 Stability Studies

There are several factors which influence the formation of polyelectrolyte complexes. Notably, factors like pH, ionic strength and temperature are of paramount importance for the polyelectrolyte formation and stability. Therefore, the stability of PECs and APECs was investigated at various temperatures (25 ˚C, 37˚C & 45˚C), ionic strengths (68mM, 103mM & 145mM NaCl) and pH (1.2, 6.6 & 7.4).

3.6.1.4.1 Effect of temperature

The effect of temperature (37˚C and 45˚C) on size and ZP of IL PECs and APECs was studied by DLS (Figure 3.10a & b). All PECs and APECs displayed no significant change in size except QPa2.5 based APECs. QPa2.5-DS demonstrated approximately 2 fold, and QPa2.5-PAA 3 fold increase in size at 45˚C (Figure 3.10a).

The increased temperature affected the ZP of all APECs except Pa2.5 based APECs. Pa2.5-PAA demonstrated the least fluctuation in ZP (≤2mV) indicating the highest stability at the temperatures tested. In contrast, QPa2.5-PAA APECs demonstrated the greatest decline in ZP of up to 20mV at 37°C and 45°C.

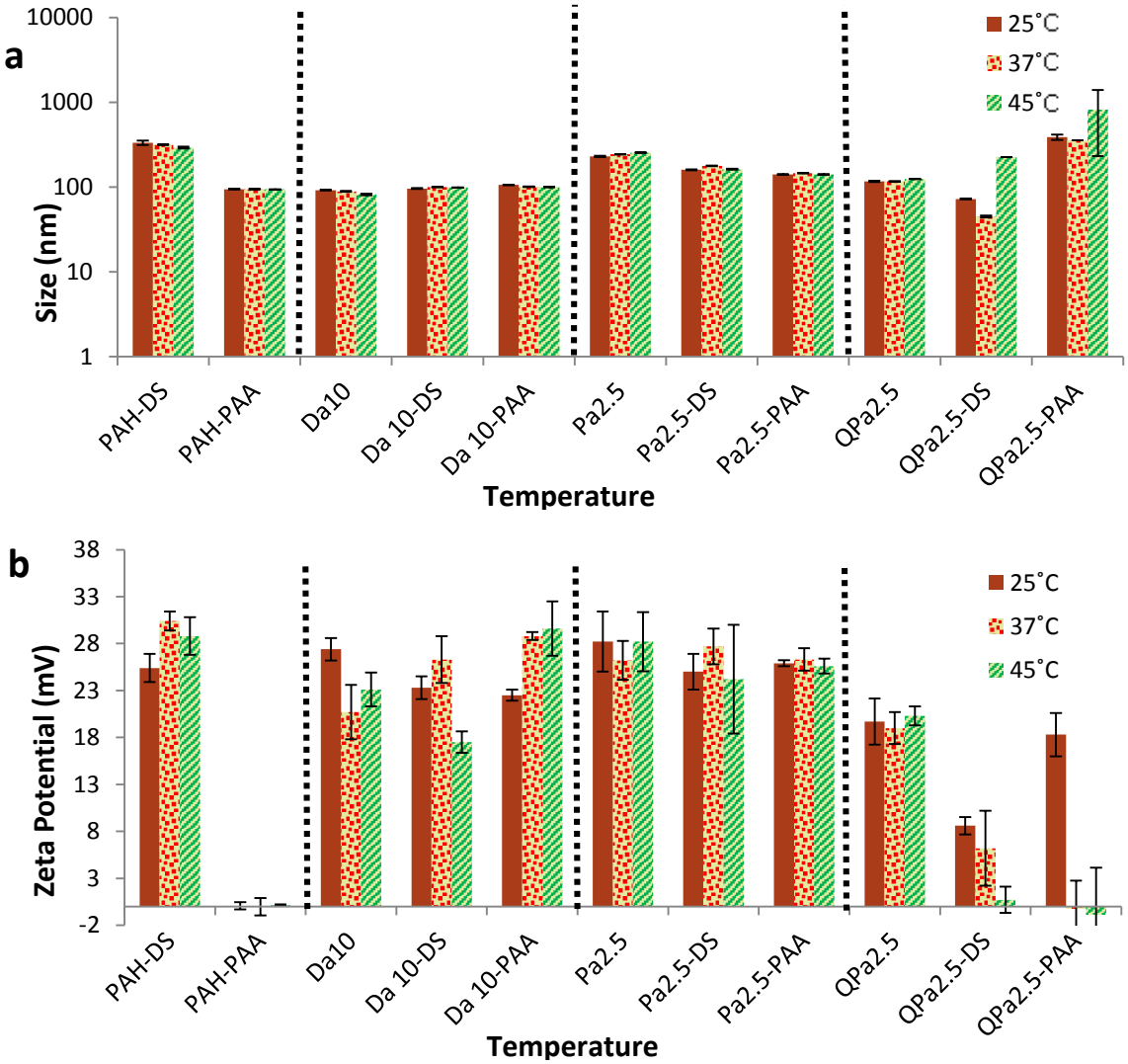

Figure 3.10 Effect of temperature on (a) Size (b) ZP of PECs and APECs incubated at 37˚C and 45˚C for 30 minutes. Each value represents mean± SE of three experimental determinations.

3.6.1.4.2 Effect of Ionic Strength

The influence of various salt concentrations (68mM, 102mM and 145mM NaCl) on the size and ZP of IL PECs and IL APECs is shown in Figure 3.11a & b. PAH-DS displayed a dramatic increase in hydrodynamic sizes at all molarities of NaCl tested, indicating destabilisation of these complexes. PAH-PAA displayed a progressive increase in size with increasing salt concentration, reaching up to 2 order of magnitude in size at the highest i.e., 145mM NaCl, indicating the initiation of destabilisation of complexes. This shows that type of polyanion had no favourable effect on the stability of PAH based APECs.

Once again, the PECs and APECs formed by hydrophobically modified PAH (Pa2.5 and Da10) displayed only minor fluctuation in size (≤180nm) at various NaCl molarities, as compared to PAH and hydrophilically modified Pa2.5 (i.e., QPa2.5). This shows that type of polycation had an effect on the stability of PECs and APECs at various ionic strength conditions. All the PECs and APECs formed by hydrophobically modified polycations (except Pa2.5-DS) presented a reduction in ZP at high salt conditions. This shows that type of polyanion had minimum effect on size of Pa2.5 and Da10 based PECs and APECs at various salt conditions, however, had considerable effect on ZP of APECs.

IL QPa2.5 PECs displayed a 2 fold increase in size at 102mM NaCl, and a 4 fold increase at 145mM NaCl signifying destabilisation of the complexes with increasing NaCl concentration. However, QPa2.5 based APECs displayed an increase in size at 68mM NaCl followed by a decrease in size at 102mM and 145mM NaCl concentration, irrespective of polyanion used. This behaviour indicates that polyanion had a favourable effect on the stability QPa2.5 based APECs at higher NaCl conditions. However, the reduction in ZP at different NaCl concentrations was more marked in QPa2.5-PAA than QPa2.5-DS indicating that DS prevented changes in the ZP.

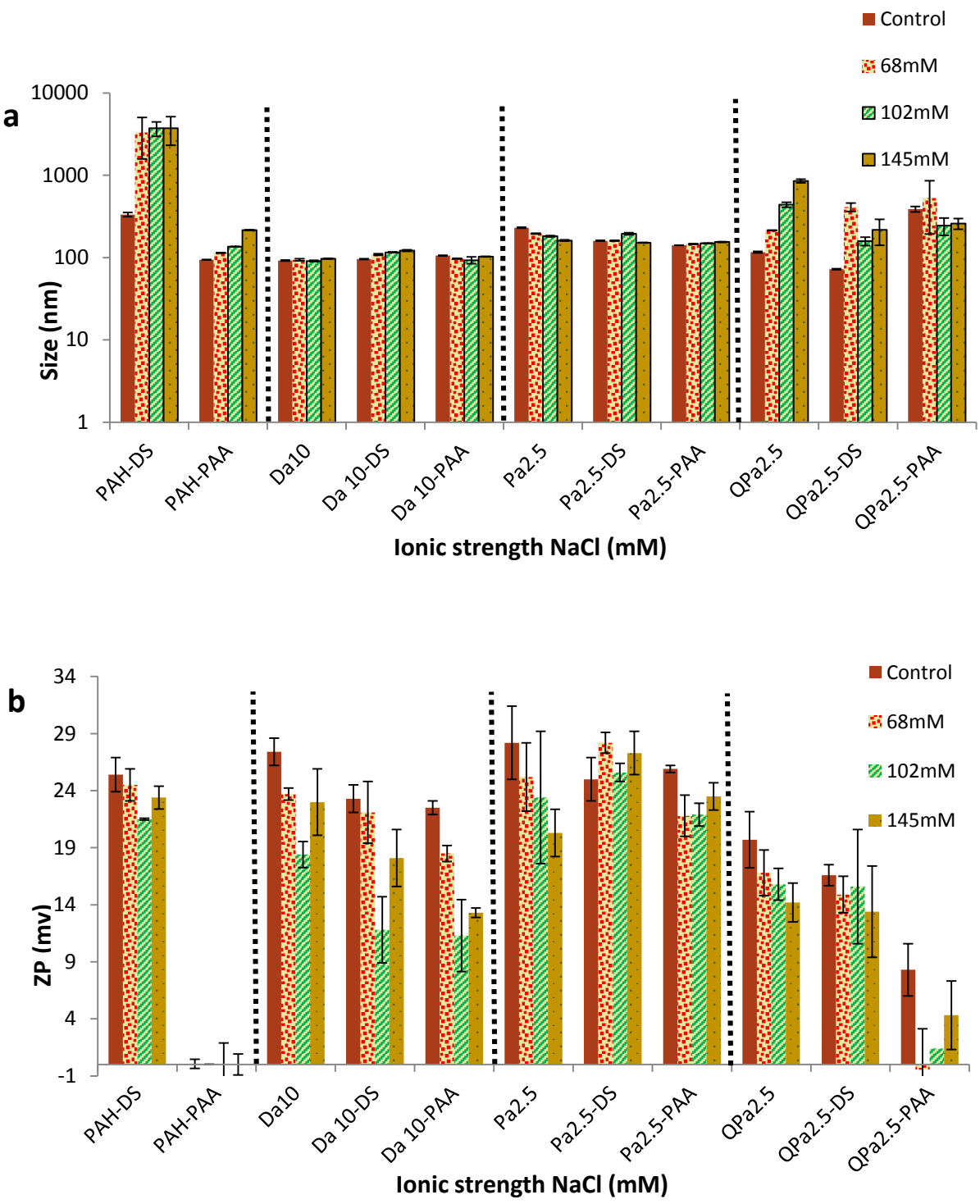

Figure 3.11 Effect of Ionic strength on (a) Size (b) ZP of PECs and APECs incubated at 68mM, 102mM and 145mM NaCl for 30 minutes. Each point represents mean± SE of three experimental determinations.

3.6.1.4.3 Effect of pH

The stability of various PECs and APECs was investigated at physiological pH in GIT by incubating them for 4h in pH 1.2 (in stomach) and 6h in pH 6.6 (small intestine) [333]. The integrity of complexes at the above mentioned pH was compared with the formulation pH 7.4 (Control). Figure 3.12a & b shows the effect of various pH on the size and ZP of IL PECs and IL APECs. All PECs showed minor fluctuation in size apart from QPa2.5 PECs. Similar to the effect of ionic strength (3.6.1.4.2), once again, PAH based APECs, whether formed with PAA or DS encountered fluctuation in size. PAH-PAA displayed a 3 fold increase in size at pH 1.2, suggesting the initiation of dissociation of complexes, whereas PAH-DS demonstrated reduction in size at the tested pH implying the stability of complexes.

All the hydrophobically modified APECs (i.e., Da10 and Pa2.5 based APECs), except Da10-PAA, maintained or reduced in size at pH 6.6 and 1.2, with minor fluctuations in ZP. Pa2.5 based PECs and APECs displayed less fluctuation in size and ZP than Da10 based APECs. Among Pa2.5 based APECs, Pa2.5-DS maintained their size while Pa2.5-PAA demonstrated a reduction in size from 137-73 indicating their stability at pH 1.2 and 6.6. Pa2.5-PAA produced less fluctuation in ZP (25-28mV) than Pa2.5-DS, signifying higher stability. On the other hand, Da10-DS exhibited less fluctuation in size and ZP than their corresponding Da10 PECs, indicating their stability over Da10 PECs. However, Da10-PAA displayed a 2 fold increment in size and a 2 fold reduction in ZP (23-12mV) at pH 1.2 indicating destabilisation of complexes.

QPa2.5 based PECs maintained their size and ZP at pH 1.2 and 6.6. Among QPa2.5 APECs, QPa2.5-PAA reduced in size whereas QPa2.5-DS increased in size at pH 6.6 and 1.2. Similar to behaviour in ionic strength (section 3.6.1.4.2), once again, the fluctuation in ZP was more marked in QPa2.5-PAA than QPa2.5-DS. These results show that the type of polyanion had an impact on the size and ZP of APECs. PAH-PAA and Da10-PAA also showed more fluctuation in size and ZP than DS based APECs, implying reduced stability at pH 1.2. All DS based APECs presented less fluctuation in size, signifying the role of DS in contributing stability to the complexes at low pH.

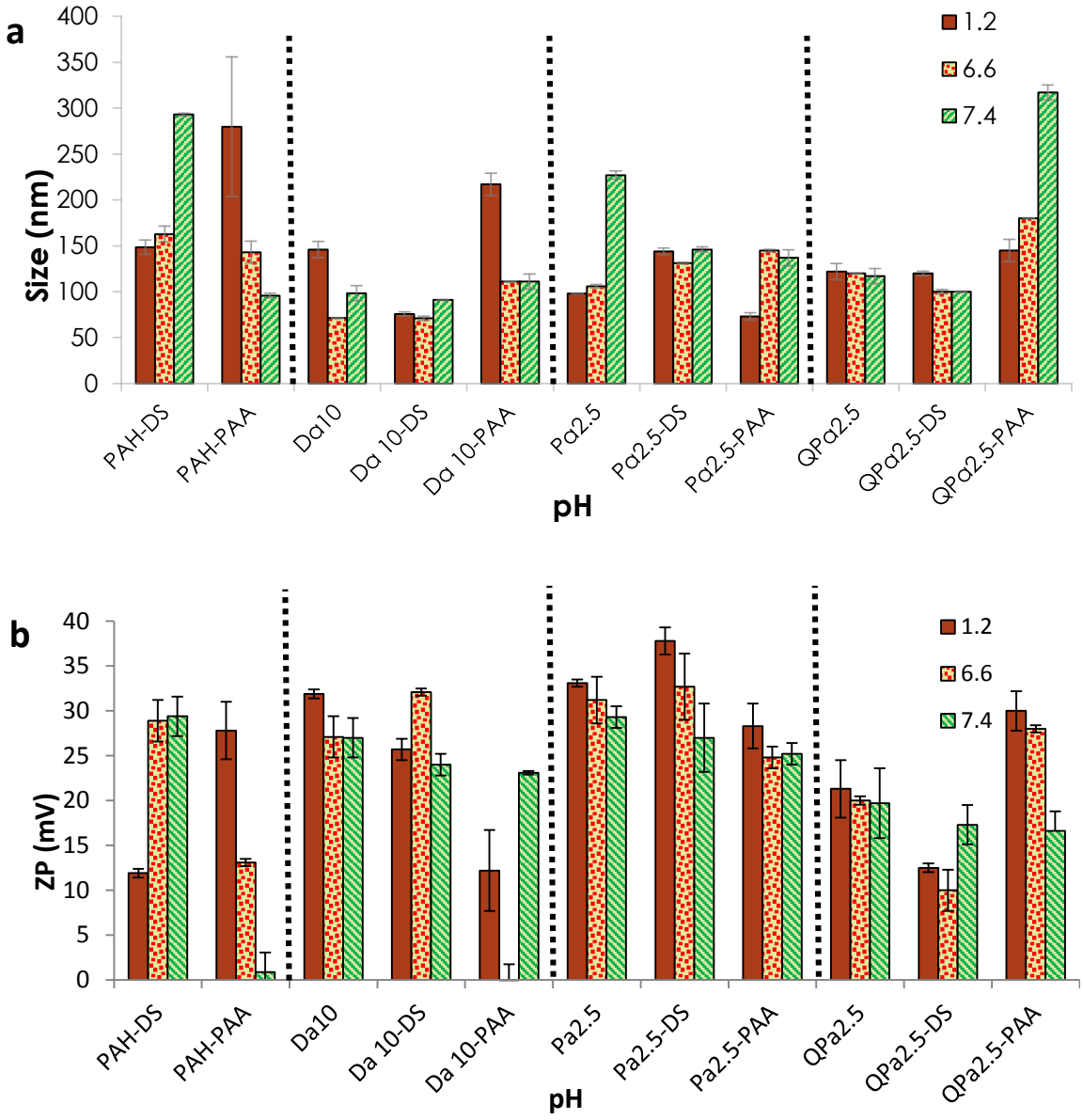

Figure 3.12 Effect of pH on (a) Size (b) ZP of PECs and APECs incubated at pH 1.2 for 4hrs and pH 6.6 for 6hrs. Each point represents mean± SE of three experimental determinations

3.7 DISCUSSION

It is well established that nanoparticles made of polyelectrolyte complexation hold tremendous promise as drug delivery systems [72]. This study describes the formation of eight NIL APECs and eight IL APECs as carrier for insulin. The NIL and IL APECs were fabricated by complexing a polycation (PAH, Pa2.5, Da10 or QPa2.5) with a polyanion (DS or PAA) in the presence of a low MW ionic cross-linker $ZnSO_4$. $ZnSO_4$ ionises in aqueous environment to give two bivalent ions i.e., Zn^{+2} and SO_4^{-2}, which cross-link the polymeric chains via electrostatic interactions [334]. In comparison to the monovalent ions, the bivalent ions (Zn^{+2} and SO_4^{-2}) play role in the formation and stabilisation of polyelectrolyte complexes, as they hold twice the charge of monovalent ions. Unlike the monovalent ions, the bivalent ions have higher affinity for charged polymer units. They form ionic cross links by interacting electrostatically with the charged polymer units in the proteins and polyelectrolyte and thus provide stability to the complexes as shown in Figure 3.13 [122, 335]. The MW of such ionic cross likers is much smaller than the MW of the polymeric chains [336]. The smaller the molecular size of the cross-linker, the faster is the crosslinking reaction, since it eases the diffusion of molecules in the complex [336].

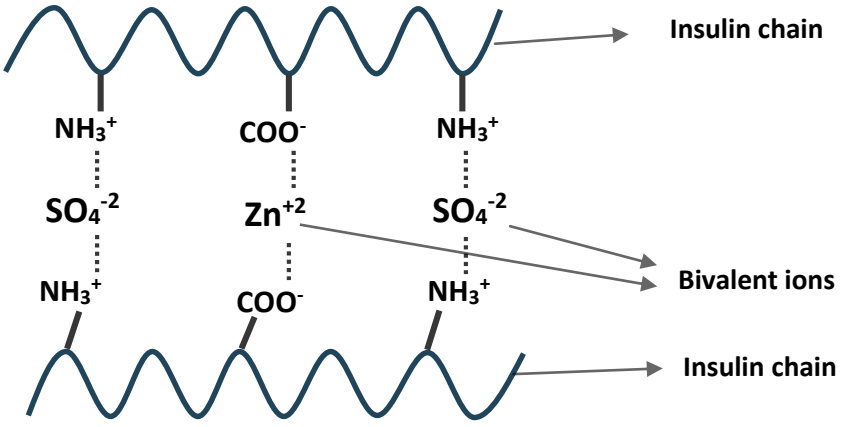

Figure 3.13 Interaction of cross-linker with insulin in APECS

The influence of cross-linker on the formation and physical stability of APECs was established in the absence and presence of 0.4µM and 4µM $ZnSO_4$ (Data not presented). Large sizes (>800nm) APECs were achieved with 0.4µM $ZnSO_4$, whereas optimum

sizes (<450nm) were achieved in the presence of 4µM $ZnSO_4$. The ionic crosslinking between the chains allowed tight stacking of the chains resulting in a decrease in the size of complexes [113]. Similar findings were achieved by Tiyaboonchai *et al.* who reported that $ZnSO_4$ stabilised the PEI-DS-insulin particles through electrostatic interactions with these particles [122]. They also showed that the mean particles size of Amphoericin B nanoparticles formed by using $ZnSO_4$ <25µM was larger than the mean particle size of complexes formulated with 25µM $ZnSO_4$ [55]. This indicates that the cross-linker and its concentration plays an important role in the formation of APECs. The Zn^{2+} and SO_4^{2-} ions promoted ion pairing interaction between unpaired charges on the polymeric chains [113]. The amino groups on the polycation and insulin, linked with the SO_4^{2-} of $ZnSO_4$, while COO^- groups of insulin and PAA, and SO_4^{2-} of DS, linked with the Zn^{2+} to form electrostatically stable complexes as shown in Figure 3.13 [55].

There was a reduction in the size and ZP of PECs upon complexation with insulin. The polymeric chains in a solution, in the un-complexed state remain in an expanded form due to the electrostatic repulsion between the like charges on the chains [116]. The like charges on the polymer backbone oppose each other and tend to prevent the chains from coiling or acquiring a self-assembled structure, leading to large sized self-assemblies [115]. However, upon complexation, the negatively charged insulin units (COO^-) bind electrostatically to the amino groups of the polycation. This behaviour reduces the number of positively charged units on the polymer chains thereby decreasing the intra-complex electrostatic repulsion between the like charges, leading to a decrease in size. Chen *et al.* has shown a similar trend whereby the introduction of a negatively charged polymer (DS) in the system was associated with a decrease in particle size and zeta potential [258]. It was shown that as the charge of chitosan was reduced by addition of DS, the chitosan molecules started to fold, resulting in the formation of condensed particles with a small size [258]. It has recently been shown that hyaluronan-chitosan nanoparticles either showed a slight decrease in size or did not change significantly upon introduction of a hyaluronan content [290].

On the other hand, unlike PECs, the IL APECs (except Pa2.5-PAA and QPa2.5-DS) displayed an increase in the hydrodynamic size, upon complexation with insulin. This effect may be attributed to the alteration in the +/- charge ratio due to the addition of two negative charges i.e., polyanion and insulin in APECs. The polycation: polyanion

charge ratio is an important factor affecting the particle size [258]. An increase in the charge ratio of polycation: polyanion above 1 is associated with a decrease in the particle size resulting from an increase in the magnitude of net charge on the particles [290]. On the other hand, as the charge ratio approaches closer to 1 by addition of polyanion, the particle mean size increases because of the reduction in charge ratio [337]. In the first step of the formation of IL APECs, the polycation was complexed with insulin which led to a significant reduction in the number of charged amino groups on the polymer backbone. This behaviour reduced the intra-complex repulsion between polymeric chains leading to a reduction in the complex size. However, in the second step, addition of polyanion led to the occupancy of the remaining un-paired charges on the polymer backbone and increased the intra-complex repulsion between the two polyanions resulting in an increased size. This effect has previously been reported by Chen *et al.* who showed that incorporation of bovine serum albumin (BSA) into the chitosan-DS nanoparticles led to an increase in the particle size which gave a good indication of the incorporation of BSA into chitosan-DS nanoparticles [258]. The authors indicated the role of the positively charged BSA to compete with chitosan to interact with DS electrostatically [258]. Similarly, the incorporation of anti angiogenic hexapeptide (ARH peptide) was also shown to increase the size of nanoparticles, compared to the empty nanoparticles [270]. Likewise, the incorporation of MTX into the glycol chitosan-DS nanoparticles [273] and of 5-aminosalicylic acid (5-ASA) into the chitosan–DS hydrogel [291] have also been shown to cause a sharp increase in the particle size of the nanoparticle dispersion.

It is well know that the association of protein in complexes alters the surface charge of complexes. Insulin is negatively charged above its isoelectric point i.e., pH 5.2, [338] therefore, complexation of insulin in PECs and APECs was expected to reduce the ZP of IL complexes. For this reason, a reduction in the ZP of PECs and APECs upon complexation with insulin indicated the association of insulin in the complexes (refer to Table 3.2). The incorporation of anti angiogenic hexapeptide (ARH peptide) in CS-DS nanoparticles has previously shown a similar trend to change the ZP of peptide-loaded nanoparticles from positive to negative, compared to the empty nanoparticles indicating that almost all the ARH peptide was incorporated into the nanoparticles [270]. Insulin is amphoteric in nature, i.e., comprises of both positively and negatively charged moieties [118]. Ionisation of these charged moieties in the insulin molecule are

responsible for the complexation of insulin in PECs and APECs by electrostatic interactions [272]. The COO^- of insulin interact electrostatically with the amino group of polycation (Figure 3.14a). The amino groups in the insulin molecule interacts with COO^- of PAA or SO_4^{2-} of DS (Figure 3.14 b & c). In this way, several different forms of electrostatically driven interaction are possible. Additionally, hydrophobic interactions, Van der Waal's associations and hydrogen bonding also contribute in the association of proteins with polyelectrolytes [121].

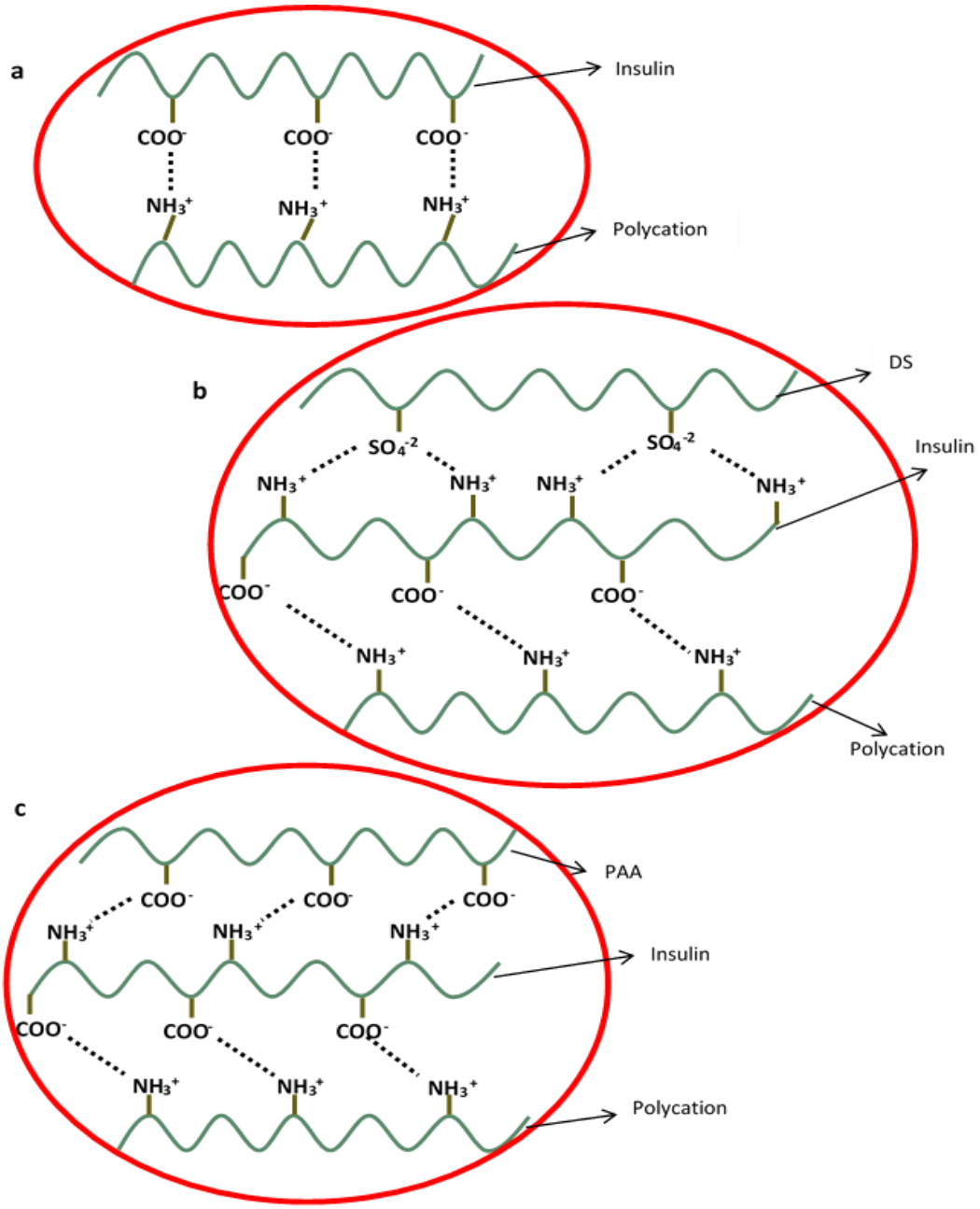

Figure 3.14 Schematic illustration of interaction between polycation, polyanion and insulin in (a) IL PEC (b) IL DS based APEC (c) IL PAA based APEC

The reduction in ZP of both NIL and IL APECs in the presence of a polyanion again indicates the complexation between polyanion and polycation. Introduction of polyanion such as DS has previously been found to reduce the cationic charge related to polycations such as PEI [55] and chitosan [296].

APECs formed by PAH and modified PAH displayed significant differences in their properties indicating that the type of polycations have an influence on the properties of polyelectrolyte complexes. Apart from NIL QPa2.5, NIL QPa2.5-DS and IL PAH-DS, all the other PECs and APECs exhibited a size < 230nm. In this way, APECs formed by hydrophobically modified PAH i.e., Pa2.5 and Da10 exhibited smaller hydrodynamic sizes and relatively higher ZP as compared to the APECs formed by QPa2.5 which displayed considerably larger sizes and low ZP values. These effects can be explained by the ability of hydrophobic grafts i.e., Pa2.5 and Da10 to allow stronger hydrophobic association with insulin leading to formation of smaller self-assemblies [121]. In contrast, the bulky nature of quaternary ammonium moieties and increased electrostatic repulsion between permanently charged quaternary ammonium moieties appeared to have driven the formation of large size PECs and APECs [129]. In addition, the hydrophilic quaternary moieties might have prevented the hydrophobic interactions due to inter-chain repulsion which further reduced the tight packing of polymer chains [119]. As a consequence, the polymer chains were set apart resulting in the large sized complexes [119]. A similar effect has been shown by Guo *et al.* who prepared ternary complexes by introduction of polyanion polyglutamic acid-graft-poly(ethylene glycol) (PGA-g-mPEG) into amphiphilic polycation polycaprolactone-graft-poly(N,N-dimethylaminoethyl methacrylate) (PCL-g-PDMAEMA). The electrostatic interaction between PGA and PDMAEMA chains led to compaction of the complexes and at the same time the hydrophilic mPEG chains increased the size of the complexes. As a result, the ternary complexes nearly maintained the constant and suitable sizes of about 130 nm [127].

The insulin association efficiency of complexes was generally found to be polymer structure dependent. In relation to the polycations, the degree of association efficiency is graded as Pa2.5>Da10>PAH>QPa2.5. Thus the PECs and APECs formed by hydrophobically grafted PAH (Pa2.5 and Da10) demonstrated higher insulin association efficiency (80%) than PAH (60%) and QPa2.5 (40%) based APECs. Among the hydrophobically grafted APECs, Pa2.5 demonstrated higher percentage

association efficiency than Da10 based APECs. The difference in the association efficiency of the two may be attributed either to (i) the difference in percentage grafting of the two, where the higher hydrophobic load of Da10 could not cope with the greater amount of insulin or (ii) the bulkier and rigid dansyl moeities might have caused some steric hindrance resulting in limited complexation. However, a detailed investigation of the underlying concepts of the complexation process is very crucial, since the overall yield of insulin strongly depends on the efficiency of the complexation process. Pa2.5-DS demonstrated the highest ability to complex insulin, i.e., 100%, which suggest that all of the insulin was complexed with polymers. In addition, PAH-DS and Da10-DS also demonstrated higher insulin association efficiency than their PAA based counterparts. These results indicate higher insulin association by DS based APECs. DS possesses a higher molecular weight (60-10KDa) than PAA which may be responsible for high association efficiency. The highly charged SO_4^{-2} of DS might have strongly interacted with NH_3^+ of insulin and trapped more insulin molecules than the less charged COO^- of PAA, allowing higher AE. Our findings correlate with the findings achieved by Sarmento *et al*. who prepared complexes between polyanions (dextran sulphate or alginate) with chitosan and reported a higher insulin association efficiency of DS based complexes than alginate based complexes [126]. In addition, Silvia *et al*. have also demonstrated high insulin complexation in the presence of dextran sulphate [339].

QPa2.5 APECs demonstrated 2 fold lower association efficiency than QPa2.5 PECs. The presence of bulky groups in the side chain of the polycation has been reported to have a notable effect on the complexation with the highly charged polyanion. The presence of bulky side chains on chitosan have been reported to have steric hindrance effects that reduced the cooperativity of the charge based interactions [292]. The addition of polyanion in IL QPa2.5 PECs might have created a competition between insulin and polyanion to complex with the bulky $N^+(CH_3)_3$. Since the complexation of insulin and polyanion with quaternary ammonium moieties resulted in a significant decline in ZP, this shows that the polyanion might have impeded the interaction of insulin with QPa2.5 and itself superseded in complexing with the QPa2.5. This might indicate a higher binding affinity of QPa2.5 for polyanion than insulin. This effect has previously been demonstrated by Tiyaboonchai *et al.* who reported a competitive interaction between Amphotericin B and DS with the positively charged chitosan [73].

The stability studies showed that the hydrophobically formed PECs and APECs were more stable at varying temperature, ionic strength and pH than PAH and QPa2.5 based complexes. They showed less fluctuation in size and minor changes in ZP at varying condition (apart from Da10 PECs and Da10-PAA APECs which displayed increase in size at pH 1.2 and fluctuation in ZP). The higher stability of complexes formed by hydrophobically modified PAH has been attributed to the generation of hydrophobic associations between hydrophobic grafts of polycation and insulin. Previously Reschel *et al.* has also shown that hydrophobic nature of poly[N-(2-aminoethyl)methacrylamide trifluoroacetate] conferred higher stability to (PAEMA)/DNA complexes than PLL/DNA complexes, [282].

Since PAH has flexible chain architecture, its chains can move about with sufficient degree of freedom. The modification of PAH with hydrophobic grafts (i.e., C_{16} long alkyl chain of Pa2.5 and aromatic group of Da10) tend to reduce the polymer chain flexibility [120]. The destabilisation experienced by PAH-DS at high ionic strength, and PAH-PAA at the tested pH is therefore ascribed to the flexible linear architecture of PAH and lack of hydrophobic association which was unable to provide sufficient strength to the complexes. It is assumed that the addition of salt created a counter-ion environment which screened the positive charges on the surface of PAH-DS. This effect led to the loss of electrostatic attraction between the PAH-DS and insulin, subsequently leading to an increase in the size and hence dissociation of the complexes [79, 113]. Similarly, at pH 1.2 the carboxylic acid groups of PAA are protonated and hence did not interact with positively charged amino groups (NH_3^+) leading to destabilisation of PAH-PAA. The PAH based APECs are not formed by additional hydrophobic associations which could stabilise these complexes. However, the hydrophobic grafting on the PAH backbone provided additional hydrophobic interactions which conferred stability to the hydrophobically modified complexes [120]. Filippov *et al.* showed that the colloid stability of P17 based polyplexes increased with increasing the hydrophobic cholesterol content in polycations [251]. The complexes prepared with the lowest content of cholesterol showed the highest coagulation rate, whereas the rate of coagulation was lower for complexes prepared with polycations bearing higher amounts of cholesterol [251]. Thus it was shown that the colloid stability of complexes increases with increasing content of side-chain cholesterol moieties which is related to the hydrophobicity of polycations [251].

The increase in temperature up to 45˚C brought no significant change in size and minor fluctuation in ZP of hydrophobically formed PECs and APECs. It is known that the hydrophobic interactions increase in strength with the increasing temperature [287]. These increasing hydrophobic associations are considered to have maintained the complex integrity. The results are consistent with the findings achieved from Mao *et al.* who reported that the increased temperature facilitates PECs formation [79]. However, on the other hand, QPa2.5 based APECs, in particular QPa2.5-PAA, demonstrated moderate increase in size and reduction in ZP at increased temperatures. The hydrophilic segments of QPa2.5 might have undergone dehydration of polymer chains caused by the desolvation of water molecules upon increase in temperature. This behaviour might have led to impairment or loss of hydrogen bonding between the polymer and water molecules resulting in the increased sizes of the self-assemblies and hence destabilised the complexes [112]. The breakage of hydrogen bonds might have caused displacement of positive surface charges which is obvious from the very low ZP of QPa2.5 based APECs. In the case of QPa2.5-insulin PECs, any breakage of the bonds upon increase in temperature appeared to have been compensated by new bond formation via hydrophobic association between reorganised QPa2.5 chains and insulin chains. The non-polar aliphatic side chains of insulin are thought to have mediated the hydrophobic associations with palmitoyl graft in QPa2.5, which maintained the integrity of QPa2.5 PECs [121]. However, this effect was essentially absent in the case of QPa2.5 based APECs as the presence of polyanion interfered with the intra-complex hydrophobic associations.

The hydrophobically modified PECs and APECs were found stable at high ionic strength conditions. It is assumed that, the addition of salt produced a counter ions environment. Since the surface of hydrophobically modified PECs and APECs was positively charged, the counter-ions bound to the surface and reduced the surface charge which is clear from the obvious reduction in ZP, however, the concentration of counter-ions was not enough to neutralise the surface charge of the complexes which could subsequently cause destabilisation of the complexes. Alternatively, QPa2.5 PECs displayed a progressive increase in size with increasing ionic strength. It is thought that the PECs formed by polyamines with bulky quaternised amine groups are less stable due to loosely coupled charges by weak electrostatic interaction [340]. This effect is ascribed to the increased distance between charges in the ion pairs. The presence of

counter-ions caused neutralisation of surface charge of QPa2.5. Since the surface charge of QPa2.5 PECs was already below (≤20mV), as compared to the hydrophobically modified PECs and APECs ≥22mV. This caused the counter ions to effectively neutralise the surface charge leading to the destabilisation of QPa2.5 PECs which clearly appeared from the progressive increase in size and decrease in ZP.

On the other hand, the presence of polyanion in QPa2.5 APECs decreased the steric hindrance and reduced the distance between the charged units, allowing stronger ion pairing. QPa2.5 APECs, although experienced the same effect of loss of surface charge by charge neutralisation at low ionic strength due to the small positive surface charge (≤16mV), however, when the small monovalent ions (Na^+ and Cl^-) penetrated deeper into the expanding complexes, they might have generated ion pairing effect with the free negative charges (SO_4^{+2} and COO^-) on the polyanion chains in the complexes which is considered to have restored the surface charge and hence provided stability to the QPa2.5 APECs at high ionic strength conditions [340]. These effects can be noticed from the compaction of size and increase in ZP at high ionic strength conditions (102mM and 145mM).

Generally, PECs and APECs formed by modified polycations (except Da10 PECs Da10-PAA APECs) were found stable at varying pH. QPa2.5 based PECs and APECs maintained or reduced in size suggesting their stability. However, slight variation in ZP was observed. All modified APECs except Da10-PAA and QPa2.5-DS displayed increase in the ZP at pH 1.2. At pH 1.2, the amino groups of polycation and insulin are predominantly protonated, thus generate a positive charge. The sulfonate groups of DS are partially ionised at pH 1.2, giving predominantly a negative charge while carboxylic group of PAA and insulin remain unionised. PAH is a weak base, PAA a weak acid and DS a strong acid [253]. The pKa of PAH and modified PAH is approximately 8.8 [341]. This means that their amino groups will be highly protonated at pH values below their pKa and de-ionised at pH above its pKa [279]. On the other hand, the pKa of polyanions DS and PAA are 1.2 and 4.75 respectively [253, 342]. The polyanions are fully ionized, at pH values higher than their pKa, however, the degree of ionization decreases rationally with the decrease in pH below their pKa [343]. DS benefits from its low pKa (pH 1.2), in complexing with polycation over a broad pH range above its pKa, which is essentially indicative of a permanently charged state. This is the reason that all DS based APECs, demonstrated considerably higher stability at the pH tested, irrespective

of the polycation used. However, since PAA has a pKa of 4.75, the degree of ionized units decreases clearly below its pKa. This is the reason that in an acidic medium (pH 1.2), PAH-PAA and Da10-PAA displayed 3 and 2 folds increase in size respectively, which is indicative of the destabilisation of these complexes. However, a reverse trend was observed for Pa2.5-PAA (145-73 nm) and QPa2.5-PAA (350-150), whereby they displayed considerable reduction in size, indicating their stability at low pH. This behaviour of how PAA conferred stability to these complexes is not fully known. These findings indicate that PEC and APEC systems can retain their therapeutic cargo in the acidic environment of the stomach and the intestine and therefore can be taken up in the intact form by the intestinal enterocytes.

3.8 CONCLUSION

APECs were formed in nano-sized range by complexing a polyanion, a polycation and insulin. Pa2.5 based APECs were found to be the most stable systems at all the conditions tested. They demonstrated higher stability at varying temperature, ionic strength, pH, and higher insulin association efficiency than unmodified, Da10 and QPa2.5 APECs. The findings imply that the hydrophobic modification of PAH had a favourable effect on the stability of PECs and APECs. In addition, DS conferred greater stability and higher insulin complexation than PAA indicating that type of polyanion also plays a role in stabilising APECs.

Chapter 4

Biocompatibility Profiling Of Ternary Polyelectrolyte Complexes

4 INTRODUCTION

Despite being efficient delivery systems, a major challenge to nanocarriers is the understanding of potential harmful effects caused by them to the cells [157, 344]. Nanocarriers can disrupt certain activities within the cells which alter the cellular metabolism and cell proliferation [344, 345]. They may cause structural damage to the cells which can even result in cell death. In addition, nanocarriers have been shown to cause increased production of inflammatory cytokines and reactive oxygen species (ROS) [148, 346]. For this reason, it is essential to investigate the potential adverse effects related to all polymeric nanostructures to evaluate their 'biocompatibility' profile (suitability for human use) [347]. The *in vitro* cell culture systems provide an efficient primary means to screen the drug delivery systems [166, 345]. However, there is a need to optimize and standardize the *in vitro* approaches for the detection of nanocarrier toxicity [345].

4.1 *IN VITRO* CELL CULTURE SYSTEMS

The cell based *in vitro* models play a very important role in analysing the toxic effects of nanomedicine on the cell lines. There are techniques to measure endpoints such as cytotoxicity, haemocompatibility, immunotoxicity and inflammatory potential to understand the underlying toxicity [166, 345, 348, 349]. Such models offer many advantages over the use of animal models. They are simple, quick and less expensive to use than animal models [166]. Additionally, *in vitro* cell culture models based on human cell lines may better represent the human cellular functions than the *in vivo* studies done on animals [350]. However, it is difficult to assess and analyse the multiple complex biological effects solely by *in vitro* cell culture models. Therefore, the accuracy and predictability of these tests is validated by comparing with the *in vivo* studies [158, 351, 352].

An essential part of *in vitro* toxicity evaluation is the selection of appropriate end points and cell types for simulating the original biological environment [160]. The cell lines are selected for their similarity to the *in vivo* phenotype. Some of the common cell types used in *in vitro* testing include phagocytic (monocyte and macrophage phenotypes), neural, hepatic, epithelial, endothelial, red blood cells (RBC's) and various cancer cell lines [157, 353-355]. The two cancer cell lines used in this study are described below.

4.1.1 Cell lines

4.1.1.1 CaCo2 Cell line

CaCo2 is a continuous cell line which is derived from the human epithelial colorectal adenocarcinoma [220]. It was chosen for this study because it mimics intestinal enterocytes both morphologically and functionally which serve as initial line of contact for the oral drug [356]. CaCo2 cells express many *in vivo* characteristics such as TJs, microvilli, several enzymes and transporters (peptidases, esterases, P-glycoprotein) (Gad, 2008; Yee, 1997), and uptake transporters for amino acids, cobalamine, and bile acids which are classically representative of ileal enterocytes [357]. One limitation of using this cell line is the absence of mucus lining. Although this limitation can typically underestimate the interaction between the carriers and mucin, but is still commonly used because it provides an alternative for ileal cells.

4.1.1.2 J774 Cell Line:

J774 cell line originated in 1968 from a female mouse suffering from plasmacytoma [358]. It is a finite cancerous cell line obtained from peritoneal lavage of the mouse. It is a rapidly growing cell line and comprises of murine macrophage-like mononuclear cells which grow with a doubling time of 22h [358]. Macrophages are the first line defence in generation of early immune responses and an essential part of the mononuclear phagocyte system [359, 360]. They take part in primary immune regulation by phagocytosis, antigen presentation and production of cytokines such as interleukin IL-6, IL-10, IL-12 and tumour necrotic factor-α (TNF α) [361, 362]. This cell line has been used in a variety of experiments such as elucidation of immune responses, macrophage function and cytotoxicity [363].

4.1.2 Cytotoxicity

An important initial aspect of biomaterial screening is the investigation of *in vitro* cytotoxicity [349]. The term cytotoxicity refers to the toxic effects mediated by a substrate on the cells [349]. There are numerous properties of nanomaterials such as size, shape, biodegradability and molecular weight which are involved in mediating toxicity, however, cationic nature is of prime importance in causing toxicity (Fischer et al., 2007). A large number of polycations such as PLL, polyethyleneamine (PEI) polyamidoamine (PAMAM) are known to be cytotoxic which has been established *in vitro* by using a variety of cell lines and cell cytotoxicity assays (Fischer et al., 2007).

The primary amine functional groups on polycation are considered as the key factor for causing cytotoxicity [153]. They are known to interact with negatively charged proteoglycans on the surface of cell membrane by electrostatic interaction [364, 365]. The conversion of primary amines to safer tertiary or quaternary amine or addition of a steric coating such as polyethylene glycol (PEG), renders them non-toxic [67, 151, 366]. In addition, approaches which can reduce the surface charge such as by complexing with a polyanion have also been shown to reduce the toxicity associated with polycations [131]. Wang *et al.* used four types of biocompatible polyanion containing carboxyl groups or sulfonic acid groups to prepare polyanion/PEI complexes [127, 131]. These complexes produced a sharp reduction in the PEI associated toxicity such that the cell viability for all polyanion-PEI complexes was more than 95% compared to only 12% of PEI alone [131].

In addition to charge density and type of amine, the polymer architecture, three-dimensional arrangement and molecular weight of polycations have also been shown to influence the cytotoxicity [157, 367]. Recently, Mao *et al.* reported a concentration and MW dependent effect of trimethyl chitosan (TMCs-400 kDa and TMCs-5kDa) and PEG grafted-TMC (PEG(5k)-g-TMC(400) on the cytotoxicity of CaCo2 cells by using 3-4,5 dimethyl thialzol2,5 diphenyl tetrazolium bromide (MTT) and lactate dehydrogenase (LDH) assay [227]. The cytotoxicity of polycation such as diethylaminoethyl-dextran (DEAE-dextran), PLL and PEI was shown to increase with the increase of their molecular weights. However, these findings applied only to the polymers having similar chemical structure and not for different types of polycations [157].

Cationic polymers comprising of a globular structure such as PAMAM have been found to be more biocompatible than linear or branched polymers (diallyl-dimethyl-ammonium chloride (DADMAC), PLL, PEI) [157]. Despite having high charge, PAMAM has been reported to produce low cytotoxicity which is attributed to its low molecular weight. Polymers with a rigid architecture e.g. DADMAC have displayed comparatively lower toxicity than flexible chain polymers [157]. It has been hypothesised that the chain stiffness makes the attachment of DADMAC to the cell surface more difficult resulting in reduced interaction and hence decreased cytotoxicity [157]. There may be many more factors responsible for causing polymeric toxicity. Further research in nanotoxicology will allow understanding of the underpinning

concepts leading to toxicity. The *in vitro* assays are essential screening tests which provide information of the structure-toxicity relationship for optimizing and standardizing the biocompatibility of polymeric delivery systems.

4.1.2.1 In Vitro Cytotoxicity assays

Cytotoxicity assays determine the loss of cell viability occurring from the distortion of structure or function of the cell membrane or cellular organelles [349, 368]. The evaluation of basal cytotoxic potential of a substrate is made by determination of its IC_{50} [160]. Exposure of cells to cytotoxins initially causes structural, biochemical or metabolic alterations in cells which act as markers for the assessment of degree and type of cell damage. The changes in cellular morphology, mitochondrial function, membrane leakage of LDH, reduced glutathione (GSH) levels, oxidative stress, haemoglobin release from erythrocytes and adenosine triphosphate (ATP) depletion are the most common endpoints used to assess the *in vitro* cytotoxicity [349, 368].

The commonly employed cytotoxicity assays include tetrazolium salt based assays particularly MTT [157, 227], 3-(4,5-dimethylthiazol-2-yl)-5-(3-carboxymethoxyphenyl)-2-(4-sulfophenyl)-2H-tetrazolium) (MTS), (2,3-bis(2-methoxy-4-nitro-5-sulfophenyl)-5-[(phenylamino)carbonyl]-2H-tetrazolium hydroxide) (XTT) [160, 345] which assess the cytotoxicity by measuring the metabolic activity of mitochondrial enzymes. Other common assays include LDH assay [157, 227], neutral red (3-amino-6-dimethylamino-2-methyl-phenazine) uptake assay and ATP [144]. LDH is a cytoplasmic enzyme present in all cells. It is released into the cell culture supernatant upon damage to the cell membrane. This forms the basis for determination of cell membrane integrity and hence the cell damage [369].

Neutral red determines the number of vital and uninjured cells in the cultures. The neutral red dye is taken up exclusively by viable cells and subsequently accumulates in the lysosomes [355]. The assessment of the dye content determines the number of live and undamaged cells.

ATP is present in all metabolically active cells. Determination of ATP content by bioluminescent measurement is directly related to the number of metabolically active cells [369]. The tetrazolium salt based colorimetric assays determine the metabolic activity of viable cells. MTT is the most widely used assay, discussed in detail in the section below.

4.1.2.1.1 MTT Assay

MTT assay is a quantitative calorimetric assay employed for measuring the effect of a substrate on the activity of the living cells [370, 371]. In other words, it studies the substrate-induced impairment of mitochondrial function [371]. MTT is a yellow water soluble tetrazole which is reduced to purple water insoluble formazan crystals in metabolically active cells by mitochondrial reductases [160, 371]. The insoluble formazan is solubilised by adding dimethyl sulfoxide (DMSO), an acidified ethanol solution, or isopropanol to form a purple solution [157, 371]. The amount of purple formazan produced by treated and untreated control cells is used as a measure of the viability of the cells. The fluorescent intensity of the coloured solution is determined at a certain wavelength (usually between 500 and 600 nm) by a spectrophotometer [370, 371]. The absorbance level reflects the amount of the reduced product which in turn is an indicator of the number of metabolically active and functionally viable cells [160].

The *in vitro* cytotoxicity assays can give a relative but not absolute index of potential toxicity of a polymeric carrier, however can set out the suitability for further investigation and subsequent *in vivo* use. MTT assay is chosen in this study due to its sensitivity and reproducibility. A number of researchers compared MTT assay with other cytotoxicity assays such as LDH assay, neutral red assay and trypan blue and have found comparable results [157, 227]. In this study, MTT assay was combined with ROS and haemolysis assay to assess the degree of cytotoxicity on CaCO2 cells and erythrocytes.

4.1.3 Haecompatibility

Haemolysis assay is a common test for the analysis of nanocarrier interaction with the blood components. It is a very easy, rapid and sensitive method [372]. Haemoglobin serves as a biomarker for the detection of haemolysis. Free haemoglobin concentration is determined spectrophometrically in the erythrocyte supernatants which is proportional to the degree of haemolysis [373]. Haemolysis can lead to serious disorders e.g., anaemia, haemocytosis and jaundice [373]. For this reason, the haemolytic potential of all nanocarriers must be evaluated as a necessary part of the development of drug delivery systems [373].

The physicochemical properties of nano-drug carriers such as cationic charge [374, 375] high molecular weight, flexible architecture and branched or linear structure [157,

376] trigger their interactions with erythrocytes leading to haemagglutination (cell aggregation) or haemolysis (destruction of red blood cells) [376, 377].

Haemagglutination is thought to occur due to non-specific ionic interactions between the positively-charged polycation and negative charges of the erythrocytes, mainly by sialic acid units located in the glycocalyx of the cell membrane [374, 378]. These interactions may also cause haemolysis via permeabilization of the lipid bilayer of erythrocytes [373, 378].

The hydrophobic subunits of quaternized tertiary polyamine have been shown to have a tendency to dissolve in the lipid membrane and destabilise erythrocyte leading to haemolysis [378]. The MW of PLL has also been shown to have an impact on haemolysis and aggregation of erythrocyte [377]. Kaminski *et al*. reported the same behaviour of the polymethacrylate derivatives to cause haemolysis with the increase of hydrophobicity and MW [376]. Fischer *et al.* reported an increase in haemolysis with the increase in the number of primary amine group in polycation [157].

Despite the cytotoxicity associated with polycations, numerous polycations have reached the clinics for drug delivery purposes such as Eudragit derivatives, chitosan and protamine [379]. A number of approaches are being used to prevent the toxicity of polycations. The efficient but toxic polycations are modified to produce safer nanocarriers such as polyethylene glycol (PEG) grafted nanocarriers to prevent their interaction at the biological surfaces, by masking their antigenic sites [92, 380, 381]. Zhu *et al*. prepared chitosan-N-trimethylaminoethylmethacrylate chloride–PEG which were able to reduce the haemolytic activity of the unmodified counterpart up to 50% [92]. In addition, Kamiński *et al.* synthesised cationic derivatives of dextran and hydroxypropylcellulose which have been reported to be free from haemolytic effects [376].

4.1.4 Oxidative Stress

Oxidative stress is caused by an imbalance of the redox state of cells which occurs under conditions such as exposure to radiations or toxic chemicals [160, 382]. It primarily occurs due to the overproduction of ROS and free radicals by the cells [383]. Although, both free radicals and ROS are naturally produced in the body as intermediates in several different metabolic reactions, however, a balance is maintained by simultaneous production of antioxidants such as glutathione (GSH) [383, 384].

ROS species are either electrophilic molecules (e.g. H_2O_2) that attract electrons or are free radicals (e.g. OH^-) containing an unpaired electron [160, 383]. Such species have substantial ability to damage DNA, proteins, and lipids by binding covalently and irreversibly to these biomolecules [385]. There are several different types of ROS such as superoxide (O_2^-), hydroxyl radical (HO^-), peroxy radical (ROO^-), and hydrogen peroxide (H_2O_2) and reactive nitrogen species (RNS) [166, 383, 385, 386].

ROS generation is one of the primary mechanisms of nanocarrier toxicity. There have been large numbers of instances when toxicity has been attributed to ROS production and oxidative stress [148, 159, 382, 387]. A diverse range of nanomaterials including carbon fullerenes, carbon nanotubes and nanoparticle metal oxides have been implicated to produce ROS [159]. ROS generation has been reported to be the plausible mechanism for the cellular apoptosis induced by the chitosan/polyoxometalate nano-complex nanocarriers [388]. It has been reported that carrageenan (a sulphated polysaccharide) produces inflammation as a consequence of free radical generation [382]. The generation of ROS by fullerenes nano-C60 has shown to produce toxic effects by causing lipid peroxidation of cell membranes [387, 389]. Lipid peroxidation is characterised as an oxidative deterioration of polyunsaturated lipids of cell membrane which is involved in causing toxic effects such as DNA damage leading to cancer [383]

It has been shown that ROS production varies with the physicochemical properties of nanocarriers. One good example is PEI-DS microparticles which produced significantly high levels of ROS with the increase of MW of PEI [390]. Recently, Nabeshi *et al*. reported that silica particles induced intracellular ROS generation which increased with decreasing particle size to less than 100 nm [391]. These findings indicate the role of high MW and small size in the ROS generation.

It is considered that the surface area to volume ratio of nanocarriers is the key factor responsible for production of ROS. The higher the ratio, the higher is the chemical reactivity and hence the biological activity of the nanocarriers, resulting in more ROS production [160, 368, 392].

Despite great advances in polymer cytotoxicity testing, the relation of the physicochemical properties of polymeric nanocarriers to the generation of ROS has not been fully explored [393]. This is the reason that the assays determining the production of ROS and free radicals hold great importance in the evaluation of toxicity generated

by polymeric systems. There are a number of assays used to measure oxidative stress such as ROS assay, lipid peroxidation assay, glutathione: oxidized glutathione assay, cytochrome C reduction assay and probe based assays such as 2′,7′-dichlorofluorescein diacetate (DCFDA) and 5-(and 6-)-chloromethyl-2',7'-dichloro-dihydrofluorescein diacetate (CM H_2DCFDA) ROS assay

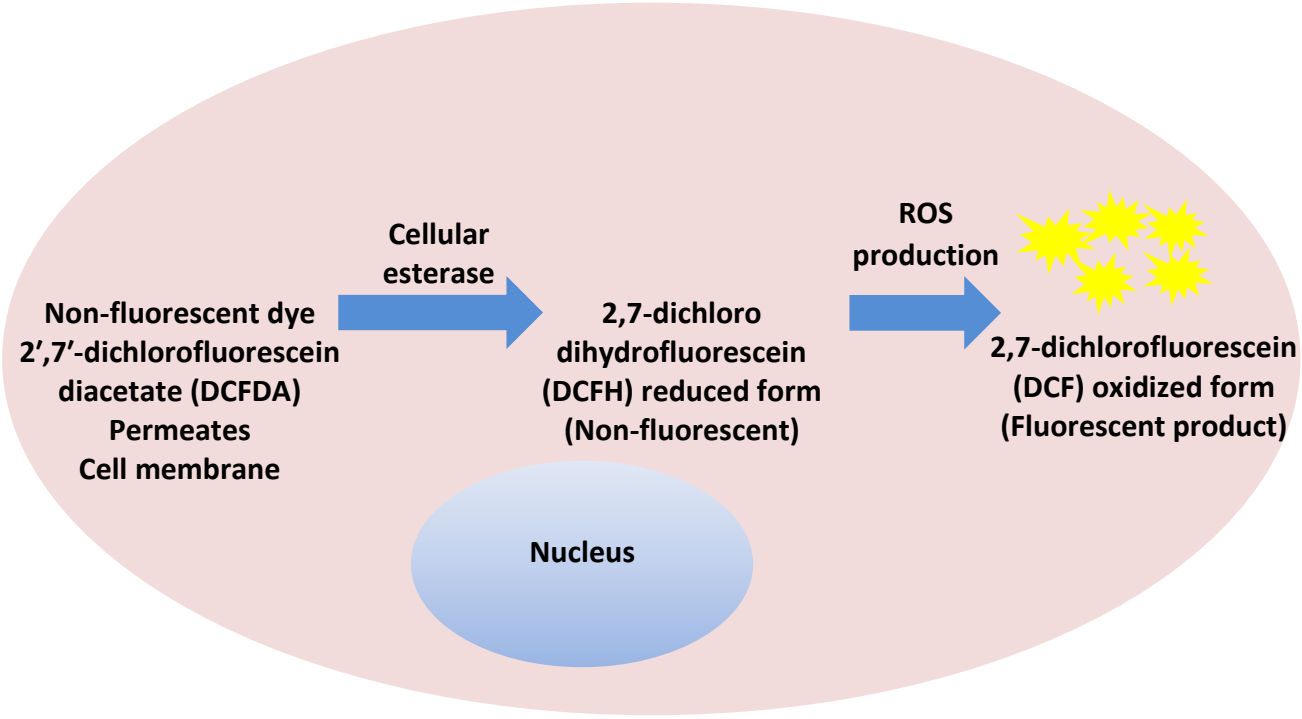

Figure 4.1 Schematic representation of probe based detection of intracellular ROS

4.1.4.1 ROS assay

The ROS assays are employed to determine the inflammatory and oxidizing potential of nanocarriers by measuring intracellular ROS. ROS production is measured using probes e.g. 2′,7′-dichlorofluorescein diacetate (DCFDA) or 5-(and 6-)-chloromethyl-2',7'-dichloro-dihydrofluorescein diacetate (CM H_2DCFDA). These fluorescent based probes can permeate the cell membrane where they are deacetylated to form 2,7-dichlorodihydrofluorescein (DCFH) [166]. In the presence of ROS, DCFH is oxidized to a fluorescent product, 2,7-dichlorofluorescein (DCF) (Figure 4.1) [166]. The evaluation of intracellular oxidative stress is made by measuring the presence of fluorescence of DCF in the sample by a fluorometer [160]. It gives an indication of

inflammation and irritation. The degree of inflammation and irritation can also be measured by evaluating the immunotoxicity profile.

4.1.5 Immunotoxicity

Immunotoxicity assessment is an important aspect of biomaterial screening of nanocarriers for their inflammatory potential. Inflammation occurs as a result of an immune response set in against the foreign antigens. It is mediated by a complex regulatory network of cells. Macrophages are activated on exposure to foreign bodies and secrete cytokines such as interleukin-6 (IL-6), IL-8 and TNFα which further generate immune response and inflammation [361, 362, 394].

Cytokines are small soluble proteins or glycoproteins which act as messengers between adjacent or distant cells particularly of hematopoietic origin [395]. They act as markers of inflammation or disease process [396]. Among the many cytokines some function as proinflammatory (TNF-α, IL-2 and IL-6) while other as anti-inflammatory bodies (IL-10) [396, 397]. TNF-α and IL-6 were chosen for the *in vitro* cytokines assay because they are produced by activated macrophages and monocytes. They are involved in acute phase pro-inflammatory reactions [396, 398]. TNF-α can induce the production of IL-6 [396] and is able to initiate a cascade of other cytokines which further mediate an inflammatory response [399]. IL-2 is predominantly produced by antigen-activated T cells [400]. In addition to TNF-α and IL-6, IL-2 was employed for *in vivo* cytokine generation assay to assess the role of second line immune cells (T cell) in immune regulation. It has both positive and negative effects on the immune response and can stimulate a cascade of cytokines that involve various interleukins, interferon and TNF-α [401].

The type and degree of cytokine production has been found to be different between different cell lines. Tryoen-To´th and coworkers cultured osteoblast-like cells (SaOS-2) and human periodontal ligament (PDL) cells on the surface of polyelectrolyte films with different terminating layers i.e., PEI, poly(sodium 4-styrenesulfonate) (PSS), PAH, poly(L-glutamic acid) (PGA), or PLL. They found significantly high levels of IL-8 (45 and 35%) than TNF-α in the culture supernatant of SaOS-2 cells grown on PAH and PEI-terminating films respectively, indicating the influence of type of polycation on cytokine production. The stimulating effect of PAH and PEI surfaces on

IL-8 production was more pronounced on PDL cells indicating cell type specific production [402].

Chellat *et al.* found that exposure of the THP-1 macrophages to different concentrations of chitosan-DNA nanoparticles did not induce proinflammatory cytokine (IL-1β, IL-6 and TNFα) at 1, 6 and 24h incubation time [361]. Similar findings have been reported by Semete *et al.* who reported that chitosan and polyethylene glycol (PEG) coated-PLGA nanoparticles were taken up by macrophages following *in vivo* exposure via oral and intraperitoneal routes but did not produce significant level of cytokine [403]. These studies indicate non-immunogenicity of these polymeric nanoparticles.

Researchers have identified the relationship of cytokine production with cytotoxicity which may adversely affect their use. A study done by Olbrich *et al.* investigated the effect of D114- solid lipid nanospheres (SLN) prepared using different surfactants on the production of pro-inflammatory cytokine IL-6, IL-12 and TNFα by RAW 264.7 cells. They reported that the IL-6 and TNFα generation reduced with the increase in concentration of formulation (from 0.00001 to 0.1%) such that no cytokine were detected at higher concentrations [404]. These findings indicated an inverse relationship of the cytokine generation with cytotoxicity. Similar findings have been reported by Scholer *et al.* who studied the generation of IL-6, IL-12 and TNFα on exposure to solid lipid nanoparticles (SLN) coated with P908, P407, P188, HS15 and T80 at 0.001% or lower concentrations. It was shown that IL-6 generation following incubation with all the above mentioned SLN formulations was reduced from 0.0001% to 0.1% in a concentration dependent manner indicating an inverse relationship of cytokine generation with cytotoxicity [405].

There may be an association of physicochemical properties of nanocarriers such as size, surface charge, biodegradability, hydrophilicity and hydrophobicity with generation of cytokines, however, the effect of these properties on the cytokine generation has not been fully explored for polymeric nano-structures. There are two important techniques of analysing and quantifying cytokines in biological fluids and tissue culture supernatant namely flow cytometric and ELISA based detection.

4.1.5.1 Enzyme linked immunosorbent assay (ELISA)

ELISA is a highly specific and sensitive method for quantifying cytokines in biological samples [406]. However, they are restricted to detection and quantification of a single cytokine per assay. Simultaneous detection of a number of cytokines can be performed by using flow cytometry [406]. The principle of sandwich ELISA is detailed in chapter 3, section 3.3.4.2.

4.2 AIM

The aim of the present study was to investigate the biocompatibility of various polycations and NIL APECs.

4.2.1 Objectives

To investigate the effect of various polycations and APECs on

- Cytotoxicity
- ROS generation
- Haemocompatibility
- *In vitro* and *in vivo* Immunotoxicity

4.3 MATERIALS AND METHODS

4.3.1 Materials

Materials used	Supplier
3-4,5 dimethyl thialzol2,5 diphenyl tetrazolium bromide (MTT)	Sigma Aldrich
CaCo2 Cells	European Collection of Cell Cultures
Cytokine ELISA kits	Bioscience
Dimethyl Sulfoxide (DMSO)	Sigma Aldrich
Dulbecos Minimal essential media	Invitrogen, UK
Dulbecos Modified Eagles Media	Invitrogen, UK
Eagles Minimal Essential Media	Sigma Aldrich
Foetal bovine serum	Sigma Aldrich
Hydrogen peroxide (H_2O_2)	Sigma Aldrich
J774 cells	European Collection of Cell Cultures
L Glycine	Sigma Aldrich
L-Glutamine	Sigma Aldrich
Lipopolysacchride (LPS)	Sigma Aldrich
Non-essential amino acids	Sigma Aldrich
Penicillin Streptomycin	Sigma Aldrich
Phosphate buffer saline 10X (PBS)	Sigma Aldrich
ROS detection assay kit	Invitrogen, UK
Triton-X	Sigma Aldrich
Trypan Blue	Sigma Aldrich
Trypsin 10X	Sigma Aldrich

4.3.2 Methods

4.3.2.1 Thawing of frozen CaCo2 cells

The media was warmed by placing in a 37°C water bath for 15min. On every occasion when the cells were thawed, the cryo-tube was taken out from the liquid nitrogen and partially immersed in the water bath at 37°C for 1-2min until the cells fully thawed. The tube was then wiped with 70% IMS to avoid contamination. The contents of the tube were slowly pipetted into a T25 flask ($75cm^2$). 9mL of pre-warmed complete medium (Eagles minimal essential medium (EMEM) supplemented with 1% non- essential amino acids (NEAA), 1% 2nM Glutamine, 10% heat inactivated foetal bovine serum (FBS) and 1% Penstrep) was added into the flask to promote the growth of cells. The flask was incubated in 5% CO_2 at 37°C.

4.3.2.2 Cell line maintenance:

CaCo2 cells grown in EMEM were examined every alternate day for their confluency and media was replaced with 10mL of fresh pre-warmed media. The cells were re-incubated in 5% CO_2 at 37°C. They were generally found to be 80-90% confluent in 3-4 days and ready for subculture. For all experiments the confluent flasks were first washed 3 times with 5mL 0.01M PBS. 3mL of 0.25% w/v trypsin was added to the CaCo2 cell flask to dislodge cells from the bottom of the flask. The flask was then swirled few times to allow contact of trypsin with all the cells. 2mL of trypsin was aspirated and the flask was incubated in 5% CO_2 at 37°C for 30sec. The flask was then gently shaken and tapped to separate cells from each other. Subsequently, the cells were examined under the microscope to confirm cell detachment from the surface of the flask. 5mL of media was then added into the flask to inactivate the trypsin. The cell suspension was transferred to a 15mL centrifuge tube and centrifuged at 1500 rpm for 5min at ambient temperature. The supernatant was aspirated by vacuum suction and the pellet was re-suspended in 1mL of fresh media. The cells were counted as detailed below (section 4.3.2.3) and transferred to new T75 flasks to grow again. The remaining cells were used for the required assay. The thawed cells were sub-cultured three times before using for an experiment.

J774 cells were cultured in dulbeco's modified eagles medium (DMEM) which was supplemented with 10% FBS and 1% penicillin/streptomycin and incubated in 5% CO_2 at 37^o C. Macrophages adhere strongly to the tissue culture plastic and hence cannot be easily trypsinized. Therefore, the cells were passaged by scraping. Once confluent

(usually within 24h) the cells were gently scraped with a cell scraper. The harvested cells were centrifuged at 1500 rpm for 5min at room temperature. The pellet was re-suspended in media and used as required.

4.3.2.3 Cell counting

100µL of cell suspension was mixed with 100µL trypan blue in an eppendorf (1:1 dilution). 10 µL of this suspension was pipetted into the haemocytometer chamber and was covered with a moist cover slip.

The number of cells were counted in the neubauer's chamber and the average number of viable cells in the suspension was determined as shown in equation 4.1.

$$\text{Average number of cells/chamber} = \frac{\text{Total number of viable cells}}{\text{Number of chambers}}$$

Equation 4.1

The original number of cells/mL were calculated as in equation 4.2.

$$\text{Original number of cells/mL} = \text{Average number of cells} \times 10^4 \times \text{dilution factor}$$

Equation 4.2

The volume of the original cell suspension required to achieve desired number of cells to grow in a flask was calculated using equation 4.3.

$$\text{Volume of original suspension} = \frac{\text{Desired number of cells}}{\text{Original number of cells}} \times \text{Total volume}$$

Equation 4.3

4.3.2.4 In vitro cytotoxicity assay

4.3.2.4.1 MTT assay

MTT assay was conducted on two different cell lines to determine the cytotoxicity of various formulations. CaCo2 cells (passage 40-70) and macrophage J774 cell line (passage 86-97) were grown at a density of 2 X 10^3 cells/well in 96 well plates under identical experimental conditions. The method described here is based in principle on the method described by Mosmann *et al.* [407].

200µL of the cell suspension (2 X 10^3cells/well) was added to the 96 wells plates. The plates were incubated at 37°C, 5% CO_2 until the desired confluency (80-90%) was achieved (usually within 1-2 days). The polymer (PAH, Pa2.5, Da10, QPa2.5) and APEC (PAH-DS, PAH-PAA, Pa2.5-DS, Pa2.5-PAA, Da10-DS, Da10-PAA, QPa2.5-DS and QPa2.5-PAA) solutions were prepared (as described in chapter 3, section 3.5.2.1.1 & 3.5.2.2.1) and were serially diluted with growth media to achieve required concentrations. The media in the 96 well plate was replaced with 200µL of each concentration into the wells (n=5). Triton X was used as a positive control while untreated media was used as a negative control. Plates were incubated in 5% CO_2 at 37°C. After 24h incubation, the polymer/APEC solutions were replaced with 200µL of fresh media and plates were incubated for another 24h. 50µL of sterile filtered MTT solution (0.5 mg/mL) prepared in distilled water was added into each well containing media. The unreacted dye was aspirated after 4h. The insoluble formazan crystals were dissolved by adding 200µL of DMSO, followed by addition of 25µL of 0.05 M glycine buffer (made up by dissolving 3.75g glycine and 2.93g NaCl in 500mL distilled water and pH adjusted to 10.5) in each well. The absorbance was read spectrophotometrically at a wavelength of 540nm with a UV plate reader (Synergy H4, Vermont, USA). The percentage cell viability was calculated using equation 4.4.

$$\%\ \text{Cell viability} = \frac{\text{Average sample absorbance} - \textit{background absorbance}}{\text{Average absorbance of negative control} - \textit{background absorbance}}\ \text{X}\ 100$$

Equation 4.4

The IC_{50} was calculated as the concentration at which the cell viability decreased to 50% of maximum cell viability (negative control cells). The experiments were performed in triplicates.

4.3.2.5 Haemolysis assay

4.3.2.5.1 Erythrocyte preparation

Fresh rat blood was kindly provided by the biological service unit (BSU) of the University of Hertfordshire. Blood was collected in a heparinized tube and washed with phosphate buffered saline (PBS buffer 0.01 M). 15mL of PBS was added to 3 - 5mL of fresh rat blood and centrifuged at 2500 rpm for 10min at 4˚C. The supernatant was

discarded and the process was repeated until the supernatant was clear. The final erythrocyte pellet was isolated and weighed. A 3% w/v dilution was made with PBS.

4.3.2.5.2 Assay procedure

Haemolysis assay was adopted from the method described by D Fischer *et al.* [157]. 80µL of the erythrocyte suspension was pipetted into each well of round bottomed 96 well plates. 20 $mgmL^{-1}$ stock solution of each polymer or APEC was made up in Tris buffer and the pH was adjusted to pH 7.4 with NaOH / HCl. Serial dilution was performed to achieve various concentrations ranging from (0.05- 10$mgmL^{-1}$) of polymer and APEC solutions by using 0.01M PBS as a diluent. 80µL of various formulation concentrations (n=5) were added into a 96 well plate. The negative control was prepared by mixing blood and PBS solutions (1:1), while the positive control was prepared by mixing blood solution and triton X (1:1). The plates were incubated at 37˚C for 4h and then centrifuged at 2500 rpm for 10min at 4˚C. 100µL of supernatant from each well was transferred to a flat bottom 96 well plate. The amount of haemoglobin released in the samples was determined spectrophotometrically at 540nm. The experiments were performed in triplicate and the percentage haemolysis was calculated in relation to the positive controls by using equation 4.5.

$$\% \text{ Haemolysis} = \frac{\text{Average sample absorbance} - \textit{background absorbance}}{\text{Average absorbance of positive control} - \textit{background absorbance}} \text{ X } 100$$

Equation 4.5

4.3.2.6 Reactive oxygen species (ROS) assay

The ROS production was investigated in the CaCo2 cells incubated with various polymers and APECs. The CaCo2 cells (2 X 10^3cells/well) were seeded into a 96-well plate and incubated for 24h. The generation of ROS was monitored by using ROS detection kit (Molecular Probes/Invitrogen) following the manufacturer's protocol.

100µL of polymer or APEC at the IC_{90} concentration (concentrations (PAH 3$µgmL^{-1}$, PAH-DS 3$µgmL^{-1}$, PAH-PAA 5$µgmL^{-1}$, Pa2.5 7$µgmL^{-1}$ Pa2.5-DS 10$µgmL^{-1}$, Pa2.5-PAA 14$µgmL^{-1}$, Da10 7$µgmL^{-1}$, Da10-DS 10$µgmL^{-1}$, Da10-PAA 14$µgmL^{-1}$, QPa2.5 11$µgmL^{-1}$, QPa2.5-DS 14$µgmL^{-1}$, QPa2.5-PAA 14$µgmL^{-1}$) determined by the MTT assay) were added to each well of 96 well plate (n=5) and plates were incubated at 37˚C

for 4h. A 10µM stock solution was prepared by first dissolving in 50µg of carboxy methyl- di-fluoro di-hydro fluorescein di-acetate (CM-H_2DCFDA- 577.8 g/mol) in 0.5mL DMSO while protected from light, followed by subsequent dilution with 11.5 mL of 0.01M PBS**.**

The cells were washed 3 times with PBS and incubated with 100µM CM-H_2DCFDA (100µL/well) at 37°C. After 30min, the cells were washed 3 times with PBS and incubated with serum free medium (100µL/well). The medium was removed after 30min and replaced with PBS. Production of the oxidation product was determined by measuring the fluorescent intensity of the samples at 560 nm (excitation) and 590 nm (emission) on a fluorescent microplate reader (Techan M200 microplate reader). The background reading of negative control (PBS) was subtracted from the actual fluorescent reading. Tert-Butyl hydrogen peroxide (TBHP- $(CH_3)_3COOH$), 100µM was used as a positive control for ROS production, as it is an inducer of a number of ROS. The ROS generation induced by the positive control was considered as 100%. The percentage of ROS production by cells incubated with various formulations was calculated in respect to the positive control cells as shown in equation 4.6.

$$\%\ \text{ROS production} = \frac{Average\ fluorescence\ intensity\ of\ samples - background\ fluorescence}{Average\ fluorescence\ intensity\ of\ positive\ control - background\ fluorescence} X100$$

Equation 4.6

4.3.2.7 Cytokine Assay:

4.3.2.7.1 *In vitro* cytokines assay

The macrophages were harvested from a confluent flask and centrifuged at 1500 rpm for 5min at room temperature. The pellet was re-suspended in media and seeded in 96 well plates (2 X 10^3 cells/well) for 24h. The cells were incubated with 200µL/well of polymers, NIL APECs at the IC_{90} concentrations (refer to section 4.3.2.6) based on the results from MTT assay. Lipopolysaccharide (LPS) was used as a positive control (1µg/mL) to induce cytokines associated with activated macrophages.

After 2-4 h incubation of the cells with the samples, the supernatants were collected for cytokine determination. The concentrations of cytokines (TNF-α and IL-6) in cell culture supernatants were determined by enzyme-linked immunosorbent assay (ELISA) according to the manufacturer's protocol (Bioscience ELISA kits).

Briefly, the plates were coated with cytokine capture antibodies (IL-6, TNF- α). The plates were sealed and kept at 4°C for 16-18h. The coated plates were washed 4 times with 300µL wash buffer per well. Afterwards, the plates were washed 4 times with 300µL wash buffer per well between all the subsequent steps. 200µL of assay diluent was added to each well to reduce the non-specific binding and the plates were re-incubated. After 1h reaction period, 100µL per well of standards and cell culture supernatants incubated with IC_{90} concentration of polymer and APECs diluted in assay diluent were added to the wells of 96 well plates and incubated for 2h on a plate shaker (200 rpm) at RT. Thereafter, the plates were incubated with 100µL per well of detection antibodies. After 1h reaction time, 100µL per well of freshly prepared TMB substrate solution was added and plates were incubated in the dark for 20min. The wells containing cytokine turned blue. 100µL per well of stop solution (1M H_2SO_4) was added to each well to stop the reaction. The amount of IL-6 and TNF-α present in each well was determined by using a microplate spectrophotometer (Synergy H4, Vermont, USA) at a wavelength of 540nm. A standard calibration curve was constructed between absorbance and known concentration (7.8-500 $pgmL^{-1}$) of cytokines (IL-6 and TNF). The cytokine concentration in unknown samples was calculated from the calibration curve. The measurements were performed in triplicates.

4.3.2.7.2 *In Vivo* cytokine assay

Male wistar mice were maintained in the BSU at UH, and used at 6-8 weeks of age. They weighed between 18 - 22g each. To examine the *in vivo* effect of the formulations, half of the mice were injected intravenously with sterile LPS (100µg/mouse) and 100-200µg/mouse of formulations prepared in 5% dextrose via the tail vein while rest half were given the formulations orally via intra gastric gavage to ensure delivery of an exact dose. The mice were bled and 100-200µL aliquots of blood were retrieved via the arterial catheter at 12h after i.v. administration and 24h of oral administration of formulations. Blood samples were centrifuged at 6000 rpm for 5 min at 4°C. The serum was aliquoted and stored at -20°C until assayed for the presence of cytokines. The serum cytokine concentrations were determined by ELISA immunoassay as described above in section 4.3.2.7.1.

4.3.2.8 Statistical analysis

All the experiments were performed in triplicates and data presented as mean ±S.E. Statistical analysis was performed using one way analysis of variance (ANOVA)

followed by post hoc, tukey's test for comparison with the control group. The statistical significance was determined at a $p<0.05$.

4.4 RESULTS

4.4.1 *In vitro* cytotoxicity analysis by MTT assay

MTT assay was performed to determine the viability of CaCo2 and J774 cells after 24h treatment with polycations or NIL APECs formulations. The principle of this assay is based on the assessment of cellular mitochondrial activity [407]. The percentage of viable cells was used as an indicator of polycation and APECs response.

4.4.1.1 MTT analysis on CaCo2 cells

The treatment of cells with DS and PAA at (0.01-10mgml^{1}) concentrations did not affect the cell viability or morphological characteristics of cells (data not shown). The polycations (PAH, Pa2.5, Da10, QPa2.5) produced a more significant decrease in the cell viability than APECs (Figure 4.2 & 4.3). The IC_{50} values of the polycations were calculated to be PAH-37.5µgmL^{-1}, Pa2.5-63µgmL^{-1}, Da10-63µgmL^{-1}, and QPa2.5-500µgmL^{-1} (Table 4.1).

A substantial increase in IC_{50} ($p<0.05$**)** was observed when the cells were incubated with APECs. The improvement in IC_{50} was more pronounced in the presence of PAA based APECs ($p<0.001$**)** than DS based APECs. The introduction of PAA was able to increase the IC_{50} of PAH by 2 fold ($p\leq0.01$), Pa2.5 (14 fold- $p\leq0.001$), Da10 (16 fold- $p\leq0.001$) and QPa2.5 (2 fold- $p\leq0.01$) compared to polycation alone (Table 4.1). On the other hand, DS based formulations i.e., Pa2.5-DS and PAH-DS did not exhibit improvement in IC_{50}, whereas Da10-DS ($p<0.01$) and QPa2.5-DS ($p<0.05$) improved the IC_{50} by 2.2 and 2 fold respectively.

Substantial changes in the morphology of the cells were noticed upon incubation with the polycations and APECs (Figure 4.4). The number of viable cells appeared significantly higher in the cells incubated with the PAA based formulations, particularly Pa2.5-PAA and Da10-PAA. The areas showing black patches on micrograph represent the dead cells.

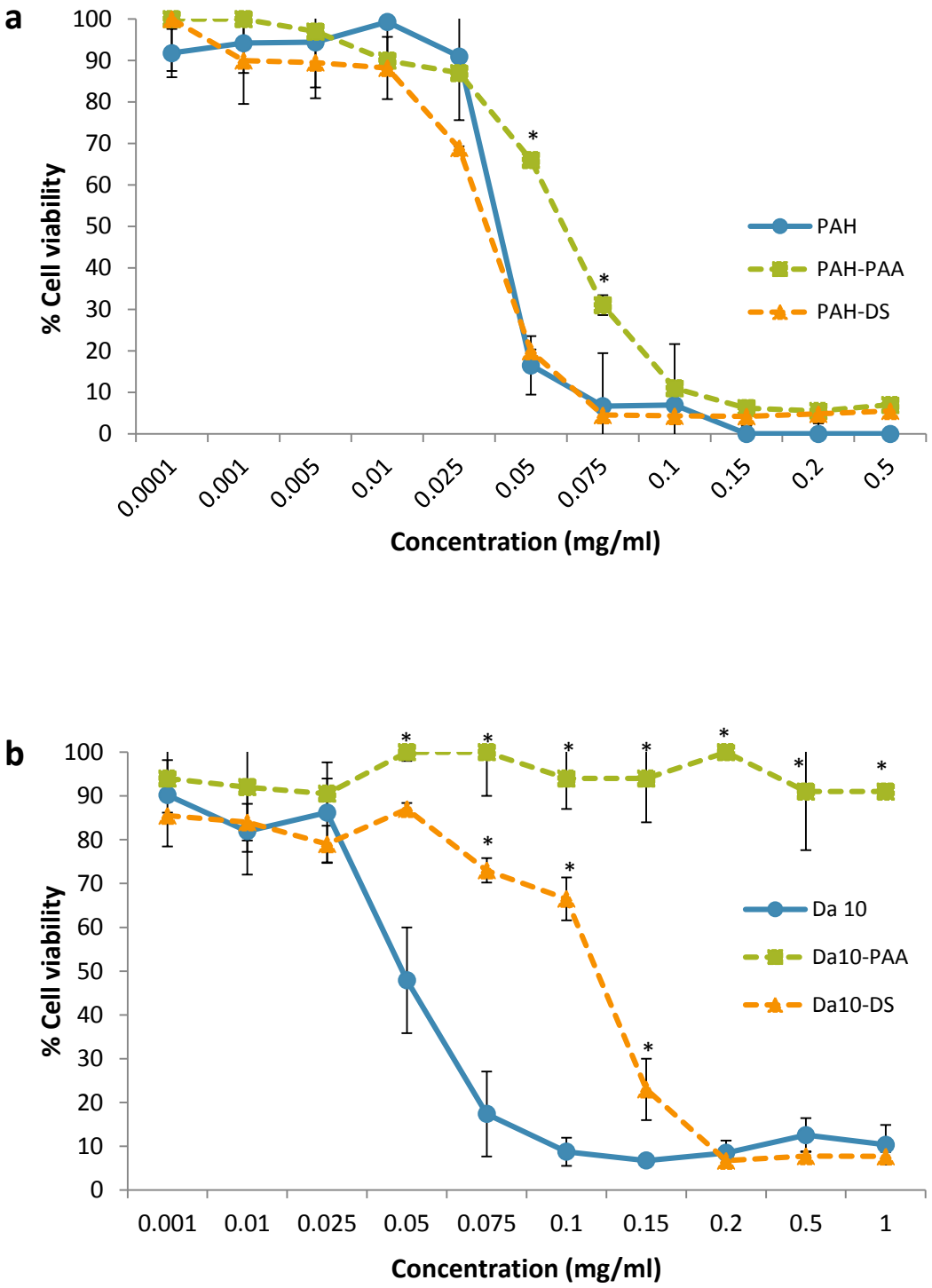

Figure 4.2 Effect of (a) PAH and corresponding APECs (b) Da10 and corresponding APECs on viability of CaCo2 cells. Each value represents mean± SE of three experimental determinations. Statistical significance was determined at a p value<0.05*.

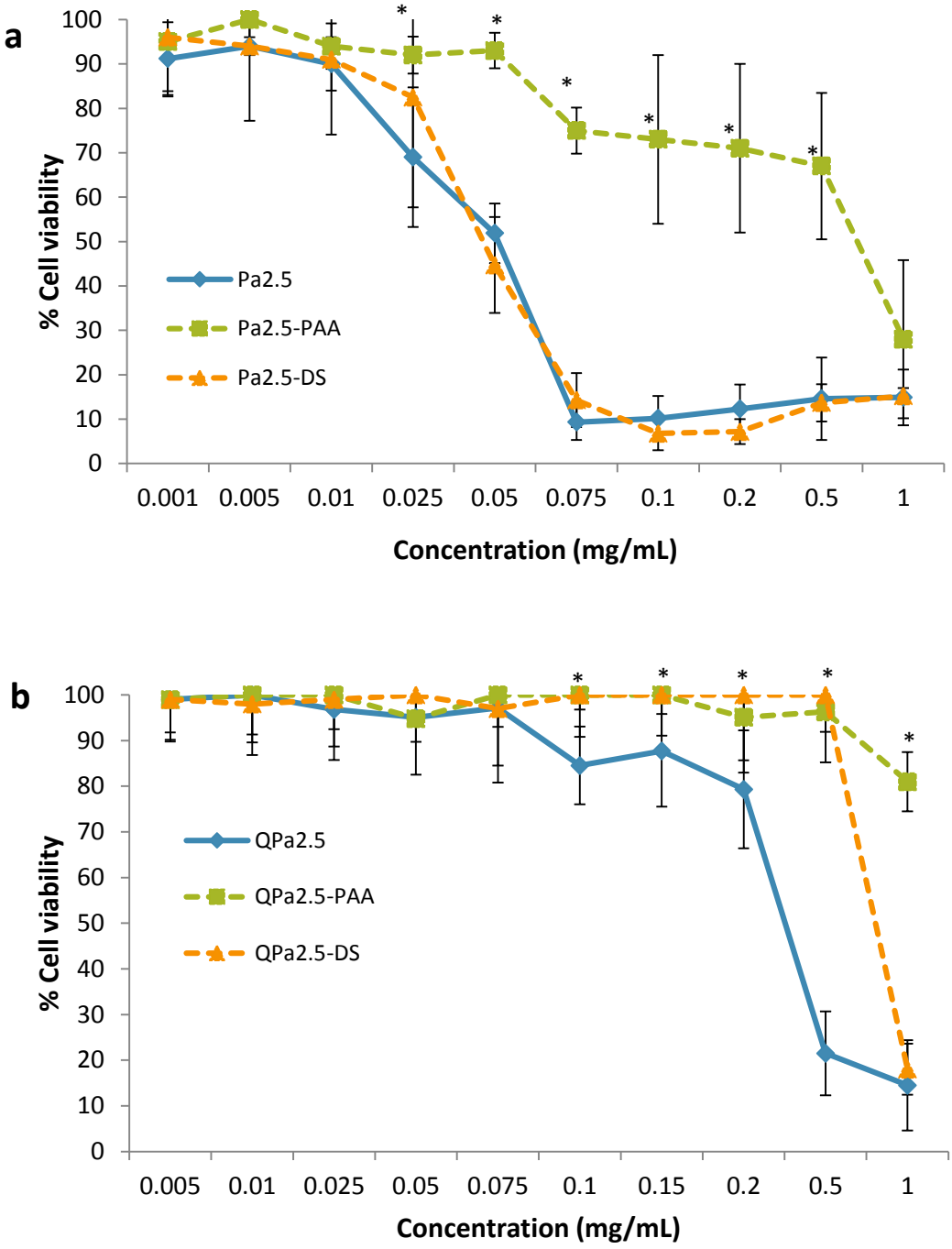

Figure 4.3 Effect of (a) Pa2.5 and corresponding APECs (b) QPa2.5 and corresponding APECs on viability of CaCo2 cells. Each value represents mean± SE of three experimental determinations. Statistical significance was determined at a p value<0.05*.

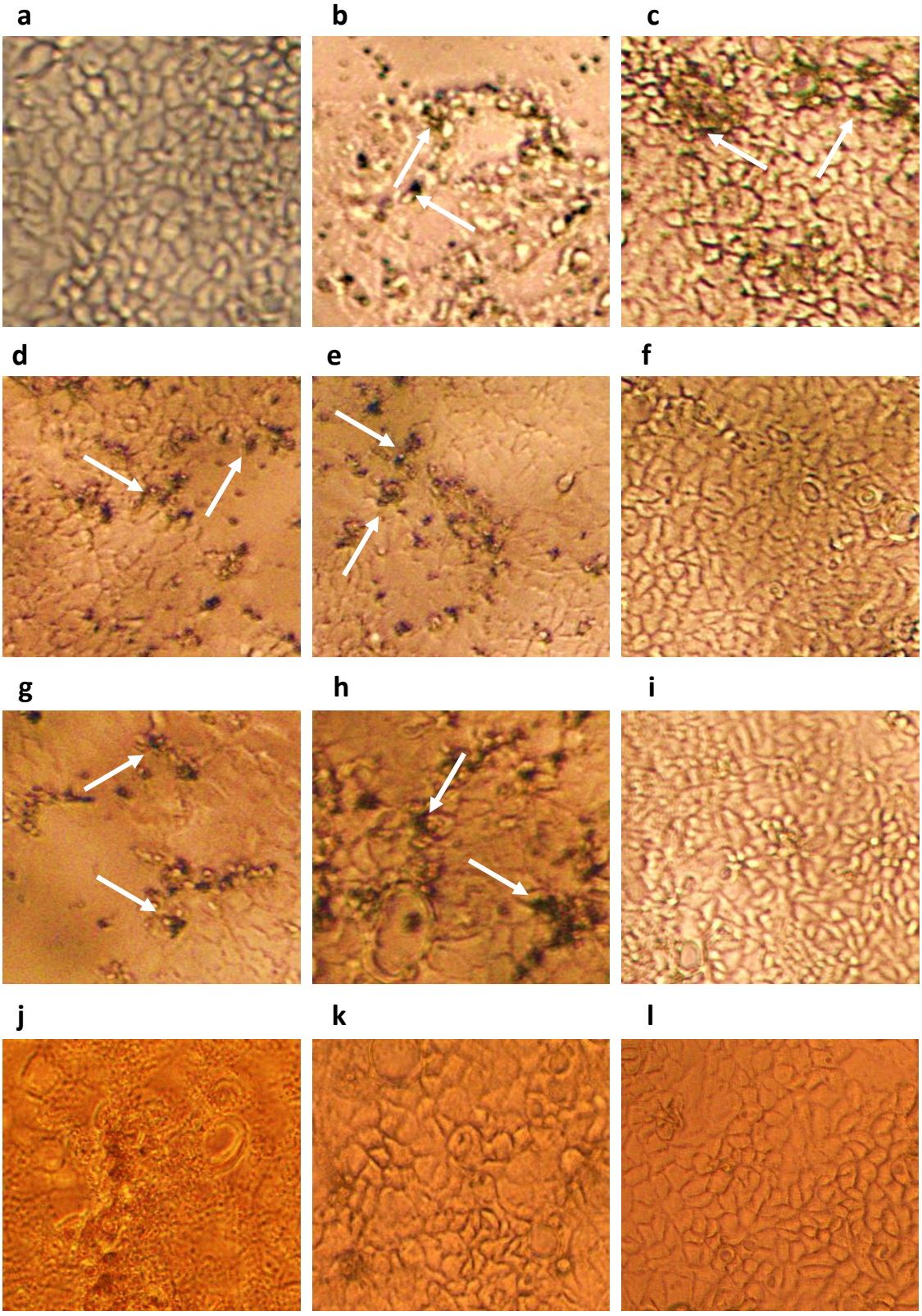

Figure 4.4 Effect of polycations and APECs on viability of CaCo2 cells (a) Untreated control, (b) PAH-DS (0.025mgmL^{-1}), (c)PAH-PAA (0.025mgmL^{-1}), (d) Da10 (0.05mgmL^{-1}), (e) Da10-DS (0.05mgmL^{-1}), (f) Da10-PAA (0.05 mgmL^{-1}), (g) Pa2.5 (0.05mgmL^{-1}), (h) Pa2.5-DS (0.05mgmL^{-1}), (i) Pa2.5-PAA (0.05mgmL^{-1}), (j) QPa2.5 *(0.5*mgmL^{-1}*), (k) QPa2.5-DS (0.5*mgmL^{-1}*), (l) QPa2.5-PAA (0.5*mgmL^{-1}). The black patches show dead cells which are indicated by arrows.**

Table 4.1 A summary of cytotoxicity profile of polycations and APECs on CaCo2 and J774 cells following 24h incubation. Each value represents mean± SD of three experimental determinations.

Polycations/ APECs	IC_{50} ($mgmL^{-1}$) on CaCo2 cells	Improvement in IC_{50} of APECs compared to related polycations	IC_{50} ($mgmL^{-1}$) on J774 cells	Improvement in IC_{50} of APECs compared to related polycations
PAH	$3.75X\ 10^{-2}$		$2.0X\ 10^{-2}$	
PAH-PAA	$7.5X\ 10^{-2}$	2 folds	$7.2X\ 10^{-2}$	3.6 folds
PAH-DS	$3.75X\ 10^{-2}$	-	$2.4X\ 10^{-2}$	1.2 folds
P2.5	$6.3X\ 10^{-2}$		$3.75X\ 10^{-2}$	
Pa2.5-PAA	$9.0X\ 10^{-1}$	14.2 folds	$3.5X\ 10^{-1}$	9.33 folds
Pa2.5-DS	$6.3X\ 10^{-2}$	-	$1.5X\ 10^{-1}$	4 folds
Da10	$6.3X\ 10^{-2}$		$3.75X\ 10^{-2}$	
Da10-PAA	1	15.8 folds	$1.4X\ 10^{-1}$	3.73 folds
Da10-DS	$1.4X\ 10^{-1}$	2.2 folds	$8.15X\ 10^{-2}$	2.17 folds
QPa2.5	$5X\ 10^{-1}$		1.15	
QPa2.5-PAA	1	2 folds	$2.1X\ 10^{-1}$	-
QPa2.5-DS	1	2 folds	$1.7X\ 10^{-1}$	-

4.4.1.2 MTT analysis on J774 cells

J774 cells were found to be more susceptible to polycations and APECs induced cytotoxicity than CaCo2 cells. The IC_{50} values varied significantly between the two cell lines. The IC_{50} values in J774 cells were found to be much lower than those found in CaCo2 cells (Table 4.1). The degree of cytotoxicity on J774 cells is rated as PAH>Pa2.5=Da10>QPa2.5 which is similar to what was found in CaCo2 cells (Figure 4.5 & 4.6). Once again, PAH was found to be more cytotoxic than its modified counterparts (Figure 4.5a) and QPa2.5 was the least cytotoxic (Figure 4.6b).

Similar to CaCo2 cells, the addition of polyanions diminished the cytotoxicity of most of the polycations in J774 cells (except QPa2.5 based APECs), however, the improvement was not as great as found in the CaCo2 cells (Table 4.1). Pa2.5-PAA and

Da10-PAA improved the IC_{50} on J774 cells by 9.3 fold ($p<0.01$) and 3.73 fold ($p<0.05$) respectively, whereas 14 – 16 fold respectively on CaCo2 cells. On the other hand, Pa2.5-DS displayed 4 fold improvements in IC_{50} ($p<0.05$), in contrast to no improvement on CaCo2 cells. Like CaCo2 cells, Da10-DS produced 2 fold improvement in IC_{50} ($p<0.05$) on J774 cells. Substantial changes in the morphology of cells were noticed after 24h incubation with polycation or APECs (Figure 4.7). The number of dead cells was seen to be higher in the cells incubated with the polycations than APECs at identical concentrations.

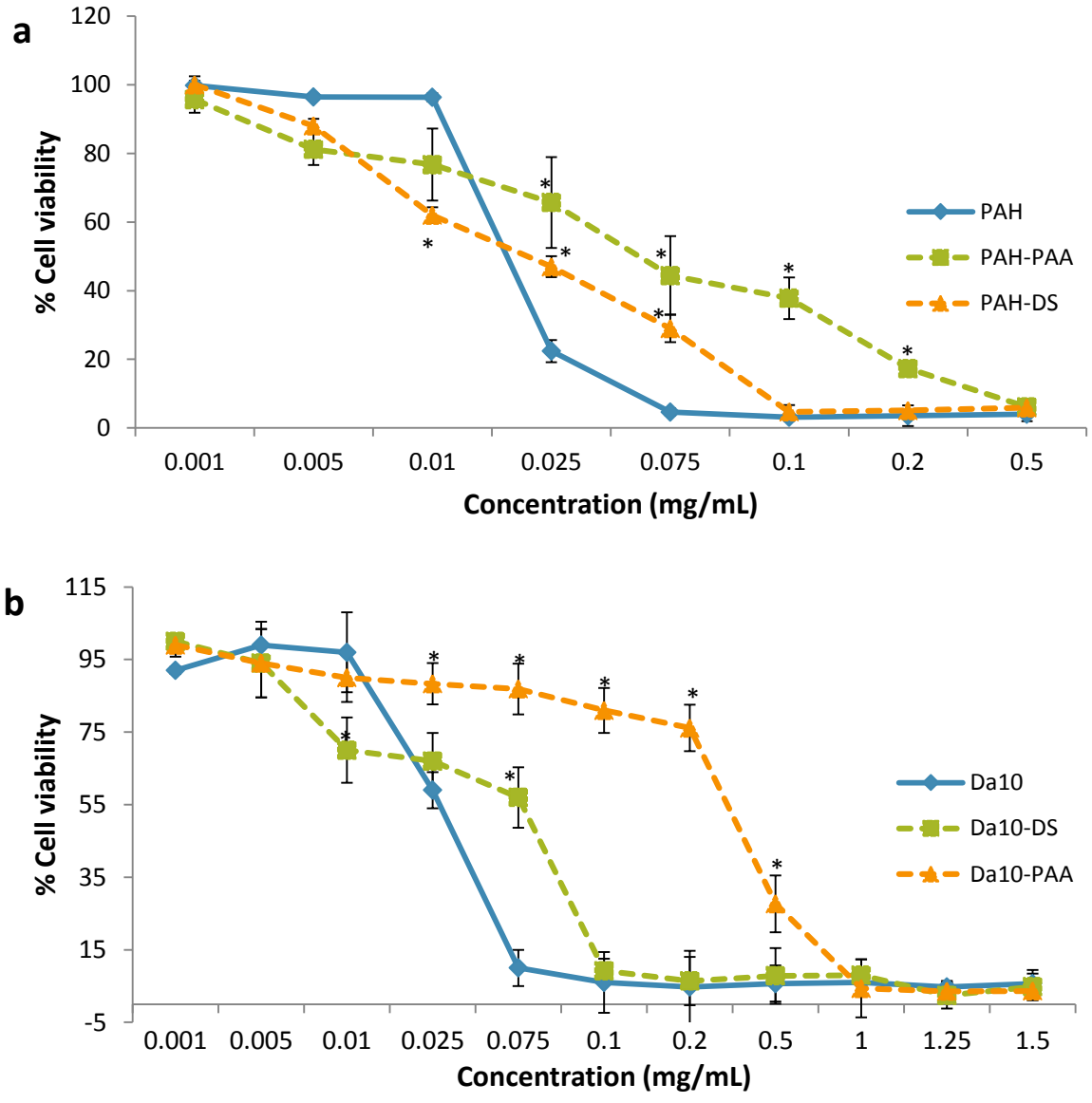

Figure 4.5 Effect of (a) PAH and corresponding APECs (b) Da10 and corresponding APECs on viability of J774 cells. Each value represents mean± SE of three experimental determinations. Statistical significance was determined at a p value<0.05*.

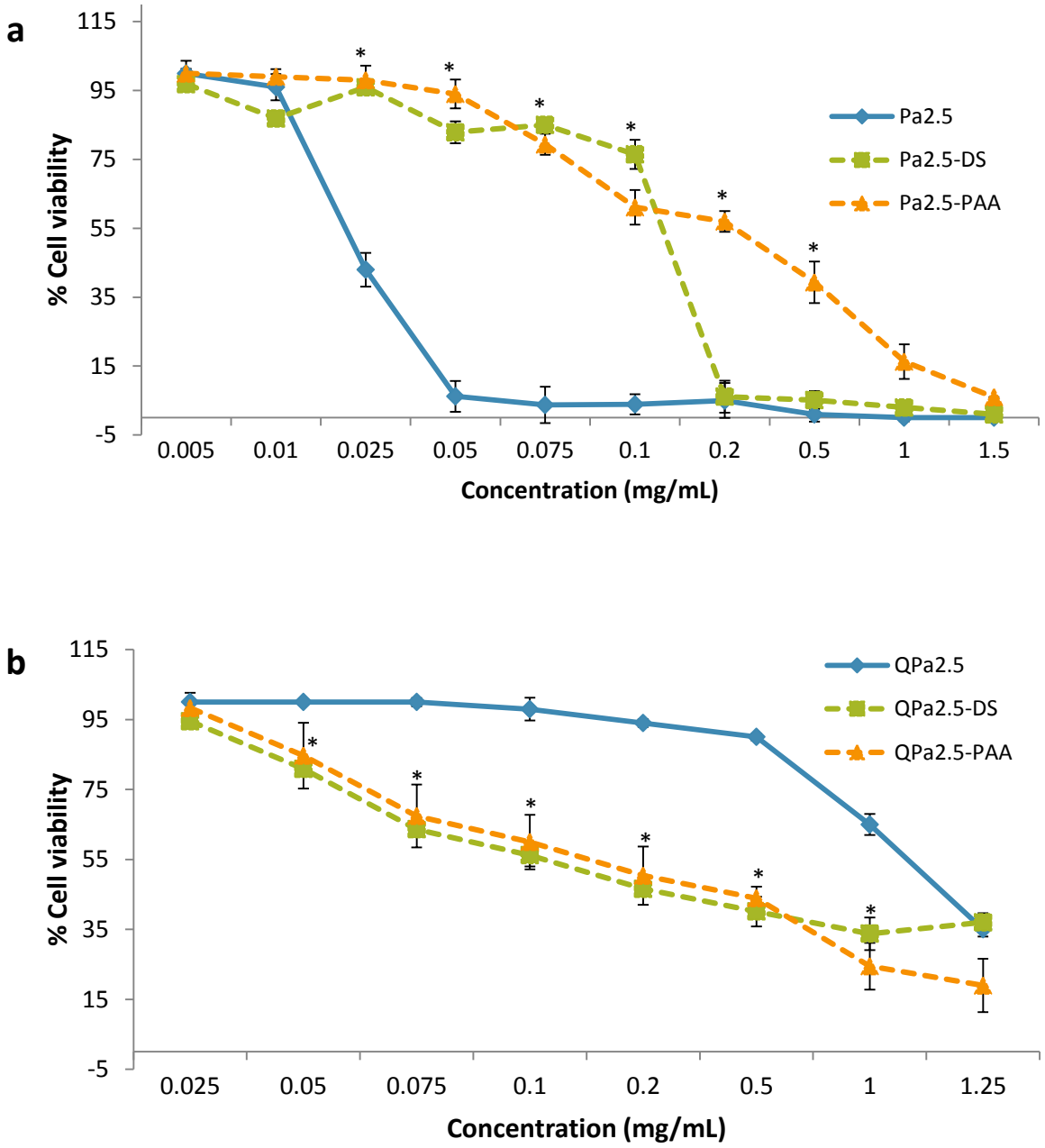

Figure 4.6 Effect of (a) Pa2.5 and corresponding APECs (b) QPa2.5 and corresponding APECs on viability of J774 cells. Each value represents mean± SE of three experimental determinations. Statistical significance was determined at a p value<0.05*.

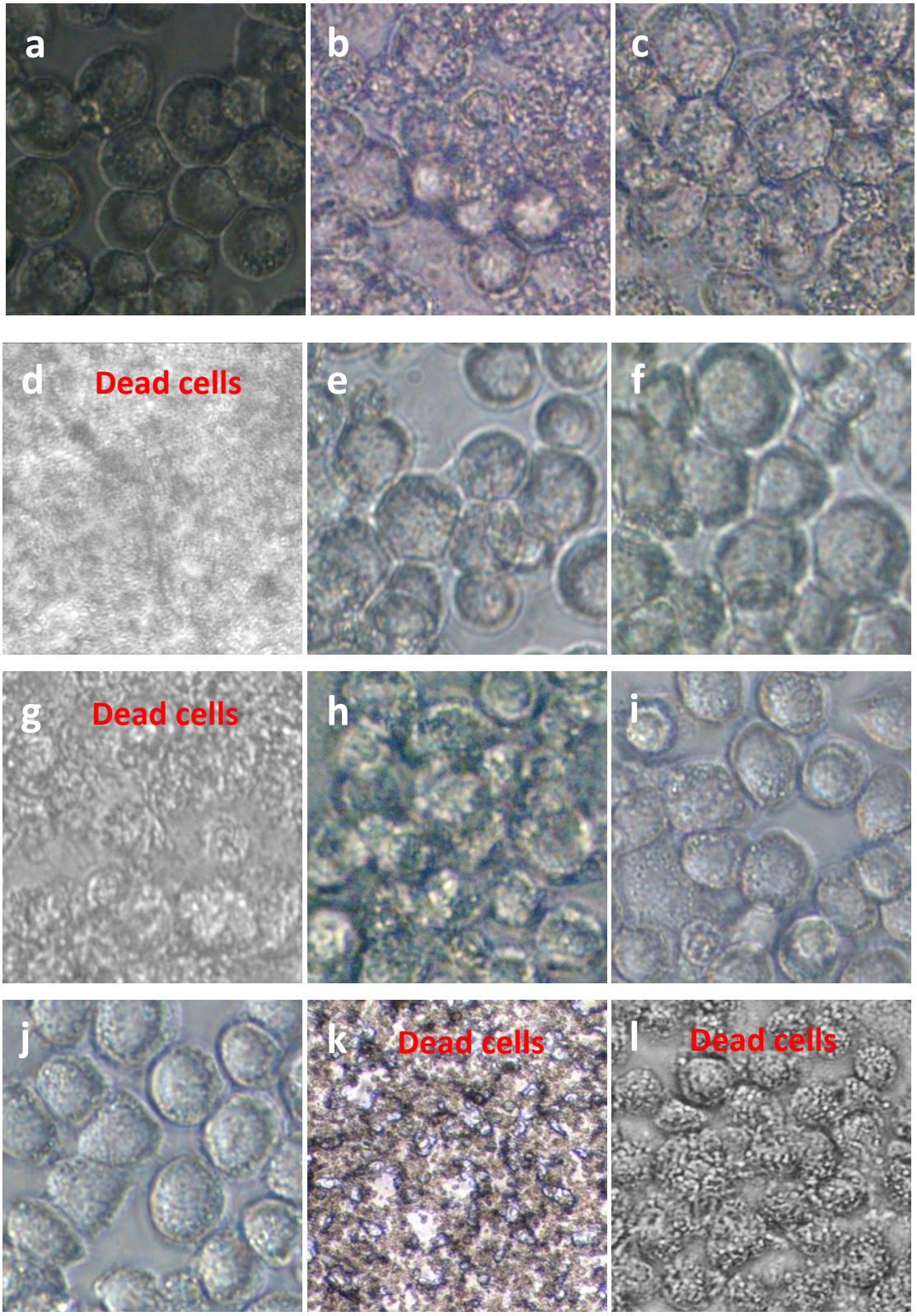

Figure 4.7 Effect of (a) Untreated control, (b) PAH-DS (0.025mgml^{-1}), (c)PAH-PAA (0.025mgml^{-1}), (d) Da10 (0.05mgml^{-1}l) (e) Da10-DS (0.05mgml^{-1}) (f) Da10-PAA (0.05mgml^{-1}), (g) Pa2.5 (0.05mgml^{-1}), (h) Pa2.5-DS, (0.05mgml^{-1}), (i) Pa2.5-PAA, (0.05mgml^{-1}), (j) QPa2.5 (0.5 mgml^{-1}), (k) QPa2.5-DS (0.5mgml^{-1}), (l) QPa2.5-PAA (0.5mgml^{-1}) on viability of J774 cells (X 40 magnification).

4.4.2 Haemolysis Assay

Haemolysis assay was employed to investigate the degree of haemolysis on exposure to polycations and APECs. The haemolytic potential of APECs was evaluated in comparison to polycations alone. Less than 10% haemolysis was considered as no significant haemolysis which is in line with Fisher *et al.* [157]. Haemoglobin measured in the erythrocyte supernatants exposed to all formulation ($\leq 5 mgmL^{-1}$) was found to be less than 10%, except Da10 based formulations (Figure 4.8a). However, at higher concentrations ($\geq 5 mgmL^{-1}$) PAH and Pa2.5 were found haemolytic (Figure 4.8b & c).

Among all polycations, Da10 appeared to be the most haemolytic. Da10 $1 mgml^{-1}$ released 20% of haemoglobin, $8 mgml^{-1}$ released approximately 34% and $10 mgml^{-1}$ released approximately 37% haemoglobin. However, Da10-DS and Da10-PAA ($8 mgmL^{-1}$ concentration) released 16% and 11% haemoglobin respectively, indicating significantly less haemolytic activity than Da10. Exposure of cells to non-haemolytic concentration of Da10 and corresponding APECs resulted in aggregation and clumping of cells (Figure 4.9j, k & l). PAH, PAH-DS, PAH-PAA, Pa2.5, Pa2.5-DS and Pa2.5-PAA demonstrated no haemolytic activity up to $5 mgml^{-1}$ (Figure 4.8b & C). Quaternary ammonium based polycations and APECs were found to be non-haemolytic at all concentrations tested in the study ($10 mgml^{-1}$) (Figure 4.8d).

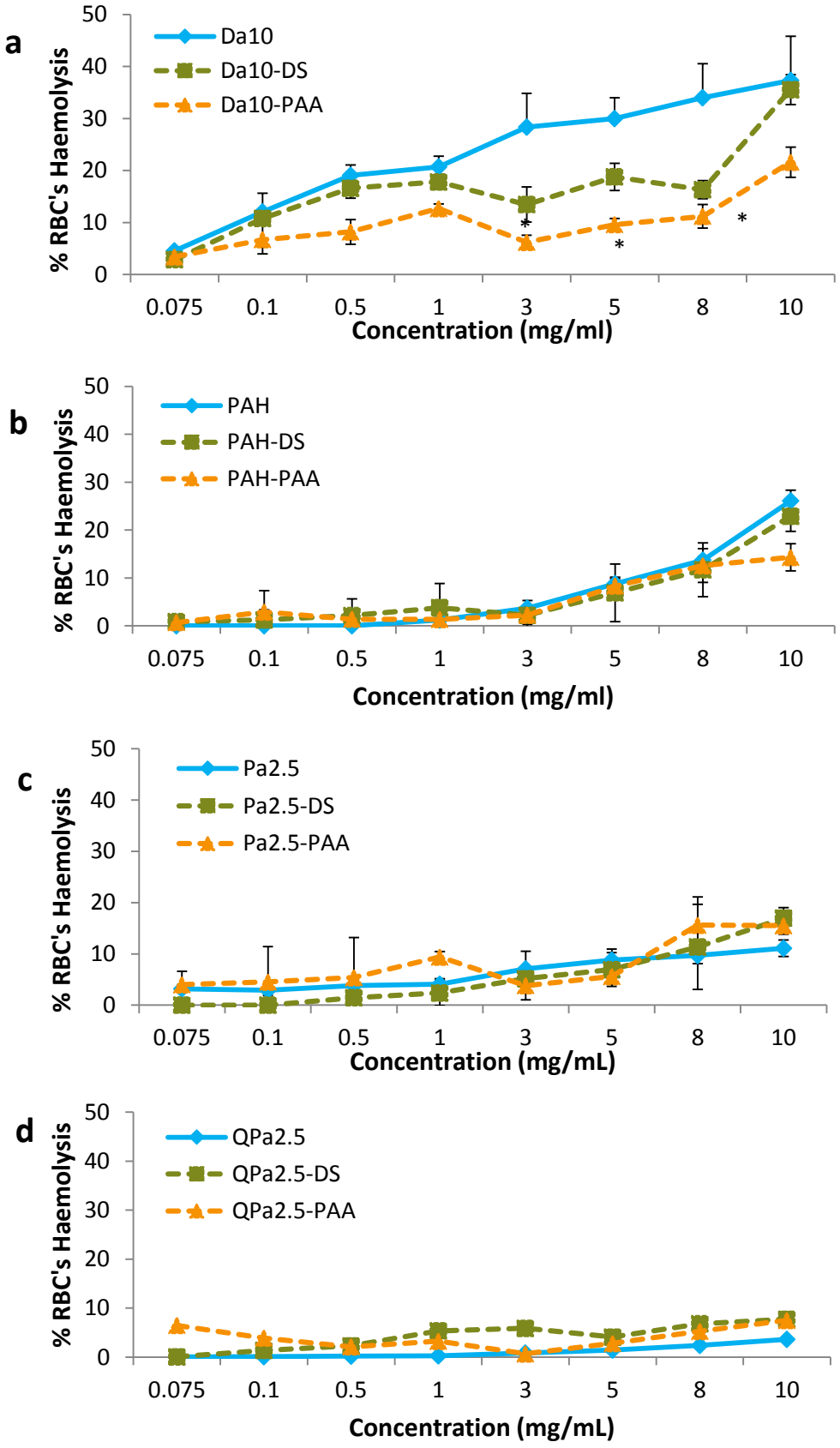

Figure 4.8 Effect of (a) Da10 and corresponding APECs (d) PAH and corresponding APECs (a) Pa2.5 and corresponding APECs (a) QPa2.5 and corresponding APECs on haemocompatibility of erythrocytes. Each value represents mean± SE of three experimental determinations. Statistical significance was determined at a p value<0.05.

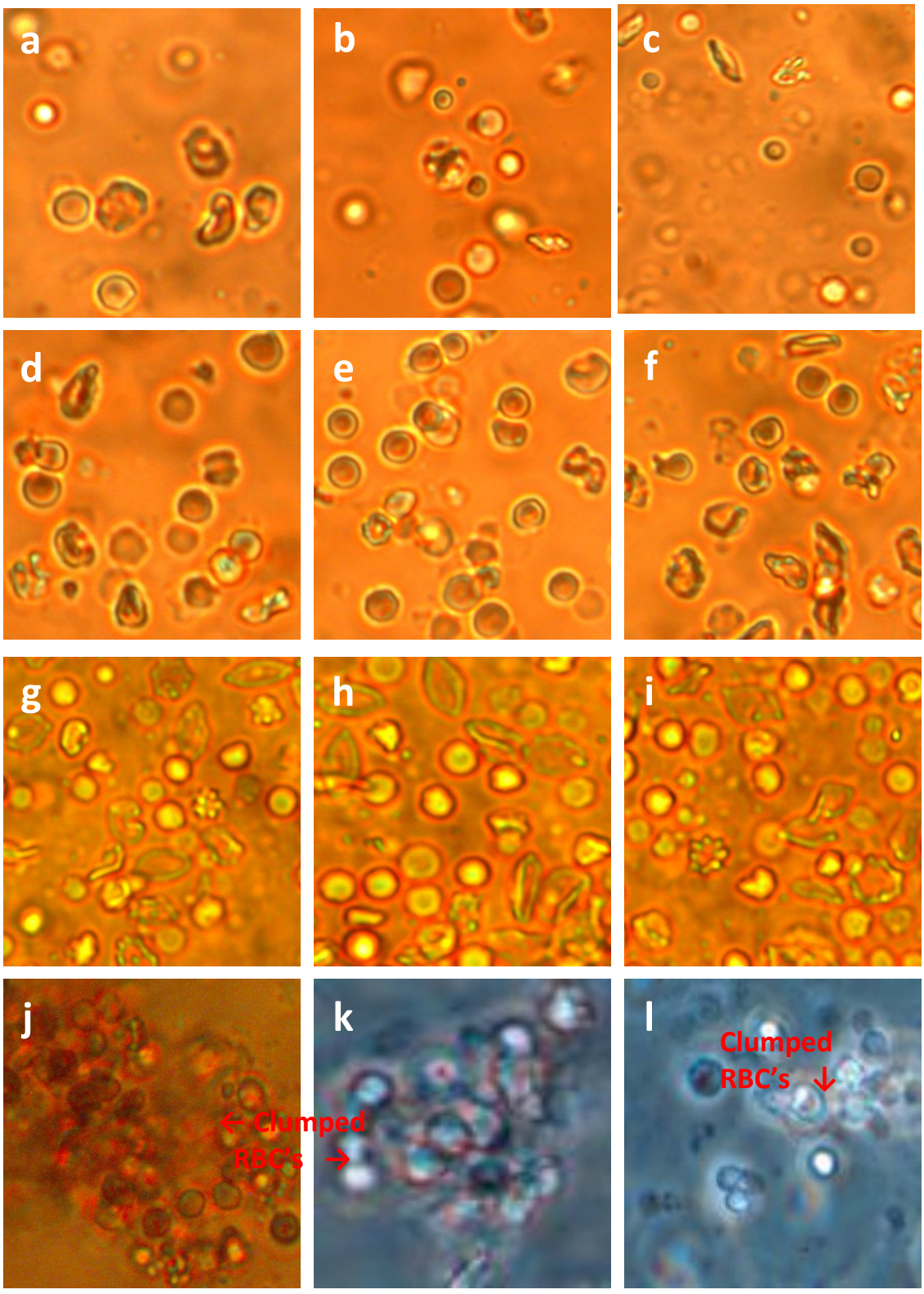

Figure 4.9 Morphology of wistar rat RBC's incubated with (a) Untreated control (b) PAH-DS (c) PAH-PAA (d) Pa2.5 (e) Pa2.5-DS (f) Pa2.5-PAA (g) QPa2.5 (h) QPa2.5-DS (i) QPa2.5-PAA (j) Da10 (k) Da10-DS (l)Da10-PAA.

4.4.3 ROS assay

Intracellular ROS generation was assessed in the supernatants of CaCo2 cells incubated with polycations and APECs (at IC_{90} as determined by the MTT assay). PAH, Pa2.5 and Da10 induced higher ROS (max 25%) in CaCo2 cells than QPa2.5 (max 12%) (Figure 4.10).

There was substantially lower ROS production on exposure of CaCo2 cells to APECs ($p<0.05$**)** than their corresponding polycations. APECs formed by Pa2.5 and QPa2.5 produced more significant reduction in polycation associated ROS production (Figure c and d) than APECs formed by PAH and Da10 (Figure a & b). PAH and Pa2.5 based APECs reduced the ROS production of corresponding polycations by 2 fold and 3 fold respectively ($p<0.05$). Da10-DS did not reduce the ROS production compared to Da10. The QPa2.5-PAA produced 3 fold ($p<0.01$) and QPa2.5-DS 2 fold ($p<0.05$) lower ROS generation than QPa2.5 ($p<0.05$).

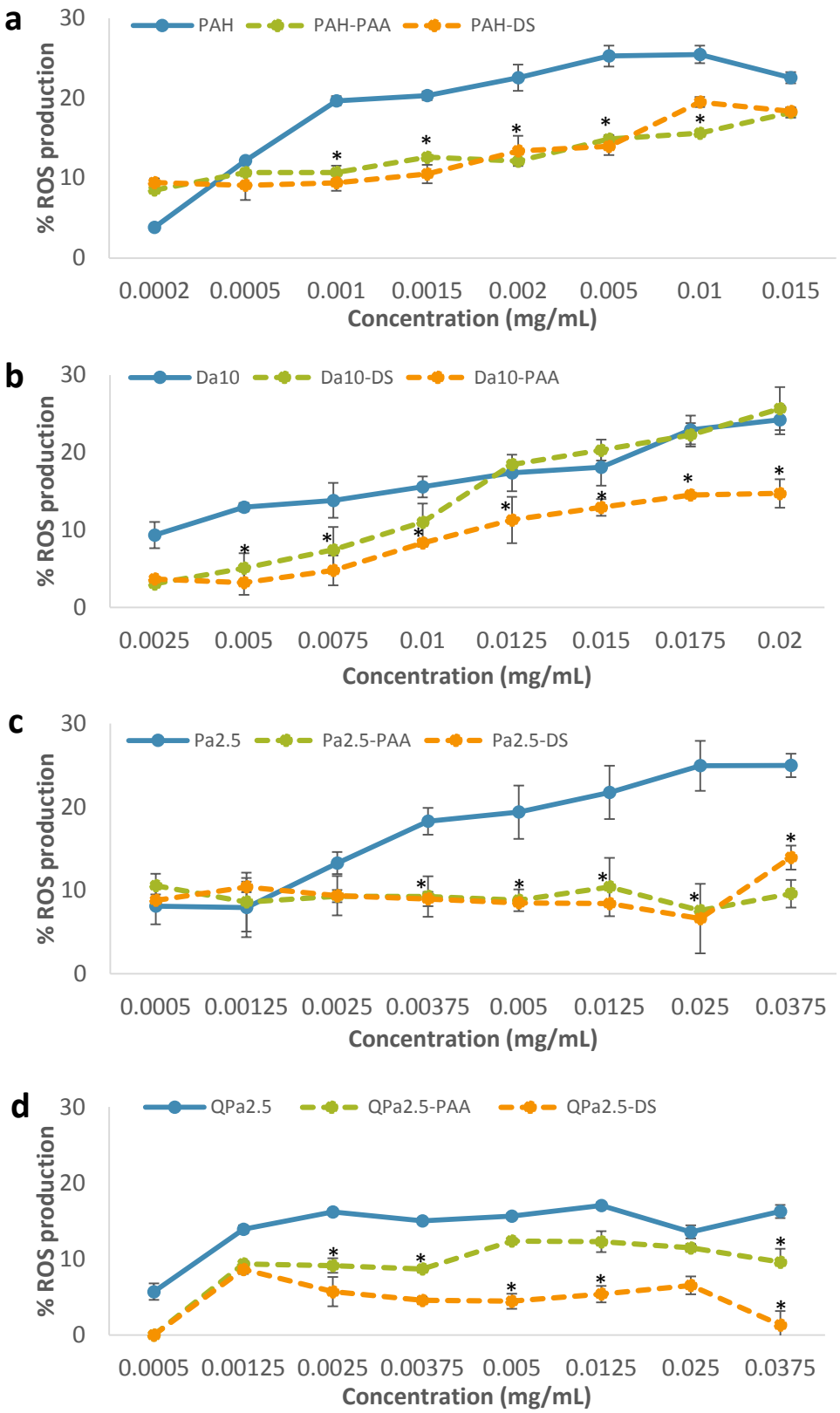

Figure 4.10 Effect of ROS production by CaCo2 cells on exposure to (a) PAH and corresponding APECs (b) Da10 and corresponding APECs (c) Pa2.5 and corresponding APECs (d) QPa2.5 and corresponding APECs. Each value represents mean± SE of three experimental determinations. Statistical significance was determined at a p value<0.05*.

4.4.4 *In Vitro* cytokine generation assay

This study was performed to determine the ability of polycations and APECs to induce cytokine production (IL-6 and TNF α) in J774 cells. IL-6 and TNFα cytokines were chosen as they are produced by macrophages and serve as an indicator for activation of macrophages and hence an early immune response.

All polycations and APECs demonstrated the ability to induce IL-6 and TNFα production (Figure 4.11). Generally, the formulations induced higher levels of IL-6 than TNFα (except QPa2.5 and QPa2.5-PAA). The IL-6 generation profile of polycations is rated as QPa2.5>Pa2.5>Da10>PAH. On the other hand, TNFα generation profile is rated as QPa2.5>Pa2.5>PAH>Da10.

QPa2.5 and its APECs demonstrated higher generation of cytokines (≥90%) than unmodified and hydrophobically modified polycations (≤75%). QPa2.5 and Da10 based APECs produced no significant reduction in corresponding polycation associated cytokine generation (except QPa2.5-PAA). The exposure of cells to Da10-DS resulted in higher levels of cytokines than their corresponding polycations.

The cytokine generation was lower in the cell supernatants exposed to PAH and Pa2.5 based APECs. Similar to MTT and haemolysis assay, the result of PAH and Pa2.5 based APECs showed more marked reduction in cytokine generation in the presence of PAA based APECs (PAH-PAA- 1.7 fold IL-6 reduction, $p<0.01$; Pa2.5-PAA 2 fold TNFα reduction and 3.5 fold IL-6 reduction, $p<0.001$) than DS based APECs (which did not show statistically significant difference in cytokine generation with their corresponding polycation). These results show that PAA based APECs, in particular Pa2.5-PAA produced the most significant reduction in cytokine generation, therefore, only PAA based APECs were selected for the *in vivo* cytokine generation study.

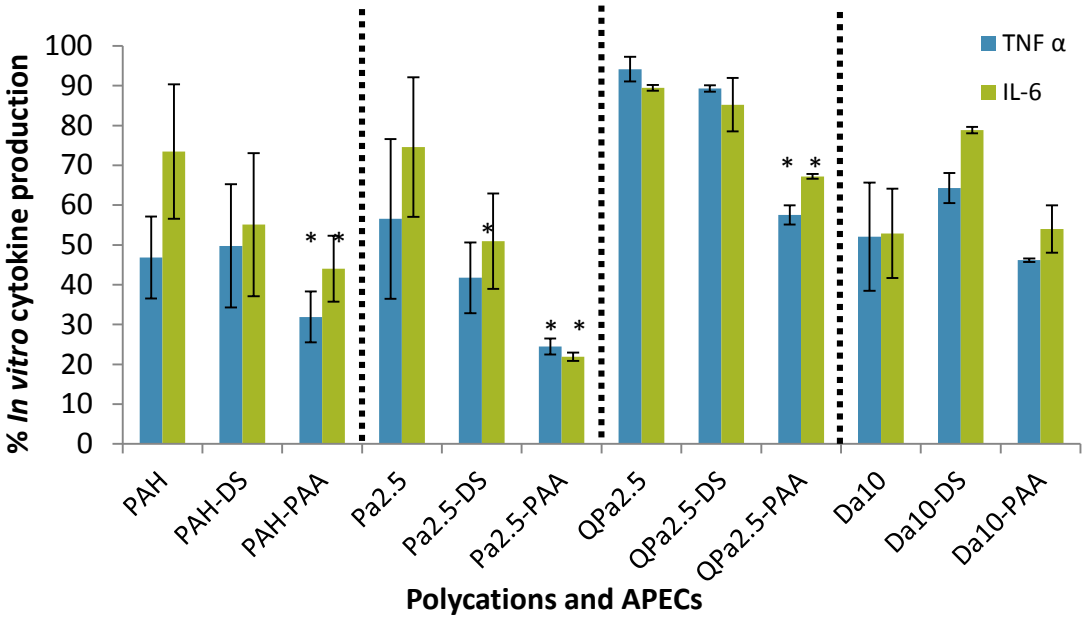

Figure 4.11 *In vitro* cytokine generation by J774 cells on exposure to polycations and APEC formulation. Each value represents mean± SE of three experimental determinations. Statistical significance was determined at a p value<0.05*.

4.4.5 *In Vivo* cytokine generation assay

The *in vivo* generation of three pro-inflammatory cytokines (IL-2, IL-6 and TNF-α) was investigated in serum samples of healthy mice treated with i.v. and oral doses of polycations or APECs. The polycations and APECs induced significantly lower levels of *in vivo* cytokines (Figure 4.12) compared to the high levels of *in vitro* cytokines (Figure 4.11) in macrophage culture supernatants. Among all the cytokines tested, the generation of IL-6 was more significant (maximum 27% i.v. administration; maximum 18% oral administration) than other cytokines which is consistent with the *in vitro* data. The cytokine generation was found higher in mice sera treated with i.v. and oral QPa2.5 than the hydrophobically modified polycations, which agrees with the *in vitro* data. There were no significant differences in the generation of IL-2 and TNFα by polycations and APECs. Pa2.5-PAA and QPa2.5-PAA brought a more marked reduction ($P<0.05$) in the polycation associated cytokine generation than Da10-PAA.

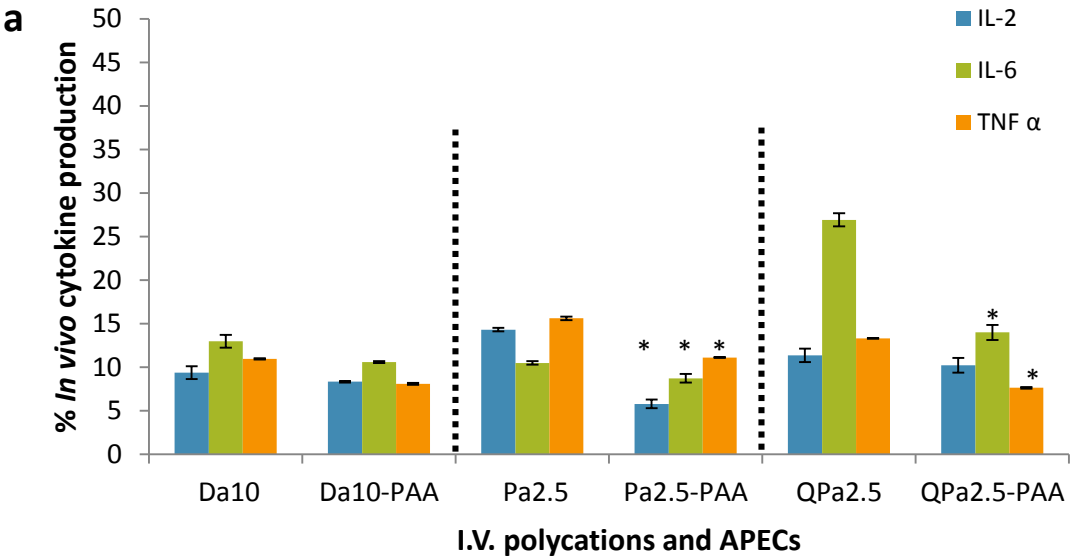

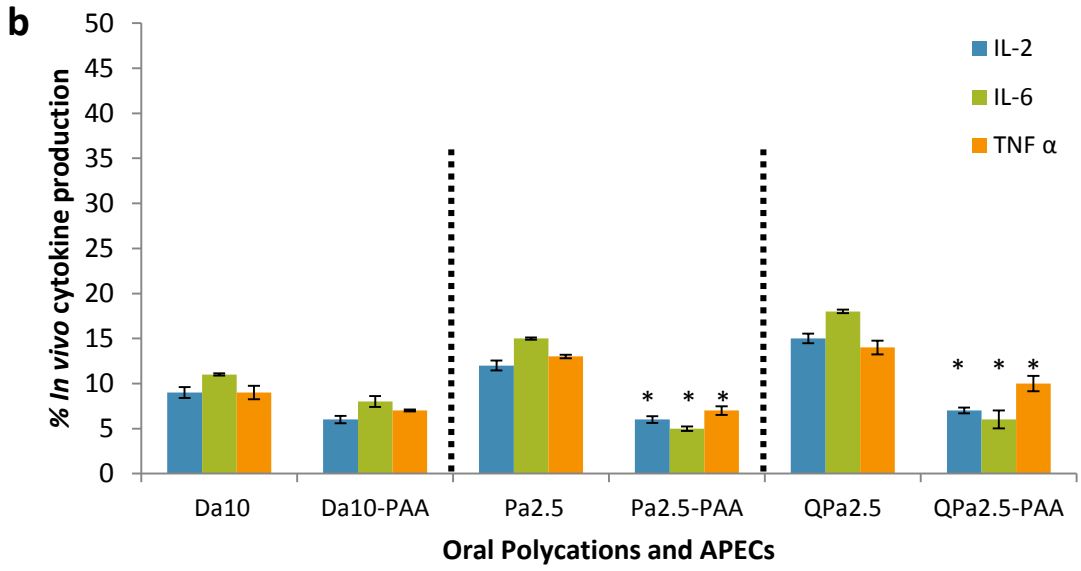

Figure 4.12 *In vivo* cytokine generation profile in serum samples of wistar mice treated with (a) i.v. polycation and APEC formulations (b) oral polycation and APEC formulations. Each value represents mean± SE of three experimental determinations. Statistical significance was determined at a p value<0.05*.

4.5 DISCUSSION

It is well known that polyelectrolyte complexes are simple and quick to formulate but complexes formed from polycations may be toxic biologically [153]. There is a well-established relationship between toxicity and the polycationic nature of polymers [157, 408]. This study aims to evaluate the biocompatibility profile of various polycations and APECs. Briefly, this study investigated and compared the cytotoxicity, haemocompatibility, ROS generation and immunotoxicity of the polycations and APECs fabricated in chapter 3 section 3.5.2.1.1 & 3.5.2.2.1.

The findings from MTT assay substantiate the contribution of polymer architecture in mediating the cytotoxic effects on CaCo2 and J774 cells (Table 4.1), whereby hydrophobically modified polymer (Pa2.5 and Da10) were more cytotoxic than the hydrophilically modified PAH (QPa2.5). The key trend of the polymer cytotoxicity remained the same i.e., PAH>Pa2.5=Da10>QPa2.5 on both the cell lines. However, J774 cells exhibited lower IC_{50} values indicating higher sensitivity to the polycations and APECs than CaCo2 cells. The varying IC_{50} on the two cell lines can be attributed to the differences in the physicochemical properties of the particles and the intrinsic difference in the properties of the two cell lines. It has been shown that different particles differ in their ability to interact with macrophages and hence in the induction of toxicity [353]. Macrophages have been shown to internalise 4 times more polystyrene-COOH than THP-1 cells which may be the reason for their higher sensitivity [307]. Recently, Calu-3 and CaCo-2 cells have also been reported to exhibit different degree of toxicity on exposure to chitosan indicating differential toxicity on different cell lines [409]. Clift *et al.* has shown significant toxicity of quantum dots (QDs) on J774 cells [353] which were found non-toxic on primary rat hepatocytes [410]. This might mean that macrophages are more sensitive to nanocarriers than other cell lines which may either be due to extensive uptake or different mechanism of uptake by them. However, unlike other formulations, QPa2.5 based complexes exhibited lower cytotoxicity to macrophage which may be due to their large size which prevented higher uptake of particles and hence the cytotoxicity.

CaCo2 cells are derived from colon adenocarcinoma, which differentiate to adapt ileal enterocyte like properties [220]. They differ significantly from the macrophages both morphologically and physiologically. Their uptake mechanism is different from the uptake by macrophages. They preferentially internalise nanoparticles in the range

of 100-200 nm by endocytosis [411]. However, the particles that are internalised by cells may also undergo efflux [412]. Conversely, the uptake by macrophages occurs primarily via phagocytosis. The extent of uptake depends on the size and shape of nanoparticles [412].

The internalisation of nanoparticles by macrophage cell lines does not behave the same as uptake by primary macrophage [412] as well as by other cell lines [413]. Macrophages have been shown to phagocytise the particles ≥200nm in diameter more efficiently than the smaller particles [307, 411]. It has been shown that macrophages were able to accumulate significantly higher level of oritavancin than the epithelial cell lines i.e., LLC-PK1 and CaCo2 indicating chances for higher cytotoxicity [413]. Therefore, it is very important to understand the molecular events leading to a higher uptake. It is also important to determine whether the uptake of nanoparticles by macrophages activates or halts the inflammatory response [412].

The unmodified PAH was more cytotoxic to both cell lines than the modified PAH. The higher cytotoxicity of PAH is attributed to the presence of a high density of primary amine groups. It is well known that polycations bearing $–NH_2$ termini such as PEI, poly-l-lysine (PLL), chitosan [207] and polyallylamine (PAH) generate significant cytotoxicity [143, 153]. Modification of PAH reduces the number of primary amines on the PAH backbone which is the most likely reason for the reduction in cytotoxicity. It has previously been shown that modification of primary amines with hydrophilic methyl glycolates [154], PEG [414] and imidazolyl grafting [152] reduces the cytotoxicity. It has also been shown by Thompson *et al.* that the modification of PAH with palmitoyl group decreased the toxicity of PAH by 2-3 fold which agree well with our data [415]. Besides, they also reported that quaternisation of palmitoyl pendant groups on the polymer backbone significantly improved the cytotoxicity which again correlates with our data [415].

Based on studies with polycations, it has been observed that macromolecules with tertiary and quaternary amino groups exhibit a much lower cytotoxicity index than primary and secondary groups [227]. This is clear from the results where hydrophilic modification of Pa2.5 with a quaternary ammonium moiety brought a more significant improvement in IC_{50} i.e., CaCo2 cells -13 fold and J774 cells - 57.5 fold. This may be due to the conversion of primary amines on the polymer backbone to less toxic quaternised amines which carry a permanent cationic charge [151]. Brownlie *et al*. has

reported a similar response of more than four-fold reduction in the toxicity of PEI by the quaternised PEI, and eight folds upon quaternisation of palmitoyl grafted PEI [151].

The polyanions, PAA and DS are non-toxic hydrophilic polymers. They did not affect the cell viability up to 10mgmL^{-1} (data not shown). Owing to their negative charge they are able to complex with polycations and reduce their overall positive charge [258]. In this way, they are expected to diminish the polycation associated cytotoxicity. As expected, the addition of the polyanions in APECs significantly reduced the ZP and hence increased the IC_{50}. Tiyaboonchai *et al.* has previously reported similar findings whereby PEI-DS complexes diminished the cytotoxicity associated with PEI [122]. Nimesh *et al.* also reported the ability of polyallylamine-dextran sulphate-DNA (PAH-DS-DNA) complexes to reduce the cytotoxicity of PAH [153]. Guo *et al*. prepared ternary complexes by coating polyglutamic acid-graft-poly(ethylene glycol)(PGA-g-mPEG) onto binary complexes of polycaprolactone-graft-poly(N,N-dimethylaminoethyl methacrylate (PCL-g-PDMAEMA). These ternary complexes demonstrated lower *in vitro* cytotoxicity in CCK-8 cells than the binary complexes [127]. The ternary complexes (polycaprolactone-graft-poly(N,N-dimethylaminoethyl methacrylate) (PCL-g-PDMAEMA) [256] and polyanion/pDNA/PEI [131] have also been shown to reduce the positive surface charge and hence toxicity associated with the corresponding binary complexes.

Among the two polyanions, the increase in IC_{50} was more pronounced in the presence of PAA based APECs than DS based APECs. These findings indicate that different polyanions exert different effects on the cell viability when complexed with the polycations. This effect of polyanions may be attributed to the low MW of PAA (1.8kDa) in comparison to high MW of DS (6-10kDa). Numerous researchers have shown that high MW polycations such as PEI and TMC are more cytotoxic than low MW ones [157, 227, 367]. The high MW of polyanion may have similar implications on cytotoxicity as high MW polycations. In addition to MW, there are distinct architectural differences between the DS and PAA which may be responsible for the trend observed. DS is an anionic polysaccharide with a dense architecture whereas PAA is a weak polyacid [261, 267] They exhibit differences in ionisation state and number of charged groups. In addition, the anionic functional units of the two i.e., SO_4^{-2} of DS and COO^- of PAA are also different. These differences may be responsible for causing

different degree of affinity for the cell membrane and leading to differences in mediation of cytotoxicity.

The *in vitro* exposures of erythrocytes to the polycations (except Da10) and APECs showed low tendency to cause haemolysis (≤12%) over the concentration range (0.075-5mgml^{-1}). The microscopic observations showed that even non-haemolytic concentrations of Da10 caused a substantial clumping and aggregation of erythrocytes presumably due to the polymer cross linking (Figure 4.9j, k & l). Changes in RBC morphology have also been observed by Malik *et al.* after only 1h incubation with non-haemolytic concentration of cationic polyamidoamine (PAMAM) and diaminobutane (DAB) dendrimers [408]. A higher haemolytic profile (37% at 10mg/mL^{-1}) of Da10 has been linked to the hydrophobic modification of its backbone. However, since hydrophobically modified Pa2.5 was not haemolytic, the effects observed may be due to the difference in the structure of hydrophobic group or degree of hydrophobic load. Da10 comprised of higher hydrophobic load i.e., 10% hydrophobic grafting in comparison to 2.5% of Pa2.5 (which indicates haemolysis due to a higher hydrophobic load. The haemolytic effects may be due to the formation mixed micelles of the hydrocarbon chains with the phospholipid bilayers [416]. The hydrophobicity of the polymers has previously been linked with the membrane-disruptive activity by Liu *et al.* [417]. It was reported that the hydrophobicity of the polymer permits partitioning of the polymer into the cell membrane. This behaviour disrupts the packing of the lipid bilayer and causes haemolysis [417]. On the other hand, hydrophilicity of polymers has been shown to reduce the haemolytic effects which agrees well with the lowest haemolysis profile of the QPa2.5 based formulations [414]. Colak *et al*. incorporated a hydrophilic, biocompatible PEG pendant groups on amphiphilic polynorbornene derivative, Poly3, and found that increasing the hydrophilicity reduced the haemolytic activities of the polymer [414].

Da10-DS and Da10-PAA were able to significantly reduce the haemolytic activity associated with Da10. The improvement in haemolytic profile may be due to the reduction in positive charge density or addition of hydrophilicity to the complexes which subsequently prevented the adverse interaction of APECs with the erythrocyte membrane. Liu *et. al.* has previously shown that the haemolytic activity may reduce by reduction in positive charge density via surface modification of polymer [417]. It is also

believed that a balance between hydrophobic and hydrophilic load is required to prevent the haemolytic activity [376].

Nanocarrier toxicity has been proposed to originate from oxidative stress induced by ROS and free radical formation [418]. There is substantial evidence that nanocarriers made from inorganic and metallic materials, such as carbon, iron, zinc and titanium dioxide (TiO_2) are potent generators of ROS [418]. However, very few polymeric nanocarriers have been explored for their ROS generation profile. Exposure of polycations and APECs to CaCo2 cells induced low levels of ROS (<26%) at IC_{90} concentration. The trend of ROS generation (PAH>Pa2.5=Da10>QPa2.5) agreed well with the cytotoxicity profile indicating a correlation between ROS production and cytotoxicity. Cationic particles have been shown to localise in mitochondria and produce a cytotoxic response via the mitochondrial injury pathway which leads to production of additional O_2 species [419]. Naha *et al.* has shown that ROS production in J774 cells exposed to PAMAM dendrimers linearly correlated with the number of surface primary amino group [420]. The higher intracellular ROS generation under the effect of PAH may also be due to the higher number of primary amino groups which caused a disruption of the mitochondrial electron transduction chain leading to higher cytotoxicity [421].

Modification of PAH led to a reduction in the number of primary amino groups and hence a reduction in ROS production and cytotoxicity. The small size (≤100nm) of nanocarriers is considered to exhibit higher reactivity, which increases their adverse effects [422]. This may also be the reason for lower ROS generation in cells exposed to QPa2.5 based formulations which exhibited larger particle sizes (≥250nm) compared to other formulations.

APECs demonstrated a significant reduction in ROS production compared to the corresponding polycations**.** No significant differences were observed in alleviation of ROS induction between PAA and DS. These findings suggest that reduction in positive charge turned down the production of ROS. These findings are in line with the study of Yang *et al*. who also demonstrated the role of positively charged poly-l-lactide glycolide in higher ROS production [393].

Oxidative stress has also been implicated in the activation of cytokine production [421]. The effect of various polycations and APECs on the induction of cytokine generation (IL-6 and TNF α) from the J774 cells was investigated by *in vitro* cytokine assay. The *in vitro* investigations was facilitated by *in vivo* cytokine production (IL-6, IL-2 and TNF α) assessed in healthy mice treated with oral and i.v. doses of polycations and APECs. All formulations demonstrated the ability to induce cytokines both *in vitro* and *in vivo*, however, there were significant differences in cytokine production between the polycations and their respective APECs and between *in vivo* and *in vitro* situations.

The *in vivo* serum cytokine levels (≤27%) were found to be significantly lower than the *in vitro* levels ≥90% (Figure 4.11 & 4.12). This disparity in the data may have been due to the difference in the *in vitro* and *in vivo* situations such as short half-life or localised *in vivo* cytokine production leading to their reduced systemic availability [423, 424]. The difference in the incubation time between the *in vitro* (2-4h) and the *in vivo* (12h following i.v. and 24h following oral administration) cytokines production may also have contributed to the disparity in data. There is a possibility that the *in vivo* cytokine levels reached a peak any time before or after they were analysed. Besides, *in vitro* assays provide only cell type-specific responses, however, do not capture intercellular effects such as cross-talk between cells which can alter the cytokine levels. One such example is of the *in vivo* stimulation of anti-inflammatory cytokines e.g., IL-10 which might have caused the down regulation of pro-inflammatory cytokines [361]. The down regulation of cytokines (IL-6, TNFα and IL-2) by IL-10 might have been responsible for low *in vivo* cytokine level.

Generally, *in vitro* and *in vivo* IL-6 generation on exposure to polycations and APECs was higher than other cytokines, except Pa2.5-PAA, QPa2.5 and QPa2.5-PAA. The differences in the cytokine generation profile between IL-6 and TNFα are attributed to the different reactivity of cells towards the different formulations. Exposure of macrophages to phorbol myristate acetate (PMA), and Phytohemagglutinin (PHA) has previously shown to induce significantly different levels of 5 different cytokine at similar experimental conditions employed [424]. It was also shown that there was no correlation between the productions of one cytokine with the other, nor was there any association between response to one stimulus or the other [424].

The degree of *in vitro* TNFα production is rated as QPa2.5>Da10>Pa2.5=PAH whereas *in vitro* IL-6 generation is rated as QPa2.5>Pa2.5=PAH>Da10. QPa2.5

showed the highest cytokine production in both *in vitro* and *in vivo* situations. This shows that cytokine generation followed a reverse trend to the cytotoxicity and ROS assay. Previously, Scholer *et al.* has also shown an inverse relationship of the cytokine generation to the cytotoxicity on exposure to solid lipid nanoparticles [405]. They also reported that cytokine generation is particle size dependent [397]. Similar finding have been reported by Zolnik *et al.* indicating that particle size is a major factor governing the type of immune response [163]. This might mean that large particle sizes of QPa2.5 (468 ±12nm) and its APECs (435 and 228 nm), compared to the unmodified and hydrophobically modified polycations may be responsible for higher cytokine generation. There may also be an association of the surface properties of QPa2.5 such as hydrophilicity or particle size with the generation of cytokine. Previously, Jones *et al.* has also linked hydrophilicity of particles with the generation of cytokines [362].

Pa2.5-PAA showed the most pronounced reduction (≤25%) in cytokine generation in cell culture supernatants. A similar trend was observed in *in vivo* study whereby Pa2.5-PAA produced ≤12% cytokine generation. Unlike *in vitro* study, QPa2.5-PAA also reduced the *in vivo* cytokine generation ($P<0.05$) indicating the role of PAA in reducing the cytokine production. However, Da10-PAA was unable to significantly reduce the *in vitro* cytokine generation. QPa2.5-DS and Da10-DS were also unable to reduce the *in vitro* cytokine production indicating no role of DS in reducing the cytokine production. Polyanions have previously been implicated in stimulation of immune system which is in agreement with the above findings [425]. These findings indicate that the type of polyanion plays a significant role in altering cytokine generation.

4.6 CONCLUSION

APECs significantly reduced the polycation associated cytotoxicity. The reduction in cytotoxicity and polycation induced ROS production was more pronounced on exposure to PAA based APECs particularly Da10-PAA and Pa2.5-PAA than DS based APECs. The polycations and APECs (except Da10 based formulations) showed no significant haemolytic activity up to $5mgml^{-1}$. Both *in vitro* and *in vivo* data demonstrated reduction in cytokine generation on exposure to APECs particularly in the presence of PAA based APECs (Pa2.5-PAA). There was little correlation between *in vitro* and *in vivo* cytokine generation which is assumed to be either due to localised *in vivo* release of cytokines or *in vivo* production of anti-inflammatory cytokines such as IL-10 which down regulated the *in vivo* cytokine levels.

Chapter 5

Uptake And Transport Of Ternary Polyelectrolyte Complexes

5 INTRODUCTION

The success of oral administration of protein is dependent on a number of factors, out of which one crucial factor is their uptake and transport by enterocytes in the gut. Nanocarriers have shown unique potential to facilitate the cellular uptake and transport of proteins. However, differences in the physicochemical properties of nanocarriers such as size, surface charge and hydrophobicity have significant implications in their cellular uptake and transport [308, 317]. Considerable efforts have been devoted to elucidate the effects of these properties on the cellular uptake and transport mechanism of nanocarriers. Some of the recent progress is briefly discussed below.

5.1 MECHANISM OF UPTAKE AND TRANSPORT

5.1.1 Paracellular Transport

Due to poor permeation of macromolecules via TJs, research is being conducted to explore approaches to improve the paracellular permeability of macromolecules [173]. The potential of nanocarriers to allow reversible opening of the TJs represent a promising way to facilitate the absorption of hydrophilic drugs across the intestinal epithelium [426]. Recently, Thompson *et al.* has shown the potential of amphiphilic PAH based polyelectrolyte nano-complexes to reversibly open the TJs and increase insulin transport through the monolayers [427]. It is also known that the paracellular permeability of proteins and peptides can be enhanced by using polymers such as chitosan and its derivatives [428, 429].

Chitosan acts by binding to the epithelial cells and causing transient reversible opening of the TJs. It is proposed that this effect is due to structural reorganization of the tight junction-associated proteins and morphological changes in F actin cytoskeleton [183]. A number of chitosan derivatives such as trimethyl chitosan and thiolated chitosan have been designed to reversibly open the TJs and hence increase the permeability of nanocarriers across the intestinal cells [430-432]. It is thought that the cationic nature of chitosan and its derivatives is responsible for their interaction with the junctional proteins leading to transient reversible opening of TJs. Recently, Sadeghi *et al.* studied four partially quaternised derivatives of chitosan - trimethyl chitosan (TMC), dimethylethyl chitosan (DMEC), diethylmethyl chitosan (DEMC) and triethyl chitosan (TEC) to evaluate their effect on the permeability of insulin across intestinal CaCo2 monolayers. It was found that all four chitosan derivatives decreased the TEER

value in the same order (TMC > DMEC > DEMC = TEC > chitosan) as was observed for the cationic charge of the various polymers. These finding indicated that the higher the cationic charge, the higher is the reduction in the TEER. It was also shown that reduction in TEER was not due to the cytotoxic effects but due to transient opening of the TJs [431].

There are reports which provide evidence that not only cationic charge but also anionic charge mediates opening of TJs. One such investigation was conducted by Kitchens *et al*. who studied the influence of surface charge of PAMAM dendrimers on the transport of ^{14}C-mannitol across CaCo2 cells [433]. It was reported that the PAMAM dendrimers with neutral surface groups (PAMAM–OH) did not significantly influence TEER or ^{14}C-mannitol permeability across CaCo2 monolayers. However, PAMAM dendrimers with negatively charged surface groups (PAMAM–COOH) had a generation-dependent effect on the TEER and ^{14}C-mannitol permeability [433].

Studies have reported the effect of physicochemical properties such as viscosity on the TJ opening and enhancement of paracellular permeation. Thanou and coworkers studied the effect of 3 different viscosity grades 20, 40 and 60 cps of N-sulfonato-N,O-carboxymethylchitosan (SNOCC), on the rate of the intestinal permeation of low molecular weight heparin (LMWH) and reviparin. The higher viscosity formulation decreased the TEER more readily and was found 51 fold more effective in enhancing the permeation of the ^{14}C-mannitol compared to the low viscosity formulation. These findings indicate the role of the higher viscosity of the nanocarrier formulation in enhanced permeation across intestinal epithelia [432].

A number of studies have implicated particle size and surface properties in enhancing paracellular transport [433-435]. Li *et al.* has shown that treatment of Calu-3 cells with carbopol polymer gel formulations resulted in molecular size-dependent permeability enhancement of desmopressin a model peptide, with a concomitant drop in the TEER [187]. The permeation enhancement ability was related to the chelation of extracellular or tight-junctional Ca^{2+} by carboxylate groups of charged polymer which led to temporary disruption of tight-junctions, thereby facilitating paracellular transport [187].

The understanding of the mechanism of opening of TJs is very crucial. Dorkoosh *et al.* studied the mechanism of opening of TJs in CaCo2 cell monolayers using superporous hydrogel (SPH) and SPH composite (SPHC) polymers as permeation

enhancers for octreotide drug delivery [436]. It was reported that the junctional proteins including actin, occludin and claudin-1 were influenced by application of SPH and SPHC polymers to the CaCo2 cell monolayers. SPH and SPHC induced noticeable changes in the staining pattern of all three proteins. There was increased expression of these proteins in the TJs which was assumed to be due to the mechanical pressure of the polymers on the junctional proteins leading to opening of the TJs [436].

There are reports which have indicated the opening of TJs under the influence of polymers, however, only a subtle passage of nanocarriers across the paracellular junctions has been observed [188, 437]. This may be due to the fact that TEER has to decrease below a threshold level of about 50% of the original values for the paracellular passage of large molecules to occur [183]. Since the TJs represent only <1% of the mucosal surface area (pore diameter between 10-50 Å) of the intestine, the passage of macromolecules will still be limited despite the opening of TJs [141, 172, 220, 438, 439].

There are studies which have reported that uptake of nanocarriers occurred via both the paracellular and transcellular pathway. El-Sayed studied the mechanism of uptake of PAMAM and found that internalisation occurred via a combination of both paracellular and transcellular transport by adsorptive endocytosis [434]. However, it is still believed that the contribution of paracellular transport is significantly lower than the transcellular transport [205]. Therefore, efforts should be made to increase the potential of nanocarriers for transcellular transport.

5.1.2 Transcellular Transport

The transcellular internalization of particles is thought to be influenced by physicochemical properties of particles such as the size, shape, surface charge and surface chemistry [304, 308, 317, 440-443]. Recently, Gratton *et al*. designed three distinct series of cationic poly(ethylene glycol)-based particles with varying sizes and shapes but similar surface charge i.e., a micrometer-sized series of cubic-shaped particles (cube side length 2 µm, 3µm and 5µm); a micrometer-sized cylindrical series with identical heights but varying diameters; and a cylindrical shaped nanoparticle series of 200 nm, 100 nm and 150 nm in diameter [440]. The cellular internalization of particles by HeLa cells was found to be particle size and shape dependent. The HeLa cells readily internalized non-spherical particles with dimensions as large as 3µm via several mechanisms of endocytosis. There was also a marked effect of charge on the

cellular internalization of particles. The positively charged nanoparticles were internalized (84%) to a significant extent within 1h, whereas the identically shaped, negatively charged particles were not internalized to any significant amount (<5%). These findings strongly support the role of particle size, shape and surface charge in the cellular internalization of particles [440].

A plethora of research has demonstrated that polycations are taken up more readily by cells than polyanions. However, there is evidence that particles containing both polyanion and polycation demonstrate efficient internalisation [131]. Woitiski *et al.* formulated multilayered nanoparticles by encapsulating insulin within a core consisting of alginate and DS, interacting with poloxamer and stabilized by layering with chitosan and subsequently coated with albumin. These nanoparticles increased the insulin permeation by 2.1 fold through CaCo2 cell monolayer, 3.7 fold through a mucus-secreting CaCo2/HT29 co-culture, and 3.9 fold through excised intestinal mucosa of Wistar rat, as compared to insulin alone [444]. Hornoff *et al.* has shown that coating a DNA/PEI polyplexes with low molecular weight anionic hyaluronan (<10 kDa) facilitated CD44 receptor-mediated uptake, leading to increased transfection efficiency [445]. Wang and co-workers have shown that polyanions/DNA/polycation ternary polyplexes exhibited significantly higher transfection efficiencies than the original DNA/polycation binary polyplex [131]. Similarly, Xu's research group showed that a DNA/crosslinked PEI/hyaluronate ternary polyplexes achieved remarkably higher transfection efficiency than other polycation systems [446]. These investigations indicate that the novel ternary complexes formed by combination of polycation and polyanion may show higher uptake than the conventional binary systems.

In addition to surface charge, surface chemistry of nanocarriers is known to influence the uptake via the transcellular pathway [441]. Yin Win and colleagues showed that the cellular uptake of nanoparticles can be improved by surface modification with vitamin E [308]. They reported that the vitamin E coated PLGA nanoparticles showed 1.4 fold higher uptake than the polyvinyl alcohol -coated PLGA nanoparticles and 4-6 fold higher than that of nude polystyrene nanoparticles [308].

A large number of polymeric nanocarriers have been reported to be internalised via endocytosis. Internalization of cationic PEG-graft-trimethyl-chitosan copolymer–insulin nanocomplexes has been reported to occur predominantly by adsorptive endocytosis [67]. Jevprasesphant and coworkers reported the endocytosis-mediated

cellular internalisation of G3 PAMAM and surface-modified (with lauroyl chains) G3 PAMAM dendrimer nanocarriers across CaCo2 cell monolayers [447]. They reported the presence of early endosomes containing electron-dense nanocomposites immediately below the apical surface. In addition, endosomes were seen to aggregate to produce multivesicular bodies found throughout the cell. These findings supported the notion that nanocomposites transported through the cells in these vesicular structures [447].

Studies have identified several different types of endocytic pathways such as classical clathrin mediated endocytosis, caveolae-mediated endocytosis, clathrin- and caveolae-independent endocytosis as detailed in chapter 1 [201, 202]. These endocytic mechanisms are distinguished by the composition of coat, size of detached vesicles, and fate of the internalized material [201]. Recently, Dombu and colleagues reported that cationic nanoparticles made of maltodextrin were quickly internalised within 3 min by clathrin mediated endocytosis and that their exocytosis was cholesterol dependent [448]. It has been shown that particles can be taken up via a combination of clathrin and caveolae mediated endocytosis or clathrin and caveolae independent pathways depending on their physicochemical properties [208, 449]. Jin *et al.* indicated the ability of insulin loaded TMC nanoparticles modified with a CSKSSDYQC (CSK) targeting peptide to be internalised via clathrin and caveolae mediated endocytosis by goblet cell-like HT29-MTX cells [449]. Harush-Frenkel and co-workers studied the differential endocytic internalisation of positively versus negatively charged nanoparticles. They showed that unlike negatively charged nanoparticles, the positively charged particles were seen to be internalised via clathrin- and caveolin pits, predominantly in the perinuclear region [208]. Qaddoumi and colleagues reported that PLGA nanoparticles are internalised in primary cultures of rabbit conjunctival epithelial cells by endocytosis mainly via clathrin- and caveolin-1- independent pathways [450]. Rejman *et al.* reported that particles size itself can determine the pathway of entry. The clathrin mediated pathway of endocytosis shows an upper size limit for internalization of approx. 200 nm. The kinetic parameters have determined almost exclusive internalization of such particles along this pathway rather than via caveolae mediated pathway [214].

Nanocarriers may be absorbed in small quantities via membranous epithelial cells in the GALT called M cells [215]. M cells have the capability of transporting

nanoparticles via transcytosis from the gut lumen to the underlying mucosal immune system. Rajapaksa's group investigated the uptake mechanism of sub-micron size PLGA particles, incorporating a recombinant protein, with or without a c-terminal peptide which had a high binding affinity for a protein (claudin 4) associated with M cell endocytosis [451]. These particles exhibited enhanced uptake by intestinal M cells [451]. However, since the number of M cells in FAE is very low, the potential for uptake via this pathway is very limited [220]. Beloqui and co-workers studied the potential of three different nanostructured lipid carriers (NLC) formulations to enhance the oral bioavailability of poorly soluble compounds using saquinavir (SQV). It was found that SQV transport across the CaCo2 monolayers enhanced up to 3.5-fold by NLCs compared to the SQV suspension. However, M cells did not enhance the transport of NLCs loaded with SQV [452]. The probability of nanocarriers not being internalised or being internalised to a negligible extent, draws attention to the need to characterise the uptake and mechanism of uptake of all novel nanocarriers. This chapter elucidates the potential of uptake and transport of the polymers, PECs and APECs (fabricated in chapter 3), using *in vitro* cell culture models, flow cytometry and fluorescent microscopy.

5.2 CHARACTERISATION OF NANOCARRIERS UPTAKE

5.2.1 *In vitro* cell culture model

The transport of drug across epithelial lining is studied using *in vitro* cell culture models (Figure 5.1). CaCo2 cell culture models are the most widely used *in vitro* models. CaCo2 cells form a confluent monolayer which serves as an *in vitro* tool to predict the absorption of orally administered drugs [220, 426, 453]. The intrinsic ability of CaCo2 cells to form TJs assist in the uptake and transport studies [454, 455].

Transport studies are simple and convenient procedures and provide reproducible data. They provide rapid assessment of the intestinal permeability of drug candidates [170]. These studies require only small quantities of drugs for absorption screening [426]. However, such models are laborious as they require 3-4 weeks to generate a confluent layer (Gad, 2008). Drug transport studies involve the culture of CaCo2 cells on porous filters in multi-well cell culture plates. The wells comprise of apical or basolateral compartments. The transport of drug is measured from the apical to basolateral direction or vice versa [426].

In vitro models can be used to monitor changes in the integrity of TJs (leaky to moderately leaky epithelium) by measuring the TEER [220, 426]. The efficiency of the opening of TJs is usually monitored by using high molecular weight paracellular markers such as mannitol and FITC-Dextran [426]. The paracellular permeability of the macromolecules essentially depends on their molecular size. Therefore, paracellular markers of different molecular sizes can be used to assess the opening of TJs [426]. This allows CaCo2 cell models to be used to investigate the mechanism of transport of drug [173]. However, they do not provide information about cellular localisation of nanocarriers, which can be obtained from techniques such as fluorescent microscopy.

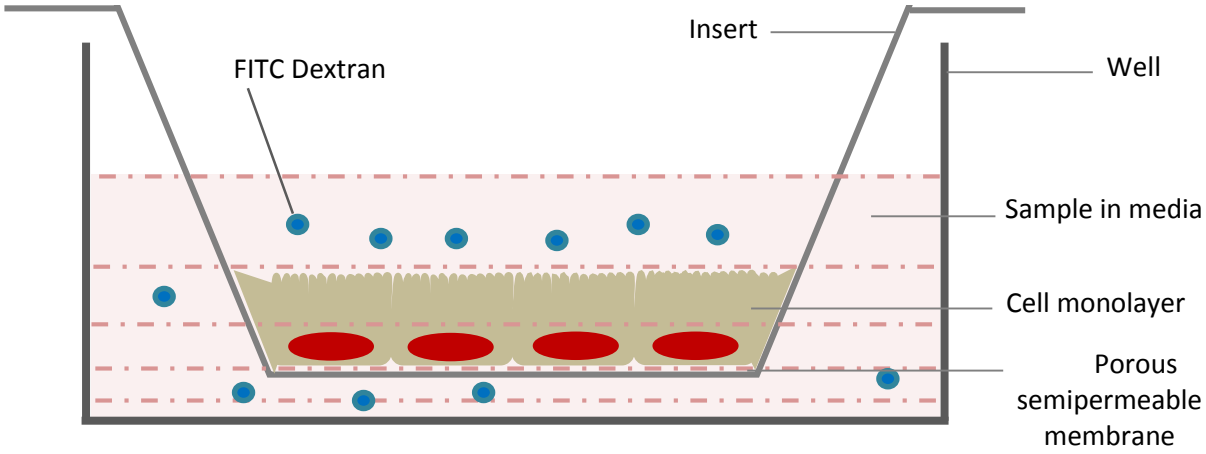

Figure 5.1 *In vitro* cell culture model of transport study showing cell monolayer in a transwell

5.2.2 Fluorescent Microscope:

Fluorescence microscopy is a powerful technique for live-cell imaging at a sub-second time scale [456, 457]. It provides opportunity not only to study the cellular structure, distribution of cellular organelles, cell health and performance but also provide insights into the cellular uptake and localisation of the nanocarriers [458]. In order to study the uptake of particles, the specimen of interest is labelled with fluorophores which reveal the locations of the particles in the cell. The cellular organelles can also be stained to elucidate the differential localisation of particles. Nam *et al*. visualised the uptake of Glycol chitosan (GC) and GC-5β- cholanic acid conjugate nanoparticles (HCG) by HeLa cells under fluorescent microscope by labelling them with carboxy succinimidyl ester cyanine 5.5. At 5 min post-incubation, the fluorescence

signal from the HGC nanoparticles was detected primarily near the cellular membrane. As the incubation time increased, the HGC fluorescence became more intense inside the cells and evenly dispersed in the cytosol. However, entry of HGC into the nucleus was somewhat unclear even at a prolonged incubation time. Evidently, some particles formed aggregates which appeared as large and strongly fluorescent red spots under the microscope [201]. Although, fluorescent microscopy generates a large amount of data, it is essentially qualitative. Other techniques such as flow cytometry are more useful in providing quantitative data.

5.2.3 Flow cytometry

Flow cytometry is a rapid, simple and sensitive method for analysing a large number of cells individually using light-scattering, fluorescence, and absorbance measurements [141, 459]. It has the ability to analyse many properties of the cells in a moving liquid stream at thousands of events per second, with simultaneous measurement of light scatter and fluorescence of each event [460, 461]. It is able to perform a broad range of functions like cell and particle sizing and sorting, determination of cell biology and pathology [462]. However, in this study, flow cytometry has been used to analyse cellular uptake of particles to elucidate the percentage internalisation of PECs and APECs.

Particle uptake is commonly determined by using intracellular markers like fluorescently labelled particles such as DiI, rhodamine or fluorescein labelled particles [190]. In a flow cytometer, the cells are transported in a fluid stream which is positioned in the centre of the laser beam. The cells flow one-by-one into the cytometer for single cell analysis which is accomplished through a pressurized laminar flow system. The sample specific lasers focus on the cell suspension, scatter light forward and on the sides and emit fluorescence [463]. The side-scattered light is proportional to cell granularity or internal complexity whereas forward scatter determines the size of particles [464]. The amount of fluorescent signal detected is proportional to the number of fluorochrome molecules in the cells [462]. Park *et al.* found that the N-acetyl histidine-conjugated glycol chitosan (NAcHis-GC) nanoparticles, were detected as green fluorescence after 10 minutes treatment of the cells with nanoparticles. DiI is virtually non-fluorescent until incorporated into lipid membranes, was seen as red fluorescence which is indicative of its entrapment into lipid membranes such as plasma, endosome, and lysosome membranes [190].

5.3 AIM

The aim of the study was to investigate the potential uptake and transport of polycations, PECs and APECs across CaCo2 cells.

5.3.1 Objectives

- Determination of the effect of free insulin, polycations, PECs and APECs on TEER of the CaCo2 cell monolayers.
- Determination of the effect of free insulin, IL PECs and IL APECs on transport of a paracellular marker i.e., FITC-Dextran (10kDa) across CaCo2 cell monolayer.
- Determination of the transport of free insulin and insulin loaded in IL PECs and IL APECs across CaCo2 cell monolayer.
- Evaluation of transcellular uptake of polycations, PECs and APECs by flow cytometry and fluorescent microscopy.

5.4 MATERIAL AND METHODS

5.4.1 Materials

Materials	Supplier
Bovine insulin ELISA kit	Mercodia, Sweden
Diamino-2-phenylindole (DAPI)	Sigma Aldrich, UK
Dimethyl sulfoxide (DMSO)	Sigma Aldrich, UK
FITC-insulin	Sigma Aldrich, UK
Foetal bovine serum (activated)	Sigma Aldrich, UK
Hank's balanced salt solution with sodium bicarbonate, magnesium and calcium (HBSS)	Sigma Aldrich, UK
Insulin from bovine pancreas (27 U/mg)	Sigma Aldrich, UK
L-Glutamine (200 mM)	Sigma Aldrich, UK
Minimum essential media eagle media (EMEM)	Sigma Aldrich, UK
Non-essential amino acids	Sigma Aldrich, UK
Penicillin/Streptomycin (10000 UmL−1/ 10000 µLmL−1)	Invitrogen
Phosphate buffer tablets (PBS)	Sigma Aldrich, UK
Rhodamine B isothiocyanate (RBITC)	Sigma Aldrich, UK
Transwell plates	Corning, UK
Trypan blue	Sigma Aldrich, UK
Trypsin-EDTA	Sigma Aldrich, UK

5.4.2 Method

5.4.2.1 Rhodamine Labelling of Amphiphilic Polymers

Rhodamine B isothiocyanate (RBITC) grafting of amphiphilic polymers (Pa2.5 and QPa2.5) was carried out using a method adapted from Thompson *et al.* [427]. Briefly, 50mg Pa2.5 was dissolved in 95mL of double-distilled water to achieve a 0.05% (w/v) solution of Pa2.5. RBITC (5mg) was initially dissolved in 5mL DMSO to achieve 1mgmL^{-1} solution which was then added drop-wise to the above prepared Pa2.5 solution over 10 min with gentle magnetic stirring. The solution was stirred for one hour at room temperature followed by dialysis against 5L of double-distilled water with a visking tube (12–14 kDa cutoff; Medicell, UK). The dialysis was carried out over 48 h, with six water changes in 24h to ensure removal of all non-bound RBITC. The dialysate was lyophilized for 24h to obtain rhodamine labelled Pa2.5 (Pa2.5R) as a deep pink fluffy solid. Pa2.5R was further quaternised as described in chapter 2, section 2.4.2.2.2 to produce RBITC-labelled QPa2.5 (QPa2.5R).

5.4.2.2 Transport Study

5.4.2.2.1 Cell culture

The CaCo2 cells were grown at a density of 2×10^4 cells/well on Transwell® filters with a pore size of 0.4 mm in 12-well polycarbonate plates. The cells were cultured for at least 15-21 days until a confluent monolayer was formed. Fresh media was added to the apical (0.5mL) and the basal compartments (1.5mL). The media was replaced from the apical compartment every alternate day until 9 days and then from both apical and basal compartments until the day when the experiment was conducted. The cell confluency and the monolayer formation were assessed by measuring the TEER with a Millicell-ERS (Millipore).

5.4.2.2.2 Monolayer integrity

Cells were grown in Transwell plates as detailed above. TEER measurements were taken routinely by using Millicell-ERS ohmmeter chopsticks (Millipore, USA) before and after media addition to assess the monolayer integrity. The transport study experiments were conducted when the resistance was within 350-650 $\Omega.cm^2$, usually within 15-21 days.

5.4.2.2.3 TEER measurements and permeation of insulin and FITC-Dextran transport across CaCo2 monolayer

The transport study was carried out by replacing the media (EMEM) from apical (0.5 mL) and basal chambers (1.5 ml) of each well with HBSS (supplemented with 1% (v/v) non-essential amino acids and 1% (v/v) L-glutamine) followed by equilibration of plates for 30 min at 37 ºC before conducting TEER measurements. The polycations, PECs and APECs were prepared in 0.01 M HCl: 0.1 M Tris buffer 87:13% (v/v) as described in chapter 3, sections 3.5.2.1 and 3.5.2.2. The samples were subsequently diluted in HBSS to their respective IC_{90} concentrations (PAH 3µgmL^{-1}, PAH-DS 3µgmL^{-1}, PAH-PAA 5µgmL^{-1}, Pa2.5 7µgmL^{-1} Pa2.5-DS 10µgmL^{-1}, Pa2.5-PAA 14µgmL^{-1}, Da10 7µgmL^{-1}, Da10-DS 10µgmL^{-1}, Da10-PAA 14µgmL^{-1}, QPa2.5 11µgmL^{-1}, QPa2.5-DS 14µgmL^{-1}, QPa2.5-PAA 14µgmL^{-1}) determined by MTT. The free insulin (5µgmL^{-1}) was used as a control.

0.5mL/well of IC_{90} concentrations of samples were added to the apical compartments. The media (200µL) was collected from the basal compartment at 0.5, 1, 1.5 and 2 h and replaced with fresh HBSS to measure the apical to basolateral flux of insulin. After 2h, the cells were washed with HBSS (three times) and samples were replaced with fresh EMEM. The plates were incubated for another 2 h. The samples (200µL) were again collected from the basal compartment of each Transwell at 3 and 4h and replaced with fresh media. The insulin concentrations of the samples collected at different time points were determined using a Mercodia bovine insulin ELISA kit (Meracodia Ltd., Sweden).

The paracellular permeability of a paracellular marker FITC-dextran (10kDa) across the cell monolayer was also monitored in the presence and absence of IL PECs and APECs. A FITC-Dextran solution (20mgmL^{-1}) was prepared in HBSS. 250µL of 20mgmL^{-1} was added to the apical side of the monolayer to achieve a final concentration of 10mgmL^{-1} and the plates were incubated at 5% CO_2, 95% humidity and 37°C. The FITC-Dextran concentration in samples from each basal chamber was determined at different time points (at 0.5, 1, 1.5 and 2 h before sample removal; at 3 and 4h after sample removal) by using a Fluorescence Multi-well Plate Reader (Perkin Elmer, LS 55) with excitation and emission wavelengths of 485 nm and 530 nm, respectively.

TEER measurements were recorded at 0 h (before addition of polycations, PECs and APECs), at 0.5, 1, 1.5 and 2 h (before removing polycations, PECs and APECs) and at

3 and 4 h (after removing polycations, PECs and APECs). The resistance of HBSS alone (10 $\Omega.cm^2$) was considered as background resistance and subtracted from each TEER value.

5.4.2.3 Uptake study

5.4.2.3.1 Determination of CaCo2 cell uptake by fluorescent imaging

The CaCo2 cells were grown and maintained as described in chapter 4 section 4.3.2. For the uptake experiments, the CaCo2 cells were seeded in 12-well polycarbonate plates at a density of 2×10^4 cells/well. The fluorescently labelled polycations (Pa2.5R, QPa2.5R); and IL PECs and APECs which were fabricated using fluorescently labelled polycations were diluted in EMEM to achieve their IC_{90} concentration reported previously in section 5.4.2.2.3. The confluent cell culture plates were washed with serum free EMEM and the cells were incubated with 2mL of IC_{90} concentrations of various polymer, PECs or APECs samples at 5% CO_2, 95% humidity and 37°C. After 2 h, the cells were washed (three times) with pre-warmed 0.1M PBS and stained with DAPI (300 nM for 5 mins) to detect and localize the cellular nuclei. The cells were stained with 4% trypan blue for 1 min to identify the presence of dead cells. Subsequently, the wells were washed (three times) with PBS and the plate was re-incubated at 5% CO_2, 95% humidity and 37°C for 0.5 h prior to imaging by fluorescence microscopy with Olympus IX2 series, inverted fluorescent microscope 1X71 Ltd., UK. The fluorescence images were acquired with the IX-TVAD TV camera, Olympus Instruments and processed using image analysis software (C*). Each experiment was carried out in triplicates.

5.4.2.3.2 Quantitative Measurement of the CaCo2 cell uptake by Flow cytometry

The cells were grown in 12 well plates at a density of 1×10^5 cells/well as detailed in chapter 4, sections 4.3.2. The IL and NIL PECs and APECs were prepared at IC_{90} concentrations as given above in section 5.4.2.2.3) using rhodamine labelled polymers (Pa2.5R and QPa2.5R). The IL PECs and APECs were prepared using fluoresceine-isothiocyanate labelled insulin (FITC-insulin). The cells were incubated with various formulations for 2h at 5% CO_2, 95% humidity and 37°C. The plates were then sub-cultured as described in chapter 4 section 4.3.2.2. The cell pellets ($\geq10^5 cell mL^{-1}$) were re-suspended in 0.1M PBS and analysed by flow cytometery (Attune® Acoustic Focusing Cytometer). The flow cytometer was equipped with a violet laser (excitation

515 nm and emission 545 nm) and a blue laser (excitation 540 nm and emission 590 nm) for detection of fluorescein and rhodamine respectively. The cells were appropriately gated by forward and side scatter and 30 000 events per sample were collected. The fluorescence was detected in BL1 channel for fluorescein and BL2 channel for rhodamine. Each experiment was carried out in triplicates.

5.4.2.4 Statistical analysis

A normality test on the data was performed to confirm the normal distribution of data. All data were compared by one-way analysis of variance (ANOVA), Post Hoc tukeys test using the SPSS 20 software. $P<0.05$ was considered to denote significance. Statistical differences were compared between the polycations, PECs and APECs. In addition, statistical differences were also compared between control i.e., free insulin samples and polycations, PECs and APECs.

5.5 RESULTS

5.5.1 Transport study

5.5.1.1 Effect of the formulations on TEER across the CaCo2 cell monolayer

The effect of various formulations on the integrity of CaCo2 cell monolayer was investigated by monitoring TEER across the CaCo2 cell monolayers (Figure 5.2 and 5.3). The CaCo2 cells incubated with free insulin exhibited no apparent variation in TEER compared to the initial values at any time point. In comparison to the free insulin, the polycations, PECs and APECs significantly decreased the original TEER ($p<0.001$) within 0.5h which signifies the opening of CaCo2 cell TJs. The reduction in TEER compared to the initial values was more significant in the presence of PECs than their respective APECs. The samples were replaced with fresh media at 2h to investigate the reversibility of opening of the TJs. All PECs and APECs (with few exceptions) demonstrated restoration of TEER to around ≥80% of their initial values within 24h. This behaviour indicates that the effect of formulations was reversible and rules out the possibility of permanent damage to the TJs. However, TEER did not recover completely for IL Pa2.5 PECs and Da10 based complexes which retained 20-40% of the original values.

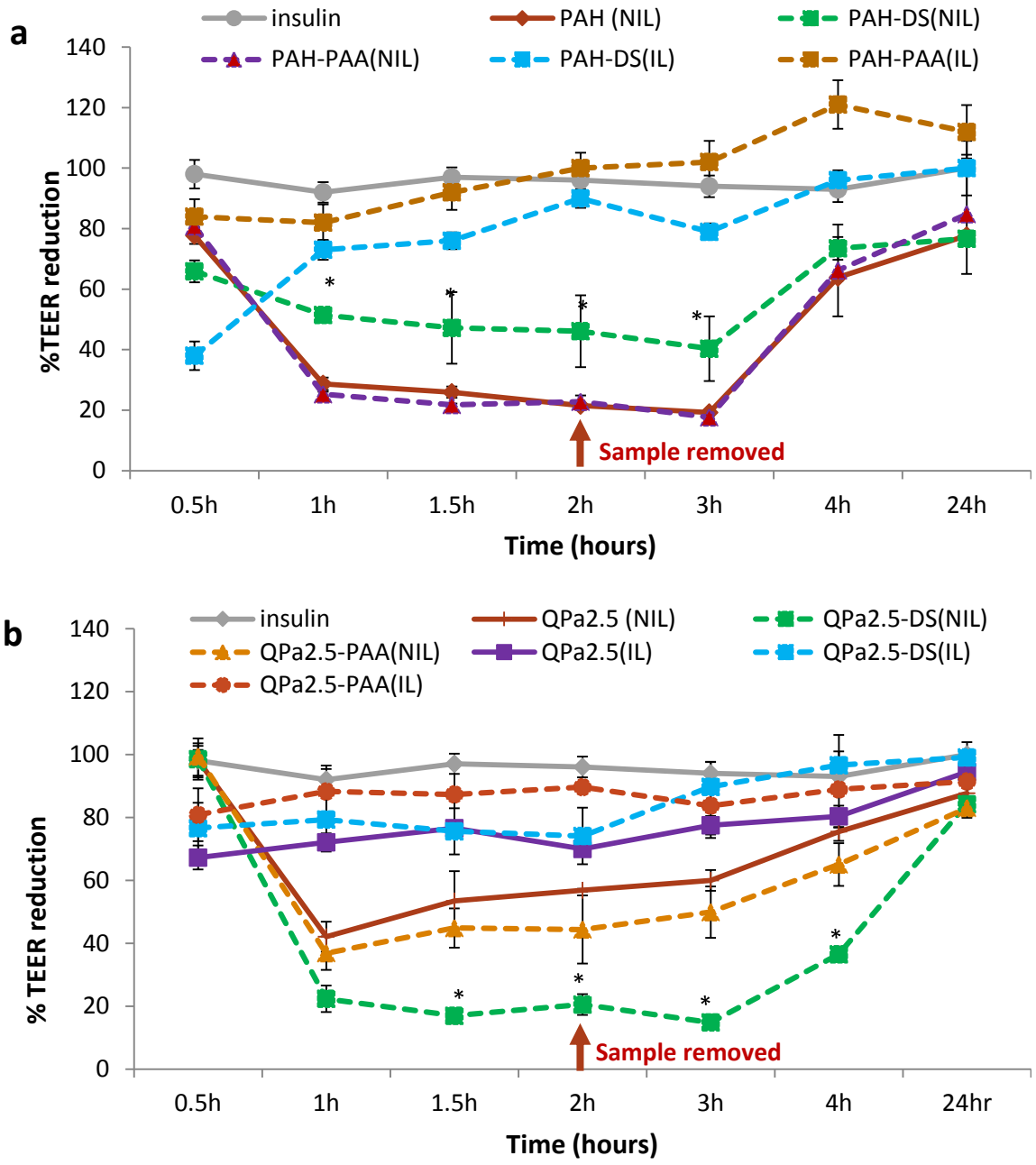

Figure 5.2 Effect of (a) PAH based formulations and (b) QPa2.5 based formulations (IC_{90} concentration) on percentage TEER of CaCo2 cells (n=3 ±SE). Values represent average percentage reduction in the original TEER. Each point represents the mean± SD of 3 replicate experiments. Insulin (5 μgmL^{-1}) demonstrated no significant decrease in original TEER. All samples were significantly different from insulin ($p<0.05$). Differences between PECs and respective APECs are expressed as $p<0.05$*.

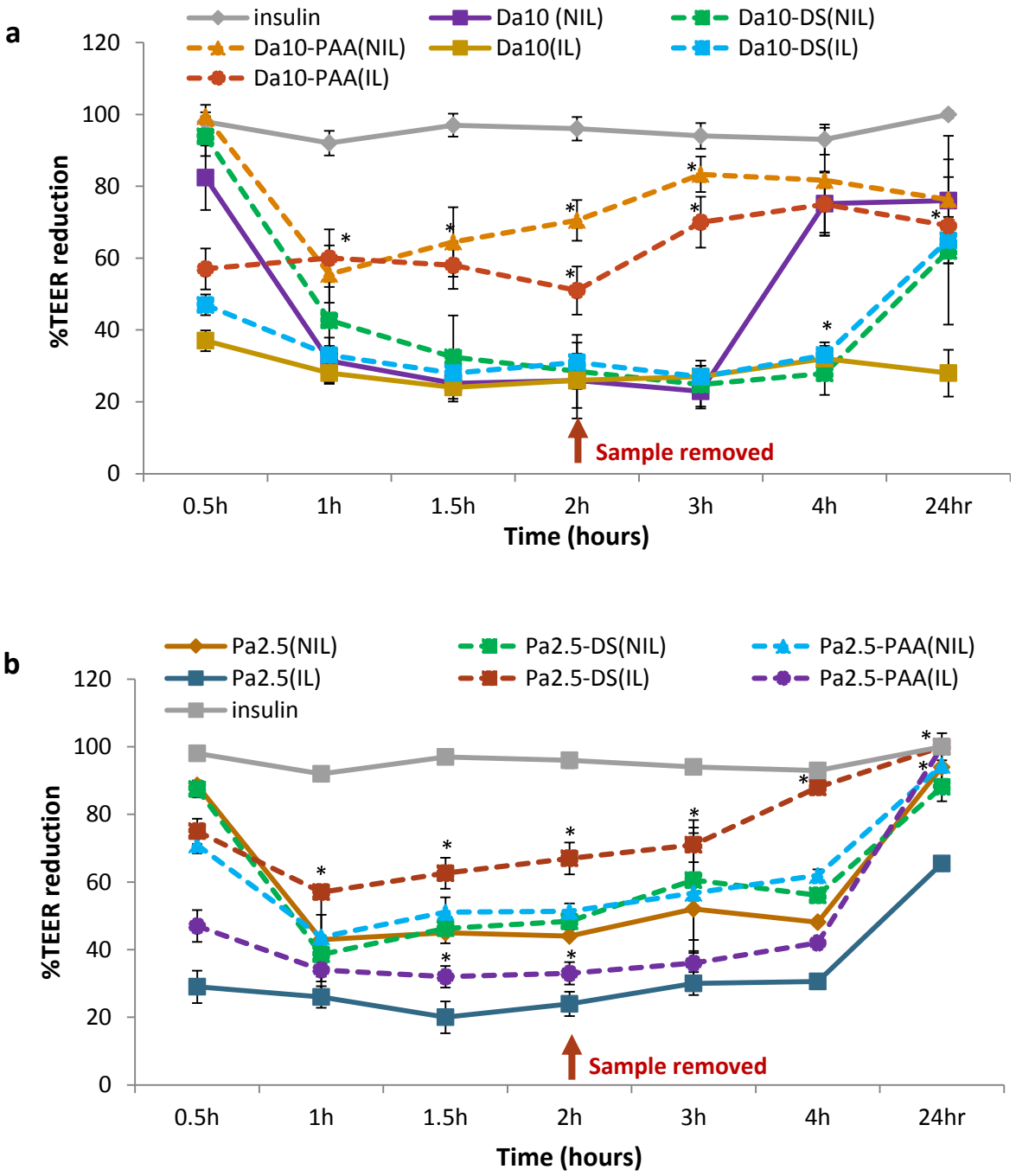

Figure 5.3 Effect of (a) Da10 based formulations and (b) Pa2.5 based formulations (IC_{90} concentration) on percentage TEER of CaCo2 cells (n=3 ±SD). Values represent average percentage reduction in the original TEER. Each point represents the mean± SE of 3 replicate experiments. Insulin (5 μgmL^{-1}) demonstrated no significant decrease in original TEER. All samples were significantly different from insulin ($p<0.05$). Differences between PECs and respective APECs are expressed as $p<0.05$*.

The NIL PAH displayed greater tendency to reduce the original TEER value than their IL counterparts (Figure 5.2a). NIL PAH and NIL PAH-PAA displayed a more marked reduction of the original TEER (5 fold, $p<0.01$) than NIL PAH-DS (2 fold). Conversely, IL PAH-DS produced greater reduction of original TEER (40-70%) than IL PAH-PAA (80%).

Similar to PAH based complexes, QPa2.5 based complexes produced greater reduction in original TEER than their IL counterparts (Figure 5.2b). The NIL QPa2.5-DS produced a more significant reduction in original TEER (5 fold, $P<0.001$) than NIL QPa2.5 and QPa2.5-PAA (2.5 fold). There were no significant differences in TEER reduction profile between the three IL QPa2.5 complexes.

The IL and NIL Da10 and Da10-DS produced significantly greater reduction in original TEER ($P<0.05$) than corresponding Da10-PAA (Figure 5.3a). The greater reduction in original TEER by NIL QPa2.5-DS, IL PAH-DS and Da10-DS indicate the role of DS in a more significant TEER reduction than PAA.

In comparison to PAH and QPa2.5 based complexes, IL Pa2.5 based complexes (except IL Pa2.5-DS) followed a reverse trend (Figure 5.3b). There was a more marked reduction in the original TEER by IL Pa2.5 and Pa2.5-PAA (40% of original- $p<0.001$) than IL Pa2.5-DS (60% of original, $p<0.05$). There was no significant difference in the TEER reduction between the NIL Pa2.5 PECs and APECs.

5.5.1.2 Effect of formulations on the permeability of FITC-Dextran (10KDa) across CaCo2 monolayers

The permeability of an otherwise impermeable marker, FITC-Dextran (10KDa) in the presence and absence of free insulin, polycations, PECs and APECs was investigated across CaCo2 cell monolayer (Figure 5.4).

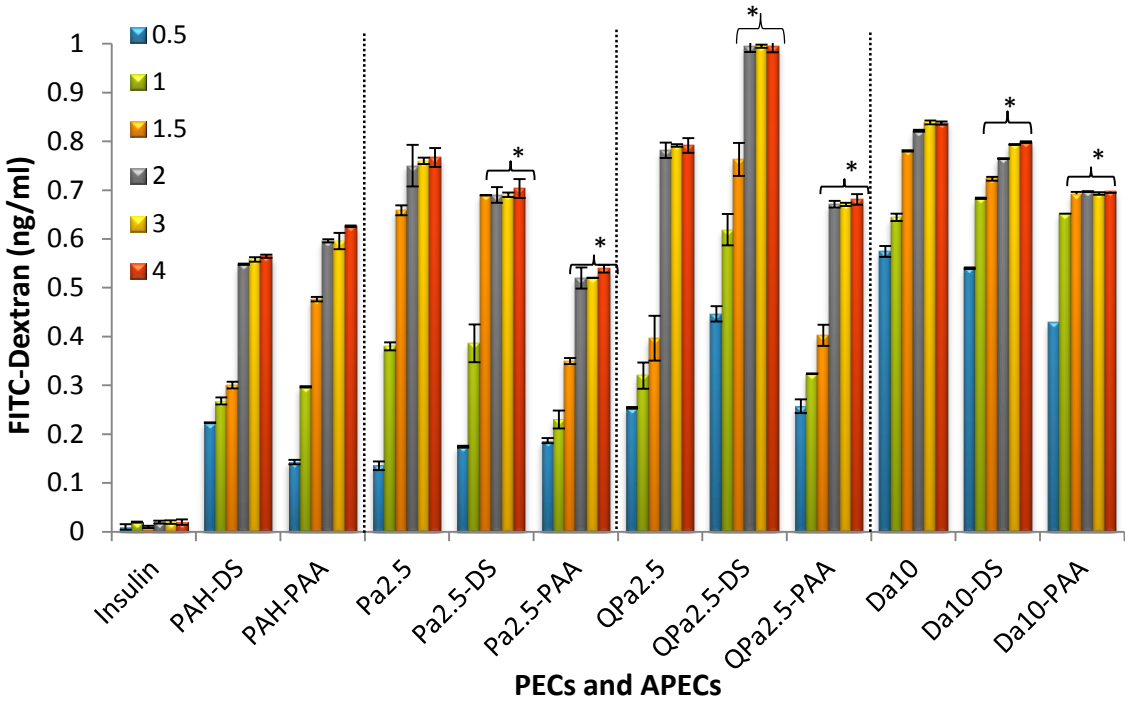

Figure 5.4 Effect of various IL PEC and APEC formulations on permeability of FITC-Dextran across CaCo2 monolayer at different time points (h) (n=3 ±SE). All samples demonstrated significant differences p<0.05 when compared with free insulin p<0.05. The statistically significant differences in FITC-Dextran permeation between PECs and their respective APECs is expressed as p<0.05*.

In the presence of free insulin, no substantial flux of FITC-Dextran was observed across the CaCo2 cell monolayer indicating that free insulin has no role in opening the TJs which correlates with the TEER findings. Likewise, cells exposed to media alone demonstrated no flux of FITC-Dextran across CaCo2 cells signifying no uptake of FITC-Dextran in the absence of PECs and APECs (data not shown). It was observed that cells exposed to PECs and APECs demonstrated statistically significant ($p<0.05$) permeation of FITC-Dextran across CaCo2 cell monolayer compared to free insulin. However, the amount of FITC-Dextran in donor chamber was found to be <0.01%, indicating no appreciable paracellular transport.

There was only a subtle difference observed in the permeability of FITC-Dextran in the cells exposed to various PECs which is graded as Da10≥QPa2.5≥Pa2.5 (0.82, 0.78, 0.75ng/ml respectively at 2h). The flux of FITC-Dextran was higher in the cells

incubated with PECs than APECs ($p<0.05$). These findings are consistent with the TEER data where IL PECs (except QPa2.5 PECs) demonstrated a higher reduction in TEER than their respective APECs. These findings indicate that PECs had a greater ability to open the TJs and to facilitate the paracellular transport than APECs.

The paracellular flux of FITC-Dextran across CaCo2 cells exposed to IL APECs is ordered as QPa2.5-DS ≥ Da10-DS ≥Da10-PAA ≥Pa2.5-DS ≥QPa2.5-PAA ≥PAH-PAA ≥PAH-DS ≥Pa2.5-PAA (Figure 5.4). Notably, IL QPa2.5-DS demonstrated a higher flux of FITC-Dextran across the CaCo2 monolayer ($p\leq0.01$) than the corresponding IL QPa2.5 PECs, despite there being no significant difference in the TEER reduction between them (Figure 5.2b).

Altogether, the findings show that DS based APECs formed by complexation with modified PAH facilitated a higher paracellular permeability of FITC dextran than PAA based APECs. These results are in line with the TEER study where DS based formulations exhibited greater reduction in TEER.

5.5.1.3 Transport of insulin across CaCo2 cell monolayer

The cumulative transport of insulin across CaCo2 cell monolayers on exposure of cells to IL PECs and IL APECs is shown in Figure 5.5 and 5.6, and summarised in Table 5.1. The findings show that there was only a minor transport of free insulin across CaCo2 cells compared to insulin complexed in PECs and APECs ($p\leq0.001$). All IL PECs and APECs increased the permeability of insulin across the epithelial barrier. These findings correlates well with the findings achieved from the TEER and FITC-Dextran permeability study which demonstrated the opening of TJs and facilitation of FITC-Dextran absorption.

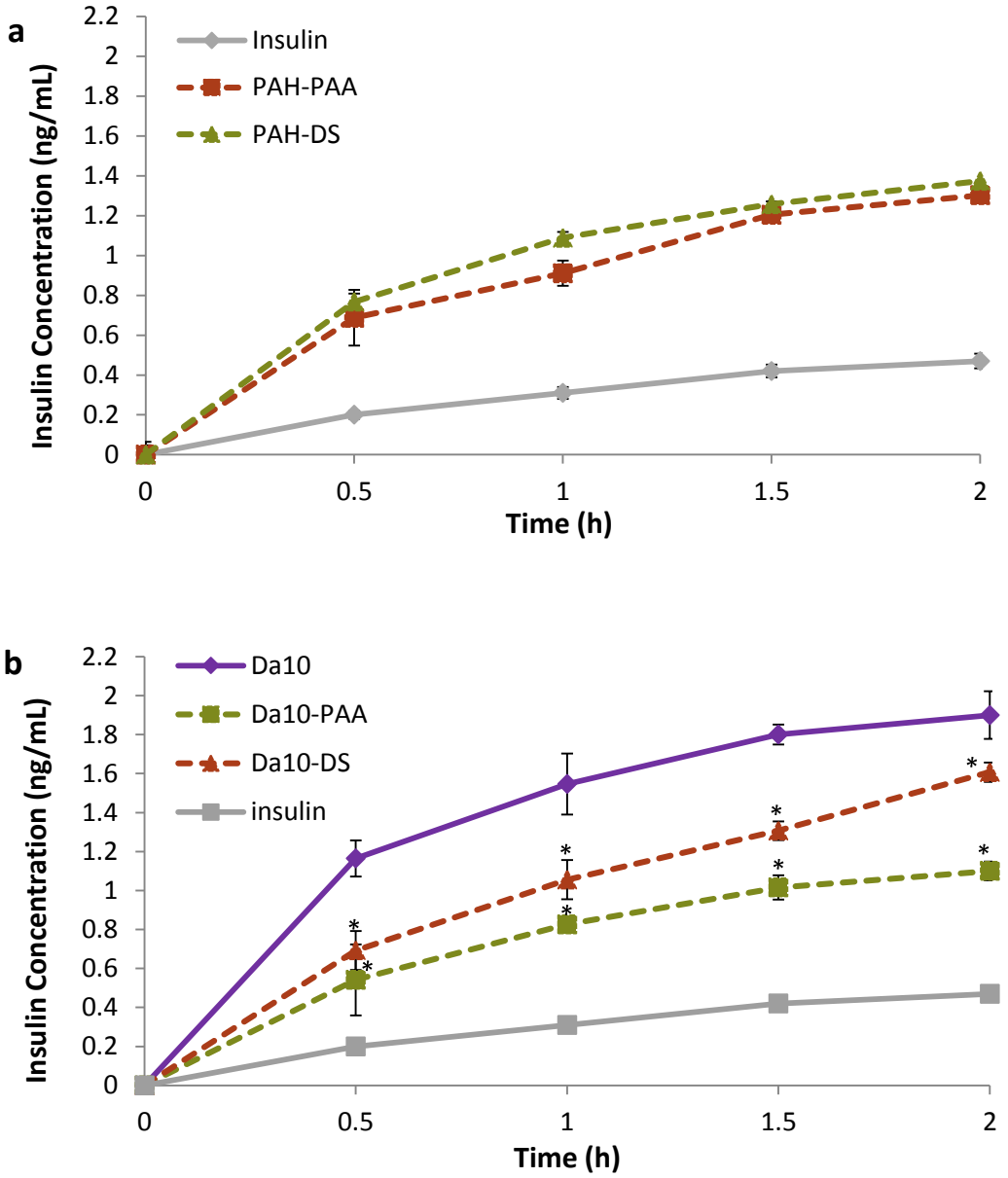

Figure 5.5 Cumulative insulin concentration in the basal compartment of transwell plates at different time points following incubation of CaCo2 cells with (a) PAH based IL PEC and APEC formulations (b) Da10 based IL PEC and APEC formulations (n=3 ±SE). All PEC and APEC formulations demonstrated significantly higher insulin permeation than free insulin ($p<0.001$). APEC formulations exhibited significantly lower insulin permeation than their respective PECs, expressed as $p<0.05$*.

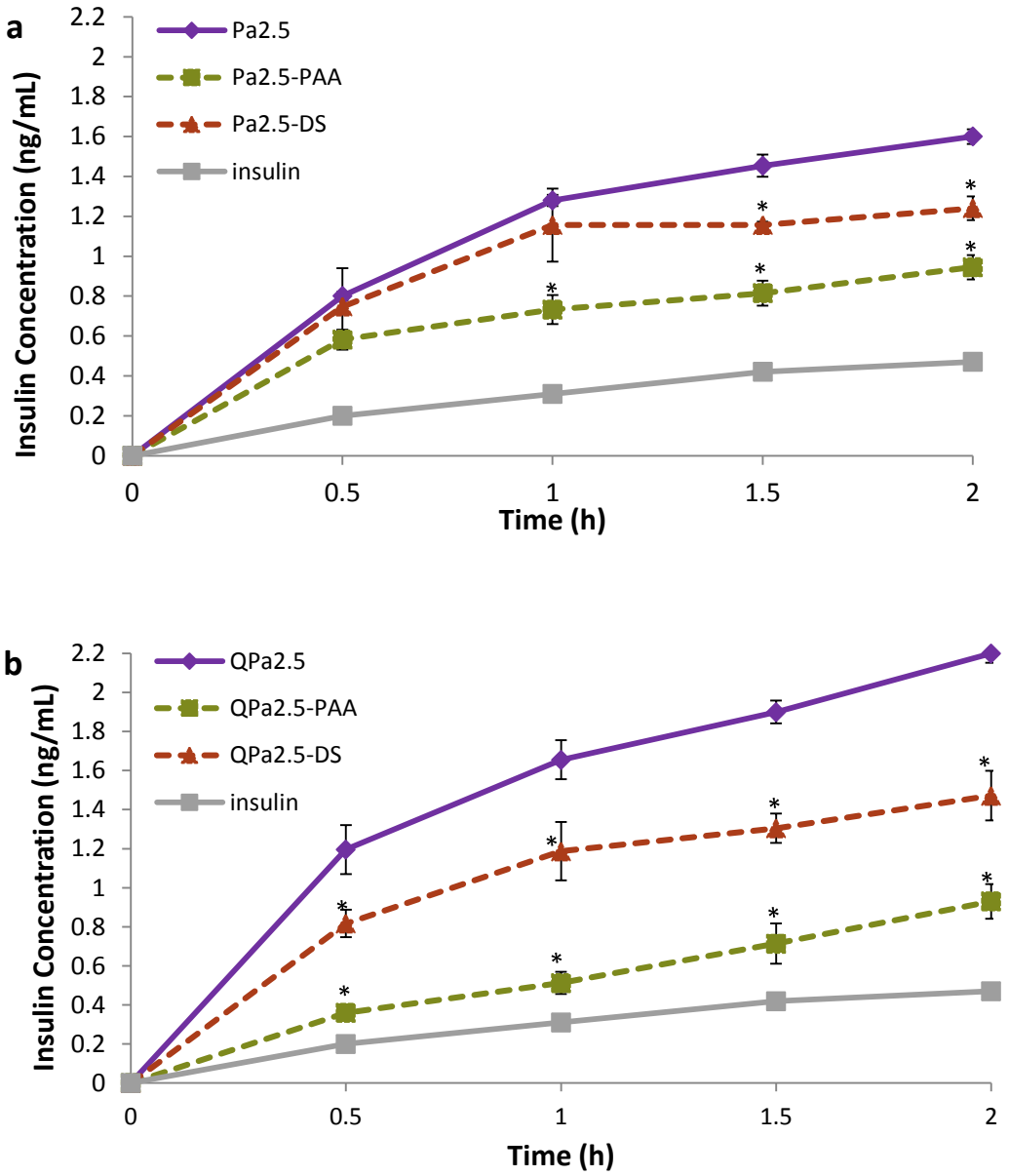

Figure 5.6 Cumulative insulin concentration in the basal compartment of Transwell plates at different time points following incubation of CaCo2 cells with (a) Pa2.5 based IL PEC and APEC formulations (b) QPa2.5 based IL PEC and APEC formulations (n=3 ±SE). All PEC and APEC formulations demonstrated significantly higher insulin permeation than free insulin ($p<0.001$). APEC formulations exhibited significantly lower insulin permeation than their respective PECs, expressed as $p<0.05$*.

Table 5.1 Cumulative insulin concentration in basal chambers of Transwell plates following incubation with IL PEC and APEC formulations for 2h

PECs and APECs	Insulin concentration (μgmL^{-1}) in basal chamber of wells of Transwell plate at 2h incubation with samples	Number of folds reduction in insulin transport by APECs as compared to PECs
Free insulin	0.4	
PAH-PAA	1.3	
PAH-DS	1.4	
Pa2.5	1.6	
Pa2.5-PAA	0.9	1.8
Pa2.5-DS	1.2	1.3
QPa2.5	2.2	
QPa2.5-PAA	0.9	2.4
QPa2.5-DS	1.5	1.5
Da10	1.9	
Da10-PAA	1.1	1.7
Da10-DS	1.6	1.2

The cells incubated with PECs demonstrated higher transport of insulin than APECs ($p<0.001$) (Table 5.1). The degree of insulin transport by cells incubated with PECs is graded as QPa2.5 ≥Da10 ≥Pa2.5 (Figure 5.5 and 5.6, Table 5.1). These findings relate to the FITC-Dextran permeability study in view that both studies demonstrated higher flux in the presence of QPa2.5 and Da10 and lowest flux in the cells exposed to Pa2.5. The findings are also consistent with the TEER data except for the IL QPa2.5 PECs which demonstrated a lower ability to open the TJs and facilitate FITC-Dextran transport compared to QPa2.5-DS.

The uptake of free insulin across CaCo2 cells was found to be <0.01% of the total amount of insulin in the apical chamber of transwell plates. The reduced uptake of free insulin may be attributed to the enzyme activity on the apical membrane of CaCo2 cells which might have degraded it prior to its uptake by cells. On the other hand, the insulin transport across CaCo2 cells incubated with PECs and DS based APECs was found to be ≥0.01%, indicating a considerably higher uptake than free insulin. The insulin

transport profile of the APECs is graded as Da10-DS ≥QP2.5-DS ≥Pa2.5-DS ≥PAH-DS = PAH-PAA ≥Da10-PAA ≥Pa2.5-PAA = QPa2.5-PAA (Figure 5.5 and 5.6). This ranking substantiates the role of DS based APECs in generating higher insulin transport than PAA based APECs. The transport of insulin across CaCo2 cells incubated with PAA based APECs was found to be ≤0.01%. This low insulin transport across cells agree well with the low TEER reduction profile, reduced permeability of FITC-Dextran and reduced uptake of complexes in cells exposed to PAA based APECs. Conversely, the high insulin transport across cells exposed to DS based APECs correspond well to the high TEER reduction profile, higher permeability of FITC-Dextran and higher uptake of complexes in cells exposed to DS based APECs.

5.5.2 Uptake study

5.5.2.1 Determination of the CaCo2 cell uptake by fluorescent imaging

The fluorescent microscopy was employed to confirm the uptake of IL PECs and APECs by CaCo2 cells. QPa2.5 and Pa2.5 based complexes were chosen for this study. Since the fluorescent microscope was not equipped with a UV filter, therefore, uptake of Da10 based complexes was not studied. Figure 5.7 and 5.8 show the fluorescent microscopy images of CaCo2 cells where internalised IL Pa2.5-R and IL QPa2.5-R based PECs and APECs are shown by arrows. The complexes are seen as red fluorescence whereas the cellular nuclei appear as blue fluorescence due to staining with DAPI nuclear stain. No fluorescence was detected in the control cells which were not exposed to the rhodamine labelled complexes, implying that there was no auto-fluorescence of the cells which could cause misinterpretation of the data (figure not shown). The complexes appeared as punctuated red spots. The Pa2.5 PECs (red fluorescence) were found predominantly close to the cell membrane (Figure 5.7-1b) while Pa2.5 APECs were found further in the cytosol (Figure 5.7-2b & 3b). On the other hand, QPa2.5 based complexes (red fluorescence) mainly localised in the cytoplasm and perinuclear areas (Figure 5.8-1b) whereas QPa2.5 Co- localised in the cytoplasm (Figure 5.8-2b & 3b). Dead and damaged cells appeared as black patches in bright field due to the treatment of cells with trypan blue. The bright field images revealed no substantial black/blue staining of cells signifying the viability of the CaCo2 cells after treatment with PECs and APECs.

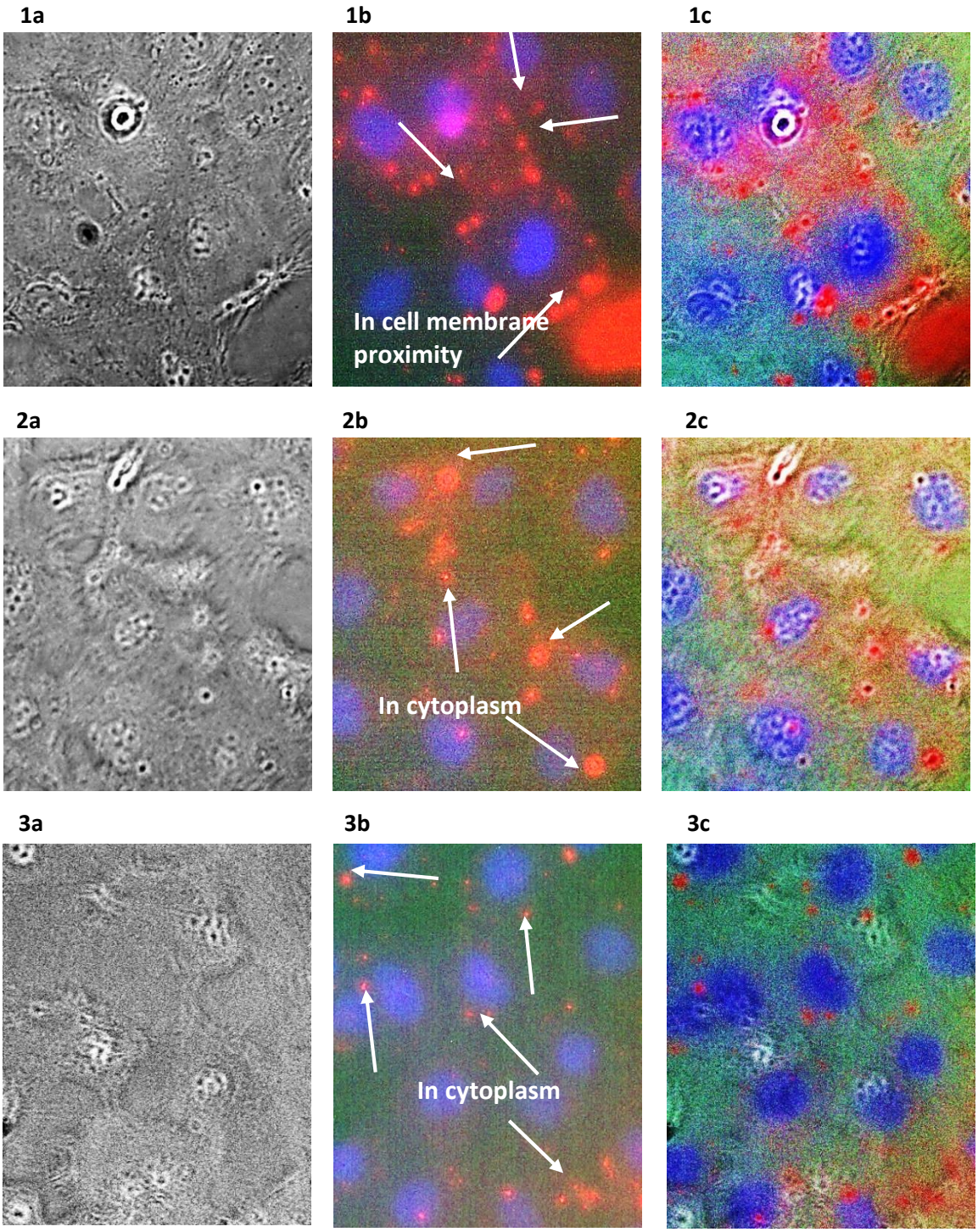

Figure 5.7 Fluorescent microscopy images (40X magnification) of CaCo2 cells incubated with various IL PECs and APECs at IC_{90} concentration (1) IL Pa2.5 (2) IL Pa2.5-DS (3) IL Pa2.5-PAA (a) Bright field image (b) Fluorescent image (c) overlay of a & b. The complexes are visualised as red fluorescence indicated by arrows and the nucleus as blue fluorescence due to staining with DAPI nuclear stain.

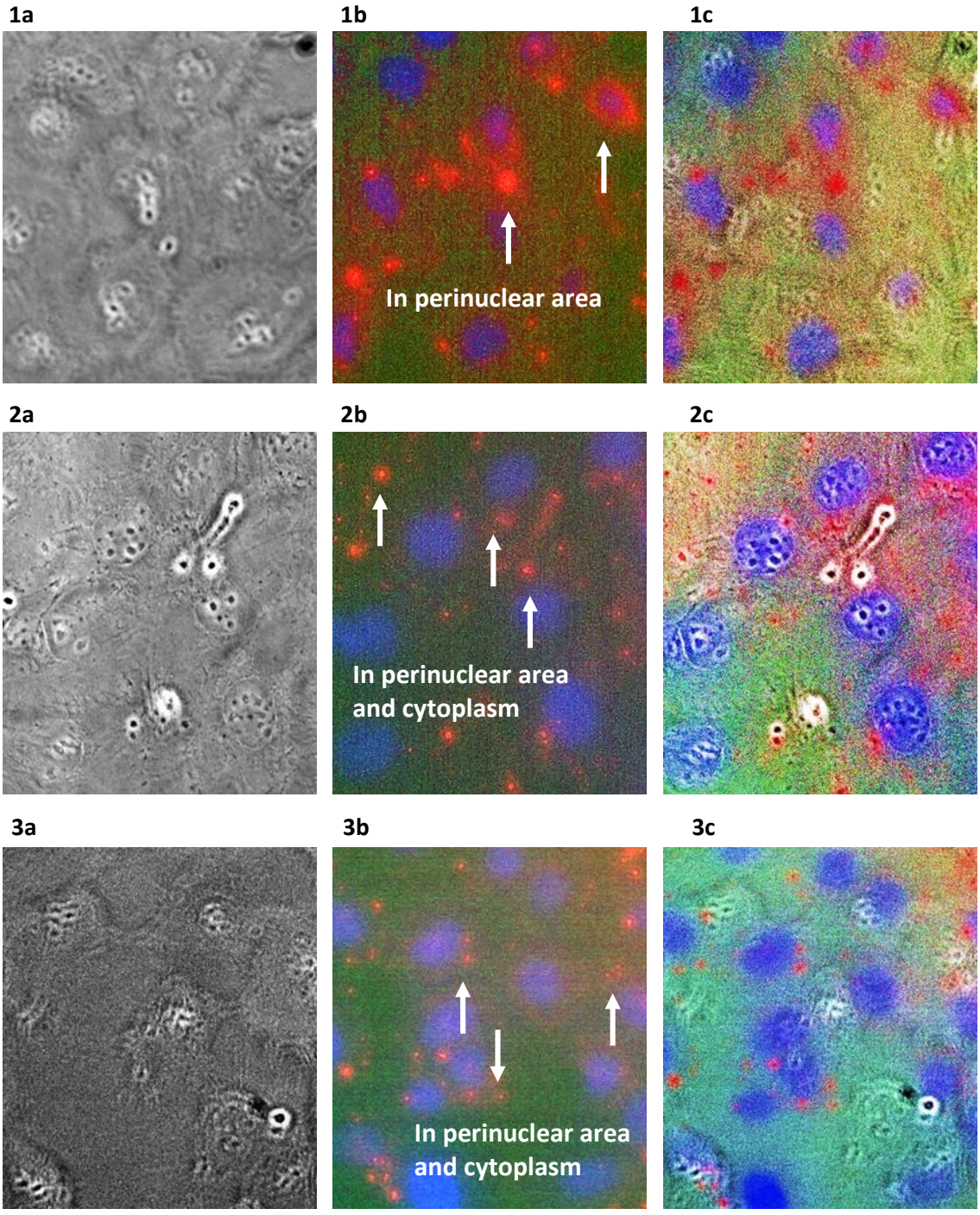

Figure 5.8 Fluorescent microscopy images (40X magnification) of CaCo2 cells incubated with various IL PECs and APECs at IC_{90} concentration (1) IL QPa2.5 (2) IL QPa2.5-DS (3) IL QPa2.5-PAA (a) Bright field image (b) Fluorescent image (c) overlay of a & b. The complexes are visualised as red fluorescence indicated by arrows and the nucleus as blue fluorescence due to staining with DAPI nuclear stain.

5.5.2.2 Quantitative measurement of the CaCo2 cell uptake by Flow cytometry

In order to determine the efficiency of uptake, a quantitative uptake study was carried out using flow cytometer (Attune® Acoustic Focusing Cytometer). Figure 5.9 and 5.10 display the plots showing the internalisation of R-Pa2.5 and R-QPa2.5 based PECs and APECs by CaCo2 cells. Each plot presents four quadrants specific to the cells i.e. left lower quadrant (cell with no uptake i.e., negative), left upper quadrant (cells presenting uptake of only rhodamine labelled complexes), right lower quadrant (cells presenting uptake of only FITC-insulin) and right upper quadrant (cells presenting uptake of both rhodamine labelled complexes and FITC-insulin).

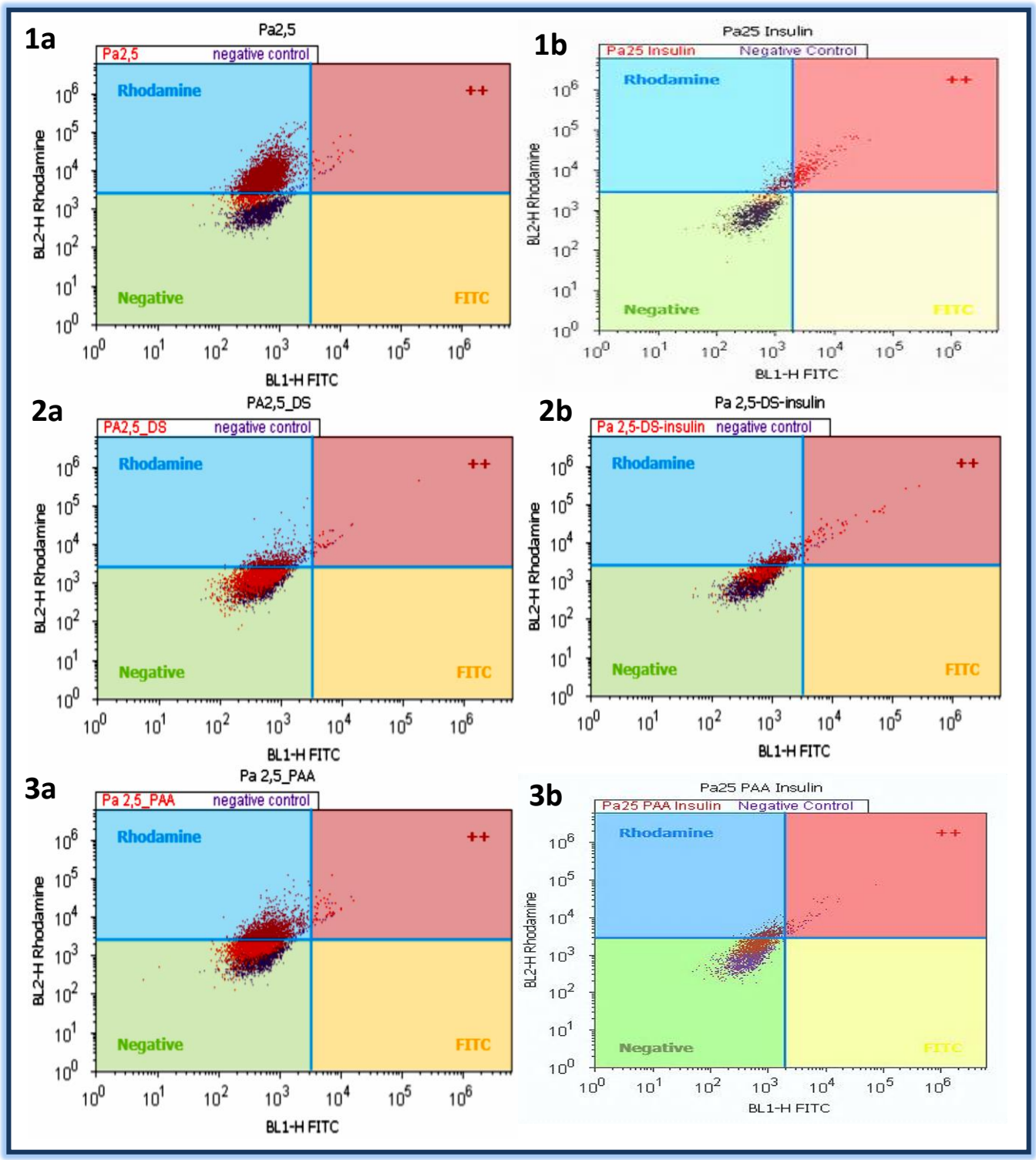

Figure 5.9 Flow cytometry plots showing the uptake profile of CaCo2 cells incubated with (1a) Pa2.5 (1b) IL Pa2.5 (2a) NIL Pa2.5-DS (2b) IL Pa2.5-DS (3a) NIL Pa2.5-PAA (3b) IL Pa2.5-PAA.

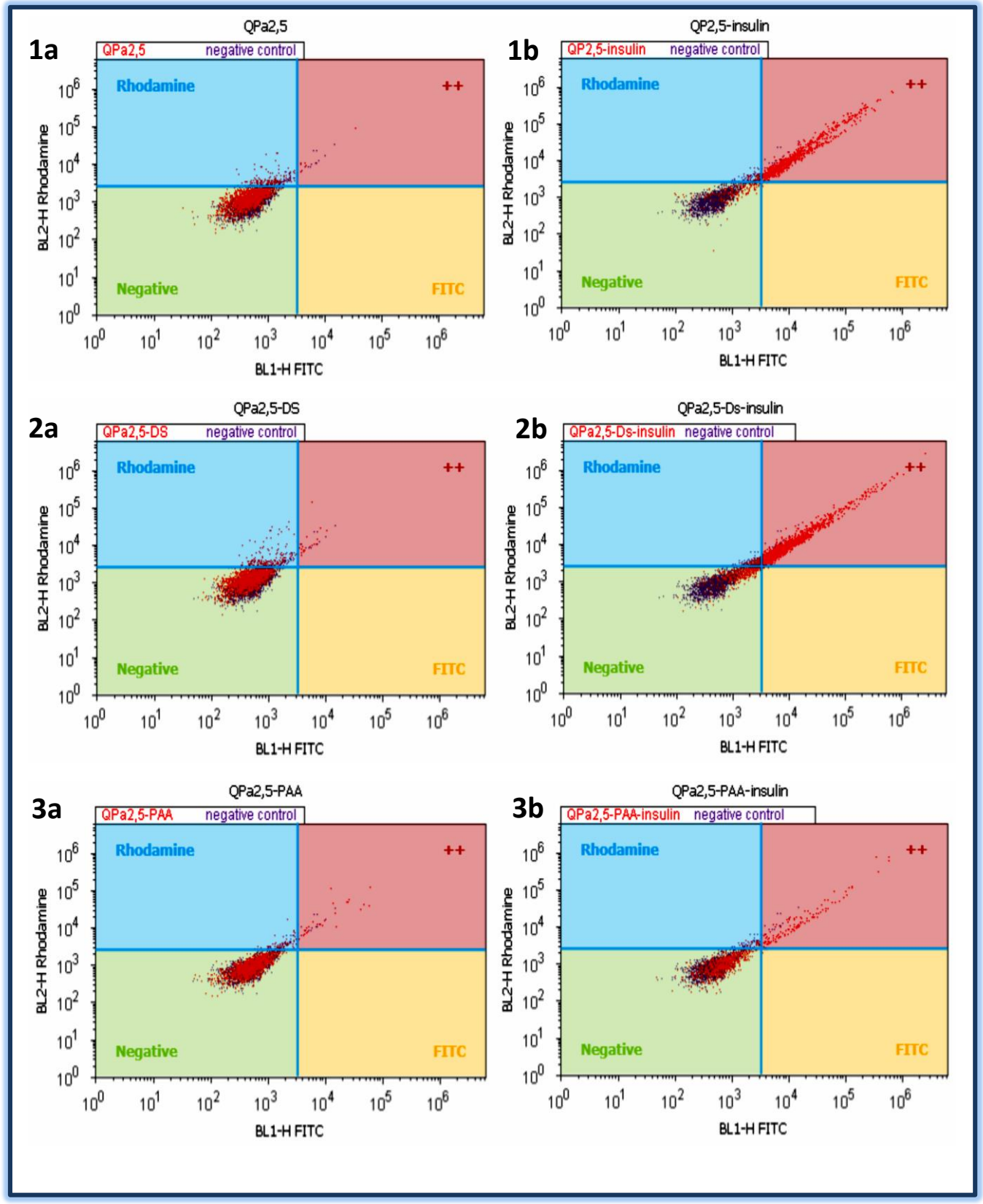

Figure 5.10 Flow cytometry plots showing the uptake profile of CaCo2 cells incubated with (1a) QPa2.5 (1b) IL QPa2.5 (2a) NIL QPa2.5-DS (2b) IL QPa2.5-DS (3a) NIL QPa2.5-PAA (3b) IL QPa2.5-PAA.

Table 5.2 Percentage uptake of polycations, PECs and APECs by CaCo2 cells determined by flow cytometry (n=3 ±SE)

PECs and APECs	% Uptake of non-loaded complexes	% Uptake of insulin loaded complexes
Pa2.5	89±2.3	44±6.8
Pa2.5-DS	25±5.4	43 ± 8.7
Pa2.5-PAA	42±6.8	29± 3.2
QPa2.5	10±2.2	73± 7.4
QPa2.5-DS	8±1.7	67± 6.2
QPa2.5-PAA	5±2.4	12± 4.2

The data in Table 5.2 summarises the uptake of NIL and IL QPa2.5 and Pa2.5 complexes by CaCo2 cells achieved from the flow cytometry study. The findings show that the uptake of Pa2.5 and QPa2.5 PECs was higher than the uptake of respective APECs.

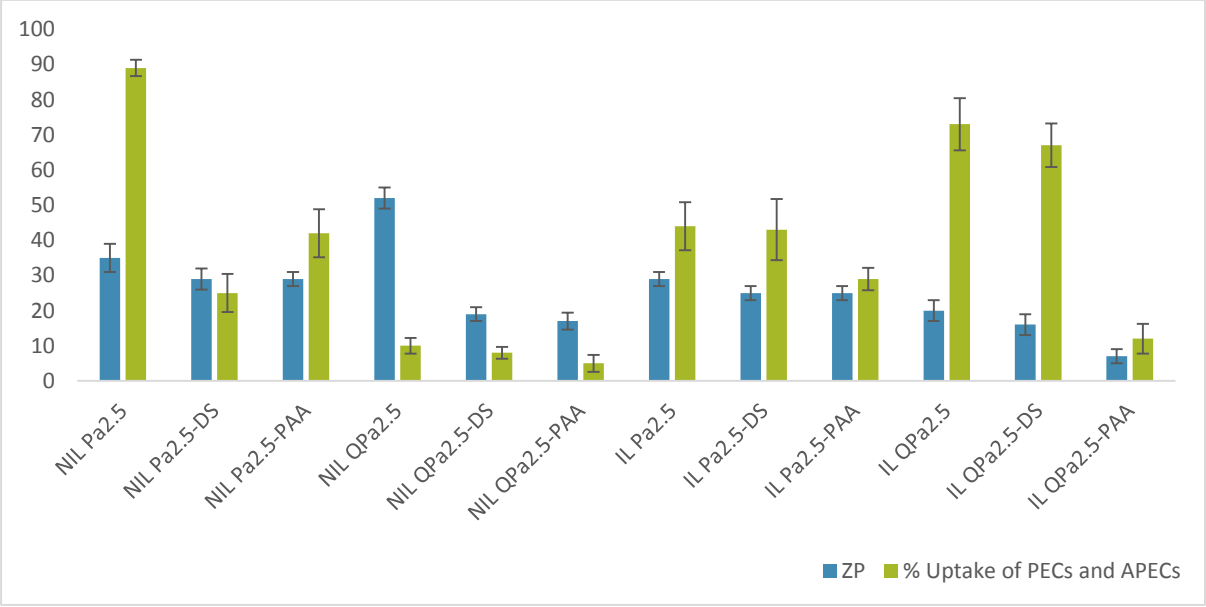

Figure 5.11 Intracellular uptake of IL and NIL complexes versus ZP (n=3 ±SE).

Overall, the uptake of the NIL Pa2.5 PECs and APECs was significantly higher than the uptake of respective IL Pa2.5 complexes (except Pa2.5-DS). The IL Pa2.5 PECs demonstrated 2 fold lower uptake (44%) than the NIL Pa2.5 PECs (89%) whereas IL Pa2.5-PAA demonstrated 1.4 fold lower uptake (29%) than NIL Pa2.5-PAA (42%). On

the other hand, the IL Pa2.5-DS (43%) followed a reverse trend i.e., 1.7 fold higher uptake by CaCo2 cell than NIL Pa2.5-DS (25%).

The uptake of IL QPa2.5 complexes (12-73%) was found higher than the respective NIL QPa2.5 complexes (5-10%). Among all QPa2.5 complexes, NIL and IL QPa2.5-PAA presented the least uptake i.e., 5% and 12% respectively. On the contrary, the IL QPa2.5 and QPa2.5-DS demonstrated considerably higher uptake. IL QPa2.5 presented 7.3 fold higher uptake (73%) than NIL QPa2.5 (10%). IL QPa2.5-DS demonstrated 8.3 fold higher uptake (67%) than NIL QPa2.5-DS (8%).

5.6 DISCUSSION

Understanding the mechanism of cellular uptake and transport of polymeric nanocarriers is critical for designing effective carriers for protein delivery [466]. It is known that certain properties of polymeric nanocarrier systems such as size surface charge, molecular weight and hydrophilicity affect their intestinal absorption [308, 317]. Each specific property may impact differently on the uptake behaviour depending on the cell type [201]. The aim of this study was to characterize the cellular uptake and transport of PAH and modified PAH based polycations, PECs and APECs and to elucidate the influence of different physicochemical properties on their uptake and transport across CaCo2 cells. The underlying mechanism of their uptake was determined by performing TEER measurements, assessment of paracellular permeability of FITC-dextran and quantification of insulin transport across CaCo2 cells. Further investigations were done to confirm their uptake by direct visualisation of particles using fluorescent microscopy and quantification of uptake by using flow cytometry.

CaCo2 cell line was selected for this study because it offers substantial similarities to the human intestinal epithelium. CaCo2 cell monolayers are characterized by formation of TJs at the apical membrane upon growth on the membrane filters [434, 467, 468]. They express a distinct and high TEER value and therefore are generally accepted to be an appropriate cell line for the transport studies [467]. TEER is a measure of TJ integrity which reduces when the junctions are opened or damaged and hence provides an essential way to determine the tightness of the cell membrane [469]. Since the mean size of the TJs is in the order of <10 A° therefore, the transport of large macromolecules is restricted unless the TJ are opened [67, 470]. TJs can open and close to a certain degree under the influence of various polymers such as chitosan, polyallylamine and their derivatives which

is determined by monitoring reduction in TEER [67, 427]. However, the reduction in TEER does not confirm the paracellular permeation, as it does not distinguish between membrane and paracellular conductance [428]. Therefore, TEER study was coupled with FITC-Dextran (10KDa) study to assess its paracellular permeability across the TJs at various time points. Since, the transport of hydrophilic macromolecules is restricted by the presence of TJs, they form an effective means to study the paracellular permeability of macromolecules across the TJs [178]

The paracellular flux of tracers can provide information about whether the opening of the TJs is accompanied by a paracellular flux or not [471]. It has been reported that chitosan solution and nanoparticles produced a sharp and reversible decrease in TEER and increased the permeability of two FITC-dextrans, MW 4kDa and 10kDa across cells [184]. Sandri and group has shown that nanoparticles based on TMC with different quaternization degree, decreased the TEER and increased the paracellular flux of Lucifer Yellow, a paracellular pathway marker, across CaCo2 cells [58].

It is well known that insulin is absorbed into the cells through the insulin receptors present in the cellular membrane of CaCo2 cells [472]. It is also known that insulin has no effect on the TJs and therefore no drop in TEER was expected in the presence of free insulin [444]. No reduction in TEER in the presence of free insulin confirmed that the permeation of free insulin does not occur via the paracellular route. The decrease in the percentage TEER and increase in the permeability of FITC-Dextran under the influence of all the formulations tested indicates that all formulations were able to promote paracellular transport.

Generally, the cells incubated with polycations and PECs produced a greater reduction in TEER and higher transport of FITC-Dextran (except QPa2.5 based APECs) and insulin as compared to their respective APECs, presumably due to a higher positive surface charge. The presence of polyanion in APECs is thought to have caused repulsive interactions between the APECs and the negatively charged membrane proteoglycans [364] leading to a reduced interaction with the cell membrane. The findings are in line with the study done by Sadeghi *et al.* on the effect of chitosan solution and nanoparticle formulations on TEER of CaCo2 monolayers [431]. They showed that, chitosan nanoparticles had a much lower effect on decreasing the TEER compared to the free-soluble chitosan. It was considered to be due to the reduced available amount of positive charge on the surface of nanoparticles, compared to the soluble form of chitosan [431].

Discrepancy in the capacity to induce TJ opening between chitosan solution and nanoparticles has also been explained by a restriction in the movement of the chitosan chains in the nanoparticulate form, which hinder the contact of these chains with the plasma membranes and TJs [473].

The NIL PAH and QPa2.5 polymers displayed greater tendency to reduce TEER than their IL counterparts. The results are in agreement with a study conducted by Sadeghi and group who showed that nanoparticles consisting of chitosan and its quaternary ammonium derivatives loaded with insulin were less effective in facilitating paracellular transport across CaCo2 cell monolayers than the corresponding free polymers [431]. It has also been shown by Ma and Lim group that soluble chitosan was more effective in opening the intercellular TJ's than chitosan nanoparticles [188]. This was explained by the possibility of a less effective interaction of chitosan nanoparticles with the cellular proteins because of their TPP-cross-linked chains [188].

The NIL QPa2.5 complexes produced a more significant reduction in original TEER (20-60%, $p<0.001$) than their IL counterparts (70-80%, $p<0.05$). The presence of insulin in IL QPa2.5 complexes significantly dropped their positive ZP (QPa2.5 PECs 52-20mV; QPa2.5-DS 19-16 and QPa2.5-PAA 17-7mV) which could have altered their interaction with the junctional proteins, subsequently preventing the TJ opening (Table 3.2).

The reduction in original TEER was more marked in the cells incubated with NIL QPa2.5 APECs than NIL QPa2.5. This may be because the methyl groups in the bulky quaternary ammonium moiety in QPa2.5 produced significant steric effects which might have affected their interaction with the junctional proteins. It has previously been shown that pyridyl-methyl group of methylated N-(-4pyridinylmethyl) chitosan (TM-Py-CS) shielded the positive charges of the quaternary ammonium moieties of chitosan and hindered their binding to the negatively charged surface on the TJs [474]. The presence of polyanion in QPa2.5 APECs might have reduced the steric hindrance and subsequently promoted their interaction with the junctional proteins, leading to a more significant decline in the original TEER. The exact mechanism of how polyanion prevented the steric hindrance and promoted binding to the TJs remains to be further studied. The findings correspond to the recent findings which have shown that polyanion containing N-trimethyl chitosan/ poly(γ-glutamic acid) nanoparticles (TMC40/γ-PGA NPs) significantly decreased the original TEER and increased the amount of insulin transported across CaCo2 cell monolayers along the paracellular pathway [186].

Kotze *et al.* has shown that the opening of the TJs is strongly dependent on the positive charge density of the polycation [475]. The positive charge (29±2mV) of NIL PAH-PAA as compared to IL PAH-PAA (0.06±3mV) (Table 3.2) facilitated their interaction with the TJ proteins leading to a more significant reduction in original TEER. However, the presence of insulin in IL PAH-PAA complexes reduced the surface charge which altered their interaction with the TJs leading to a less significant reduction in original TEER (up to only 15%, $p<0.05$) than NIL PAH-PAA. Similar effect was observed for NIL PAH-DS (39±2mV) which showed higher TEER reduction than IL PAH-DS (25±3mV) due to their high positive surface charge.

On the other hand, IL Pa2.5 based complexes showed greater reduction in original TEER than their NIL counterparts. A comparable TEER reduction (max 60%) by NIL Pa2.5 PAA and Pa2.5-DS APECs is attributed to the identical ZP (29mV). A more significant reduction in original TEER by IL Pa2.5 PECs (max 75%- $p<0.05$) than their corresponding APECs is ascribed to their more positive ZP (29mV) than the corresponding APECs (25mV) which might have promoted their interaction with the junctional proteins.

There is evidence that higher positive charge density plays an important role in binding and internalisation of nanocarriers [476]. Positive charge has been shown to be responsible for interaction of nanocarriers with the TJ proteins and to promote their re-organization, subsequently opening the TJ [60, 431]. The alteration in the staining pattern of TJ proteins such as claudin [177] zonnula occludens (ZO-1) [186], CLDN4 [178] and JAM-1 [477] have been associated with transient opening of TJs. The ability of transient opening of TJs has also been associated with interaction of polycation such as chitosan with Protein Kinase C pathway [478].

The role of positive charge in opening the TJ and paracellular permeation of hydrophilic molecular tracers has previously been established by a number of research groups [471, 474]. The high charge density has been shown as a necessary factor to substantially improve the paracellular permeability of TMC across intestinal epithelia [58, 475]. Florea *et al.* has ascribed the difference in permeation enhancement between quaternised chitosan derivatives i.e., TMC20 and TMC60, to the stronger cationic charge density of TMC60 which makes it apparently more effective in modulating the tight-junctional barrier [476]. Hamman *et al.* reported that the effect TMC on the TEER reduction and transport of hydrophilic macromolecular compounds was associated with

the number of available positive charges on the TMC [479]. The higher FITC-Dextran and insulin transport in the cells incubated with PEC than their respective APECs are therefore attributed to their high positive surface charge. Among APECs, all DS based APECs showed higher TEER reduction and FITC-Dextran and insulin permeation across CaCo2 monolayer than PAA based APECs. These effects are attributed to the flexible architecture and high MW of DS. However, altogether the flux of FITC-Dextran across CaCo2 monolayer was ≤0.01% of original concentration of FITC-Dextran introduced in the apical chamber indicating very low paracellular transport. It has been reported by Woitiski *et al.* that detection of FITC-Dextran <0.01% of original concentration in the donor chamber indicates either no sufficient permeation of FITC-Dextran or intact integrity of intestinal mucosa [444]. The opening of the TJs by absorption enhancers is considered to be only 20-50 nm in width [186]. It could be that the paracellular pathway was not adequately widened to allow the passage of large sized complexes across the cell monolayer [188]. Therefore, altogether the findings infer that all the formulations were able to open the TJs, but there was very low paracellular permeation across the TJs. This effect has previously been reported by Mao *et al.* who demonstrated that PEG(5K) 40g-TMC(100 copolymer complexes were not internalised through paracellular route despite the TJ opening, demonstrating that the paracellular transport was not the main route of their uptake [67]. Similarly, Woitiski *et al.* reported the uptake of multi-layered chitosan nanoparticles predominantly by transcellular route despite the significant opening of the TJ [444].

Flow cytometry study showed a higher uptake of NIL Pa2.5 complexes than IL Pa2.5 complexes; and of IL QPa2.5 complexes than NIL QPa2.5 complexes. This shows that the presence of insulin interfered in the uptake of Pa2.5 complexes whereas promoted the uptake of QPa2.5 complexes (Table 5.2). This behaviour is once again considered to be due to the reduction in ZP upon introduction of insulin in Pa2.5 complexes which subsequently reduced their uptake by impairing their interaction with the membrane proteins. Conversely, the presence of insulin in IL QPa2.5 complexes prevented the steric hindrance and subsequently facilitated their interaction with the membrane proteins.

The considerably low uptake of NIL QPa2.5 based complexes (Table 5.2) indicate that they were not efficiently internalised via the transcellular route due to their large size (228-468nm) (Table 3.2). In particular, the NIL QPa2.5-PAA (228±1nm) and IL QPa2.5-PAA (388± 29nm) are assumed to have not been significantly internalised due to their large size (Table 3.2). The higher uptake of IL QPa2.5 and QPa2.5-DS and insulin transport across

CaCo2 cells substantiates the ground for uptake predominantly by a transcellular route Figure 5.12. The small size of IL QPa2.5 (117±2.4nm) and IL QPa2.5-DS (72±0.9nm) is assumed to have allowed efficient internalisation by transcellular route.

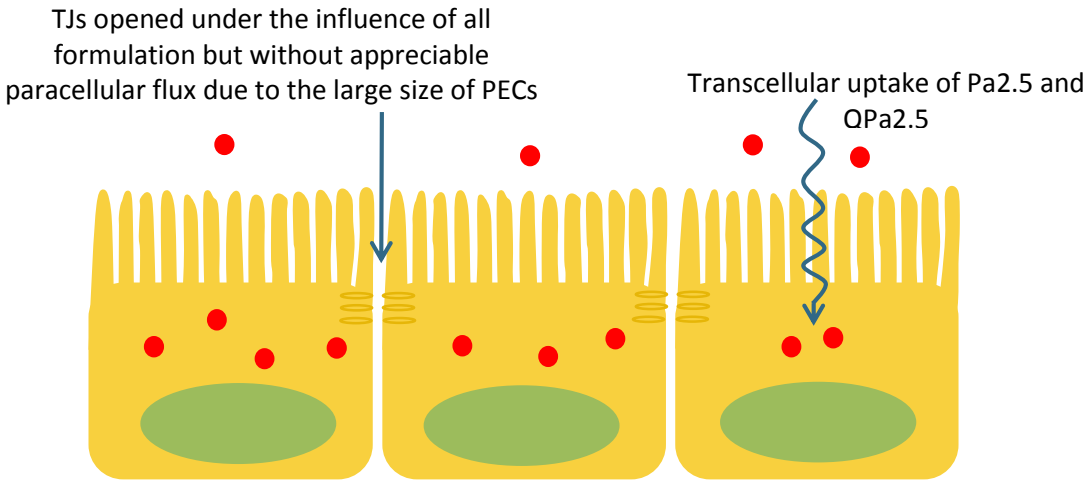

Figure 5.12 Mechanism of uptake of Pa2.5 and QPa2.5 based PECs and APECs

Thompson *et al*. reported that the internalisation of QPa2.5 PECs is not inhibited by blocking/down regulation of insulin receptor suggesting that their uptake is receptor independent [427]. It was also reported that QPa2.5 PECs demonstrated uptake despite blockage of endocytosis by nocodazole and cytochalasin D and in the absence of calcium in the media. These findings ruled out the possibility of uptake by endocytosis. This led them to consider the mechanism of uptake by an active process like organic cationic transporters [427]. Human organic cationic transporters represent a family of transporters likely to be involved in the disposition of small hydrophilic organic cations e.g., ranitidine and famotidine, however, their role in the transport of high molecular weight cations is yet to be elucidated [480]. The findings may well reflect the possibility of QPa2.5 PECs to be absorbed transcellularly via the interaction with the cationic transporters [481].

The higher uptake of IL QPa2.5-DS than IL QPa2.5-PAA points towards polyanion dependent uptake. In addition, the small size and high positive ZP of IL QPa2.5-DS (size 72±0.1; ZP 16±3) as compared to low positive ZP and larger size of IL QPa2.5-PAA (size 388± 29; ZP 7mV) might have facilitated their uptake (Figure 5.11). These findings support the role of surface charge and size-selective uptake of the QPa2.5-DS complexes.

Since the ZP of QPa2.5-DS is less than the QPa2.5 PECs (Figure 5.11), there appears to be a reduced possibility of their uptake by cationic transporters. There is evidence that complexes formed of polyanions such as DS and hyaluronic acid are internalised via receptor mediated endocytosis [445, 482]. The uptake of DS by glomerular endothelial cells has been reported to occur via receptors associated with the cell-surface heparin sulphate [483]. More recently, it has been shown that coating a DNA/PEI polyplex with a low molecular weight anionic hyaluronan (<10 kDa) facilitates the receptor-mediated uptake of polyplexes [445]. Another similar study has shown that coating a DNA/polycation polyplex with poly(c-glutamic acid) (c-PGA), a polyanion, increased the cellular uptake by a c-PGA-specific receptor-mediated energy-dependent process [484].

Yin Win *et al.* has shown size dependent uptake of polystyrene nanoparticles. They showed that 100 nm particles produced 2.3-fold greater uptake compared to that of 50nm particles, 1.3-fold to that of 500 nm particles, about 1.8 fold to 1000 nm particles [308]. Thus, nanoparticles of 100–200 nm size have shown to acquire the best properties for cellular uptake [308, 442]. Such small particles have been shown to be taken up by clathrin mediated endocytosis, as clathrin baskets due to their geometry can accommodate only a maximum size of 100 nm [485]. Based on all these reports, it may be considered herein that the QPa2.5-DS APECs initially bound to the receptors followed by events leading to receptor mediated endocytosis. However, further studies are needed to address these hypotheses. The size of nanoparticles may not be the only dominant factor influencing the uptake [486]

The surface chemistry of nanocarriers also plays an important role in the uptake and transport. There have been contrasting findings related to the effect of hydrophilicity or hydrophobicity of nanocarriers on their uptake [201, 442, 487, 488]. Clare *et al.* has shown that PAH modified with 5% hydrophobic cholesteryl pendants enhanced the oral absorption of a model drug, griseofulvin, when administered intra-gastrically in rats [416]. The enhancement of hydrophilicity of nanoparticles has been linked to a declined cellular interaction and transcellular transport of the nanocarriers [442, 487]. Nam and colleagues investigated the cellular uptake mechanism and the intracellular fate of the hydrophobically modified glycol chitosan (HGC) [201]. These nanoparticles showed higher internalisation efficiency, compared to the parent hydrophilic GC polymers. These findings are in line with the NIL hydrophobically modified PAH based complexes (NIL Pa2.5 based complexes) which showed higher internalisation than their hydrophilic

counter-part (QPa2.5 based complexes) (Table 5.2). However, introduction of insulin in Pa2.5 complexes might have reduced their hydrophobicity leading to reduced uptake. Sahoo *et al.* showed that lower intracellular uptake of nanoparticles with higher amount of residual Polyvinyl alcohol was due to higher hydrophilicity of the nanoparticle surface [488]. It is thought that the positively charged NIL Pa2.5 complexes electrostatically interacted with negatively charged proteoglycans of the cell membrane, followed by non-specific adsorptive endocytosis [67], whereas Pa2.5-DS internalised via receptor mediated endocytosis. However, further work should be performed to confirm these assumptions.

It may be considered herein that the hydrophobic long alkyl chain of the palmitoyl group reduced the uptake of IL Pa2.5 complexes by CaCo2 cells. The long alkyl chain strengthened the interaction of complexes with the cell membrane such that the complexes were either not internalised efficiently or remained essentially close to the cell membrane. This effect was observed on the microscopic observations where IL Pa2.5 PECs were found in close proximity to the cell membrane. However, this assumption may not be valid as the NIL Pa2.5 complexes were taken up much more efficiently despite being equally hydrophobic. Since the uptake of Pa2.5 based APECs was significantly less than the corresponding PECs. This leads to a possibility of the role of positive surface charge in more efficient uptake. These findings are not in agreement with Wang and group who recently showed that the cellular entry of four DNA ternary polyplexes was more efficient than the DNA binary polyplexes [131]. Several other research groups have reported findings contrary to our results. It has been shown that addition of polyanions (such as PGA, hyaluronic acid and anionic polyampholyte PEG derivatives) to a polycation system, forming polyanion/DNA/polycation ternary polyplexes, significantly improved the gene delivery efficiency in comparison to their original pDNA/polycation binary polyplexes [445, 446, 484].

IL Pa2.5 complexes exhibited lower positive ZP values and hence lower uptake than their corresponding NIL counterparts (Figure 5.11). Likewise, IL and NIL Pa2.5 PECs presented higher positive ZP and hence higher uptake than their corresponding APECs. These findings clearly indicate that high positive charges are associated with a higher uptake. However, since the difference in uptake profile between the IL and NIL Pa2.5 based complexes and between PECs and APECs is not proportional to the decrease in the positive ZP. These findings raise the possibility of uptake of these complexes followed by their efflux by efflux pump e.g., P-gp efflux pump [489]. P-gp, is a transmembrane protein

of approximately 170kDa molecular mass which forms an energy-dependent drug efflux pump [354]. They present as one of the key elements in limiting drug absorption via the oral route [354]. A major limitation of tumor cell lines such as CaCo2 cells is the possibility of overexpression of P-gp pumps which may lead to a higher efflux and subsequently lower permeability in the absorptive direction [489]. P-gp pumps have shown to secrete a variety of lipophilic and cationic compounds out of cells including some anticancer agents such as anthracyclines, taxanes, vinca alkaloids, and epipodophyllotoxins consequently reducing their intracellular concentration [354]. The finding point to a P-gp mediated efflux of IL Pa2.5 PECs and IL Pa2.5-PAA. Future studies should be performed to explore the type of endocytic pathways involved in uptake of nanocarriers.

5.7 CONCLUSION

The amphiphilic PECs and APECs have ability to facilitate the transport of insulin across CaCo2 cell monolayers. PECs demonstrated greater TEER reduction, FITC-Dextran and insulin transport and transcellular uptake by CaCo2 cells than their corresponding APECs. The differences in the cellular uptake profile, localisation within the cells and mechanism of uptake of Pa2.5 and QPa2.5 based PECs and APECs are ascribed to the differences in size, surface charge and the surface chemistry of complexes. NIL QPa2.5 based complexes demonstrated minor uptake due to their large sizes. IL QPa2.5 and QPa2.5-DS demonstrated higher uptake by a transcellular route than their NIL counterparts due to their small size. DS based APECs (i.e., QPa2.5-DS and Pa2.5-DS) demonstrated higher uptake by CaCo2 cells than their respective PAA based APECs. Further investigations should be done to elucidate the mechanism of transcellular uptake by using endocytosis specific inhibitors or by subjecting cells to low temperature to distinguish between energy dependent endocytosis and energy independent mechanism.

Chapter 6

CONCLUSION AND FUTURE WORK

6 CONCLUSION AND FUTURE WORK

6.1 CONCLUSION

Oral delivery of proteins has always been preferred because of its convenience and long term compliance. However, it is limited due to the enzymatic susceptibility and physical and chemical instability of protein in the GIT [3, 68]. The high molecular weight, hydrophilic nature and proteolytic degradation prevents protein absorption through the intestinal mucosa [439, 490].

A growing number of strategies have been designed to deliver insulin to the site of absorption and facilitate its permeation through the intestinal membrane to achieve pharmacological effects [57, 67, 96, 444, 491]. These strategies include mucoadhesive polymers [13, 492], permeation enhancers [2, 34, 493] and enzyme inhibitors [28]. However, mucoadhesives such as chitosan based systems are associated with reduced stability at physiological conditions and non-specific mucoadhesion [62], while, permeation enhancers and enzyme inhibitors are associated with toxicity related issues [26, 27, 36]. Such limitations have severely restricted their use.

In recent years, the polyelectrolyte complexes have been explored for their ability to complex protein drugs and protect them against chemical and enzymatic degradation. Polyelectrolyte complexes are formed by association of the oppositely charged polymers/proteins through intermolecular interactions [3, 68, 97]. The process of fabrication is devoid of potentially harmful organic solvents and heat. For this reason, polyelectrolyte complexes emerge as a very useful means for the delivery of protein drugs. The conventional binary polyelectrolyte systems (PECs) have mainly been formed by using polycations. It is well known that polycations are associated with charge related toxicity and non-specific interactions. Therefore, the development of polycation based binary systems present a substantial challenge in this field.

Recently, a simple, novel approach has been developed to fabricate ternary polyelectrolyte complexes (APECs), which involve addition of a biocompatible polyanion to the binary complexes, to improve the stability and reduce the toxicity and non-specific bio-interactions associated with the former systems. This thesis aims to fabricate novel ternary complexes based on amphiphilic polyallylamine, for oral

delivery of proteins to overcome the aforementioned problems of toxicity and non-specific bio-interactions.

Eight NIL APECs were fabricated in a nano-size range (78-435nm) between a polycation (PAH, Pa2.5, QPa2.5 and Da10) and a polyanion (DS and PAA) at a mass ratio of (2:1) in the presence of a cross-linker $ZnSO_4$ (4µM). The IL counterparts were fabricated by adding a model protein i.e., insulin in a polycation prior to adding the polyanion in the presence $ZnSO_4$ (4µM). It is thought that the cross-linker linked the polymeric chain by forming ionic bridges and thus provided stability to the complexes. In addition, the COO^- of insulin interacted electrostatically with the $NH_3^+$of the polycation and the NH_3^+ on the polycation and insulin interacted with COO^- of PAA and SO_4^{-2} of DS leading to the formation of nano-sized APECs.

The APECs formed by the hydrophobically modified PAH i.e., Pa2.5 and Da10 exhibited smaller hydrodynamic sizes (100-200 nm) and higher ZP (22-35mV) compared to the complexes formed by the QPa2.5 (size-72-388nm, ZP- 7-20mV). The hydrophobic portions of the hydrophobically modified PAH chains is thought to provide hydrophobic association which strengthened the interaction between polymeric chains leading to smaller self-assemblies [119]. However, due to the presence of permanently charged bulky quaternary ammonium moieties, a solvation layer is formed around the complexes, which resulted in increased hydrodynamic sizes of QPa2.5 based complexes [119].

As expected, the introduction of insulin and polyanion in complexes reduced the ZP of complexes confirming their association in the complexes. Insulin association efficiency was affected by the type of polycation and polyanion. The insulin association efficiency was found to be higher in PECs and APECs formed by the hydrophobically modified PAH based complexes (Pa2.5 and Da10, >75%) than the complexes formed by PAH and QPa2.5 based complexes (≤60%). Among hydrophobically grafted complexes, Da10 based APECs showed lower insulin complexation efficiency than Pa2.5 based complexes due to higher hydrophobic load which prevented their association with insulin. The bulky and rigid naphthalene rings in the dansyl moieties are also thought to have hindered insulin complexation by generating steric hindrance effects. On the other hand, the presence of polyanion in QPa2.5 APECs created a competitive interaction between two negative charges to complex with the polycation. The polyanion superseded in complexing with the QPa2.5 and thus impeded the

interaction of insulin with the QPa2.5. The competitive interaction took place particularly in QPa2.5 APECs because of the added steric hindrance mediated by the bulky quaternary ammonium moieties in the complexes.

DS based APECs displayed a higher insulin association efficiency than the PAA based APECs, which is ascribed to the higher molecular weight (60-10KDa) of DS than PAA. The dense and branched architecture of DS, with more charged units (SO_4^{-2}) than the less charged (COO^-) PAA, is thought to have interacted more strongly with the NH_3^+ of the insulin, and hence DS were able to trap more insulin molecules leading to higher association efficiency.

The PECs and APECs formed by the hydrophobically modified PAH (i.e., Da10 and Pa2.5) were found to be more stable at varying temperature (37ºC and 45ºC), ionic strength (68mM, 102mM and 145mM) and pH (7.4, 6.6 and 1.2) (except Da10-PAA) than the unmodified and QPa2.5 based complexes. The hydrophobic modification of PAH with C_{16} long alkyl chain grafted on Pa2.5 or naphthalene group grafted on Da10) reduced the chain flexibility and allowed the chains to remain linked even at high ionic strength, temperature and pH conditions. The hydrophobic grafts appeared to generate hydrophobic interactions with the insulin chain thus providing stability to the complexes [118]. The hydrophobic interactions are essentially absent in the case of PAH based complexes which caused destabilisation of these complexes.

The increase in temperature up to 45˚C facilitated the formation of PECs and APECs. It is known that the hydrophobic interactions increase in strength with the increase in the temperature [287]. These increasing hydrophobic associations are considered to have maintained the complex integrity. However, the QPa2.5 based PECs and APECs increased in size upon increase in the temperature due to the loss of hydrogen bonding between the hydrophilic QPa2.5 chains and water molecules upon increase in the thermal energy which subsequently led to the destabilisation of the complexes.

The size and ZP of QPa2.5 based PECs increased progressively upon increasing ionic strength. This is possibly due to the shielding of surface charge of the polymeric chains by counterions which diminished the attractive interactions between the polymer chains and insulin leading to large sizes. The low positive surface charge (≤20mV) of QPa2.5 PECs, as compared to the hydrophobically modified PECs and APECs (≥22mV), was observed to be neutralised more effectively by the counterions which caused the

destabilisation of QPa2.5 PECs. Alternatively, the QPa2.5 APECs reduced in size and showed restoration of ZP at higher ionic strengths conditions (102mM and 145mM) indicating the role of higher concentration of salt in providing stability to these complexes by preventing charge neutralisation. The small monovalent ions (Na^+ and Cl^-) are assumed to have generated ion pairing effect with the free negative charges on the polymeric chains in the complexes subsequently providing stability to the complexes.

On the other hand, the addition of salt in the hydrophobically modified PECs and APECs did not cause destabilisation of complexes. The counter ions are thought to have bound to the surface, which is clear from a reduction in the ZP. However, the concentration of counter ions was not enough to neutralise the surface charge of the complexes which could cause destabilisation of the complexes. In addition, the hydrophobic association is also thought to have prevented the complex destabilisation.

The PECs and APECs formed by the modified polymers (Pa2.5, Da10 and QPa2.5) were more stable at varying pH (except Da10 and Da10-PAA) than complexes formed by unmodified PAH owing to the presence of hydrophobic associations. The protonation of carboxylic groups of PAA in Da10-PAA and PAH-PAA at low pH due to a higher pKa (2.5) than pKa of DS (1.2) suppressed the electrostatic interaction between the polymeric chains and insulin leading to destabilisation of these complexes. This data showed that presence of PAA in APECs altered the stability of complexes at low pH. PAH-PAA lost stability as no contributory hydrophobic associations were present to prevent destabilisation of complexes. On the other hand, similar to low insulin complexation efficiency shown by Da10, destabilisation of Da10 PECs and Da10-PAA at low pH is also attributed to the bulky and rigid naphthalene ring in Da10 which conferred steric hindrance and prevented stronger interaction with insulin leading to destabilisation of complexes. However, unlike Da10 based complexes, Pa2.5 based PECs and APECs showed stability irrespective of polyanion used. This effect might mean that long hydrocarbon chain (C_{16}) in Pa2.5 promoted stronger hydrophobic interactions than the bulky and rigid naphthalene ring in Da10.

The cytotoxicity of polycations and APECs was determined by MTT assay on the CaCo2 cells and J774 cells. The cytotoxicity of modified polycations was significantly less than the unmodified counterparts (PAH>Da10=Pa2.5>QPa2.5). The hydrophobic and hydrophilic grafting reduced the number of primary amines on the polymer

backbone and hence the cationic charge thereby reducing the PAH associated cytotoxicity. The hydrophilic quaternary moieties on polymer backbone contributed to most significant reduction in toxicity.

Macrophages (J774 cells) were seen to be more sensitive to the effect of various polycations and APECs than the CaCo2 cells; however, the main pattern of the cytotoxicity remained the same on both the cell lines. The varying IC_{50} on the two cell lines is attributed to the difference in the morphological and physiological properties of the two cell lines. The enterocytes preferentially internalise nanocarriers in the range of 100- 200 nm by endocytosis [411] whereas, macrophages internalise particles ≤500nm in diameter by phagocytosis [307, 411].

The presence of polyanion in the APECs reduced the polycation associated toxicity on both the cell lines by reducing the positive charge density. PAA based complexes exhibited less cytotoxic profile probably due to low MW of PAA than high MW DS based APECs. The administration of PAH-PAA brought more significant improvement in IC_{50} due to its low positive ZP (29mV) compared to the high positive ZP (39mV) of PAH-DS. QPa2.5 APECs produced a comparable reduction in cytotoxicity irrespective of polyanions probably due to the similar ZP value (17-19 mV) of both APECs. Pa2.5-PAA and Da10-PAA were clearly less cytotoxic than their DS based counterparts and brought most significant improvement in the IC_{50} of Pa2.5 and Da10 i.e., 14 fold and 16 fold respectively on CaCo2 cells and 9.3 fold and 3.73 fold respectively on J774 cells. However, this improvement in cytotoxicity was not due to the low ZP of PAA based APECs, as there was no considerable difference in the ZP between PAA and DS based APECs. These findings show that not only surface charge but parameters such as MW and structure of polyanions may influence the cytotoxicity profile of complexes. Thus the higher cytotoxicity of DS based APECs is ascribed to the high molecular weight and the dense branched architecture of DS.

The *in vitro* haemolytic profile showed minor haemolytic activity (≤12%) by all polycations and APECs (0.075-5mgmL^{-1}) (except Da10). Da10 produced a maximum haemolytic activity of approximately 37% at 10mgmL^{-1}. The hydrophobicity of the polymers has previously been linked with the membrane-disruptive activity by Liu *et al* [417]. It is thought that the hydrocarbon chains formed mixed micelles with the phospholipid bilayers [416]. However, since Pa2.5 did not produce any haemolytic effect, the haemolytic activity of Da10 is ascribed to the higher hydrophobic load i.e.,

10% hydrophobic grafting than Pa2.5 (2.5%). The Da10-DS and Da10-PAA APECs (8mgmL^{-1}) clearly reduced the haemolytic activity associated with Da10. The improvement in the haemolytic activity is assumed to be due to the combined effects of reduction in the positive charge density as well as the structure and MW of polyanion which subsequently reduced the disruption of the erythrocyte membrane.

The reactive oxygen specie assay showed that the polycations and APECs stimulated production of low levels of ROS (≤26%) in the CaCo2 cells at the experimental conditions employed. The degree of ROS generation (PAH≥Pa2.5=Da10≥QPa2.5) followed the same trend as the cytotoxicity profile indicating a direct association of ROS production with the cytotoxicity. The APECs demonstrated significant reduction in the polycations induced ROS production which is again due to the reduction in cationic charge. However, reduction in the ROS generation was not sufficiently sensitive enough to differentiate between PAA and DS based APECs.

The cytokine generation assay (IL-6, IL-2 and TNF α) showed conflicting results between the *in vitro* and *in vivo* situations. The level of *in vivo* serum cytokine production was significantly less (≤ 27%) than the *in vitro* situation (90%). This disparity in the data can be explained by the difference in the *in vitro* and *in vivo* situations such as short half-life and localised *in vivo* production of cytokines leading to reduced systemic availability. In addition, there might have been *in vivo* stimulation of anti-inflammatory cytokines (IL-10) which caused down regulation of the pro-inflammatory cytokines leading to low *in vivo* level of cytokines [361].

Among APECs the reduction in *in vitro* and *in vivo* cytokine generation (<25%) was most significant on exposure to Pa2.5-PAA. Conversely, Da10 based APECs showed less ability to reduce cytokine generation. Da10-PAA marginally reduced the TNF-α generation whereas Da10-DS increased the *in vitro* secretion of IL-6 and TNF-α. These findings indicate the role of DS in raising immune response which correlates with their higher cytotoxicity, haemocompatibility and ROS generation than PAA based APECs. The biocompatibility of PAA based APECs is ascribed to the low MW PAA (1.8kDa) than DS (6-10kDa). For this reason, only PAA based APECs were selected for the *in vivo* cytokine generation study.

The induction of cytokines was greatest upon exposure to QPa2.5 and its APECs, in both the *in vitro* and *in vivo* situations. These findings do not correlate with cytotoxicity

and ROS assay where QPa2.5 based complexes were found to be the least cytotoxic and did not induce ROS. This reverse trend with cytotoxicity supports an inverse relationship of the cytokine generation with the cytotoxicity. The generation of cytokine on exposure to QPa2.5 is attributed to its hydrophilicity and large particle sizes (250-468nm). Literature shows that the small sized particles are more immunogenic than the larger particles, however, immunogenicity of larger particles has been shown to depend on their chemical composition [494]. Macrophages have been shown to adhere better to the hydrophillic surfaces which activate them to produce higher levels of cytokine [362].

The transport study showed a transient decline in the percentage TEER of CaCo2 cells on exposure to most of the formulations indicating reversible opening of the CaCo2 cell TJs. The reduction in the percentage TEER was more pronounced on exposure to the NIL QPa2.5 (58-78%) and NIL PAH complexes than their IL counterparts (20-30%). The application of polymeric nanocarriers to the CaCo2 cell monolayers has been reported to influence the junctional proteins, including actin, occludin, and claudin-1, leading to reversible opening of TJs [436]. The reduction in the positive ZP of NIL QPa2.5 PECs and APECs from (ZP- NIL 52-20mV) to (ZP IL-20-17mV) upon complexation with insulin is thought to have altered their interaction with the junctional proteins and prevented the TJ opening by IL QPa2.5 and IL PAH based complexes. The higher positive charge of PECs than APECs allowed better interaction with cell membrane proteins resulting in higher transport of FITC-Dextran and insulin across CaCo2 cells (except QPa2.5-DS). Among APECs, the FITC Dextran and insulin flux was higher in the cells incubated with DS based APECs than PAA based APECs.

The uptake study revealed internalisation of APECs by a transcellular route. Slight differences in particle size and surface charge have been shown to have significant implications in the cellular uptake of nanocarriers and mechanisms of uptake process [317]. The small sizes and high positive ZP of IL QPa2.5 PECs (size 117±2.4; ZP 20±3) and IL QPa2.5-DS (size 72±0.1; ZP 16±3) as compared to large sizes and low positive ZP of IL QPa2.5-PAA (size 388± 29; ZP 7mV) are thought to have promoted higher uptake of complexes i.e., 73% and 67% respectively. The low ZP of QPa2.5-PAA is assumed to have reduced the electrostatic interaction with the membrane proteins and prevented the uptake of the complexes. The large size particles require a stronger

driving force and additional energy for internalization thus prevent effective uptake of complexes [495].

Since DS based formulations have previously been shown to be taken up by receptor mediated uptake [482, 483], therefore it is thought that QPa2.5-DS are internalised via receptor mediated endocytosis, whereas QPa2.5-PAA appears to be taken up by non-specific adsorptive endocytosis.

By contrast, the IL Pa2.5 PECs and IL Pa2.5-PAA showed significantly lower uptake than the NIL counterparts. Among APECs, the uptake of IL Pa2.5-DS was significantly higher than IL Pa2.5-PAA. The uptake of Pa2.5 complexes was not observed to be affected by size or ZP but hydrophobic-hydrophilic balance. The presence of insulin in complexes altered the hydrophobic-hydrophilic balance resulting in reduced uptake of insulin loaded Pa2.5 complexes. There is a possibility that the uptake of these complexes was followed by their efflux by efflux pump e.g., P glycoprotein efflux pump [489]. P glycoprotein efflux pump have previously been shown to secrete a variety of lipophilic and cationic compounds out of cells [354]. However, further work should be performed to confirm these assumptions. It is thought that both IL and NIL Pa2.5 PECs and Pa2.5-PAA electrostatically interacted with the negatively charged proteoglycans of the cell membrane, followed by non-specific adsorptive endocytosis [67], whereas Pa2.5-DS internalised via receptor mediated endocytosis.

Altogether the data on the APECs indicate that DS based APECs showed a higher insulin association efficiency and stability; however were found to be more cytotoxic and immunogenic than their PAA based counterparts. The DS based complexes (IL PAH-DS, QPa2.5-DS, and Da10-DS) produced a more significant reduction in the percentage TEER, more efficient uptake, higher insulin permeation and FITC-Dextran flux than their PAA based counterparts, indicating the influence of polyanion on cellular uptake. The findings show that the biocompatibility, internalization and transport of the complexes are governed by the physicochemical properties such as surface chemistry, size, surface charge and the type of the polyanion complexed. The presence of polyanion may be able to reduce the toxicity of the delivery system by reducing the overall positive. However, the reduced positive charge and hence interaction with the cell membrane may have implication in cellular uptake and transport of complexes.

6.2 FUTURE WORKS

Development of drug delivery systems by polyelectrolyte complexation offer opportunities to tailor the properties of complexes to achieve desired systems. The novel ternary complexes (APECs) fabricated in this project were effective in improving the biocompatibility of the complexes, however, reduced the insulin complexation efficiency and eventual uptake and transport of the complexes. In regards to this limitation, optimisation of formulation to prepare more sophisticated delivery system which can improve the uptake and transport is crucial. Modification of the delivery system by using polyethylene glycol grafted PAH may increase the protein complexation efficiency as well as biocompatibility of complexes.

In order to fully functionalise the potential of the ternary complexes, the precise behaviour and stability of ternary complexes should be studied in biological mediums (i.e., simulated gastric and intestinal fluids) and the release profile should also be elucidated. It is desirable to carry out a long term stability testing of the formulations to determine their potential as pharmaceutical excipients.

Monitoring particle internalization by confocal microscopy can provide a more complete understanding of intracellular localization of complexes [440]. Besides, it will be useful to conduct study at different time points to determine the time taken by the formulation to be taken up. It will also help to study the transport and release of bioactive protein from the nanocarriers and determine where the polymer and protein reside inside the cell.

In addition to the microscopic study, cellular internalisation should also be studied to determine the mechanism of cellular uptake. Endocytosis specific biochemical inhibitors such as cytochlasin D (endocytosis inhibitor), chlorpromazine (inhibitor of clathrin-mediated endocytosis), dynasore (inhibitor of dynamin-dependent endocytosis), genistein (inhibitor of caveolin-mediated endocytosis), [440, 441, 496] should be used to elucidate specific endocytosis mechanisms. Once detailed *in vitro* study has been conducted, the oral *in vivo* studies should be done to elucidate the various APEC formulations as effective pharmaceutical therapies.

REFERENCES

1. Marschütz, M.K., P. Caliceti, and A. Bernkop-Schnürch, *Design and in vivo evaluation of an oral delivery system for insulin.* Pharmaceutical research, 2000. **17**(12): p. 1468-1474.
2. Gupta, V., et al., *A Permeation Enhancer for Increasing Transport of Therapeutic Macromolecules across the Intestine.* Journal of Controlled Release, 2013. **172**(2): p. 541-549
3. Cegnar, M. and J. Kerc, *'Self-Assembled Polyelectrolyte Nanocomplexes of Alginate, Chitosan and Ovalbumin.* Acta Chim. Slov, 2010. **57**(2): p. 431-441.
4. Jintapattanakit, A., et al., *Peroral delivery of insulin using chitosan derivatives: A comparative study of polyelectrolyte nanocomplexes and nanoparticles.* International journal of pharmaceutics, 2007. **342**(1-2): p. 240-249.
5. Goldberg, M. and I. Gomez-Orellana, *Challenges for the oral delivery of macromolecules.* Nature reviews Drug discovery, 2003. **2**(4): p. 289-295.
6. Bowman, K. and K. Leong, *Chitosan nanoparticles for oral drug and gene delivery.* International Journal of Nanomedicine, 2006. **1**(2): p. 117.
7. Chen, M.-C., et al., *A review of the prospects for polymeric nanoparticle platforms in oral insulin delivery.* Biomaterials, 2011. **32**(36): p. 9826-9838.
8. Del Curto, M.D., et al., *Oral delivery system for two-pulse colonic release of protein drugs and protease inhibitor/absorption enhancer compounds.* Journal of pharmaceutical sciences, 2011. **100**(8): p. 3251-3259.
9. Aoki, Y., et al., *Region-dependent role of the mucous/glycocalyx layers in insulin permeation across rat small intestinal membrane.* Pharmaceutical research, 2005. **22**(11): p. 1854-1862.
10. Khanvilkar, K., M.D. Donovan, and D.R. Flanagan, *Drug transfer through mucus.* Advanced drug delivery reviews, 2001. **48**(2): p. 173-193.
11. Aoki, Y., M. Morishita, and K. Takayama, *Role of the mucous/glycocalyx layers in insulin permeation across the rat ileal membrane.* International journal of pharmaceutics, 2005. **297**(1): p. 98-109.
12. Morishita, M., et al., *A novel approach using functional peptides for efficient intestinal absorption of insulin.* Journal of controlled release, 2007. **118**(2): p. 177-184.
13. Ma, Z., T.M. Lim, and L.-Y. Lim, *Pharmacological activity of peroral chitosan–insulin nanoparticles in diabetic rats.* International journal of pharmaceutics, 2005. **293**(1): p. 271-280.
14. Werle, M. and H. Takeuchi, *Strategies to Overcome the Enzymatic Barrier*, in *Oral Delivery of Macromolecular Drugs*. 2009, Springer. p. 65-83.
15. Plapied, L., et al., *Fate of polymeric nanocarriers for oral drug delivery.* Current opinion in colloid & interface science, 2011. **16**(3): p. 228-237.
16. George, M. and T. Abraham, *Polyionic hydrocolloids for the intestinal delivery of protein drugs: alginate and chitosan--a review.* Journal of Controlled Release, 2006. **114**(1): p. 1-14.
17. Soppimath, K.S., et al., *Biodegradable polymeric nanoparticles as drug delivery devices.* Journal of Controlled Release, 2001. **70**(1): p. 1-20.
18. Carino, G.P. and E. Mathiowitz, *Oral insulin delivery.* Advanced drug delivery reviews, 1999. **35**(2): p. 249-257.
19. Lee, H.J., *Protein drug oral delivery: the recent progress.* Archives of pharmacal research, 2002. **25**(5): p. 572-584.
20. Pinto Reis, C., et al., *Nanoencapsulation I. Methods for preparation of drug-loaded polymeric nanoparticles.* Nanomedicine: Nanotechnology, Biology and Medicine, 2006. **2**(1): p. 8-21.
21. Van Der Walle, C., *Peptide and protein delivery*: Academic Press, 2011.
22. Mahato, R.I., et al., *Emerging trends in oral delivery of peptide and protein drugs.* Critical reviews in therapeutic drug carrier systems, 2003. **20**(2-3): p. 153-214.
23. Cohen, M.H., et al., *FDA drug approval summary: gefitinib (ZD1839)(Iressa®) tablets.* The oncologist, 2003. **8**(4): p. 303-306.

24. Cohen, M.H., et al., *Approval summary for imatinib mesylate capsules in the treatment of chronic myelogenous leukemia.* Clinical Cancer Research, 2002. **8**(5): p. 935-942.
25. Morishita, M., et al., *Novel oral insulin delivery systems based on complexation polymer hydrogels: Single and multiple administration studies in type 1 and 2 diabetic rats.* Journal of Controlled Release, 2006. **110**(3): p. 587-594.
26. Shah, R.B., A. Palamakula, and M.A. Khan, *Cytotoxicity evaluation of enzyme inhibitors and absorption enhancers in Caco-2 cells for oral delivery of salmon calcitonin.* Journal of pharmaceutical sciences, 2004. **93**(4): p. 1070-1082.
27. Werle, M. and A. Bernkop-Schnurch, *5 Inhibition of Enzymes and Secretory Transport.* Enhancement in Drug Delivery: 2010. p. 85,.
28. Merzlikine, A., et al., *Effect of chitosan glutamate, carbomer 974P, and EDTA on the in vitro Caco-2 permeability and oral pharmacokinetic profile of acyclovir in rats.* Drug development and industrial pharmacy, 2009. **35**(9): p. 1082-1091.
29. Lueßen, H.L., et al., *Mucoadhesive polymers in peroral peptide drug delivery. II. Carbomer and polycarbophil are potent inhibitors of the intestinal proteolytic enzyme trypsin.* Pharmaceutical research, 1995. **12**(9): p. 1293-1298.
30. Yamamoto, A., et al., *Effects of various protease inhibitors on the intestinal absorption and degradation of insulin in rats.* Pharmaceutical research, 1994. **11**(10): p. 1496-1500.
31. Su, F.-Y., et al., *Protease inhibition and absorption enhancement by functional nanoparticles for effective oral insulin delivery.* Biomaterials, 2012. **33**(9): p. 2801-2811.
32. Brayden, D.J. and R.J. Mrsny, *Oral peptide delivery: Prioritizing the leading technologies.* Therapeutic Delivery, 2011. **2**(12): p. 1567-1573.
33. Lane, M.E., C.M. O'Driscoll, and O.I. Corrigan, *Quantitative estimation of the effects of bile salt surfactant systems on insulin stability and permeability in the rat intestine using a mass balance model.* Journal of pharmacy and pharmacology, 2005. **57**(2): p. 169-175.
34. Chun, I.K., et al., *Effects of bile salts on gastrointestinal absorption of pravastatin.* Journal of pharmaceutical sciences, 2012. **101**(7): p. 2281-2287.
35. Junginger, H.E. and J. Verhoef, *Macromolecules as safe penetration enhancers for hydrophilic drugs—a fiction?* Pharmaceutical Science & Technology Today, 1998. **1**(9): p. 370-376.
36. Sohi, H., et al., *Critical evaluation of permeation enhancers for oral mucosal drug delivery.* Drug development and industrial pharmacy, 2010. **36**(3): p. 254-282.
37. Tillman, L.G., R.S. Geary, and G.E. Hardee, *Oral delivery of antisense oligonucleotides in man.* Journal of pharmaceutical sciences, 2008. **97**(1): p. 225-236.
38. Wang, X., S. Maher, and D.J. Brayden, *Restoration of rat colonic epithelium after in situ intestinal instillation of the absorption promoter, sodium caprate.* Therapeutic Delivery, 2010. **1**(1): p. 75-82.
39. Fan, D., et al., *Enhancement by sodium caprate and sodium deoxycholate of the gastrointestinal absorption of berberine chloride in rats.* Drug Development and Industrial Pharmacy, 2012(00): p. 1-10.
40. Jones, S.W., et al., *Characterisation of cell-penetrating peptide-mediated peptide delivery.* British journal of pharmacology, 2005. **145**(8): p. 1093-1102.
41. Green, M. and P.M. Loewenstein, *Autonomous functional domains of chemically synthesized human immunodeficiency virus tat trans-activator protein..* Cell, 1988. **55**(6): p. 1179-1188.
42. Derossi, D., et al., *Cell internalization of the third helix of the Antennapedia homeodomain is receptor-independent.* Journal of Biological Chemistry, 1996. **271**(30): p. 18188-18193.
43. Pooga, M., et al., *Cellular translocation of proteins by transportan.* The FASEB Journal, 2001. **15**(8): p. 1451-1453.
44. Matsui, H., et al., *Protein therapy: in vivo protein transduction by polyarginine (11R) PTD and subcellular targeting delivery.* Current Protein and Peptide Science, 2003. **4**(2): p. 151-157.
45. Fawell, S., et al., *Tat-mediated delivery of heterologous proteins into cells.* Proceedings of the National Academy of Sciences, 1994. **91**(2): p. 664-668.

46. Wadia, J.S., R.V. Stan, and S.F. Dowdy, *Transducible TAT-HA fusogenic peptide enhances escape of TAT-fusion proteins after lipid raft macropinocytosis.* Nature medicine, 2004. **10**(3): p. 310-315.
47. Fittipaldi, A., et al., *Cell membrane lipid rafts mediate caveolar endocytosis of HIV-1 Tat fusion proteins.* Journal of Biological Chemistry, 2003. **278**(36): p. 34141-34149.
48. Richard, J.P., et al., *Cellular uptake of unconjugated TAT peptide involves clathrin-dependent endocytosis and heparan sulfate receptors.* Journal of Biological Chemistry, 2005. **280**(15): p. 15300-15306.
49. Pan, Y., et al., *Bioadhesive polysaccharide in protein delivery system: chitosan nanoparticles improve the intestinal absorption of insulin in vivo.* International journal of pharmaceutics, 2002. **249**(1): p. 139-147.
50. Tahtat, D., et al., *Oral delivery of insulin from alginate/chitosan crosslinked by glutaraldehyde.* International Journal of Biological Macromolecules, 2013. **58**(0): p. 160-168.
51. Zhao, S.-h., et al., *N-(2-hydroxyl) propyl-3-trimethyl ammonium chitosan chloride nanoparticle as a novel delivery system for Parathyroid Hormone-Related Protein 1–34.* International journal of pharmaceutics, 2010. **393**(1): p. 269-273.
52. Gan, Q. and T. Wang, *Chitosan nanoparticle as protein delivery carrier—systematic examination of fabrication conditions for efficient loading and release.* Colloids and Surfaces B: Biointerfaces, 2007. **59**(1): p. 24-34.
53. Sadeghi, A.M.-M., et al., *Preparation, characterization and antibacterial activities of chitosan, -trimethyl chitosan (TMC) and diethylmethyl chitosan (DEMC) nanoparticles loaded with insulin using both the ionotropic gelation and polyelectrolyte complexation methods.* International Journal of Pharmaceutics, 2008. **355**(1): p. 299-306.
54. Sun, W., et al., *Self-assembled polyelectrolyte nanocomplexes between chitosan derivatives and enoxaparin.* European journal of pharmaceutics and biopharmaceutics, 2008. **69**(2): p. 417-425.
55. Tiyaboonchai, W. and N. Limpeanchob, *Formulation and characterization of amphotericin B–chitosan–dextran sulfate nanoparticles.* International journal of pharmaceutics, 2007. **329**(1): p. 142-149.
56. Tiyaboonchai, W., *Chitosan nanoparticles: a promising system for drug delivery.* Naresuan University Journal, 2003. **11**(3): p. 51-66.
57. Thanou, M., J. Verhoef, and H. Junginger, *Oral drug absorption enhancement by chitosan and its derivatives.* Advanced drug delivery reviews, 2001. **52**(2): p. 117-126.
58. Sandri, G., et al., *Insulin-loaded nanoparticles based on N-trimethyl chitosan: in vitro (Caco-2 model) and ex vivo (excised rat jejunum, duodenum, and ileum) evaluation of penetration enhancement properties.* Aaps Pharmscitech, 2010. **11**(1): p. 362-371.
59. Xu, Y., et al., *Preparation and modification of (2-hydroxyl) propyl-3-trimethyl ammonium chitosan chloride nanoparticle as a protein carrier.* Biomaterials, 2003. **24**(27): p. 5015-5022.
60. Bravo-Osuna, I., et al., *Mucoadhesion mechanism of chitosan and thiolated chitosan-poly (isobutyl cyanoacrylate) core-shell nanoparticles.* Biomaterials, 2007. **28**(13): p. 2233-2243.
61. Krauland, A.H., D. Guggi, and A. Bernkop-Schnürch, *Oral insulin delivery: the potential of thiolated chitosan-insulin tablets on non-diabetic rats.* Journal of Controlled Release, 2004. **95**(3): p. 547-555.
62. Iqbal, J., et al., *Thiolated chitosan: development and in vivo evaluation of an oral delivery system for leuprolide.* European Journal of Pharmaceutics and Biopharmaceutics, 2012. **80**(1): p. 95-102.
63. Leitner, V.M., G.F. Walker, and A. Bernkop-Schnürch, *Thiolated polymers: evidence for the formation of disulphide bonds with mucus glycoproteins.* European Journal of Pharmaceutics and Biopharmaceutics, 2003. **56**(2): p. 207-214.
64. Föger, F., T. Schmitz, and A. Bernkop-Schnürch, *In vivo evaluation of an oral delivery system for P-gp substrates based on thiolated chitosan.* Biomaterials, 2006. **27**(23): p. 4250-4255.

65. Werle, M., *Natural and synthetic polymers as inhibitors of drug efflux pumps.* Pharmaceutical research, 2008. **25**(3): p. 500-511.
66. Park, J., et al., *Polymeric nanomedicine for cancer therapy.* Progress in Polymer Science, 2008. **33**(1): p. 113-137.
67. Mao, S., et al., *Uptake and transport of PEG-graft-trimethyl-chitosan copolymer–insulin nanocomplexes by epithelial cells.* Pharmaceutical research, 2005. **22**(12): p. 2058-2068.
68. Jintapattanakit, A., et al., *Peroral delivery of insulin using chitosan derivatives: a comparative study of polyelectrolyte nanocomplexes and nanoparticles.* International journal of pharmaceutics, 2007. **342**(1): p. 240-249.
69. Hans, M. and A. Lowman, *Biodegradable nanoparticles for drug delivery and targeting.* Current Opinion in Solid State and Materials Science, 2002. **6**(4): p. 319-327.
70. Moghimi, S., et al., *Polymeric nanoparticles as drug carriers and controlled release implant devices*, 2006: p. 29-42.
71. Tiyaboonchai, W., *Chitosan nanoparticles: a promising system for drug delivery.* Naresuan University Journal, 2003. **11**(3).
72. Sarmento, B., et al., *Development and characterization of new insulin containing polysaccharide nanoparticles.* Colloids and Surfaces B: Biointerfaces, 2006. **53**(2): p. 193-202.
73. Tiyaboonchai, W., J. Woiszwillo, and C. Middaugh, *Formulation and characterization of DNA-polyethylenimine-dextran sulfate nanoparticles.* European Journal of Pharmaceutical Sciences, 2003. **19**(4): p. 191-202.
74. Mao, H.-Q., et al., *Chitosan-DNA nanoparticles as gene carriers: synthesis, characterization and transfection efficiency.* Journal of Controlled Release, 2001. **70**(3): p. 399-421.
75. Torres-Lugo, M. and N.A. Peppas, *Preparation and characterization of P (MAA-g-EG) nanospheres for protein delivery applications.* Journal of Nanoparticle Research, 2002. **4**(1-2): p. 73-81.
76. Zhao, M., et al., *Redox-responsive nanocapsules for intracellular protein delivery.* Biomaterials, 2011. **32**(22): p. 5223-5230.
77. Yan, M., et al., *A novel intracellular protein delivery platform based on single-protein nanocapsules.* Nature Nanotechnology, 2009. **5**(1): p. 48-53.
78. O'Reilly, R.K., C.J. Hawker, and K.L. Wooley, *Cross-linked block copolymer micelles: functional nanostructures of great potential and versatility.* Chem. Soc. Rev., 2006. **35**(11): p. 1068-1083.
79. Mao, S., et al., *Self assembled polyelectrolyte nanocomplexes between chitosan derivatives and insulin.* Journal of pharmaceutical sciences, 2006. **95**(5): p. 1035-1048.
80. Kumari, A., S.K. Yadav, and S.C. Yadav, *Biodegradable polymeric nanoparticles based drug delivery systems.* Colloids and Surfaces B: Biointerfaces, 2010. **75**(1): p. 1-18.
81. Sosnik, A., A. Carcaboso, and D.A. Chiappetta, *Polymeric Nanocarriers: New endeavors for the optimization of the technological aspects of drugs.* Recent Pat Biomed Eng, 2008. **1**(1): p. 43-59.
82. Liu, Y., et al., *Biocompatibility, cellular uptake and biodistribution of the polymeric amphiphilic nanoparticles as oral drug carriers.* Colloids and Surfaces B-Biointerfaces, 2013. **103**: p. 345-353.
83. Müller, C., et al., *Preparation and characterization of spray-dried polymeric nanocapsules.* Drug development and industrial pharmacy, 2000. **26**(3): p. 343-347.
84. Pinto Reis, C., et al., *Nanoencapsulation II. Biomedical applications and current status of peptide and protein nanoparticulate delivery systems.* Nanomedicine: Nanotechnology, Biology and Medicine, 2006. **2**(2): p. 53-65.
85. Vauthier, C. and K. Bouchemal, *Methods for the preparation and manufacture of polymeric nanoparticles.* Pharmaceutical research, 2009. **26**(5): p. 1025-1058.
86. Li, S., et al., *In vitro release of protein from poly (butylcyanoacrylate) nanocapsules with an aqueous core.* Colloid and Polymer Science, 2005. **283**(5): p. 480-485.

87. Rao, J.P. and K.E. Geckeler, *Polymer nanoparticles: preparation techniques and size-control parameters.* Progress in Polymer Science, 2011. **36**(7): p. 887-913.
88. Mohanraj, V. and Y. Chen, *Nanoparticles-a review.* Tropical Journal of Pharmaceutical Research, 2007. **5**(1): p. 561-573.
89. Chalasani, K.B., et al., *A novel vitamin B12-nanosphere conjugate carrier system for peroral delivery of insulin.* Journal of Controlled Release, 2007. **117**(3): p. 421-429.
90. Minimol, P.F., W. Paul, and C.P. Sharma, *PEGylated starch acetate nanoparticles and its potential use for oral insulin delivery.* Carbohydrate polymers, 2013. **95**(1): p. 1-8.
91. Li, Y.-P., et al., *PEGylated PLGA nanoparticles as protein carriers: synthesis, preparation and biodistribution in rats.* Journal of controlled release, 2001. **71**(2): p. 203-211.
92. Zhu, S., et al., *Synthesis and characterization of PEG modifiedtrimethylaminoethylmethacrylate chitosan nanoparticles.* European polymer journal, 2007. **43**(6): p. 2244-2253.
93. Gref, R., et al., *The controlled intravenous delivery of drugs using PEG-coated sterically stabilized nanospheres.* Advanced drug delivery reviews, 2012. **16**(2): p. 215-233.
94. Damgé, C., C.P. Reis, and P. Maincent, *Nanoparticle strategies for the oral delivery of insulin.* 2008: p. 45-68.
95. Shu, S., et al., *Gradient cross-linked biodegradable polyelectrolyte nanocapsules for intracellular protein drug delivery.* Biomaterials, 2010. **31**(23): p. 6039-6049.
96. Sarmento, B., et al., *Oral bioavailability of insulin contained in polysaccharide nanoparticles.* Biomacromolecules, 2007. **8**(10): p. 3054-3060.
97. Yin, L., et al., *Drug permeability and mucoadhesion properties of thiolated trimethyl chitosan nanoparticles in oral insulin delivery.* Biomaterials, 2009. **30**(29): p. 5691-5700.
98. Rawat, M., et al., *Nanocarriers: promising vehicle for bioactive drugs.* Biological and Pharmaceutical Bulletin, 2006. **29**(9): p. 1790-1798.
99. Jeong, B., et al., *New biodegradable polymers for injectable drug delivery systems.* Journal of Controlled Release, 1999. **62**(1): p. 109-114.
100. Torchilin, V., *Micellar nanocarriers: pharmaceutical perspectives.* Pharmaceutical research, 2007. **24**(1): p. 1-16.
101. Rösler, A., G.W. Vandermeulen, and H.-A. Klok, *Advanced drug delivery devices via self-assembly of amphiphilic block copolymers.* Advanced Drug Delivery Reviews, 2012. **64**(0): p. 270-279.
102. Kataoka, K., A. Harada, and Y. Nagasaki, *Block copolymer micelles for drug delivery: design, characterization and biological significance.* Advanced drug delivery reviews, 2012. **47**(1): p. 13-131.
103. Lavasanifar, A., J. Samuel, and G. Kwon, *Poly (ethylene oxide)-block-poly (-amino acid) micelles for drug delivery.* Advanced drug delivery reviews, 2002. **54**(2): p. 169-190.
104. Cheng, W., et al., *In vitro and in vivo characterisation of a novel peptide delivery system: Amphiphilic polyelectrolyte-salmon calcitonin nanocomplexes.* Journal of Controlled Release, 2010. **147**(2): p. 289-297.
105. Kaparissides, C., et al., *Recent advances in novel drug delivery systems.* Journal of Nanotechnology, Online, 2006. **2**: p. 1-11.
106. Aliabadi, H.M., et al., *Micelles of methoxy poly (ethylene oxide)- poly (ε-caprolactone) as vehicles for the solubilization and controlled delivery of cyclosporine. A.* Journal of Controlled Release, 2005. **104**(2): p. 301-311.
107. Li, N., et al., *The use of polyion complex micelles to enhance the oral delivery of salmon calcitonin and transport mechanism across the intestinal epithelial barrier.* Biomaterials, 2012. **33**(34): p. 8881-8892.
108. Lee, Y., et al., *Charge-Conversional Polyionic Complex Micelles—Efficient Nanocarriers for Protein Delivery into Cytoplasm.* Angewandte Chemie, 2009. **121**(29): p. 5413-5416.

109. Mishra, B., B.B. Patel, and S. Tiwari, *Colloidal nanocarriers: a review on formulation technology, types and applications toward targeted drug delivery.* Nanomedicine: Nanotechnology, Biology and Medicine, 2010. **6**(1): p. 9-24.
110. Ma, R.J., et al., *Phenylboronic Acid-Based Complex Micelles with Enhanced Glucose-Responsiveness at Physiological pH by Complexation with Glycopolymer.* Biomacromolecules, 2012. **13**(10): p. 3409-3417.
111. Zhao, L., et al., *Glucose-sensitive polypeptide micelles for self-regulated insulin release at physiological pH.* Journal of Materials Chemistry, 2012. **22**(24): p. 12319-12328.
112. Sarmento, B., et al., *Characterization of insulin-loaded alginate nanoparticles produced by ionotropic pre-gelation through DSC and FTIR studies.* Carbohydrate polymers, 2006. **66**(1): p. 1-7.
113. Zheng, Y., et al., *Nanoparticles based on the complex of chitosan and polyaspartic acid sodium salt: Preparation, characterization and the use for 5-fluorouracil delivery.* European journal of pharmaceutics and biopharmaceutics, 2007. **67**(3): p. 621-631.
114. Schatz, C., et al., *Formation and properties of positively charged colloids based on polyelectrolyte complexes of biopolymers.* Langmuir, 2004. **20**(18): p. 7766-7778.
115. Hartig, S.M., et al., *Multifunctional nanoparticulate polyelectrolyte complexes.* Pharmaceutical research, 2007. **24**(12): p. 2353-2369.
116. Tonge, S. and B. Tighe, *Responsive hydrophobically associating polymers: a review of structure and properties.* Advanced drug delivery reviews, 2001. **53**(1): p. 109-122.
117. Kitano, T., et al., *Conformation of Polyelectrolyte in Aqueous Solution.* Macromolecules, 1980. **13**(1): p. 57-63.
118. Cheng, W.P., et al., *In vitro and in vivo characterisation of a novel peptide delivery system: Amphiphilic polyelectrolyte–salmon calcitonin nanocomplexes.* Journal of Controlled Release, 2010. **147**(2): p. 289-297.
119. Thompson, C.J., et al., *The effect of polymer architecture on the nano self-assemblies based on novel comb-shaped amphiphilic poly (allylamine).* Colloid & Polymer Science, 2008. **286**(13): p. 1511-1526.
120. Thompson, C., et al., *The effect of polymer architecture on the nano self-assemblies based on novel comb-shaped amphiphilic poly (allylamine).* Colloid & Polymer Science, 2008. **286**(13): p. 1511-1526.
121. Thompson, C., et al., *The complexation between novel comb shaped amphiphilic polyallylamine and insulin—Towards oral insulin delivery.* International journal of pharmaceutics, 2009. **376**(1): p. 46-55.
122. Tiyaboonchai, W., et al., *Insulin containing polyethylenimine–dextran sulfate nanoparticles.* International journal of pharmaceutics, 2003. **255**(1): p. 139-151.
123. Shu, X. and K. Zhu, *A novel approach to prepare tripolyphosphate/chitosan complex beads for controlled release drug delivery.* International Journal of Pharmaceutics, 2000. **201**(1): p. 51-58.
124. Jintapattanakit, A., T. Kissel, and V.B. Junyaprasert, *Effect of Tripolyphosphate on Physical and Enzymatic Stabilities of Insulin Loaded Nanoparticles of N-Trimethyl Chitosan.* Journal of Pharmaceutical Sciences, 2008. **35**(1-4): 1-7.
125. Berger, J., et al., *Structure and interactions in chitosan hydrogels formed by complexation or aggregation for biomedical applications.* European journal of pharmaceutics and biopharmaceutics, 2004. **57**(1): p. 35-52.
126. Sarmento, B., et al., *Alginate/chitosan nanoparticles are effective for oral insulin delivery.* Pharmaceutical Research, 2007. **24**(12): p. 2198-2206.
127. Guo, S., et al., *Ternary complexes of amphiphilic polycaprolactone-graft-poly (N, N-dimethylaminoethyl methacrylate), DNA and polyglutamic acid-graft-poly (ethylene glycol) for gene delivery.* Biomaterials, 2011. **32**(18): p. 4283-4292.

128. Sharma, S., et al., *Enhanced immune response against pertussis toxoid by IgA-loaded chitosan–dextran sulfate nanoparticles.* Journal of pharmaceutical sciences, 2012. **101**(1): p. 233-244.
129. Thompson, C.J., L. Tetley, and W. Cheng, *The influence of polymer architecture on the protective effect of novel comb shaped amphiphilic poly(allylamine) against in vitro enzymatic degradation of insulin—Towards oral insulin delivery.* International journal of pharmaceutics, 2010. **383**(1): p. 216-227.
130. Wang, B., et al., *Effects of hydrophobic and hydrophilic modifications on gene delivery of amphiphilic chitosan based nanocarriers.* Biomaterials, 2011. **32**(20): p. 4630-4638.
131. Wang, C., et al., *Influence of polyanion on physicochemical properties and biological activities of polyanion/DNA/polycation ternary polyplex.* Acta Biomaterialia, 2012. **8**(8): p 3014-3026.
132. Sotiropoulou, M., G. Bokias, and G. Staikos, *Water-soluble complexes through Coulombic interactions between bovine serum albumin and anionic polyelectrolytes grafted with hydrophilic nonionic side chains.* Biomacromolecules, 2005. **6**(4): p. 1835-1838.
133. Hamman, J.H., *Chitosan based polyelectrolyte complexes as potential carrier materials in drug delivery systems.* Marine drugs, 2010. **8**(4): p. 1305-1322.
134. Dautzenberg, H. and W. Jaeger, *Effect of charge density on the formation and salt stability of polyelectrolyte complexes.* Macromolecular Chemistry and Physics, 2002. **203**(14): p. 2095-2102.
135. Shovsky, A., et al., *Formation and stability of water-soluble, molecular polyelectrolyte complexes: effects of charge density, mixing ratio, and polyelectrolyte concentration.* Langmuir, 2009. **25**(11): p. 6113-6121.
136. Burova, T.V., et al., *Ternary Interpolyelectrolyte Complexes for Oral Delivery of Insulin: Insulin-Poly (methylaminophosphazene)-Dextran Sulfate.* Langmuir, 2013. **29**(7): p 2273-2281.
137. Delair, T., *Colloidal polyelectrolyte complexes of chitosan and dextran sulfate towards versatile nanocarriers of bioactive molecules.* European journal of pharmaceutics and biopharmaceutics, 2011. **78**(1): p. 10-18.
138. Kovacevic, D., et al., *Kinetics of formation and dissolution of weak polyelectrolyte multilayers: role of salt and free polyions.* Langmuir, 2002. **18**(14): p. 5607-5612.
139. Müller, M., et al., *Polyelectrolyte complex nanoparticles of poly (ethyleneimine) and poly (acrylic acid): preparation and applications.* Polymers, 2011. **3**(2): p. 762-778.
140. Salmaso, S. and P. Caliceti, *Self assembling nanocomposites for protein delivery: Supramolecular interactions of soluble polymers with protein drugs.* International Journal of Pharmaceutics, 2013. **440**(1): p. 111-123.
141. Jung, T., et al., *Biodegradable nanoparticles for oral delivery of peptides: is there a role for polymers to affect mucosal uptake?* European Journal of Pharmaceutics and Biopharmaceutics, 2000. **50**(1): p. 147-160.
142. Bayat, A., et al., *Preparation and characterization of insulin nanoparticles using chitosan and its quaternized derivatives.* Nanomedicine: Nanotechnology, Biology and Medicine, 2008. **4**(2): p. 115-120.
143. Sethuraman, V.A., K. Na, and Y.H. Bae, *pH-responsive sulfonamide/PEI system for tumor specific gene delivery: an in vitro study.* Biomacromolecules, 2006. **7**(1): p. 64-70.
144. Hillegass, J.M., et al., *Assessing nanotoxicity in cells in vitro.* Wiley Interdisciplinary Reviews: Nanomedicine and Nanobiotechnology, 2010. **2**(3): p. 219-231.
145. Soenen, S.J., et al., *Cellular toxicity of inorganic nanoparticles: Common aspects and guidelines for improved nanotoxicity evaluation.* Nano Today, 2011. **6**(5): p. 446-465.
146. Sargent, L., et al., *Induction of aneuploidy by single-walled carbon nanotubes.* Environmental and molecular mutagenesis, 2009. **50**(8): p. 708-717.
147. Murray, A., et al., *Oxidative stress and inflammatory response in dermal toxicity of single-walled carbon nanotubes.* Toxicology, 2009. **257**(3): p. 161-171.
148. Shvedova, A.A., et al., *Mechanisms of carbon nanotube-induced toxicity: focus on oxidative stress.* Toxicology and applied pharmacology, 2012. **261**(2): p. 121-133.

149. Alexis, F., et al., *Factors affecting the clearance and biodistribution of polymeric nanoparticles.* Molecular pharmaceutics, 2008. **5**(4): p. 505-515.
150. Lv, H., et al., *Toxicity of cationic lipids and cationic polymers in gene delivery.* Journal of Controlled Release, 2006. **114**(1): p. 100-109.
151. Brownlie, A., I. Uchegbu, and A. Schätzlein, *PEI-based vesicle-polymer hybrid gene delivery system with improved biocompatibility.* International journal of pharmaceutics, 2004. **274**(1): p. 41-52.
152. Pathak, A., et al., *Engineered polyallylamine nanoparticles for efficient in vitro transfection.* Pharmaceutical research, 2007. **24**(8): p. 1427-1440.
153. Nimesh, S., R. Kumar, and R. Chandra, *Novel polyallylamine–dextran sulfate–DNA nanoplexes: highly efficient non-viral vector for gene delivery.* International journal of pharmaceutics, 2006. **320**(1): p. 143-149.
154. Boussif, O., et al., *Synthesis of polyallylamine derivatives and their use as gene transfer vectors in vitro.* Bioconjugate chemistry, 1999. **10**(5): p. 877-883.
155. Zanta, M.-A., et al., *In vitro gene delivery to hepatocytes with galactosylated polyethylenimine.* Bioconjugate chemistry, 1997. **8**(6): p. 839-844.
156. Fischer, D., et al., *A novel non-viral vector for DNA delivery based on low molecular weight, branched polyethylenimine: effect of molecular weight on transfection efficiency and cytotoxicity.* Pharmaceutical research, 1999. **16**(8): p. 1273-1279.
157. Fischer, D., et al., *In vitro cytotoxicity testing of polycations: influence of polymer structure on cell viability and hemolysis.* Biomaterials, 2003. **24**(7): p. 1121-1131.
158. Fischer, H.C. and W.C. Chan, *Nanotoxicity: the growing need for in vivo study.* Current opinion in Biotechnology, 2007. **18**(6): p. 565-571.
159. Bottini, M., et al., *Multi-walled carbon nanotubes induce T lymphocyte apoptosis.* Toxicology letters, 2006. **160**(2): p. 121-126.
160. Stone, V., H. Johnston, and R.P.F. Schins, *Development of in vitro systems for nanotoxicology: methodological considerations.* Critical reviews in toxicology, 2009. **39**(7): p. 613-626.
161. Maurer-Jones, M.A., et al., *Toxicity of therapeutic nanoparticles.* Nanomedicine, 2009. **4**(2): p. 219-241.
162. Liu, X., et al., *The influence of polymeric properties on chitosan/siRNA nanoparticle formulation and gene silencing.* Biomaterials, 2007. **28**(6): p. 1280-1288.
163. Zolnik, B.S., et al., *Minireview: nanoparticles and the immune system.* Endocrinology, 2010. **151**(2): p. 458-465.
164. El-Ansary, A. and S. Al-Daihan, *On the toxicity of therapeutically used nanoparticles: an overview.* Journal of toxicology, 2009.
165. Gaspar, R. and R. Duncan, *Polymeric carriers: preclinical safety and the regulatory implications for design and development of polymer therapeutics.* Advanced drug delivery reviews, 2009. **61**(13): p. 1220-1231.
166. Marquis, B.J., et al., *Analytical methods to assess nanoparticle toxicity.* Analyst, 2009. **134**(3): p. 425-439.
167. Love, S.A., et al., *Assessing Nanoparticle Toxicity.* Annual Review of Analytical Chemistry, 2012. **5**: p. 181-205.
168. Liebler, D.C. and F.P. Guengerich, *Elucidating mechanisms of drug-induced toxicity.* Nature reviews Drug discovery, 2005. **4**(5): p. 410-420.
169. Behrens, I., et al., *Comparative uptake studies of bioadhesive and non-bioadhesive nanoparticles in human intestinal cell lines and rats: the effect of mucus on particle adsorption and transport.* Pharmaceutical research, 2002. **19**(8): p. 1185-1193.
170. Balimane, P.V. and S. Chong, *Cell culture-based models for intestinal permeability: a critique.* Drug discovery today, 2005. **10**(5): p. 335-343.
171. Si-Shen, F., et al., *Nanoparticles of biodegradable polymers for clinical administration of paclitaxel.* Current medicinal chemistry, 2004. **11**(4): p. 413-424.

172. des Rieux, A., et al., *Nanoparticles as potential oral delivery systems of proteins and vaccines: a mechanistic approach.* Journal of Controlled Release, 2006. **116**(1): p. 1-27.
173. Artursson, P., K. Palm, and K. Luthman, *Caco-2 monolayers in experimental and theoretical predictions of drug transport.* Advanced drug delivery reviews, 2012. **46**(1): p 27-43.
174. Van Itallie, C.M. and J.M. Anderson, *Claudins and epithelial paracellular transport.* Annu. Rev. Physiol., 2006. **68**: p. 403-429.
175. Watson, C., M. Rowland, and G. Warhurst, *Functional modeling of tight junctions in intestinal cell monolayers using polyethylene glycol oligomers.* American Journal of Physiology-Cell Physiology, 2001. **281**(2): p. C388-C397.
176. Oliveira, S. and J. Morgado-Diaz, *Claudins: multifunctional players in epithelial tight junctions and their role in cancer.* Cellular and molecular life sciences, 2007. **64**(1): p. 17-28.
177. Martien, R., et al., *Thiolated chitosan nanoparticles: transfection study in the Caco-2 differentiated cell culture.* Nanotechnology, 2008. **19**(4): p. 045101.
178. Yeh, T.-H., et al., *Mechanism and consequence of chitosan-mediated reversible epithelial tight junction opening.* Biomaterials, 2011. **32**(26): p. 6164-6173.
179. Lin, Y.-H., et al., *Preparation and characterization of nanoparticles shelled with chitosan for oral insulin delivery.* Biomacromolecules, 2007. **8**(1): p. 146-152.
180. Van Itallie, C.M., et al., *ZO-1 stabilizes the tight junction solute barrier through coupling to the perijunctional cytoskeleton.* Molecular biology of the cell, 2009. **20**(17): p. 3930-3940.
181. Rosenthal, R., et al., *The effect of chitosan on transcellular and paracellular mechanisms in the intestinal epithelial barrier.* Biomaterials, 2012. **33**(9): p 2791-2800.
182. Smith, J., E. Wood, and M. Dornish, *Effect of chitosan on epithelial cell tight junctions.* Pharmaceutical Research, 2004. **21**(1): p. 43-49.
183. Ranaldi, G., et al., *The effect of chitosan and other polycations on tight junction permeability in the human intestinal Caco-2 cell line.* The Journal of nutritional biochemistry, 2002. **13**(3): p. 157-167.
184. Vllasaliu, D., et al., *Tight junction modulation by chitosan nanoparticles: comparison with chitosan solution.* International journal of pharmaceutics, 2010. **400**(1): p. 183-193.
185. Lin, Y.-H., et al., *Novel nanoparticles for oral insulin delivery via the paracellular pathway.* Nanotechnology, 2007. **18**(10): p. 105102.
186. Mi, F.-L., et al., *Oral delivery of peptide drugs using nanoparticles self-assembled by poly (γ-glutamic acid) and a chitosan derivative functionalized by trimethylation.* Bioconjugate chemistry, 2008. **19**(6): p. 1248-1255.
187. Li, L., et al., *Carbopol-mediated paracellular transport enhancement in Calu-3 cell layers.* Journal of pharmaceutical sciences, 2006. **95**(2): p. 326-335.
188. Ma, Z. and L.-Y. Lim, *Uptake of chitosan and associated insulin in Caco-2 cell monolayers: a comparison between chitosan molecules and chitosan nanoparticles.* Pharmaceutical Research, 2003. **20**(11): p. 1812-1819.
189. Malatesta, M., et al., *Diaminobenzidine photoconversion is a suitable tool for tracking the intracellular location of fluorescently labelled nanoparticles at transmission electron microscopy.* European journal of histochemistry: EJH, 2012. **56**(2): p 123-128.
190. Park, J.S., et al., *N-acetyl histidine-conjugated glycol chitosan self-assembled nanoparticles for intracytoplasmic delivery of drugs: Endocytosis, exocytosis and drug release.* Journal of controlled release, 2006. **115**(1): p. 37-45.
191. Hillaireau, H. and P. Couvreur, *Nanocarriers' entry into the cell: relevance to drug delivery.* Cellular and molecular life sciences, 2009. **66**(17): p. 2873-2896.
192. Ben-Dov, N. and R. Korenstein, *Enhancement of cell membrane invaginations, vesiculation and uptake of macromolecules by protonation of the cell surface.* PLoS one, 2012. **7**(4): p. e35204.
193. Cho, Y.W., J.D. Kim, and K. Park, *Polycation gene delivery systems: escape from endosomes to cytosol.* Journal of pharmacy and pharmacology, 2003. **55**(6): p. 721-734.

194. Arote, R.B., et al., *The therapeutic efficiency of FP-PEA/TAM67 gene complexes via folate receptor-mediated endocytosis in a xenograft mice model.* Biomaterials, 2010. **31**(8): p. 2435-2445.
195. Yang, S.-J., et al., *Folic acid-conjugated chitosan nanoparticles enhanced protoporphyrin IX accumulation in colorectal cancer cells.* Bioconjugate chemistry, 2010. **21**(4): p. 679-689.
196. Zheng, Y., et al., *Receptor-mediated gene delivery by folate-poly (ethylene glycol)-grafted-trimethyl chitosan in vitro.* Journal of drug targeting, 2011. **19**(8): p. 647-656.
197. Navaroli, D.M., et al., *Rabenosyn-5 defines the fate of the transferrin receptor following clathrin-mediated endocytosis.* Proceedings of the National Academy of Sciences, 2012. **109**(8): p. E471-E480.
198. Wang, J., et al., *The complex role of multivalency in nanoparticles targeting the transferrin receptor for cancer therapies.* Journal of the American Chemical Society, 2010. **132**(32): p. 11306-11313.
199. Wang, Y., et al., *Preparation and evaluation of paclitaxel-loaded nanoparticle incorporated with galactose-carrying polymer for hepatocyte targeted delivery.* Drug Development and Industrial Pharmacy, 2012. **38**(9): p. 1039-1046.
200. Chen, S., et al., *Mechanism-based tumor-targeting drug delivery system. Validation of efficient vitamin receptor-mediated endocytosis and drug release.* Bioconjugate chemistry, 2010. **21**(5): p. 979-987.
201. Nam, H.Y., et al., *Cellular uptake mechanism and intracellular fate of hydrophobically modified glycol chitosan nanoparticles.* Journal of Controlled Release, 2009. **135**(3): p. 259-267.
202. Kiss, A.L. and E. Botos, *Endocytosis via caveolae: alternative pathway with distinct cellular compartments to avoid lysosomal degradation?* Journal of cellular and molecular medicine, 2009. **13**(7): p. 1228-1237.
203. Le Roy, C. and J.L. Wrana, *Clathrin-and non-clathrin-mediated endocytic regulation of cell signalling.* Nature Reviews Molecular Cell Biology, 2005. **6**(2): p. 112-126.
204. Doherty, G.J. and H.T. McMahon, *Mechanisms of endocytosis.* Annual review of biochemistry, 2009. **78**: p. 857-902.
205. Huang, M., et al., *Uptake of FITC-chitosan nanoparticles by A549 cells.* Pharmaceutical research, 2002. **19**(10): p. 1488-1494.
206. Tahara, K., et al., *Improved cellular uptake of chitosan-modified PLGA nanospheres by A549 cells.* International journal of pharmaceutics, 2009. **382**(1): p. 198-204.
207. Huang, M., E. Khor, and L.-Y. Lim, *Uptake and cytotoxicity of chitosan molecules and nanoparticles: effects of molecular weight and degree of deacetylation.* Pharmaceutical Research, 2004. **21**(2): p. 344-353.
208. Harush-Frenkel, O., et al., *Targeting of nanoparticles to the clathrin-mediated endocytic pathway.* Biochemical and biophysical research communications, 2007. **353**(1): p. 26-32.
209. Kirkham, M. and R.G. Parton, *Clathrin-independent endocytosis: new insights into caveolae and non-caveolar lipid raft carriers.* Biochimica et Biophysica Acta (BBA)-Molecular Cell Research, 2005. **1745**(3): p. 273-286.
210. Pelkmans, L., *Secrets of caveolae-and lipid raft-mediated endocytosis revealed by mammalian viruses.* Biochimica et Biophysica Acta (BBA)-Molecular Cell Research, 2005. **1746**(3): p. 295-304.
211. Pelkmans, L. and A. Helenius, *Endocytosis via caveolae.* Traffic, 2002. **3**(5): p. 311-320.
212. Chung, Y.-C., T.-Y. Cheng, and T.-H. Young, *The role of adenosine receptor and caveolae-mediated endocytosis in oligonucleotide-mediated gene transfer.* Biomaterials, 2011. **32**(19): p. 4471-4480.
213. Van der Aa, M., et al., *Cellular uptake of cationic polymer-DNA complexes via caveolae plays a pivotal role in gene transfection in COS-7 cells.* Pharmaceutical research, 2007. **24**(8): p. 1590-1598.

214. Rejman, J., et al., *Size-dependent internalization of particles via the pathways of clathrin-and caveolae-mediated endocytosis.* Biochem. J, 2004. **377**: p. 159-169.
215. Florence, A.T., *Nanoparticle uptake by the oral route: Fulfilling its potential?* Drug discovery today: technologies, 2005. **2**(1): p. 75-81.
216. Forchielli, M.L. and W.A. Walker, *The role of gut-associated lymphoid tissues and mucosal defence.* British Journal of Nutrition, 2005. **93**(1): p. 41-48.
217. Hunter, A.C., et al., *Polymeric particulate technologies for oral drug delivery and targeting: A pathophysiological perspective.* Nanomedicine: Nanotechnology, Biology and Medicine, 2012. **8**: p. S5-S20.
218. Kraehenbuhl, J.-P. and M.R. Neutra, *Epithelial M cells: differentiation and function.* Annual review of cell and developmental biology, 2000. **16**(1): p. 301-332.
219. Mowat, A.M., *Anatomical basis of tolerance and immunity to intestinal antigens.* Nature Reviews Immunology, 2003. **3**(4): p. 331-341.
220. O'Neill, M.J., et al., *Intestinal delivery of non-viral gene therapeutics: physiological barriers and preclinical models.* Drug discovery today, 2011. **16**(5): p. 203-218.
221. Garinot, M., et al., *PEGylated PLGA-based nanoparticles targeting M cells for oral vaccination.* Journal of Controlled Release, 2007. **120**(3): p. 195-204.
222. Gullberg, E., et al., *Identification of cell adhesion molecules in the human follicle-associated epithelium that improve nanoparticle uptake into the Peyer's patches.* Journal of Pharmacology and Experimental Therapeutics, 2006. **319**(2): p. 632-639.
223. Alexandridis, P. and B. Lindman, *Amphiphilic block copolymers: self-assembly and applications*. Elsevier Science, 2000.
224. Wang, C., Z. Wang, and X. Zhang, *Amphiphilic building blocks for self-assembly: From amphiphiles to supra-amphiphiles.* Accounts of Chemical Research, 2012. **45**(4): p. 608-618.
225. Yoon, H.-J. and W.-D. Jang, *Polymeric supramolecular systems for drug delivery.* Journal of Materials Chemistry, 2010. **20**(2): p. 211-222.
226. Hoskins, C., P.K. Thoo-Lin, and W.P. Cheng, *A review on comb-shaped amphiphilic polymers for hydrophobic drug solubilization.* Therapeutic Delivery, 2012. **3**(1): p. 59-79.
227. Mao, S., et al., *Synthesis, characterization and cytotoxicity of poly (ethylene glycol)-graft-trimethyl chitosan block copolymers.* Biomaterials, 2005. **26**(32): p. 6343-6356.
228. Wang, Y. and S.M. Grayson, *Approaches for the preparation of non-linear amphiphilic polymers and their applications to drug delivery.* Advanced drug delivery reviews, 2012. **64**(9): p. 852-865.
229. Park, S., et al., *Graphene oxide sheets chemically cross-linked by polyallylamine.* The Journal of Physical Chemistry C, 2009. **113**(36): p. 15801-15804.
230. Chertow, G.M., et al., *Poly [allylamine hydrochloride](RenaGel): a noncalcemic phosphate binder for the treatment of hyperphosphatemia in chronic renal failure.* American journal of kidney diseases, 1997. **29**(1): p. 66-71.
231. Nimesh, S., R. Kumar, and R. Chandra, *Novel polyallylamine-dextran sulfate-DNA nanoplexes: Highly efficient non-viral vector for gene delivery.* International journal of pharmaceutics, 2006. **320**(1-2): p. 143-149.
232. Garrigues, S. and M. de la Guardia, *Non-invasive analysis of solid samples.* TrAC Trends in Analytical Chemistry, 2012. . **43**: p. 161-173.
233. Saldivar-Guerra, E. and E. Vivaldo-Lima, *Handbook of Polymer Synthesis, Characterization, and Processing*. ohn Wiley and sons, 2013.
234. Braun, D., et al., *Polymer synthesis: theory and practice: fundamentals, methods, experiments*. Springer, 2004.
235. Pavia, D.L., *Introduction to spectroscopy*. cengage learning, 2008.
236. Braun, D., H. Cherdron, and M. Rehahn, *Polymer synthesis: theory and practice*. Springer, 2013.
237. Dugan, G., *ELEMENTAL ANALYSIS,* 1974.

238. Durand, B. and J. Monin, *Elemental analysis of kerogens (C, H, O, N, S, Fe).* Kerogen: Paris, Editions Technip, 1980: p. 113-142.
239. Rezl, V. and J. Janák, *Elemental analysis by gas chromatography.* Journal of Chromatography A, 1973. **81**(2): p. 233-260.
240. Aiken, A.C., P.F. DeCarlo, and J.L. Jimenez, *Elemental analysis of organic species with electron ionization high-resolution mass spectrometry.* Analytical Chemistry, 2007. **79**(21): p. 8350-8358.
241. Izunobi, J.U. and C.L. Higginbotham, *Polymer Molecular Weight Analysis by 1H NMR Spectroscopy.* Journal of Chemical Education, 2011. **88**(8): p. 1098-1104.
242. Bruch, M., *NMR spectroscopy techniques*. Vol. 21. CRC, 1996.
243. Guerrini, M., et al., *A novel computational approach to integrate NMR spectroscopy and capillary electrophoresis for structure assignment of heparin and heparan sulfate oligosaccharides.* Glycobiology, 2002. **12**(11): p. 713-719.
244. Nanny, M.A., R.A. Minear, and J.A. Leenheer, *Nuclear magnetic resonance spectroscopy in environmental chemistry*. 1997: Oxford University Press, USA. 1997.
245. Keeler, J., *Understanding NMR spectroscopy*. Wiley, 2011.
246. Andrew, E.R., *Nuclear magnetic resonance.* Nuclear Magnetic Resonance. Vol. 1. Cambridge Monographs on Physics, 2009.
247. Holzgrabe, U., I. Wawer, and B. Diehl, *NMR spectroscopy in pharmaceutical analysis*. Elsevier Science, 2008.
248. Richards, S.A. and J.C. Hollerton, *Essential practical NMR for organic chemistry*. Wiley, 2010.
249. Takamura, K., *Polymer dispersions and their industrial applications.* Wiley-VCH, 2002.
250. Chung, Y.C., et al., *PEGylated Guanidinylated Polyallylamine as Gene-Delivery Carrier.* Journal of Biomaterials Science, Polymer Edition, 2011. **22**(14): p. 1829-1843.
251. Filippov, S.K., et al., *Effect of hydrophobic interactions on properties and stability of DNA–polyelectrolyte complexes.* Langmuir, 2010. **26**(7): p. 4999-5006.
252. Tiyaboonchai, W., J. Woiszwillo, and C.R. Middaugh, *Formulation and characterization of amphotericin B–polyethylenimine–dextran sulfate nanoparticles.* Journal of pharmaceutical sciences, 2001. **90**(7): p. 902-914.
253. Hu, Y., et al., *Synthesis and characterization of chitosan–poly (acrylic acid) nanoparticles.* Biomaterials, 2002. **23**(15): p. 3193-3201.
254. Woodle, M., et al., *Sterically stabilized polyplex: ligand-mediated activity.* Journal of Controlled Release, 2001. **74**(1): p. 309-311.
255. Hsu, S.-W., et al., *Polyelectrolyte-Templated Synthesis of Bimetallic Nanoparticles.* Langmuir, 2011. **27**(13): p. 8494-8499.
256. Huang, Y., et al., *Binary and ternary complexes based on polycaprolactone-graft-poly (N, N-dimethylaminoethyl methacrylate) for targeted siRNA delivery.* Biomaterials, 2012. **33**(18): p. 4653-4664.
257. Peng, J., et al., *Influence of anions on the formation and properties of chitosan-DNA nanoparticles.* Journal of nanoscience and nanotechnology, 2005. **5**(5): p. 713-717.
258. Chen, Y., et al., *Designing chitosan-dextran sulfate nanoparticles using charge ratios.* Aaps Pharmscitech, 2007. **8**(4): p. 131-139.
259. Shu, S., et al., *Delivery of protein drugs using nanoparticles self-assembled from dextran sulfate and quaternized chitosan.* Journal of Controlled Release, 2011. **152**: p. e170-e172.
260. Wang, Q., J. Perez, and T. Webster, *Inhibited growth of Pseudomonas aeruginosa by dextran- and polyacrylic acid-coated ceria nanoparticles.* International Journal of Nanomedicine, 2013. **8**: p. 3395-3399.
261. Ma, Y.-H., et al., *Magnetically targeted thrombolysis with recombinant tissue plasminogen activator bound to polyacrylic acid-coated nanoparticles.* Biomaterials, 2009. **30**(19): p. 3343-3351.

262. Gao, X., et al., *Biodegradable pH-responsive polyacrylic acid derivative hydrogels with tunable swelling behavior for oral delivery of insulin.* Polymer, 2013. **54**(7): p. 1786- 1793.
263. Zhang, C. and D.E. Hirt, *Layer-by-layer self-assembly of polyelectrolyte multilayers on cross-section surfaces of multilayer polymer films: A step toward nano-patterning flexible substrates.* Polymer, 2007. **48**(23): p. 6748-6754.
264. Khairnar, G. and F. Sayyad, *Development of buccal drug delivery system based on mucoadhesive polymers.* International Journal of PharmTech Research, 2010. **2**(1): p. 719-735.
265. Reineke, J., et al., *Can bioadhesive nanoparticles allow for more effective particle uptake from the small intestine?* Journal of Controlled Release, 2013. **170**(3): p. 477-484.
266. Li, Z. and E. Ruckenstein, *Water-soluble poly (acrylic acid) grafted luminescent silicon nanoparticles and their use as fluorescent biological staining labels.* Nano letters, 2004. **4**(8): p. 1463-1467.
267. Sonia, T. and C.P. Sharma, *An overview of natural polymers for oral insulin delivery.* Drug discovery today, 2012. **17**(13): p. 784-792.
268. Terg, R.A., *Large-Volume Paracentesis: Which Plasma Expander?* 2011. p. 32-39.
269. Tiyaboonchai, W., J. Woiszwillo, and C.R. Middaugh, *Formulation and characterization of DNA–polyethylenimine–dextran sulfate nanoparticles.* European journal of pharmaceutical sciences, 2003. **19**(4): p. 191-202.
270. Chen, Y., V.J. Mohanraj, and J.E. Parkin, *Chitosan-dextran sulfate nanoparticles for delivery of an anti-angiogenesis peptide.* Letters in Peptide Science, 2003. **10**(5-6): p. 621-629.
271. Anitha, A., et al., *Preparation, characterization, in vitro drug release and biological studies of curcumin loaded dextran sulphate–chitosan nanoparticles.* Carbohydrate polymers, 2011. **84**(3): p. 1158-1164.
272. Sarmento, B., et al., *Development and comparison of different nanoparticulate polyelectrolyte complexes as insulin carriers.* International Journal of Peptide Research and Therapeutics, 2006. **12**(2): p. 131-138.
273. Saboktakin, M.R., et al., *Synthesis and characterization of pH-dependent glycol chitosan and dextran sulfate nanoparticles for effective brain cancer treatment.* International journal of biological macromolecules, 2011. **49**(4): p. 747-751.
274. Phenrat, T., et al., *Stabilization of aqueous nanoscale zerovalent iron dispersions by anionic polyelectrolytes: adsorbed anionic polyelectrolyte layer properties and their effect on aggregation and sedimentation.* Journal of Nanoparticle Research, 2008. **10**(5): p. 795-814.
275. Sabín, J., G. Prieto, and F. Sarmiento, *Studying Colloidal Aggregation Using Liposomes*, in *Liposomes*. 2010, Springer. p. 189-198.
276. Vlachy, V., *Ionic effects beyond Poisson-Boltzmann theory.* Annual review of physical chemistry, 1999. **50**(1): p. 145-165.
277. Liang, Y., et al., *Interaction forces between colloidal particles in liquid: Theory and experiment.* Advances in Colloid and Interface Science, 2007. **134**: p. 151-166.
278. Sun, J., et al., *Aqueous latex/ceramic nanoparticle dispersions: colloidal stability and coating properties.* Journal of colloid and interface science, 2004. **280**(2): p. 387-399.
279. Krasemann, L., A. Toutianoush, and B. Tieke, *Self-assembled polyelectrolyte multilayer membranes with highly improved pervaporation separation of ethanol/water mixtures.* Journal of Membrane Science, 2001. **181**(2): p. 221-228.
280. Gucht, J.v.d., et al., *Polyelectrolyte complexes: bulk phases and colloidal systems.* Journal of colloid and interface science, 2011. **361**(2): p. 407-422.
281. Lee, K.Y., et al., *Physicochemical characteristics of self-aggregates of hydrophobically modified chitosans.* Langmuir, 1998. **14**(9): p. 2329-2332.
282. Reschel, T., et al., *Physical properties and in vitro transfection efficiency of gene delivery vectors based on complexes of DNA with synthetic polycations.* Journal of controlled release, 2002. **81**(1): p. 201-217.

283. Romanini, D., M.J. Braia, and M.C. Porfiri, *Applications of Calorimetric Techniques in the Formation of Protein-Polyelectrolytes Complexes,* 2013.
284. Holappa, S., et al., *Soluble polyelectrolyte complexes composed of poly (ethylene oxide)-block -poly (sodium methacrylate) and poly (methacryloyloxyethyl trimethylammonium chloride).* Polymer, 2003. **44**(26): p. 7907-7916.
285. Yousefpour, P., et al., *Polyanionic carbohydrate doxorubicin–dextran nanocomplex as a delivery system for anticancer drugs: in vitro analysis and evaluations.* International journal of nanomedicine, 2011. **6**: p. 1487.
286. Ganta, S., et al., *A review of stimuli-responsive nanocarriers for drug and gene delivery.* Journal of Controlled Release, 2008. **126**(3): p. 187-204.
287. Chandler, D., *Interfaces and the driving force of hydrophobic assembly.* Nature, 2005. **437**(7059): p. 640-647.
288. Ruel-Gariépy, E. and J.-C. Leroux, *In situ-forming hydrogels—review of temperature-sensitive systems.* European journal of pharmaceutics and biopharmaceutics, 2004. **58**(2): p. 409-426.
289. Kleinen, J. and W. Richtering, *Rearrangements in and release from responsive microgel–polyelectrolyte complexes induced by temperature and time.* The Journal of Physical Chemistry B, 2011. **115**(14): p. 3804-3810.
290. Umerska, A., et al., *Exploring the assembly process and properties of novel crosslinker-free hyaluronate-based polyelectrolyte complex nanocarriers.* International Journal of Pharmaceutics, 2012. **436**(1): p. 75-87.
291. Saboktakin, M.R., et al., *Synthesis and characterization of superparamagnetic chitosan–dextran sulfate hydrogels as nano carriers for colon-specific drug delivery.* Carbohydrate Polymers, 2010. **81**(2): p. 372-376.
292. Strand, S.P., et al., *Molecular design of chitosan gene delivery systems with an optimized balance between polyplex stability and polyplex unpacking.* Biomaterials, 2010. **31**(5): p. 975-987.
293. De la Fuente, M., B. Seijo, and M. Alonso, *Bioadhesive hyaluronan–chitosan nanoparticles can transport genes across the ocular mucosa and transfect ocular tissue.* Gene therapy, 2008. **15**(9): p. 668-676.
294. Boddohi, S., et al., *Polysaccharide-based polyelectrolyte complex nanoparticles from chitosan, heparin, and hyaluronan.* Biomacromolecules, 2009. **10**(6): p. 1402-1409.
295. Mao, S., et al., *Self-assembled polyelectrolyte nanocomplexes between chitosan derivatives and insulin.* Journal of pharmaceutical sciences, 2006. **95**(5): p. 1035-1048.
296. Sarmento, B., et al., *Development and characterization of new insulin containing polysaccharide nanoparticles.* 2006. **53**(2): 193-202.
297. Jiang, J., G. Oberdörster, and P. Biswas, *Characterization of size, surface charge, and agglomeration state of nanoparticle dispersions for toxicological studies.* Journal of Nanoparticle Research, 2009. **11**(1): p. 77-89.
298. Bootz, A., et al., *Comparison of scanning electron microscopy, dynamic light scattering and analytical ultracentrifugation for the sizing of poly (butyl cyanoacrylate) nanoparticles.* European journal of pharmaceutics and biopharmaceutics, 2004. **57**(2): p. 369-375.
299. Brar, S.K. and M. Verma, *Measurement of nanoparticles by light-scattering techniques.* TrAC Trends in Analytical Chemistry, 2011. **30**(1): p. 4-17.
300. Lead, J.R. and E.L. Smith, *Environmental and human health impacts of nanotechnology*. 2009: Wiley Online Library. Hoboken (NJ): Wiley, 2009.
301. Pecora, R., *Dynamic light scattering measurement of nanometer particles in liquids.* Journal of Nanoparticle Research, 2000. **2**(2): p. 123-131.
302. Gaumet, M., et al., *Nanoparticles for drug delivery: the need for precision in reporting particle size parameters.* European journal of pharmaceutics and biopharmaceutics, 2008. **69**(1): p. 1-9.

303. Attivi, D., et al., *Formulation of insulin-loaded polymeric nanoparticles using response surface methodology.* Drug development and industrial pharmacy, 2005. **31**(2): p. 179-189.
304. He, C., et al., *Size-dependent absorption mechanism of polymeric nanoparticles for oral delivery of protein drugs.* Biomaterials, 2012. **33**(33): p. 8569-8578.
305. Kulkarni, S.A. and S.-S. Feng, *Effects of particle size and surface modification on cellular uptake and biodistribution of polymeric nanoparticles for drug delivery.* Pharmaceutical research, 2013: p. 1-11.
306. Liu, X.-M., et al., *The effect of salt and pH on the phase-transition behaviors of temperature-sensitive copolymers based on N-isopropylacrylamide.* Biomaterials, 2004. **25**(25): p. 5659-5666.
307. Lunov, O., et al., *Differential uptake of functionalized polystyrene nanoparticles by human macrophages and a monocytic cell line.* ACS nano, 2011. **5**(3): p. 1657-1669.
308. Yin Win, K. and S.-S. Feng, *Effects of particle size and surface coating on cellular uptake of polymeric nanoparticles for oral delivery of anticancer drugs.* Biomaterials, 2005. **26**(15): p. 2713-2722.
309. Zhang, S., et al., *Size-Dependent Endocytosis of Nanoparticles.* Advanced Materials, 2009. **21**(4): p. 419-424.
310. Yin Win, K. and S.S. Feng, *Effects of particle size and surface coating on cellular uptake of polymeric nanoparticles for oral delivery of anticancer drugs.* Biomaterials, 2005. **26**(15): p. 2713-2722.
311. Kirby, B.J. and E.F. Hasselbrink, *Zeta potential of microfluidic substrates: 1. Theory, experimental techniques, and effects on separations.* Electrophoresis, 2004. **25**(2): p. 187-202.
312. Travesset, A. and S. Vangaveti, *Electrostatic correlations at the Stern layer: Physics or chemistry?* The Journal of chemical physics, 2009. **131**: p. 185102.
313. Pearson, C.R., et al., *Zeta potential as a measure of polyelectrolyte flocculation and the effect of polymer dosing conditions on cell removal from fermentation broth.* Biotechnology and bioengineering, 2004. **87**(1): p. 54-60.
314. Weiner, B.B., W.W. Tscharnuter, and D. Fairhurst. *Zeta potential: A new approach*. in *Canadian Mineral Analysts Meeting, Winnipeg Manitoba, Canada*, 1993.
315. Akkar, A. and R. Müller, *Formulation of intravenous Carbamazepine emulsions by SolEmuls® technology.* European journal of pharmaceutics and biopharmaceutics, 2003. **55**(3): p. 305-312.
316. Wang, L.K., Y.-T. Hung, and N.K. Shammas, *Physicochemical treatment processes*. Vol. 3. 2005: Humana Press. Vol. 3. Humana Press, 2005.
317. He, C., et al., *Effects of particle size and surface charge on cellular uptake and biodistribution of polymeric nanoparticles.* Biomaterials, 2010. **31**(13): p. 3657-3666.
318. Murdock, R.C., et al., *Characterization of nanomaterial dispersion in solution prior to in vitro exposure using dynamic light scattering technique.* Toxicological Sciences, 2008. **101**(2): p. 239-253.
319. Lawrie, A., et al., *Microparticle sizing by dynamic light scattering in fresh-frozen plasma.* Vox sanguinis, 2009. **96**(3): p. 206-212.
320. Kornbrekke, R., I. Morrison, and T. Oja, *Electrophoretic mobility measurements in low conductivity media.* Langmuir, 1992. **8**(4): p. 1211-1217.
321. Wang, Z., *Transmission electron microscopy of shape-controlled nanocrystals and their assemblies.* The Journal of Physical Chemistry B, 2000. **104**(6): p. 1153-1175.
322. Buseck, P., J. Cowley, and L.R. Eyring, *High-Resolution Transmission Electron Microscopy: And Associated Techniques*. 1989: Oxford University Press, USA, 1989.
323. Sospedra, I., et al., *Rapid whole protein quantification of staphylococcal enterotoxin B by liquid chromatography.* Food Chemistry, 2012. **133**(1): p. 163-166.

324. Ständker, L., et al., *Quantitative enzyme-linked immunosorbent assay determination of an abundant hemoglobin-derived anti-infective peptide in human placenta.* Analytical biochemistry, 2010. **401**(1): p. 53-60.
325. Mero, A., et al., *Covalent conjugation of poly (ethylene glycol) to proteins and peptides: strategies and methods*, in *Bioconjugation Protocols*. 2011, Springer. p. 95-129.
326. Meyer, V.R., *Practical high-performance liquid chromatography*. John Wiley and Sons, 2010.
327. Aguilar, M.-I., *HPLC of Peptides and Proteins*. Springer, 2004.
328. Zhou, S., et al., *An immunoassay method for quantitative detection of proteins using single antibodies.* Analytical biochemistry, 2010. **400**(2): p. 213-218.
329. Kalathil, S., et al., *Variable characteristics with insulin assays.* Practical Diabetes, 2013. **30**(3): p. 118-120.
330. Wild, D.G., *The Immunoassay Handbook: Theory and applications of ligand binding, ELISA and related techniques*. Newnes, 2013.
331. Martin, R.M., et al., *Filter paper blood spot enzyme linked immunoassay for insulin and application in the evaluation of determinants of child insulin resistance.* PLoS one, 2012. **7**(10): p. e46752.
332. Lu, X., et al., *Polyelectrolyte complex nanoparticles of amino poly (glycerol methacrylate) s and insulin.* International journal of pharmaceutics, 2011. . **423**(2): p. 195-201.
333. Fallingborg, J., *Intraluminal pH of the human gastrointestinal tract.* Danish medical bulletin, 1999. **46**(3): p. 183.
334. Liu, Z., et al., *Polysaccharides-based nanoparticles as drug delivery systems.* Advanced drug delivery reviews, 2008. **60**(15): p. 1650-1662.
335. Thünemann, A.F., et al., *Polyelectrolyte complexes.* Polyelectrolytes with defined molecular architecture II, 2004: p. 19-33.
336. Berger, J., et al., *Structure and interactions in covalently and ionically crosslinked chitosan hydrogels for biomedical applications.* European journal of pharmaceutics and biopharmaceutics, 2004. **57**(1): p. 19-34.
337. Polexe, R.C. and T. Delair, *Elaboration of Stable and Antibody Functionalized Positively Charged Colloids by Polyelectrolyte Complexation between Chitosan and Hyaluronic Acid.* Molecules, 2013. **18**(7): p. 8563-8578.
338. Park, W., et al., *Multi-arm histidine copolymer for controlled release of insulin from poly (lactide-co-glycolide) microsphere.* Biomaterials, 2012. **33**(34): 8848-8857.
339. Silva, C.M., et al., *Insulin release from alginate microspheres reinforced with dextran sulfate.* Chemical Industry and Chemical Engineering Quarterly/CICEQ, 2006. **12**(1): p. 40-46.
340. Izumrudov, V.A., M.V. Zhiryakova, and S.E. Kudaibergenov, *Controllable stability of DNA-containing polyelectrolyte complexes in water–salt solutions.* Biopolymers, 1999. **52**(2): p. 94-108.
341. Jaber, J.A. and J.B. Schlenoff, *Counterions and water in polyelectrolyte multilayers: a tale of two polycations.* Langmuir, 2007. **23**(2): p. 896-901.
342. Cranford, S.W., C. Ortiz, and M.J. Buehler, *Mechanomutable properties of a PAA/PAH polyelectrolyte complex: rate dependence and ionization effects on tunable adhesion strength.* Soft Matter, 2010. **6**(17): p. 4175-4188.
343. Goicoechea, J., et al., *Study and optimization of self-assembled polymeric multilayer structures with neutral red for pH sensing applications.* Journal of sensors, 2007.
344. Fadeel, B. and A.E. Garcia-Bennett, *Better safe than sorry: understanding the toxicological properties of inorganic nanoparticles manufactured for biomedical applications.* Advanced drug delivery reviews, 2010. **62**(3): p. 362-374.
345. Soenen, S.J., et al., *Cellular toxicity of inorganic nanoparticles: Common aspects and guidelines for improved nanotoxicity evaluation.* Nano Today, 2011. **6**(5): p. 446-465.

346. Luna-Velasco, A., et al., *Inorganic nanoparticles enhance the production of reactive oxygen species (ROS) during the autoxidation of L-3, 4-dihydroxyphenylalanine (L-dopa).* Chemosphere, 2011. **85**(1): p. 19-25.
347. Sgouras, D. and R. Duncan, *Methods for the evaluation of biocompatibility of soluble synthetic polymers which have potential for biomedical use: 1—Use of the tetrazolium-based colorimetric assay (MTT) as a preliminary screen for evaluation ofin vitro cytotoxicity.* Journal of Materials Science: Materials in Medicine, 1990. **1**(2): p. 61-68.
348. Duncan, R. and R. Gaspar, *Nanomedicine (s) under the Microscope.* Molecular Pharmaceutics, 2011. **8**(6): p. 2101-2141.
349. Freshney, I., *Application of cell cultures to toxicology.* Cell biology and toxicology, 2001. **17**(4): p. 213-230.
350. Yadav, P., *Cell Culture*. Educa Books, 2008.
351. Shenoy, M., *Animal Biotechnology*. Firewall Media, 2007.
352. Stacey, G., A. Doyle, and M. Ferro, *Cell culture methods for in vitro toxicology*. Springer, 2001.
353. Clift, M.J., et al., *The impact of different nanoparticle surface chemistry and size on uptake and toxicity in a murine macrophage cell line.* Toxicology and Applied Pharmacology, 2008. **232**(3): p. 418-427.
354. Bromberg, L. and V. Alakhov, *Effects of polyether-modified poly (acrylic acid) microgels on doxorubicin transport in human intestinal epithelial Caco-2 cell layers.* Journal of Controlled Release, 2003. **88**(1): p. 11-22.
355. Fotakis, G. and J.A. Timbrell, *In vitro cytotoxicity assays: comparison of LDH, neutral red, MTT and protein assay in hepatoma cell lines following exposure to cadmium chloride.* Toxicology letters, 2006. **160**(2): p. 171-177.
356. García-Lorenzo, A., et al., *Cytotoxicity of selected imidazolium-derived ionic liquids in the human Caco-2 cell line. Sub-structural toxicological interpretation through a QSAR study.* Green chemistry, 2008. **10**(5): p. 508-516.
357. Hunter, J., et al., *Functional expression of P-glycoprotein in apical membranes of human intestinal Caco-2 cells. Kinetics of vinblastine secretion and interaction with modulators.* Journal of Biological Chemistry, 1993. **268**(20): p. 14991-14997.
358. Baumgartner, C., *Biomagnetism: Fundamental Research and Clinical Applications: Proceedings of the 9th International Conference on Biomagnetism*. Vol. 7. Ios PressInc, 1995.
359. Cooper, E.L. and N. Yamaguchi, *Complementary and alternative approaches to biomedicine*. Vol. 546. Plenum Publishing Corporation, 2004.
360. Morita, H., et al., *Cytokine production by the murine macrophage cell line J774. 1 after exposure to lactobacilli.* Bioscience, biotechnology, and biochemistry, 2002. **66**(9): p. 1963-1966.
361. Chellat, F., et al., *Metalloproteinase and cytokine production by THP-1 macrophages following exposure to chitosan-DNA nanoparticles.* Biomaterials, 2005. **26**(9): p. 961-970.
362. Jones, J.A., et al., *Proteomic analysis and quantification of cytokines and chemokines from biomaterial surface-adherent macrophages and foreign body giant cells.* Journal of Biomedical Materials Research Part A, 2007. **83**(3): p. 585-596.
363. Mahor, S., et al., *Mannosylated Polyethyleneimine–Hyaluronan Nanohybrids for Targeted Gene Delivery to Macrophage-Like Cell Lines.* Bioconjugate Chemistry, 2012. **23**(6): p. 1138-1148.
364. Sandgren, S., F. Cheng, and M. Belting, *Nuclear targeting of macromolecular polyanions by an HIV-Tat derived peptide Role for cell-surface proteoglycans.* Journal of Biological Chemistry, 2002. **277**(41): p. 38877-38883.
365. Peng, S.-F., et al., *Effects of incorporation of poly (γ-glutamic acid) in chitosan/DNA complex nanoparticles on cellular uptake and transfection efficiency.* Biomaterials, 2009. **30**(9): p. 1797-1808.

366. Jintapattanakit, A., et al., *Physicochemical properties and biocompatibility of< i> N</i>-trimethyl chitosan: Effect of quaternization and dimethylation.* European Journal of Pharmaceutics and Biopharmaceutics, 2008. **70**(2): p. 563-571.
367. Kunath, K., et al., *Low-molecular-weight polyethylenimine as a non-viral vector for DNA delivery: comparison of physicochemical properties, transfection efficiency and in vivo distribution with high-molecular-weight polyethylenimine.* Journal of Controlled Release, 2003. **89**(1): p. 113-125.
368. Jones, C.F. and D.W. Grainger, *In vitro assessments of nanomaterial toxicity.* Advanced drug delivery reviews. **61**(6): p. 438-456.
369. Weyermann, J., D. Lochmann, and A. Zimmer, *A practical note on the use of cytotoxicity assays.* International journal of pharmaceutics, 2005. **288**(2): p. 369-376.
370. Nogi, K., M. Naito, and T. Yokoyama, *Nanoparticle Technology Handbook*. Elsevier, 2012.
371. Hughes, D., *Cell Proliferation and Apoptosis*. BIOS Scientific Publ, 2003.
372. Duncan, R. and L. Izzo, *Dendrimer biocompatibility and toxicity.* Advanced drug delivery reviews, 2005. **57**(15): p. 2215-2237.
373. Dobrovolskaia, M.A., et al., *Method for analysis of nanoparticle hemolytic properties in vitro.* Nano letters, 2008. **8**(8): p. 2180-2187.
374. Cerda-Cristerna, B.I., et al., *Hemocompatibility assessment of poly (2-dimethylamino ethylmethacrylate)(PDMAEMA)-based polymers.* Journal of Controlled Release, 2011. **153**(3): p. 269-277.
375. Kainthan, R.K., et al., *Blood compatibility of novel water soluble hyperbranched polyglycerol-based multivalent cationic polymers and their interaction with DNA.* Biomaterials, 2006. **27**(31): p. 5377-5390.
376. Kamiński, K., et al., *Cationic derivatives of dextran and hydroxypropylcellulose as novel potential heparin antagonists.* Journal of medicinal chemistry, 2011. **54**(19): p. 6586-6596.
377. Moreau, E., et al., *Biocompatibility of polycations: in vitro agglutination and lysis of red blood cells and in vivo toxicity.* Journal of drug targeting, 2002. **10**(2): p. 161-173.
378. Moreau, É., et al., *Interactions between red blood cells and a lethal, partly quaternized tertiary polyamine.* Journal of controlled release, 2000. **64**(1): p. 115-128.
379. Riquelme, B.D., et al., *Hemocompatibility and biofunctionality of two poly (2-(dimethylamino) ethyl methacrylate-co-poly (ethyleneglycol) copolymers.* Journal of Biomedical Materials Research Part A, 2011. **99**(3): p. 445-454.
380. Gorochovceva, N. and R. Makuška, *Synthesis and study of water-soluble chitosan-O-poly (ethylene glycol) graft copolymers.* European Polymer Journal, 2004. **40**(4): p. 685-691.
381. Cui, L., C. Tang, and C. Yin, *Effects of quaternization and PEGylation on the biocompatibility, enzymatic degradability and antioxidant activity of chitosan derivatives.* Carbohydrate Polymers, 2012. **87**(4): p. 2505-2511.
382. Swarnakar, N.K., et al., *Oral bioavailability, therapeutic efficacy and reactive oxygen species scavenging properties of coenzyme Q10-loaded polymeric nanoparticles.* Biomaterials, 2011. **32**(28): p. 6860-6874.
383. Grotto, D., et al., *Importance of the lipid peroxidation biomarkers and methodological aspects for malondialdehyde quantification.* Quimica Nova, 2009. **32**(1): p. 169-174.
384. Leeuwenburgh, C. and J. Heinecke, *Oxidative stress and antioxidants in exercise.* Current medicinal chemistry, 2001. **8**(7): p. 829-838.
385. Shafirovich, V., et al., *Role of free radical reactions in the formation of DNA damage.* The Chemical Biology of DNA Damage, 2010: p. 81-104.
386. Lee, J., N. Koo, and D. Min, *Reactive oxygen species, aging, and antioxidative nutraceuticals.* Comprehensive reviews in food science and food safety, 2004. **3**(1): p. 21-33.
387. Sayes, C.M., et al., *Nano-C60 cytotoxicity is due to lipid peroxidation.* Biomaterials, 2005. **26**(36): p. 7587-7595.

388. Menon, D., et al., *A novel chitosan/polyoxometalate nano-complex for anti-cancer applications.* Carbohydrate polymers, 2011. **84**(3): p. 887-893.
389. Shinohara, N., et al., *Is lipid peroxidation induced by the aqueous suspension of fullerene C60 nanoparticles in the brains of Cyprinus carpio?* Environmental Science & Technology, 2008. **43**(3): p. 948-953.
390. Yang, Y.-W. and P.Y.-J. Hsu, *The effect of poly (d, l-lactide- co-glycolide) microparticles with polyelectrolyte self-assembled multilayer surfaces on the cross-presentation of exogenous antigens.* Biomaterials, 2008. **29**(16): p. 2516-2526.
391. Nabeshi, H., et al., *Amorphous nanosilica induce endocytosis-dependent ROS generation and DNA damage in human keratinocytes.* Particle and fibre toxicology, 2011. **8**(1): p. 1.
392. Singh, M., et al., *Nanotechnology in medicine and antibacterial effect of silver nanoparticles.* Digest J. Nanomater. Biostructures, 2008. **3**(3): p. 115-122.
393. Yang, Y.W. and P.Y.J. Hsu, *The effect of poly (d, l-lactide- co-glycolide) microparticles with polyelectrolyte self-assembled multilayer surfaces on the cross-presentation of exogenous antigens.* Biomaterials, 2008. **29**(16): p. 2516-2526.
394. Stevenson, R., et al., *Nanoparticles and inflammation.* The Scientific World JOURNAL, 2011. **11**: p. 1300-1312.
395. Mogi, M., et al., *Interleukin (IL)-1β, IL-2, IL-4, IL-6 and transforming growth factor-α levels are elevated in ventricular cerebrospinal fluid in juvenile parkinsonism and Parkinson's disease.* Neuroscience letters, 1996. **211**(1): p. 13-16.
396. Akira, S., et al., *Biology of multifunctional cytokines: IL 6 and related molecules (IL 1 and TNF).* The FASEB journal, 1990. **4**(11): p. 2860-2867.
397. Schöler, N., et al., *Effect of lipid matrix and size of solid lipid nanoparticles (SLN) on the viability and cytokine production of macrophages.* International journal of pharmaceutics, 2002. **231**(2): p. 167-176.
398. Xing, Z., et al., *IL-6 is an antiinflammatory cytokine required for controlling local or systemic acute inflammatory responses.* Journal of Clinical Investigation, 1998. **101**(2): p. 311.
399. Leon, L.R., *Invited review: cytokine regulation of fever: studies using gene knockout mice.* Journal of Applied Physiology, 2002. **92**(6): p. 2648-2655.
400. Malek, T.R. and I. Castro, *Interleukin-2 receptor signaling: at the interface between tolerance and immunity.* Immunity, 2010. **33**(2): p. 153-165.
401. Malek, T.R. and A.L. Bayer, *Tolerance, not immunity, crucially depends on IL-2.* Nature Reviews Immunology, 2004. **4**(9): p. 665-674.
402. Tryoen-Tóth, P., et al., *Viability, adhesion, and bone phenotype of osteoblast-like cells on polyelectrolyte multilayer films.* Journal of biomedical materials research, 2002. **60**(4): p. 657-667.
403. Semete, B., et al., *In vivo evaluation of the biodistribution and safety of PLGA nanoparticles as drug delivery systems.* Nanomedicine: Nanotechnology, Biology and Medicine, 2010. **6**(5): p. 662-671.
404. Olbrich, C., et al., *Cytotoxicity studies of Dynasan 114 solid lipid nanoparticles (SLN) on RAW 264.7 macrophages—impact of phagocytosis on viability and cytokine production.* Journal of pharmacy and pharmacology, 2004. **56**(7): p. 883-891.
405. Schöler, N., et al., *Surfactant, but not the size of solid lipid nanoparticles (SLN) influences viability and cytokine production of macrophages.* International journal of pharmaceutics, 2001. **221**(1-2): p. 57-67.
406. Carson, R.T. and D.A.A. Vignali, *Simultaneous quantitation of 15 cytokines using a multiplexed flow cytometric assay.* Journal of immunological methods, 1999. **227**(1): p. 41-52.
407. Mosmann, T., *Rapid colorimetric assay for cellular growth and survival: application to proliferation and cytotoxicity assays.* Journal of immunological methods, 1983. **65**(1-2): p. 55-63.

408. Malik, N., et al., *Dendrimers:: Relationship between structure and biocompatibility in vitro, and preliminary studies on the biodistribution of 125I-labelled polyamidoamine dendrimers in vivo.* Journal of Controlled Release, 2000. **65**(1): p. 133-148.
409. Vllasaliu, D., et al., *Absorption-promoting effects of chitosan in airway and intestinal cell lines: a comparative study.* International journal of pharmaceutics, 2012. **430**(1): p. 151-160.
410. Derfus, A.M., W.C. Chan, and S.N. Bhatia, *Probing the cytotoxicity of semiconductor quantum dots.* Nano letters, 2004. **4**(1): p. 11-18.
411. Paur, H.-R., et al., *In-vitro cell exposure studies for the assessment of nanoparticle toxicity in the lung—a dialog between aerosol science and biology.* Journal of Aerosol Science, 2011. **42**(10): p. 668-692.
412. Fadeel, B., *Clear and present danger? Engineered nanoparticles and the immune system.* Swiss Med. Wkly, 2012. **142**: p. w13609.
413. Van Bambeke, F., et al., *Cellular pharmacokinetics and pharmacodynamics of the glycopeptide antibiotic oritavancin (LY333328) in a model of J774 mouse macrophages.* Antimicrobial agents and chemotherapy, 2004. **48**(8): p. 2853-2860.
414. Colak, S., et al., *Hydrophilic modifications of an amphiphilic polynorbornene and the effects on its hemolytic and antibacterial activity.* Biomacromolecules, 2009. **10**(2): p. 353-359.
415. Thompson, C., et al., *The complexation between novel comb shaped amphiphilic polyallylamine and insulin--Towards oral insulin delivery.* International journal of pharmaceutics, 2009. **376**(1-2): p. 46-55.
416. Clare, H., et al., *The use of nano polymeric self-assemblies based on novel amphiphilic polymers for oral hydrophobic drug delivery.* Pharmaceutical research, 2012. **29**(3): p. 782-794.
417. Liu, Z., et al., *Interactions between solubilized polymer molecules and blood components.* Journal of Controlled Release, 2012. **160**(1): p. 14-24.
418. Oberdörster, G., et al., *Principles for characterizing the potential human health effects from exposure to nanomaterials: elements of a screening strategy.* Particle and fibre toxicology, 2005. **2**(1): p. 8.
419. Xia, T., et al., *Cationic polystyrene nanosphere toxicity depends on cell-specific endocytic and mitochondrial injury pathways.* ACS nano, 2007. **2**(1): p. 85-96.
420. Naha, P.C., et al., *Reactive oxygen species (ROS) induced cytokine production and cytotoxicity of PAMAM dendrimers in J774A. 1 cells.* Toxicology and applied pharmacology, 2010. **246**(1): p. 91-99.
421. Donaldson, K., et al., *Combustion-derived nanoparticles: a review of their toxicology following inhalation exposure.* Particle and Fibre Toxicology, 2005. **2**(1): p. 10.
422. Nel, A., et al., *Toxic potential of materials at the nanolevel.* Science, 2006. **311**(5761): p. 622-627.
423. Finkelman, F.D. and S.C. Morris, *Development of an assay to measure in vivo cytokine production in the mouse.* International immunology, 1999. **11**(11): p. 1811-1818.
424. Sullivan, K.E., et al., *Measurement of cytokine secretion, intracellular protein expression, and mRNA in resting and stimulated peripheral blood mononuclear cells.* Clinical and diagnostic laboratory immunology, 2000. **7**(6): p. 920-924.
425. Thatte, S., K. Datar, and R.M. Ottenbrite, *Perspectives on: Polymeric drugs and drug delivery systems.* Journal of bioactive and compatible polymers, 2005. **20**(6): p. 585-601.
426. Ward, P.D., T.K. Tippin, and D.R. Thakker, *Enhancing paracellular permeability by modulating epithelial tight junctions.* Pharmaceutical Science & Technology Today, 2000. **3**(10): p. 346-358.
427. Thompson, C., et al., *Uptake and Transport of Novel Amphiphilic Polyelectrolyte-Insulin Nanocomplexes by Caco-2 Cells—Towards Oral Insulin.* Pharmaceutical research, 2011. **28**(4): p. 886-896.

428. Kowapradit, J., et al., *Methylated N-(4-N, N-dimethylaminobenzyl) chitosan, a novel chitosan derivative, enhances paracellular permeability across intestinal epithelial cells (Caco-2).* AAPS PharmSciTech, 2008. **9**(4): p. 1143-1152.
429. Kowapradit, J., et al., *Methylated N-(4-N, N-dimethylaminocinnamyl) chitosan enhances paracellular permeability across Caco-2 cells.* Drug delivery, 2010. **17**(5): p. 301-312.
430. Thanou, M., et al., *Effect of degree of quaternization of N-trimethyl chitosan chloride for enhanced transport of hydrophilic compounds across intestinal Caco-2 cell monolayers.* Journal of Controlled Release, 2000. **64**(1): p. 15-25.
431. Sadeghi, A., et al., *Permeation enhancer effect of chitosan and chitosan derivatives: comparison of formulations as soluble polymers and nanoparticulate systems on insulin absorption in Caco-2 cells.* European Journal of Pharmaceutics and Biopharmaceutics, 2008. **70**(1): p. 270-278.
432. Thanou, M., et al., *A novel polymeric absorption enhancer for the oral delivery of macromolecules.* Journal of controlled release, 2007. **117**(2): p. 171-178.
433. Kitchens, K.M., M.E. El-Sayed, and H. Ghandehari, *Transepithelial and endothelial transport of poly (amidoamine) dendrimers.* Advanced drug delivery reviews, 2005. **57**(15): p. 2163-2176.
434. El-Sayed, M., et al., *Transport mechanism (s) of poly (amidoamine) dendrimers across Caco-2 cell monolayers.* International journal of pharmaceutics, 2003. **265**(1): p. 151-157.
435. Kitchens, K.M., et al., *Transport of poly (amidoamine) dendrimers across Caco-2 cell monolayers: influence of size, charge and fluorescent labeling.* Pharmaceutical research, 2006. **23**(12): p. 2818-2826.
436. Dorkoosh, F.A., et al., *Transport of octreotide and evaluation of mechanism of opening the paracellular tight junctions using superporous hydrogel polymers in Caco-2 cell monolayers.* Journal of pharmaceutical sciences, 2004. **93**(3): p. 743-752.
437. Borchard, G., et al., *The potential of mucoadhesive polymers in enhancing intestinal peptide drug absorption. III: Effects of chitosan-glutamate and carbomer on epithelial tight junctions in vitro.* Journal of Controlled Release, 1996. **39**(2): p. 131-138.
438. Anderson, J. and C. Van Itallie, *Tight junctions and the molecular basis for regulation of paracellular permeability.* American Journal of Physiology-Gastrointestinal and Liver Physiology, 1995. **269**(4): p. G467-G475.
439. Morishita, M. and N.A. Peppas, *Is the oral route possible for peptide and protein drug delivery?* Drug discovery today, 2006. **11**(19): p. 905-910.
440. Gratton, S.E., et al., *The effect of particle design on cellular internalization pathways.* Proceedings of the National Academy of Sciences, 2008. **105**(33): p. 11613-11618.
441. Harush-Frenkel, O., et al., *Surface charge of nanoparticles determines their endocytic and transcytotic pathway in polarized MDCK cells.* Biomacromolecules, 2008. **9**(2): p. 435-443.
442. Gaumet, M., R. Gurny, and F. Delie, *Interaction of biodegradable nanoparticles with intestinal cells: the effect of surface hydrophilicity.* International journal of pharmaceutics, 2010. **390**(1): p. 45-52.
443. Desai, M.P., et al., *The mechanism of uptake of biodegradable microparticles in Caco-2 cells is size dependent.* Pharmaceutical research, 1997. **14**(11): p. 1568-1573.
444. Woitiski, C.B., et al., *Facilitated nanoscale delivery of insulin across intestinal membrane models.* International journal of pharmaceutics, 2011. **412**(1): p. 123-131.
445. Hornof, M., et al., *Low molecular weight hyaluronan shielding of DNA/PEI polyplexes facilitates CD44 receptor mediated uptake in human corneal epithelial cells.* The journal of gene medicine, 2008. **10**(1): p. 70-80.
446. Xu, P., G.K. Quick, and Y. Yeo, *Gene delivery through the use of a hyaluronate-associated intracellularly degradable crosslinked polyethyleneimine.* Biomaterials, 2009. **30**(29): p. 5834-5843.
447. Jevprasesphant, R., et al., *Transport of dendrimer nanocarriers through epithelial cells via the transcellular route.* Journal of controlled release, 2004. **97**(2): p. 259-267.

448. Dombu, C.Y., et al., *Characterization of endocytosis and exocytosis of cationic nanoparticles in airway epithelium cells.* Nanotechnology, 2010. **21**(35): p. 355102.
449. Jin, Y., et al., *Goblet cell-targeting nanoparticles for oral insulin delivery and the influence of mucus on insulin transport.* Biomaterials, 2012. **33**(5): p. 1573-1582.
450. Qaddoumi, M.G., et al., *Clathrin and caveolin-1 expression in primary pigmented rabbit conjunctival epithelial cells: role in PLGA nanoparticle endocytosis.* Mol Vis, 2003. **9**: p. 559-568.
451. Rajapaksa, T.E., et al., *Claudin 4-targeted protein incorporated into PLGA nanoparticles can mediate M cell targeted delivery.* Journal of Controlled Release, 2010. **142**(2): p. 196-205.
452. Beloqui, A., et al., *Mechanism of transport of saquinavir-loaded nanostructured lipid carriers across the intestinal barrier.* Journal of Controlled Release, 2012. **166**(2): p. 115-123.
453. Yee, S., *In vitro permeability across Caco-2 cells (colonic) can predict in vivo (small intestinal) absorption in man—fact or myth.* Pharmaceutical research, 1997. **14**(6): p. 763-766.
454. Kotzé, A.F., et al., *Enhancement of paracellular drug transport with highly quaternized N-trimethyl chitosan chloride in neutral environments: In vitro evaluation in intestinal epithelial cells (Caco-2).* Journal of pharmaceutical sciences, 1999. **88**(2): p. 253-257.
455. Ingels, F., et al., *Simulated intestinal fluid as transport medium in the Caco-2 cell culture model.* International journal of pharmaceutics, 2002. **232**(1): p. 183-192.
456. Jackson, C., R.F. Murphy, and J. Kovacevic, *Intelligent acquisition and learning of fluorescence microscope data models.* Image Processing, IEEE Transactions on, 2009. **18**(9): p. 2071-2084.
457. Brown, C.M., *Fluorescence microscopy-avoiding the pitfalls.* Journal of cell science, 2007. **120**(10): p. 1703-1705.
458. Swedlow, J.R. and M. Platani, *Live cell imaging using wide-field microscopy and deconvolution.* Cell structure and function, 2002. **27**(5): p. 335-341.
459. Rieseberg, M., et al., *Flow cytometry in biotechnology.* Applied microbiology and biotechnology, 2001. **56**(3): p. 350-360.
460. Kuckuck, F.W., B.S. Edwards, and L.A. Sklar, *High throughput flow cytometry.* Cytometry, 2001. **44**(1): p. 83-90.
461. Jaroszeski, M.J. and G. Radcliff, *Fundamentals of flow cytometry.* Molecular biotechnology, 1999. **11**(1): p. 37-53.
462. Haynes, J.L., *Principles of flow cytometry.* Cytometry, 2005. **9**(S3): p. 7-17.
463. Carter, N. and M.G. Ormerod, *Introduction to the principles of flow cytometry.* Flow Cytometry: A Practical Approach, ed, 2000. **2**: p. 1-25.
464. Krysko, D.V., et al., *Methods for distinguishing apoptotic from necrotic cells and measuring their clearance.* Methods in enzymology, 2008. **442**: p. 307-341.
465. Lan, K., et al., *Intra-herb pharmacokinetics interaction between quercetin and isorhamentin1.* Acta Pharmacologica Sinica, 2008. **29**(11): p. 1376-1382.
466. Song, Q., et al., *Cellular internalization pathway and transcellular transport of pegylated polyester nanoparticles in Caco-2 cells.* International journal of pharmaceutics, 2013. **445**(1): p. 58-68.
467. Neuhaus, W., et al., *A novel tool to characterize paracellular transport: the APTS–dextran ladder.* Pharmaceutical research, 2006. **23**(7): p. 1491-1501.
468. Tavelin, S., et al., *Prediction of the oral absorption of low-permeability drugs using small intestine-like 2/4/A1 cell monolayers.* Pharmaceutical research, 2003. **20**(3): p. 397-405.
469. Hsu, L.-W., et al., *Elucidating the signaling mechanism of an epithelial tight-junction opening induced by chitosan.* Biomaterials, 2012. **33**(26): p. 6254-6263.
470. Wen, H., et al., *Selective decrease in paracellular conductance of tight junctions: role of the first extracellular domain of claudin-5.* Molecular and cellular biology, 2004. **24**(19): p. 8408-8417.

471. Kowapradit, J., et al., *Structure–activity relationships of methylated N-aryl chitosan derivatives for enhancing paracellular permeability across Caco-2 cells.* Carbohydrate Polymers, 2011. **83**(2): p. 430-437.
472. Ichikawa, H. and N.A. Peppas, *Novel complexation hydrogels for oral peptide delivery: In vitro evaluation of their cytocompatibility and insulin-transport enhancing effects using Caco-2 cell monolayers.* Journal of Biomedical Materials Research Part A, 2003. **67**(2): p. 609-617.
473. Prego, C., et al., *Transmucosal macromolecular drug delivery.* Journal of controlled release, 2005. **101**(1): p. 151-162.
474. Suksamran, T., et al., *Oral Methylated N-Aryl Chitosan Derivatives for Inducing Immune Responses to Ovalbumin.* Tropical Journal of Pharmaceutical Research, 2013. **11**(6): p. 899-908.
475. Kotzé, A.F., et al., *Effect of the degree of quaternization of N-trimethyl chitosan chloride on the permeability of intestinal epithelial cells (Caco-2).* European Journal of Pharmaceutics and Biopharmaceutics, 1999. **47**(3): p. 269-274.
476. Florea, B.I., et al., *Enhancement of bronchial octreotide absorption by chitosan and N-trimethyl chitosan shows linear in vitro/in vivo correlation.* Journal of controlled release, 2006. **110**(2): p. 353-361.
477. Sonaje, K., et al., *Opening of Epithelial Tight Junctions and Enhancement of Paracellular Permeation by Chitosan: Microscopic, Ultrastructural, and Computed-Tomographic Observations.* Molecular pharmaceutics, 2012. **9**(5): p. 1271-1279.
478. Smith, J.M., M. Dornish, and E.J. Wood, *Involvement of protein kinase C in chitosan glutamate-mediated tight junction disruption.* Biomaterials, 2005. **26**(16): p. 3269-3276.
479. Hamman, J., C. Schultz, and A. Kotzé, *N-trimethyl chitosan chloride: optimum degree of quaternization for drug absorption enhancement across epithelial cells.* Drug development and industrial pharmacy, 2003. **29**(2): p. 161-172.
480. Bourdet, D.L., J.B. Pritchard, and D.R. Thakker, *Differential substrate and inhibitory activities of ranitidine and famotidine toward human organic cation transporter 1 (hOCT1; SLC22A1), hOCT2 (SLC22A2), and hOCT3 (SLC22A3).* Journal of Pharmacology and Experimental Therapeutics, 2005. **315**(3): p. 1288-1297.
481. Kim, M.K. and C.-K. Shim, *The transport of organic cations in the small intestine: current knowledge and emerging concepts.* Archives of pharmacal research, 2006. **29**(7): p. 605-616.
482. Chalasani, K.B., et al., *Effective oral delivery of insulin in animal models using vitamin B12-coated dextran nanoparticles.* Journal of Controlled Release, 2007. **122**(2): p. 141-150.
483. Russo, L., et al., *The normal kidney filters nephrotic levels of albumin retrieved by proximal tubule cells: retrieval is disrupted in nephrotic states.* Kidney international, 2007. **71**(6): p. 504-513.
484. Ito, T., et al., *DNA/polyethyleneimine/hyaluronic acid small complex particles and tumor suppression in mice.* Biomaterials, 2010. **31**(10): p. 2912-2918.
485. Lerch, S., et al., *Polymeric nanoparticles of different sizes overcome the cell membrane barrier.* European journal of pharmaceutics and biopharmaceutics, 2013. **84**(2): p. 265-274.
486. Kim, Y.H., et al., *Structural characteristics of size-controlled self-aggregates of deoxycholic acid-modified chitosan and their application as a DNA delivery carrier.* Bioconjugate Chemistry, 2001. **12**(6): p. 932-938.
487. Wang, M. and M. Thanou, *Targeting nanoparticles to cancer.* Pharmacological Research, 2010. **62**(2): p. 90-99.
488. Sahoo, S.K., et al., *Residual polyvinyl alcohol associated with poly (D, L-lactide-co-glycolide) nanoparticles affects their physical properties and cellular uptake.* Journal of controlled release, 2002. **82**(1): p. 105-114.
489. Antunes, F., et al., *Establishment of a triple co-culture in vitro cell models to study intestinal absorption of peptide drugs.* European journal of pharmaceutics and biopharmaceutics, 2012. **83**(3): p. 427-435.

490. Hamman, J.H., G.M. Enslin, and A.F. Kotzé, *Oral delivery of peptide drugs: barriers and developments.* BioDrugs, 2005. **19**(3): p. 165-177.
491. Sarmento, B.F.C.C., *Improvement of Peptidic Drugs Oral Availability Througt Their Encapsulation In Polyelectrolytes Complexes-Made Nano Particles.* 2011.
492. Goycoolea, F.M., et al., *Chitosan-alginate blended nanoparticles as carriers for the transmucosal delivery of macromolecules.* Biomacromolecules, 2009. **10**(7): p. 1736-1743.
493. Bernkop-Schnürch, A., C. Kast, and D. Guggi, *Permeation enhancing polymers in oral delivery of hydrophilic macromolecules: thiomer/GSH systems.* Journal of Controlled Release, 2003. **93**(2): p. 95-103.
494. Ovrevik, J. and P.E. Schwarze, *Chemical composition and not only total surface area is important for the effects of ultrafine particles.* Mutation Research/Fundamental and Molecular Mechanisms of Mutagenesis, 2006. **594**(1): p. 201-202.
495. Gao, H., W. Shi, and L.B. Freund, *Mechanics of receptor-mediated endocytosis.* Proceedings of the National Academy of Sciences of the United States of America, 2005. **102**(27): p. 9469-9474.
496. Jiang, X., et al., *Specific effects of surface amines on polystyrene nanoparticles in their interactions with mesenchymal stem cells.* Biomacromolecules, 2010. **11**(3): p. 748-753.